COUPLED MICROSTRIP AND ITS APPLICATION TO BROADBAND MICROWAVE STRUCTURES

Submitted By:
J.D. MILLER, B.Sc. (Hons.), M.Sc.

A Thesis Submitted for the Degree of Doctor of Philosophy at the University of Warwick, U.K.

December, 1991

ACKNOWLEDGEMENTS

I would like to acknowledge the contribution of the following persons towards my successfully completing this course of study:

To my supervisor Dr. H.V Shurmer for his direction, encouragement and guidance.

Professor Cullyer for his analyses and valuable suggestions on reviewing the interim reports.

Dr. Narendra Utukuri for his assistance and valuable discussions particularly in the area of computer-aided analysis.

Lucas Aerospace and TRL Microwave Technology for corporate support.

Mrs. Manjit Gill for her patience and accuracy in typing the thesis and Chris Senger and Bishu Sarkar for CAD drawings of figures.

My son, Jason and my wife Elizabeth for their understanding and support when I had to study instead of doing the things that normal fathers do.

ABSTRACT

As the most frequently used waveguide type in microwave and millimeter wave integrated circuits, microstrip theory occupies an important position in understanding the behaviour of such structures.

In this thesis it is shown that coupled microstrip, through its several degrees of freedom can be used to achieve predictable state of the art performance of active devices such as a multioctave medium power amplifier operating over the 2 - 18 GHz frequency band with +29 dBm saturated output power and 20 percent power added efficiency. Both quasi-static and full wave and analytical techniques are covered for coupled microstrip lines.

In depth analysis of edge-coupled multiconductor suspended microstrip with tuning septum, as well as multiconductor broadside coupled lines with position dependent coupling coefficient, are presented. Important relationships between the mechanical dimensions and such parameters as coupling factor and phase velocity are also derived.

The technique based on spectral domain analysis uses considerable analytical preprocessing to eliminate the need for the sophisticated computer facilities which would perviously be required to analyze such complex structures.

Based on the above mentioned technique, novel broadband planar hybrids, magic-T's and matching structures are proposed and analyzed.

TABLE OF CONTENTS

CHAPTER 5

CHAPTER 6

CHAPTER 1

MICROSTRIP ANALYSIS TECHNIQUES

1.0 INTRODUCTION

Coupled microstrip structures can be divided into three main types (a) edge-coupled (b) slot coupled (c) broadside coupled. Examples of these are indicated in figure 1.1 (a) through (ℓ).

The forms of microstrip lines shown in figure 1.1 can support various modes depending on the degree of dielectric non-homogeneity when the structures are viewed in cross-section. Such modes may be divided into pure TEM, quasi-TEM and hybrid modes.

1.1 TEM MODE

The structures in Figs. 1.1 (d), 1.1 (j), 1.1 (k) will support a TEM mode if $\ell = 0$, $s = 0$ and $\epsilon_{r1} = \epsilon_0$; for the frequency range $0 \leq f \leq \infty$. An additional condition for a pure TEM mode to propagate is that one of the two conductors must have a finite dimension. ϵ_r is relative dielectric constant, an isotropic scalar quantity and ϵ_0 permittivity of free space.

The pure TEM mode is characterised by having its magnetic and electric field components only transverse to the direction of propagation. The current vector then has non-zero magnitude only in the direction of propagation.

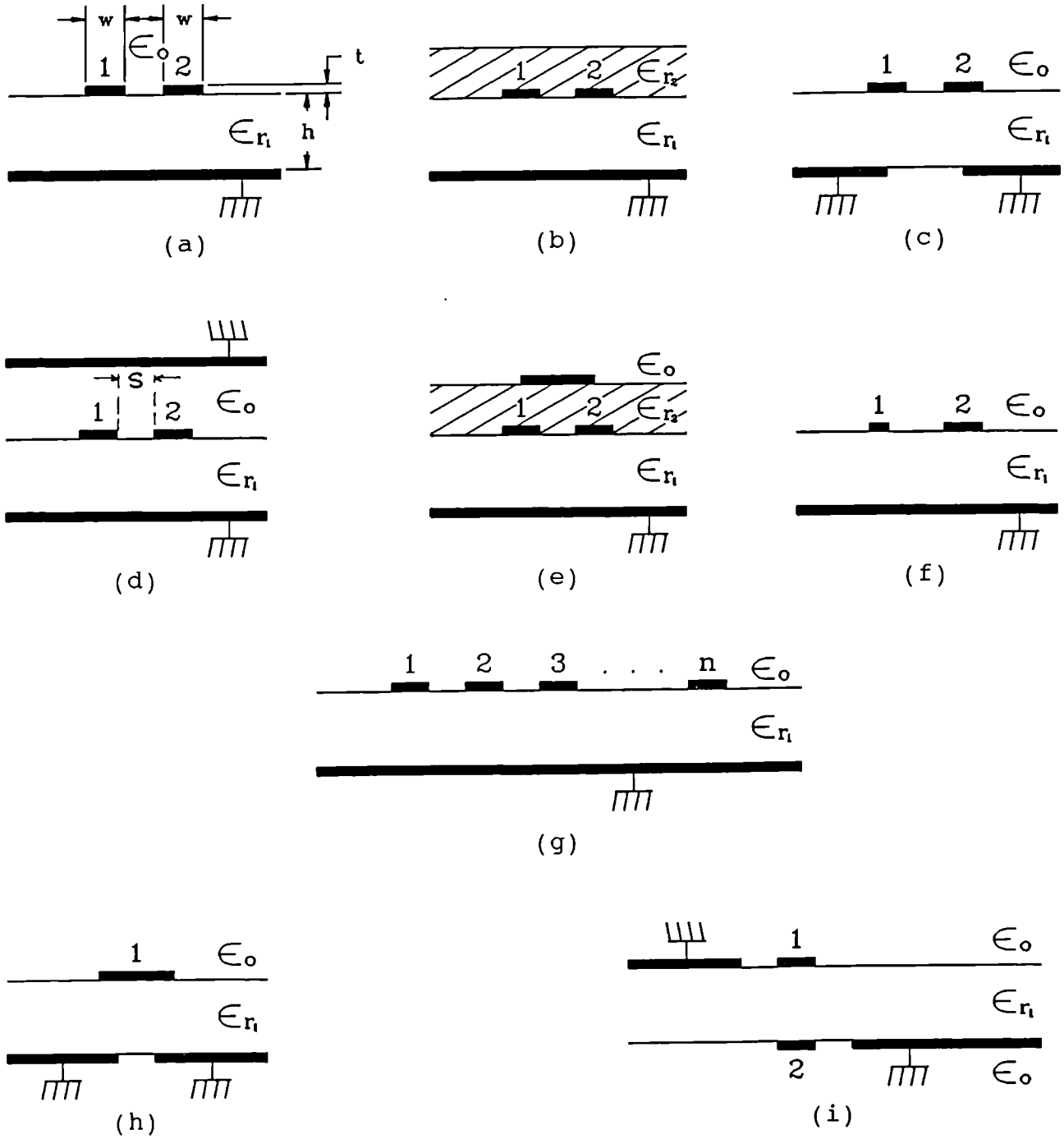

Figure 1.1(a-i): Microstrip configurations

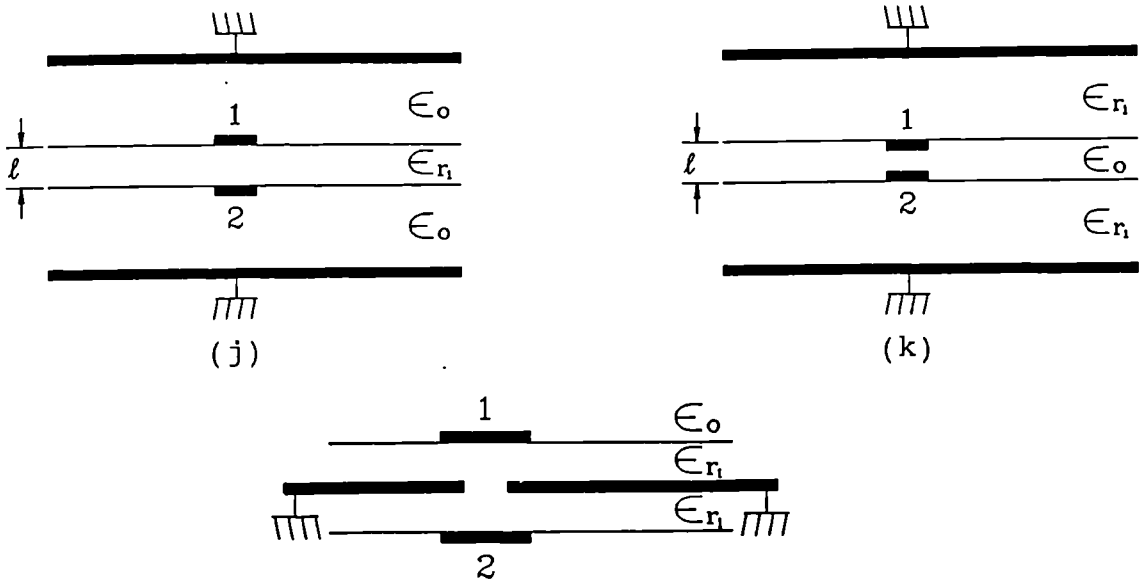

Figure 1.1(j-l): Microstrip configurations

(a) Symmetrical edge coupled pair

(b) Same as (a) with dielectric overlay

(c) Same as (a) with tuning septum

(d) Same as (a) with lid in close proximity

(e) Same as (b) with extra strip at floating potential

(f) Asymmetrical edge coupled pair

(g) Multi-line edge coupled system

(h) Microstrip slot coupled same as (c) with s = 0

(i) Coupled micro line

(j) Broadside coupled suspended microstrip lines, a variation of 1.1 (a)

(k) Broadside coupled inverted microstrip lines, a variation of 1.1 (j)

(l) Broadside Coupled Microstrip line with tuning septum.

Characteristic impedance Z_o and phase velocity V_p of the TEM line are given by

$$Z_o = \frac{1}{c\sqrt{C_a C_s}} \qquad (1.1)$$

$$V_p = \frac{c}{\sqrt{\epsilon_{eff}}} \qquad (1.2)$$

$$\epsilon_{eff} = \frac{C_s}{C_a} \qquad (1.3)$$

where c, C_a, C_s, ϵ_{effe} are speed of light in a vacuum, capacitance of the strip conductor per unit length in the absence of a dielectric, capacitance per unit length of the strip conductor in the presence of a dielectric and effective dielectric constant respectively. For the TEM line $\epsilon_{eff} = \epsilon_r$ and Z_o, V_p are single valued ie. independent of position on the line. In addition Z_o, V_p are single valued with respect to frequency.

1.2 HYBRID MODES

Microstrip will in general not support a pure TEM mode due to the dielectric non-homogeneity associated with the structure. As proof of this consider figure 1.2 [1.2]

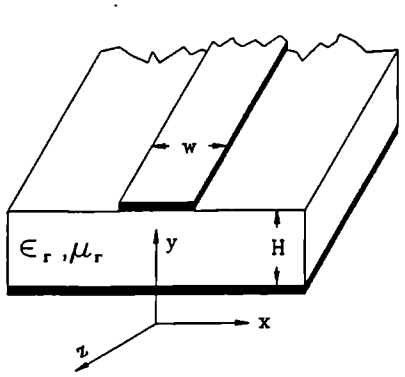

Figure 1.2 Microstrip Structure

If the dielectric above the structure is air, the tangential electric field E_x equality at any point, (x, H) at the interface between air and the substrate results in

$$(\overline{\nabla} x \overline{H})_x|_s = \epsilon_r (\overline{\nabla} x \overline{H})_x|_a \qquad (1.5)$$

where a and s refer to air and substrate respectively.

Equation 1.5 is derived from Maxwell's equations.

$$\bar{\nabla} x \bar{H}(\bar{r}, t) = \bar{J} + \frac{d\bar{D}}{dt}(\bar{r}, t)$$

$$and\ \bar{D}(\bar{r}, t) = \epsilon \epsilon_o \bar{E}(\bar{r}, t)$$

$$Expanding\ (1.5) \quad \bar{\nabla} x \bar{H} = \bar{k} \frac{\delta H_y}{\delta_x} - \bar{j} \frac{\delta H_z}{\delta_x} - \bar{k} \frac{\delta H_x}{\delta_y} + \bar{i} \frac{\delta H_z}{\delta y} + \bar{j} \frac{\delta H_x}{\delta_z} - i \frac{\delta H_y}{\delta_z}$$

$$where \bar{i}, \bar{j}, \bar{k}$$

are unit vectors in the x, y, z directions respectively. Applying (1.5) and taking into account the continuity of the normal component of displacement at the dielectric interface we arrive at

$$\epsilon_r \frac{\delta H_z}{\delta_y}\Big|_a - \frac{\delta H_z}{\delta_y}\Big|_s = (\epsilon_r - 1) \frac{\delta H_y}{\delta_z} \qquad (1.6)$$

From (1.6), since $H_y \neq 0$ and $\epsilon_r \neq 1$, H_z must be non-zero. Similarly it can be proven that $E_z \neq 0$ by using Maxwell's equation

$$\bar{\nabla} x \bar{E}(\bar{r}, t) = -\frac{\delta \bar{B}}{\delta_t}(\bar{r}, t)$$

Therefore in order to satisfy Maxwell's equation the structure must support longitudinal components of E and H fields. There is then a total transverse current density J_t along the x direction in

addition to the total tangential current density J_z along the Z direction. Due to J_t the total conductor current I is no longer uniquely defined and due to E_z the voltage $U = \int E.\ ds$ is now path dependent. Therefore characteristic impedance U/I is multivalued and frequency dependent, as will be shown later. J_t although small compared with J_z cannot be neglected if the complete dispersive nature of microstrip is to be accounted for and plays a particularly important role in characteristic impedance dispersion.

The fundamental mode behaviour can be predicted by taking into account the fact that an arbitrary electromagnetic field can be represented by a combination of TE and TM fields. A rigorous full wave analysis of the characteristic impedance and propagation constant is achieved by using the charge/current formulation [1.4] which follows:

Consider figure 1.2 where open microstrip is assumed with $\mu_r = 1$, $\epsilon_r \neq 1$, conducting strip thickness t=0, total charge on the upper and lower surface of the conducting strip = ρ_s, and phase factor is exp j ($\omega t - \gamma z$). By applying the charge continuity condition

$$\frac{\delta J_t}{\delta x} + \frac{\delta J_z}{\delta z} = \frac{-\delta \rho_s}{\delta t}$$

$$ie. \frac{\delta J_t}{\delta x} = j(\gamma J_z - \omega \rho_s) \qquad (1.7)$$

where ω is angular frequency and γ is the propagation constant.

Bhat and Koul [1.4] has shown that the fundamental mode charge functions $f_z(x)$, $g_t(x)$ associated with J_z, J_t can in general be approximately represented by

$$f_z(x) = \frac{1}{\sqrt{(\frac{w}{2})^2 - x^2}}$$

$$g_t(x) = x\sqrt{(\frac{w}{2})^2 - x^2}$$

Figure 1.3 is a graphical representation of the fundamental mode J_z and J_t based on [1.4]. The known charge singularities at the edges of the strip related to J_z is demonstrated.

At $x = \pm w/2$, $J_t (\pm w/2) = o$ (1.8) since J_t is the sum of the current densities on both surfaces (upper and lower) of the conducting strip. From (1.7) and (1.8)

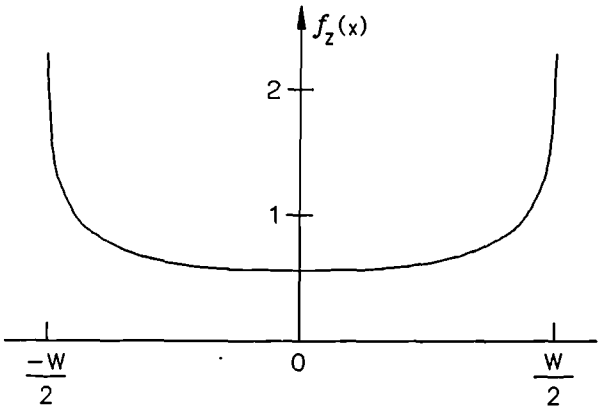

Longitudinal Current Distribution on Microstrip, $f_z(x)$ [1.4]

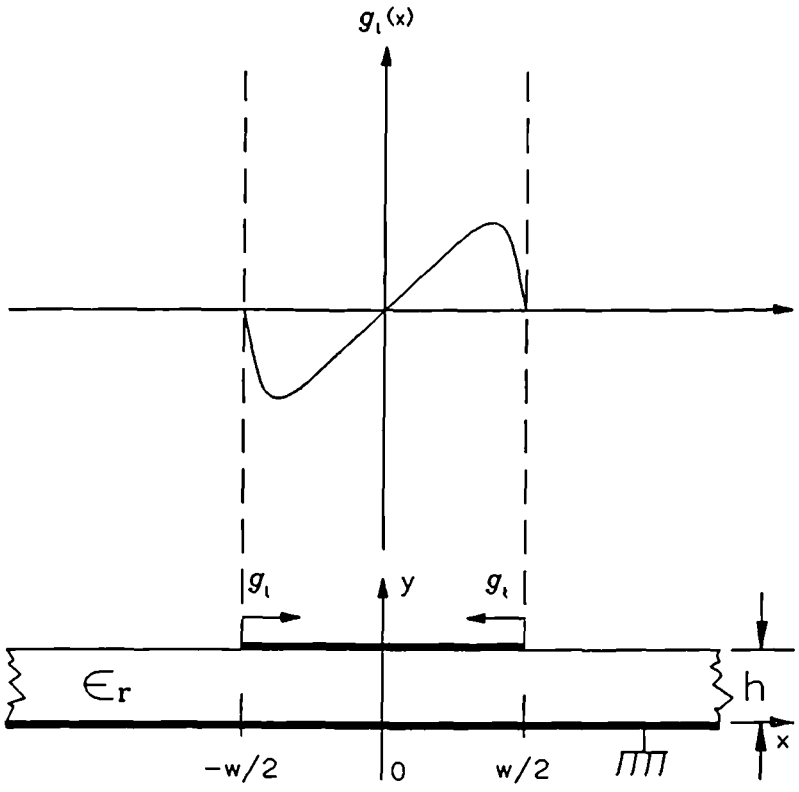

Transverse Current Distribution on Microstrip, $g_t(x)$ [1.4]

$$\int_{-w/2}^{w/2} \delta J_t = \int_{-w/2}^{w/2} j(\gamma J_z - \omega \rho_s)\, dx = o \qquad (1.9(a))$$

$$Then \quad \gamma J = \omega Q \qquad (1.9(b))$$

where J,Q are total current density and total charge per unit length of the conducting strip and

$$J = \int_{-\frac{w}{2}}^{\frac{w}{2}} J_z\, dx \qquad (1.9(c))$$

$$Q = \int_{-\frac{w}{2}}^{\frac{w}{2}} \rho_s\, dx \qquad (1.9(d))$$

For the open structure in figure 1.2 J_z, ρ_s, J_t can be determined by considering the radiation energy associated with strip current source J.

Under these conditions the following field equations (Maxwell's equations) can be written, where time dependence jwt is assumed and a perfect dielectric is assumed.

$$\overline{\nabla} x \overline{E} = -j\omega\mu\overline{H} \qquad (1.10(a))$$

$$\nabla x \overline{H} = j\,\omega\,\epsilon\,\overline{E} + \overline{J} \qquad (1.10(b))$$

In a homogenous medium (in this case air) $\nabla \cdot B = o$

1.10(c))

and since any divergenceless vector is the curl of another vector.

$$\overline{B} = \nabla x \overline{A} \qquad (1.10(d))$$

where $\bar{A}$ is defined as the electric vector potential. Substituting (1.10(d)) into (1.10(a)) results in

$$\nabla x\,(\overline{E} + j\,\omega\,\overline{A}) = 0 \qquad (1.10(e))$$

and since any curl free vector is the gradient of a scalar

$$\overline{E} = -\,j\,\omega\,\overline{A} - \nabla\phi \qquad (1.10(f))$$

where Φ is defined as the electric scalar potential

then

$$\frac{\delta^2 \phi}{\delta x^2} + \frac{\delta^2 \phi}{\delta y^2} + (\kappa^2 - \gamma^2)\,\phi = 0 \qquad (1.11(a))$$

$$\frac{\delta^2 A}{\delta x^2} + \frac{\delta^2 A}{\delta y^2} + (\kappa^2 - \gamma^2)\,A = 0 \qquad (1.11(b))$$

from (1.10(a)) where κ is the wave number in air =

$$\omega \sqrt{\varepsilon_o \mu_o}$$

As shown in [1.5] $\bar{A}$ and Φ can be expressed as functions of J_z, J_t, and ρ_s as follows:

$$\phi = \frac{1}{2\pi \varepsilon_o} \int_{-\frac{w}{2}}^{\frac{w}{2}} G_e (x-x') \rho_s (x') dx' \qquad (1.12(a))$$

$$A_x = \frac{\mu_o}{2\pi} \int_{-\frac{w}{2}}^{\frac{w}{2}} G_h(x-x') J_t(x') dx'$$

$$+\frac{1}{j\omega} \cdot \frac{1}{2\pi\epsilon_o} \int_{-\frac{w}{2}}^{\frac{w}{2}} \frac{\delta}{\delta_x} M(x-x') \rho_s (x') dx' \qquad (1.12(b))$$

$$Ay = 0, \qquad (1.12(c))$$

since the zero thickness strip ensures that there are no y directed currents.

$$A_z = \frac{\mu_o}{2\pi} \int_{-\frac{w}{2}}^{\frac{w}{2}} G_h (x-x') J_z (x') dx'$$

$$-\frac{\gamma}{w} \cdot \frac{1}{2\pi \varepsilon_o} \int_{-\frac{w}{2}}^{\frac{w}{2}} M(x-x') \rho_s (x') dx' \qquad (1.12(d))$$

where G_e (x-x'), G_h (x-x'), M (x-x') are Green's functions associated with unit charge at point (x') and given by:

$$G_h (x) = 2 \int_o^\infty \tilde{G}_h (\alpha) \cos(\alpha x) d\alpha \qquad (1.13(a))$$

$$M(x) = 2\int_o^\infty \tilde{M}(\alpha)\cos(\alpha x)\,d\alpha \qquad (1.13(b))$$

$$G_e(x) = 2\int_o^\infty \tilde{G}_e(\alpha)\cos(\alpha x)\,d\alpha \qquad (1.13(c))$$

$$\tilde{G}_h(\alpha), \tilde{M}(\alpha), \tilde{G}_e(\alpha)$$

represent Fourier transforms and are given by

$$\tilde{G}_h(\alpha) = \frac{1}{\kappa_0 + \frac{1}{\mu_r}\kappa_1 \coth(\kappa_1 H)} \qquad (1.13(d))$$

$$\tilde{M}(\alpha) = \frac{(\varepsilon_r \mu_r - 1)\kappa^2}{(\mu_r \kappa_o + \kappa_1 \coth(\kappa_1 H))(\varepsilon_r \kappa_o + \kappa_1 \tanh(\kappa_1 H))\kappa_o} \qquad (1.13(e))$$

$$\tilde{G}e(\alpha) = \frac{1}{\kappa_1 + \varepsilon_r \kappa_o \coth(\kappa_1 H)} \cdot \frac{\kappa_1}{\kappa_o} \qquad (1.13(f))$$

$$= G_h(\alpha) - \frac{\alpha^2+\gamma^2}{\kappa^2}\tilde{M}(\alpha) \qquad (1.13(g))$$

where $\kappa_o = \sqrt{\alpha^2 + \gamma^2 - \kappa^2}$ $\qquad (1.13(h))$

$$\kappa_1 = \sqrt{\alpha^2 + \gamma^2 - \varepsilon_r \mu_r \kappa^2} \qquad (1.13(i))$$

Since the Green's functions must satisfy the boundary and interface conditions of the configuration under consideration these functions would be modified accordingly for closed microstrip.

From (1.10 (e)) and (1.12 (a))

$$E_x = j\omega A_x - \frac{\delta \phi}{\delta x}$$

$$\begin{aligned} &= -j\omega \frac{\mu_o}{2\pi} \int_{-\frac{w}{2}}^{\frac{w}{2}} G_h (x-x') J_t (x') \, dx' \\ &- \frac{1}{2\pi \varepsilon_o} \int_{-\frac{w}{2}}^{\frac{w}{2}} \frac{\delta}{\delta_x} [G_e (x-x') + M(x-x')] \rho_s (x') \, dx' \end{aligned} \qquad (1.14(a))$$

$$\begin{aligned} E_z &= -j\omega A_z + j\gamma \phi \\ &= -j\omega \frac{\mu_o}{2\pi} \int_{-\frac{w}{2}}^{\frac{w}{2}} G_h (x-x') J_z (x') \, dx' \\ &+ J\gamma \cdot \frac{1}{2\pi \epsilon_o} \int_{-\frac{w}{2}}^{\frac{w}{2}} [G_e (x-x') + M(x-x')] \rho_s (x') \, dx' \end{aligned} \qquad (1.14(b))$$

By applying the boundary conditions $E_x = 0$, $E_z = 0$ on the conducting strip and applying condition (1.8) ie. $J_t (\pm w/2) = 0$ ρ_s and J_z can be found.

The propagation constant γ can then be found by using equation (1.9) since both J_z and ρ_s are now known. The other dispersive

parameter of interest is the characteristic impedance.

Characteristic impedance can be expressed by three different relations:

(a) Voltage - Current ($|V/I|$)

(b) Power - Current ($2P/II^*$)

(c) Voltage - Power ($VV^*/2P$)

All the definitions give different values. Definitions (a) and (c) give an infinite number of values.

In this analysis the characteristic impedance Z_0 is defined as the ratio of the total electromagnetic power P flowing along the conducting strip to the square of the total longitudinal current J_z [1.5].

ie. $Z_0 = \frac{2P}{II^*}$ (1.15) where P is total average

power in the z direction

$$P = \frac{1}{2}\int \overline{E} x \overline{H}\, dS \qquad (1.16)$$

Applying equation (1.10) in (1.16) it can be shown [1.8] that

$P = P_{11} + P_{22} + P_{12}$ (1.17)

Where

$$P_{11} = \frac{1}{2} \int\int Z_{11}\,(x-x') \,.\, [J_z\,(x')\,J_z{*}\,(x) + J_t\,(x')\,J_t{*}\,(x)]\; dx'dx \qquad (1.18(a))$$

$$P_{22} = \frac{1}{2} \int\int Z_{22}\,(x-x')\;(\frac{\omega}{\gamma}\rho_s(x')\;(\frac{\omega}{\gamma}\rho_s{*}\,(x))\,dx'dx \qquad (1.18(b))$$

$$P_{12} = \int\int Z_{12}\,(x-x')\;J_z\,(x')\;(\frac{\omega}{\gamma}\rho_s{*}(x))\;dx'dx \qquad (1.18(c))$$

Z_{11} (x-x'), Z_{22} (x-x') and Z_{12} (x-x') are defined as distributed mutual impedances between points x and x' and the double

integration is over the strip

ie. $-\frac{w}{2}$ to $\frac{w}{2}$

$$Z_{11}(x-x')\,,\,Z_{22}(x-x')\,,\,Z_{12}(x-x')$$

are given by

$$Z_{11}\,(x) = 2\int_o^\infty \tilde{Z}_{11}\,(\alpha)\,\cos\,(\alpha\,x)\,d\alpha \qquad (1.19(a))$$

$$Z_{22}\,(x) = 2\int \tilde{Z}_{22}\,(\alpha)\,\cos\,(\alpha x)\;d\alpha \qquad (1.19(b))$$

$$Z_{12}(x) = 2\int \tilde{Z}_{12}\,(\alpha)\,\cos\,(\alpha x)\,d\,\alpha \qquad (1.19(c))$$

$$\tilde{Z}_{11}(\alpha) = -\frac{\omega}{2} \cdot \frac{\mu_o}{2\pi} \frac{\delta}{\delta\gamma} G_h(\alpha) \qquad (1.20(a))$$

$$\tilde{Z}_{22}(\alpha) = \frac{\omega}{2} \left(\frac{\gamma}{\omega}\right)^2 \cdot \frac{1}{2\pi\varepsilon_o} \frac{\delta}{\delta\gamma} [\tilde{G}_e(\alpha) + \tilde{M}(\alpha)] \qquad (1.20(b))$$

$$\tilde{Z}_{12}(\alpha) = \frac{\gamma}{\omega} \cdot \frac{1}{4\pi\varepsilon_o} [\tilde{G}_e(\alpha) + \tilde{M}(\alpha)] \qquad (1.20(c))$$

Letting

$$P_{11} = \frac{1}{2} Z_{11} II^*, P_{22} = \frac{1}{2} Z_{22} II^*, P_{12} = \frac{1}{2} Z_{12} II^* \text{ then } Z_0 = Z_{11} + Z_{22} + Z_{12} \qquad (1.21)$$

Therefore the dispersive characteristic impedance includes three terms, of these, as shown in [1.5], Z_{11}, Z_{22} are the most heavily frequency dependent. This frequency dependence increases as w/H decreases. The term Z_{12} is the TEM mode characteristic impedance.

To analyze bounded microstrip other techniques such as the variational method or the spectral domain method can be used. These techniques are discussed later in this chapter.

1.3 QUASI-TEM MODE (Quasi-Static Analysis)

The Quasi-TEM mode is a special case of the hybrid modes where $E_T >> E_L$ and $H_T >> H_L$ where E_T, H_T, E_L, H_L are transverse electric and magnetic and longitudinal electric and magnetic fields respectively. The accuracy of these assumptions increases as frequency decreases. In addition Eaves and Bolle [1.7] has shown that if the radiating modes are not considered then microstrip propagation can be considered to be approximately TEM. This approximation approaches the exact condition at as $\epsilon_r \to \infty$ or $\epsilon_r \to \epsilon_o$ or at frequencies where the dimensions of the structure represents a very small fraction of guide wavelength. Under any of these conditions the Quasi-TEM assumption can be made and quasi-static analysis techniques used. The approximation becomes increasingly inaccurate as frequency is increased.

Therefore instead of solving the time dependent wave equation

$$\nabla^2 \overline{E} - \mu \epsilon \frac{\delta^2 \overline{E}}{\delta t^2} = o$$

which is what is required for the full wave analysis, Poisson's equation

$$\nabla \overline{E} = \nabla^2 \phi = - \rho / \epsilon$$

or Laplace's equation

$$\nabla^2\phi = 0$$

When

$$\rho = o$$

are solved for the Quasi-TEM case.

$$\overline{E}, \phi$$

are electric field and scalar potential functions respectively. The propagation constant has to be determined in the full wave analysis, whereas in the quasi-TEM analysis the emphasis is on determining the static capacitance, from which the characteristic impedance is determined using equation (1.1). C_a and C_s in (1.1) are obtained by considering

$$C_r = \frac{Q_r}{V_o} \qquad (1.22)$$

where r= a,s and V_o is the known potential of the strip with respect to ground.

$$Q_r = \int_{-\frac{w}{2}}^{\frac{w}{2}} \rho_r(x')\, dx' \qquad (1.23)$$

where $\rho_r(x')$ is the unknown charge distribution on the conducting strip which has to be determined. The core problem in quasi-static analysis is therefore the determination or accurate definition of $\rho_r(x')$. Using Green's function potential allows the transformation from a differential equation in Φ to an integral equation where the unknown is the change density ρ_r. Considering figure 1.2 the scalar potential at a given point (x,y) is given by

$$\phi(x,y) = \int_{-\frac{w}{2}}^{\frac{w}{2}} \rho_r(x')\, G_r(x-x', y-H)\, dx' \qquad (1.24)$$

where $G_r(x-x', y-H)$ is the Green's function associated with a unit charge at $x=x'$, The Green's function by definition satisfies Poisson's equation

$$\nabla^2 G(x,y/x_o,y_o) = \frac{1}{\epsilon}\, \delta(x-x_o)\, .\, \delta(y-y_o) \qquad (1.25)$$

$G(x,y/x_o y_o)$ in addition must satisfy the boundary conditions of the system. The Green's function can also be found by applying Laplace's equation

$$\overline{\epsilon}_r\, \overline{\nabla}^2 \phi(x,y) = 0 \qquad (1.26)$$

where ϵ_r is a tensor which reduces to

$$\epsilon_r \nabla^2 \phi(x,y) = o \qquad (1.27)$$

for an isotropic dielectric.

Equation (1.24) can be rewritten

$$V_o = \int_{-\frac{W}{2}}^{\frac{W}{2}} \rho_r (x') G_r (x-x') dx' \qquad |x'| \leq \frac{W}{2}, |x| \leq \frac{W}{2} \qquad (1.28)$$

Equation (1.28) is applied to a coupled line configuration with strip spacing 'S' by applying voltages + V_o, + V_o and + V_o, - V_o to the two conducting strips to represent the even and odd mode conditions.

The double strip coupled configuration can then be reduced to single strip conditions by taking advantage of the symmetry axis at x=o. The applicable boundary conditions then include a magnetic wall at x=o for the even mode (Neuman conditions) and electric wall at x=o for the odd mode (Derichlet's conditions) in addition to the other physical boundary conditions.

The even and odd mode characteristic impedances are from (1.1)

$$Z_o(^{e}/_{o}) = \frac{1}{c\sqrt{C_a(^{e}/_{o})\, C_s(^{e}/_{o})}} \qquad (1.29)$$

$$and\ Q_r(^{e}/_{o}) = C_r(^{e}/_{o})\, V_o = C_r^{e}/_{o} \int_{\frac{s}{2}}^{\frac{s}{2}+W} \rho_r(^{e}/_{o})\ (x')\, dx' \qquad (1.30)$$

(e/o) designates even or odd mode. When V_0 = 1 and S is the spacing between the two conducting strips $\rho_r^{(e/o)}$ is found from (1.28) with V_0 = 1 and appropriate limits of integration.

$$ie. 1 = \int_{\frac{s}{2}}^{\frac{s}{2}+W} \rho_r(^{e}/_{o})\ (x')\ G_r(^{e}/_{o})\ (x-x')\, dx' \qquad (1.31)$$

where for the even and odd modes

$$G_r^{e} = G_r\ (x-x') + G_r\ (x+x'+S) \qquad (1.32)$$

$$G_r^{o} = G_r\ (x-x') - G_r\ (x+x'+S) \qquad (1.33)$$

reflecting the charge sources on each strip.

Crampagne et al [1.8] give a simple method of determining the Green's function of multidielectric microstrip configurations by using a transmission line equivalence. The method assumes infinitely thin conducting strips. Das and Pozar [1.13] have in addition presented a technique based on solving Maxwell's equation in the Fourier transform domain.

Once G_r is known the problem is reduced to determining $\rho_r(x)$ and ultimately C_r. Several numerical methods exist for determining $\rho_r(x)$, C_r, among these are:

(1) The Moments Method

(2) The Variational Method

(3) Spectral Domain Approach

1.4 METHOD OF MOMENTS

The method of moments [1.7] can be used to find the total charge per unit length and thus characteristic impedance and effective dielectric constant of two coupled microstrip lines in the following manner. The unknown charge function $\rho_r(x)$ on the strip can be expressed as a linear combination of known basis functions $f_n(x)$ such that

$$\rho_r^e(x) = \sum_{n=1}^{N} a_n^e \, f_n(x) \qquad 1.34(a)$$

$$\rho_r^o(x) = \sum_{n=1}^{N} a_n^o \, f_n(x) \qquad 1.34(b)$$

where the a_n are unknown weighting constants which are to be determined and n = 1, 2, 3----N .

The superscript 'o' and 'e' refer to odd and even modes.
In order to achieve accurate solutions for $\rho_r(x)$ with a low value of N, the basis functions must be chosen to closely reflect the physical conditions. For example the basis functions should ideally display a singularly at the edges of the strips. They must, in addition, be non-zero only on the conducting strip(s).

Substituting (1.34) into (1.31) we get

$$1 = \sum_{n=1}^{N} a_n^e \int_{\frac{s}{2}}^{\frac{s}{2}+W} G_r^e (x-x') f_n (x') dx' \qquad 1.35(a)$$

$$1 = \sum_{n=1}^{N} a_n^o \int_{\frac{s}{2}}^{\frac{s}{2}+W} G_r^o (x-x) f_n (x') dx' \qquad 1.35(b)$$

The inner product of (1.35) is then taken with another set of generally different known basis functions $g_m(x)$, m = 1,2,----N to get

$$\langle 1, g_m(x) \rangle = \beta_m^e = \sum_{n=1}^{N} a_n^e \cdot \langle g_m(x), \int_{\frac{s}{2}}^{\frac{s}{2}+W} G^e (x-x') f_n(x') dx' \rangle \qquad (136(a))$$

$$\langle 1, g_m(x) \rangle = \beta_m^o = \sum_{n=1}^{N} a_n^o \cdot \langle g_m(x), \int_{\frac{s}{2}}^{\frac{s}{2}+W} G^o (x-x') f_n(x') dx' \rangle \qquad 1.36(b)$$

the inner product being defined as

$$\langle g_m (x), f_n(x) \rangle = \int_{\frac{s}{2}}^{\frac{s}{2}+W} g_n(x) f_n(x) dx \qquad (1.37)$$

(if f_n (x) = g_m (x) we have Gellerkin's method)

Equation (1.36) is a set of linear equations of size N X N and can be expressed in Matrix form

$$[\beta_m] = [g_{mn}]\ [a_n] \qquad (1.38)$$

ie. the a_n are given by $[a_n] = [g_{mn}]^{-1}\ [\beta_m]$ (1.39)

$$\text{where } g^e_{mn} = \langle g_m(x)\ ,\ \int_{\frac{s}{2}}^{\frac{s}{2}+W} G^e\ (x-x')\ f_n\ (x')\ dx' \rangle \qquad (1.40)$$

$$\text{and} \quad g^o_{mn} = \langle\ g_m(x)\ ,\ \int_{\frac{s}{2}}^{\frac{s}{2}+W} G^o\ (x-x')\ f_n\ (x')\ dx' \rangle \qquad (1.41)$$

Substituting (1.40), (1.41) into (1.23) we get

$$Q^e_r = \sum_{n=1}^{N}\ a^e_n \int_{\frac{s}{2}}^{\frac{s}{2}+W} f_n\ (x)\ dx = C^e_r \qquad (1.42(a))$$

$$Q^o_r = \sum_{n=1}^{N}\ a^o_n \int_{\frac{s}{2}}^{\frac{s}{2}+W} f_n\ (x)\ dx = C^o_r \qquad (1.42(b))$$

for V equals unity.

For the method to be applicable the appropriate Green's function for the structure under consideration must of course be found.

1.5 THE VARIATIONAL METHOD

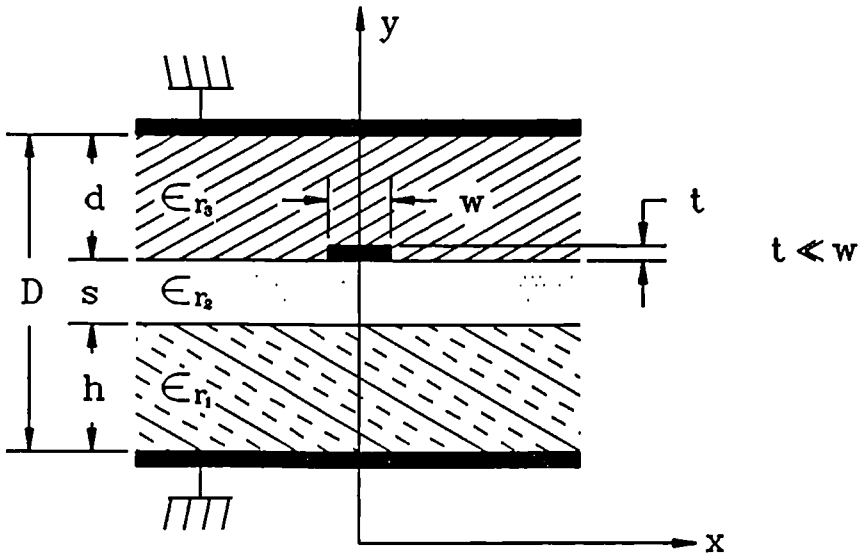

Figure (1.4) SHIELDED MICROSTRIP

So far open microstrip with t→0 has been considered, figure 1.4 shows, a microstrip structure with lid and a layered dielectric medium ϵ_{r1}, ϵ_{r2}, ϵ_{r3}. In this case o ≠ t << w. When s=o, ϵ_{r3}=1 we have regular microstrip.

The variational method of determining distributed capacitance C_r based on the approach given in [1.11] begins with Poisson's equation in two dimensions linking the scalar potential Φ (x,y) and the charge density function ρ(x,y)

$$\nabla^2\phi(x,y) = -\frac{1}{\epsilon_o\epsilon_r}\rho(x,y) \qquad (1.42)$$

where $\rho(x,y)$ is represented by the Dirac delta function ie.

$$\rho(x,y) = \delta(y-h-s-p) f(x) \qquad (1.43)$$

The spacing p between the strip and dielectric being introduced to equalize the number of variable and equations later [1.11]. One of the space variables in (1.42) is eliminated by taking the Fourier transform of all functions. ie.

$$ie.\ \tilde{f}(\beta) = \int_{-\infty}^{\infty} \tilde{f}(x)\, e^{j\beta x}\, dx \qquad (1.44)$$

where $\tilde{f}(\beta)$ denotes the Fourier transform with variable β. Taking the inverse transform of (1.44) we get

$$f(x) = \frac{1}{2\pi} \int_{-\infty}^{\infty} \tilde{f}(\beta)\, e^{-j\beta x}\, d\beta \qquad (1.45)$$

Therefore (1.42) becomes

$$\frac{d^2}{dy^2}\tilde{\phi}(\beta,y) - \beta^2 \phi(\beta,y) = o, \quad (y \neq h+s+p) \qquad (1.46)$$

The general solution of (1.46) is of the form

$$\tilde{\phi}_1(\beta,y) = A_n \sinh \beta y \qquad (1.47(a))$$

$$\tilde{\Phi}_2(\beta, y) = B_n \exp(\beta y) + C_n \exp(-\beta y) \qquad (1.47(b))$$

$$\tilde{\Phi}_3(\beta, y) = D_n \sinh \beta (D-y) \qquad (1.47(c))$$

where A_n, B_n, C_n, D_n are constants to be solved. The Φ_1, Φ_3 terms are expressed as hyperbolic functions to emphasize the fact that $\Phi_1(\beta,0)$, $\Phi_3(\beta,D) = 0$ on the ground planes. When $D \to \infty$ Φ_3 takes the form $D_n \exp(-\beta y)$. The general boundary conditions for the structure are then established in the Fourier transform domain

ie.
$$\tilde{\Phi}_1(\beta,0) = 0 \qquad (1.48(a))$$

$$\tilde{\Phi}_3(\beta,D) = 0 \qquad (1.48(b))$$

$$\tilde{\Phi}(\beta,h) = \tilde{\Phi}_2(\beta,h) \qquad (1.48(c))$$

$$\epsilon_{r1} \frac{d}{dy}(\tilde{\Phi}_1(\beta,h)) = \epsilon_{r2} \frac{d}{dy}(\tilde{\Phi}_2(\beta,h)) \qquad (1.48(d))$$

$$\tilde{\Phi}_2(\beta, h+s) = \tilde{\Phi}_o(\beta, h+s) \qquad (.148(e))$$

$$\epsilon_{r2} \frac{d}{dy}(\tilde{\Phi}_2(\beta, h+s) = \frac{d}{dy}(\tilde{\Phi}_o(\beta, h+s) \qquad (1.48(f))$$

$\tilde{\Phi}_o$ is associated with the air spacing p.

$$\tilde{\Phi}_o(\beta, h+s+p) = \tilde{\Phi}_3(\beta, h+s+p) \qquad (1.48(g))$$

$$\frac{d}{dy}\left(\tilde{\Phi}_o(\beta, h+s+p)\right) = \epsilon_{r3}\frac{d}{dy}\left(\tilde{\Phi}_3(\beta, h+s+p)\right) \qquad (1.48(h))$$

in the charge free region.

where ϵr_1, ϵr_2, 1, ϵr_3 are the relative dielectric constants of the layers and

$$\tilde{\Phi}_1(\beta, y), \tilde{\Phi}_2(\beta, y), \tilde{\Phi}_o(\beta, y)\ \tilde{\Phi}_3(\beta, y)$$

are Fourier transforms of the potential functions in each dielectric layer. By substituting (1.48) into (1.47) the solution

$$\tilde{\Phi}(\beta, h+s) = \frac{1}{\epsilon_o}\tilde{f}(\beta)\ \tilde{g}(\beta) \qquad (1.49)$$

is achieved [1.11] where

$$\tilde{g}(\beta) = [\epsilon_{r1}\coth(|\beta|h) + \epsilon_{r2}\coth(|\beta|s)] \div$$
$$[|\beta|\{\epsilon_{r1}\coth(|\beta|h))\ [\epsilon_{r3}\coth(|\beta|d)$$
$$+ \epsilon_{r2}\coth(|\beta|s) + \epsilon_{r2}[\epsilon_{r2} + \epsilon_{r3}\coth(|\beta|s)]\}]]$$

The variational expression of C_r is then taken

$$\frac{1}{C_r} = \frac{1}{Q^2}\int_{-\infty}^{\infty} f(x)\,\phi(x, h+s)\,dx \qquad (1.50)$$

where Q is total charge given by

$$Q = \int_{-\infty}^{\infty} f(x)\, dx = \int_{-\frac{w}{2}}^{\frac{w}{2}} f(x)\, dx \qquad (1.51)$$

Rather than taking the inverse transform of (1.49) we use the integral form of Parseval's equation [1.12] which is generally

$$\int_{-\infty}^{\infty} f(x)\, g^*(x)\, dx = \frac{1}{2\pi} \int_{-\infty}^{\infty} \tilde{f}(k)\, \tilde{g}(k)\, dk$$

to get

$$\frac{1}{C_r} = \frac{1}{2\pi Q^2} \int_{-\infty}^{\infty} \tilde{f}(\beta)\, \tilde{\Phi}(\beta, h+s)\, d\beta \qquad (1.51(a))$$

for t = o

If the thickness of the strip is taken to be t ≠ 0

$$\frac{1}{C_r} = \frac{1}{\pi Q^2 \epsilon_o} \int_{o}^{\infty} [\tilde{f}(\beta)]^2\, \tilde{g}(\beta)\, \tilde{h}(\beta)\, d\beta$$

where

$$\tilde{h}(\beta) = \frac{1}{2} \left\{ 1 + \frac{\sin h(|\beta| d - |\beta| t)}{\sin h(|\beta| d)} \right\} \qquad (1.51(b))$$

C_r is then evaluated by choosing an $f(x)$ trial function which closely matches the physical charge conditions and taking the fourier transform to get $\tilde{f}(\beta)$. (1.51) is a stationery formula and the value of C_r is not very dependent on the choice of $f(x)$.

The capacitance calculated by this method is lower bound ie. it is always less than the actual value, therefore one criteria of choosing $f(x)$ is to maximise C_r. Although this method provides a fairly accurate value of C_r, generally, the trial function $f(x)$ may not always be reliable depending on the configuration, therefore an upper bound of C_r should be determined to contain the margin of error. Araki and Naito [1.12] have presented a method for determining the upper bound of C_r in terms of a potential trial function V(x) at the interface containing the strip, rather than a charge function.

This method also uses the variational technique in Fourier Transform domain.

The variational expression is then

$$C_r = \frac{\epsilon_o}{2\pi} \frac{1}{V^2} \int_{-\infty}^{\infty} |\tilde{V}(\beta)|^2 |\beta| . (1 + \epsilon_r Coth(\beta) H) \, d\beta \qquad (1.52)$$

1.6 THE SPECTRAL DOMAIN APPROACH

The spectral domain approach is generally an application of Fourier transforms to the solution of boundary value problems such as coupled microstrip. The method which reduces partial differential equations encountered in the space domain to ordinary equations in the transform domain is applicable to the determination of both

static and frequency dependent parameters of planar circuits. The main difference between the spectral domain approach and other moments methods is the application of Gellerkin's method in the transform domain ie. the transform of the set of expansion basis functions are the same as the transforms of the set of testing functions. Both full wave and quasi-static analysis are possible with this method by recognising that the partial differential equation considered in the approach for full wave analysis is the wave equation, and that for static analysis Laplace or Poisson's equation is considered.

The spectral domain approach is well suited for open or closed structures including multidielectric interfaces such as overlay couplers with conductors at several of these interfaces. In general the method has been applied under the following conditions:

(1) The conductors are assumed to have ideal conductivity σ

(2) Infinitesimal thickness t

(3) No discontinuities parallel to the dielectric interface

(4) Lossless dielectrics

As pointed out in [1.14] limitations (1) and (2) would cause the method to be in applicable to such important multilevel structures as MMICs. In such cases the finite strip thickness is treated by considering the thick conducting strip as a separate layer and dielectric loss (or radiation loss) is treated as a perturbation after the lossless calculations are completed. The spectral domain

method is used later in this thesis to analyze several complex microstrip coupled structures.

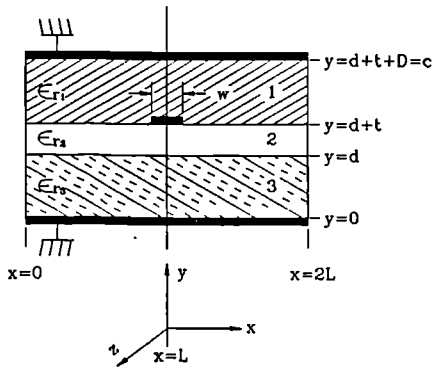

Figure (1.5) Shielded Microstrip Cross-Section

Consider figure 1.5 which has dielectric regions 1, 2, 3 with scalar effective dielectric constant E_{r1}, E_{r2}, E_{r3} and interfaces at y=d and y=d+t. Both the strip of width w and the walls at y=0 and y=d + t + D = C are assumed to be perfect conductors.

To demonstrate the general spectral domain approach to the solution of microstrip structures the approach of Bhat and Koul [1.4] is followed by defining the Hertz potential functions

$$\phi^e(x,y,z) \text{ and } \phi^h(x,y,z)$$

as follows:

Starting with Maxwell's equations in a source free region

$$\overline{\nabla} x \overline{E} = -\frac{\delta \overline{B}}{\delta t} \qquad (1.53(a))$$

$$\overline{\nabla} x \overline{H} = \frac{\delta D}{\delta t} \qquad (1.53(b))$$

$$\nabla . \overline{D} = 0 \qquad (1.53(c))$$

$$\nabla . \overline{B} = 0 \qquad (1.53(d))$$

$$\nabla . J = \frac{-\delta \rho}{\delta t} \qquad (1.53(e))$$

(1.53(d)) implies, as stated earlier, that

$$\overline{B} = \nabla x \overline{A}^e \qquad (1.54)$$

where $\bar{A}^e$ is the electric vector potential. From (1.53(a)) and (1.54)

$$\nabla x (\overline{E} + \frac{\delta \overline{A}^e}{\delta t}) = 0 \qquad (1.55)$$

as proven in (1.10(e)) which implies (1.10(f)) that

$$\overline{E} = -\nabla \Phi^e - \frac{\delta \overline{A}^e}{\delta t} \qquad (1.56)$$

where Φ^e is electric scalar potential.

Substituting (1.54) and (1.56) into (1.53(b)) and using the identities

$$\nabla x (\nabla x \bar{A}) = \nabla(\nabla . \bar{A}) - \nabla^2 \bar{A}$$

$$\bar{D} = \epsilon \bar{E}$$

$$B = \mu \bar{H}$$

$$\nabla x \nabla \bar{A}^e = \mu\epsilon \frac{\delta}{\delta t} (-\nabla\Phi^e - \frac{\delta \bar{A}^e}{\delta t})$$

or

$$-\nabla^2 \bar{A}^e + \mu\epsilon \frac{\delta^2 \bar{A}^e}{\delta t^2} + \nabla\left[(\nabla . \bar{A}^e) + \mu\epsilon \frac{\delta \Phi^e}{\delta t}\right] = 0 \qquad (1.57)$$

Using the Lorentz condition [1.4]

$$\nabla . \bar{A}^e + \mu\epsilon \frac{\delta \Phi^e}{\delta t} = 0 \qquad (1.58)$$

(1.57) becomes

$$\nabla^2 \bar{A}^e - \mu\epsilon \frac{\delta^2 \bar{A}^e}{\delta t^2} = 0 \qquad (1.59)$$

From (1.53(c)) $\bar{D}$ can be expressed as

$$\overline{D} = -\nabla x \overline{A}^h \qquad (1.60)$$

Where $\bar{A}^h$ is magnetic vector potential

Substituting (1.60) into (1.53(b)) we get

$$\overline{\nabla} x \overline{H} + \frac{\delta}{\delta t} (\nabla x \overline{A}^h) = 0$$

ie.

$$\nabla x (H + \frac{\delta}{\delta t} \overline{A}^h) = 0$$

and by definition

$$\overline{H} + \frac{\delta}{\delta t} \overline{A}^h = -\nabla \Phi^h$$

$$\overline{H} = -\frac{\delta}{\delta t} \overline{A}^h - \nabla \Phi^h \qquad (1.61)$$

where Φ^h is magnetic scalar potential. By substituting (1.60) and (1.61) into (1.53(a)) we get

$$\nabla^2 \overline{A}^h - \mu\epsilon \frac{\delta^2 \overline{A}^h}{\delta t^2} - \nabla\left[(\nabla . \overline{A}^h) + \mu\epsilon \frac{\delta \Phi^h}{\delta t}\right] = 0 \qquad (1.62)$$

and again imposing the Lorentz condition

$$\nabla . \overline{A}^h + \mu\epsilon \frac{\delta \phi^h}{\delta t} = 0 \qquad (1.63)$$

(1.62) becomes

$$\nabla^2 A^h - \mu\epsilon \frac{\delta^2 \overline{A}^h}{\delta t^2} = 0 \qquad (1.64)$$

Setting

$$A^e = \mu\epsilon \frac{\delta \overline{\pi}^e}{\delta t} \qquad (1.65(a))$$

and

$$\overline{A}^h = \mu\epsilon \frac{\delta \overline{\pi}^h}{\delta t} \qquad (1.65(b))$$

where

$\overline{\pi}^e$, $\overline{\pi}^h$ are Hertzian vector potentials

and combining (1.65(a)) with (1.58) we get

$$\mu\epsilon \frac{\delta}{\delta t} \nabla . \overline{\pi}^e + \mu\epsilon \frac{\delta \Phi^e}{\delta t} = 0 \qquad (1.66(a))$$

ie.

$$\Phi^e = - \nabla . \overline{\pi}^e \qquad (1.66(b))$$

Using (1.66(b)) and (1.56) we arrive at

$$\overline{E} = -\nabla(\nabla \cdot \overline{\pi}^e) - \frac{\delta}{\delta t}\mu\epsilon\frac{\delta\overline{\pi}^e}{\delta t} \qquad (1.67(a))$$

and using (1.54) and (1.65(a)) we get

$$\overline{B} = \nabla x\,\mu\epsilon\frac{\delta\overline{\pi}^e}{\delta t} \qquad (1.67(b))$$

Similarly using (1.65(b)) in (1.63) we get

$$\Phi^h = -\nabla \cdot \overline{\pi}^h \qquad (1.68)$$

and using (1.68) with (1.65(b)) in (1.61) we get

$$\overline{H} = -\frac{\delta}{\delta t}\mu\epsilon\frac{\delta\overline{\pi}^h}{\delta t} + \nabla(\nabla \cdot \overline{\pi}^h)$$

$$\overline{H} = \nabla(\nabla \cdot \overline{\pi}^h) - \mu\epsilon\frac{\delta^2\overline{\pi}^h}{\delta t^2} \qquad (1.69)$$

and using (1.68) with (1.65(b)) we get

$$\overline{D} = -\mu\epsilon\frac{\delta}{\delta t}\nabla x\,\overline{\pi}^h \qquad (1.70)$$

if time dependence exp jωt is assumed and $k^2 = \omega^2\,\mu\epsilon$ then following [1.4] from (1.67(a)), (1.67(b)), (1.70) and (1.69)

$$\overline{E}^e = -\nabla(\nabla \cdot \overline{\pi}^e) - k^2\overline{\pi}^e \qquad (1.71(a))$$

$$\overline{H}^e = j\omega\epsilon\overline{\nabla} x \overline{\pi}^e \qquad (1.71(b))$$

$$\overline{E}^h = -j\omega\mu\nabla x \pi^h \qquad (1.71(c))$$

$$\overline{H}^h = \overline{\nabla}(\overline{\nabla} . \overline{\pi}^h) - k^2 \overline{\pi}^h \qquad (1.71(d))$$

where

$$\overline{E}^e , \overline{H}^e , \overline{E}^h , \overline{H}^h$$

are electric and magnetic field quantities associated with the vector potentials

$$\overline{\pi}^e , \overline{\pi}^h$$

and

$$\nabla^2 \overline{\pi}^e + k^2 \overline{\pi}^e = 0 \qquad (1.72(a))$$

$$\nabla^2 \overline{\pi}^h + k^2 \pi^h = 0 \qquad (1.72(b))$$

since

$$\overline{\pi}^h, \overline{\pi}^e$$

satisfy the general wave equation

$$\nabla^2 \overline{\pi}^i - \mu\epsilon \frac{\delta^2 \overline{\pi}^i}{\delta t^2} = 0$$

where i = e,h

Bhat and Koul [3.4] express the Hertz scalar potential

$$\overline{\pi}^e, \overline{\pi}^h$$

in the following terms

$$\overline{\pi}^e = \overline{z}\,\phi^e(x,y,z) \text{ for E waves (TM)} \qquad (1.73(a))$$

$$\overline{\pi}^h = \overline{z}\,\phi^h(x,y,z) \text{ for H waves (TE)} \qquad (1.73(b))$$

where a superposition of TE to Z and TM to Z modes are considered to represent the hybrid modes associated with the structure in figure (1.5). $\overline{Z}$ is a unit vector in the Z direction. Φ^e (x,y,z), Φ^h (x,y,z) are defined as Hertz scalar potential functions.

Then the wave equations (1.72) can be rewritten

$$\nabla^2 \phi^e + k^2 \phi^e = 0 \qquad (1.74(a))$$

$$\nabla^2 \phi^h + k^2 \phi^h = 0 \qquad (1.74(b))$$

and the set of equations (1.71) can be rewritten

$$\overline{E}^e = (\nabla \frac{\delta}{\delta z} + k^2 \overline{z}) \phi^e \qquad (1.75(a))$$

$$\overline{H}^e = j\omega\epsilon \nabla x \phi^e \overline{z} \qquad (1.75(b))$$

$$\overline{E}^h = -j\omega\mu \nabla x \phi^h \overline{z} \qquad (1.75(c))$$

$$\overline{H}^h = (\nabla \frac{\delta}{\delta z} + k^2 \overline{z}) \phi^h \qquad (1.75(d))$$

Equation (1.75) proves that the transverse field components can be deduced from the longitudinal component.

Equation (1.75) is then expanded

$$\overline{E}^e = \overline{x} \frac{\delta^2 \phi^e}{\delta x \delta z} + \overline{y} \frac{\delta^2 \phi^e}{\delta y \delta z} + \overline{Z} \left(\frac{\delta^2 \phi^e}{\delta z^2} + k^2 \phi^e \right) \qquad (1.76(a))$$

$$\overline{H}^e = j\omega\epsilon (\overline{x} \frac{\delta \phi^e}{\delta y} - \overline{y} \frac{\delta \phi^e}{\delta x} \qquad (1.76(b))$$

$$\bar{E}^h = -j\omega\mu \left(\bar{x}\frac{\delta\phi^h}{\delta y} - \bar{y}\frac{\delta\phi^h}{\delta x}\right) \qquad (1.76(c))$$

$$\bar{H}^h = \bar{x}\frac{\delta^2\phi^h}{\delta x\delta z} + \bar{y}\frac{\delta^2\phi^h}{\delta y\delta z} + \bar{Z}\left(\frac{\delta^2\phi^h}{\delta z^2} + k^2\phi^h\right) \qquad (1.76(d))$$

The total $\bar{E}$ and $\bar{H}$ field are given by the following

$$\bar{E} = \bar{E}^e + \bar{E}^h \qquad (1.77(a)) \quad [1.4]$$

$$\bar{H} = \bar{H}^e + \bar{H}^h \qquad (1.77(b)) \quad [1.4]$$

Now referring to figure (1.5) and assuming that the structure supports a hybrid mode which can be represented as a superposition of TM to Z and TE to Z modes, then the electric and magnetic fields in the structure can be expressed as follows: where i = 1, 2, 3 refers to the different dielectric regions, from equations (1.76) and (1.77) and assuming that the relative permeability of all dielectrics is unity. Assume also that the Z dependence is exp $j\beta Z$ (ie. propagation in the (-Z) direction).

From (1.76(a))

$$E_{zi}(x,y,z) = \left(\frac{\delta^2}{\delta z^2} + k^2\right)\phi_i^e(x,y,z) \qquad (1.78(a))$$

From (1.76(d))

$$H_{zi}(x,y,z) = \left(\frac{\delta^2}{\delta z^2} + k^2\right)\phi_i^h(x,y,z) \qquad (1.78(b))$$

From (1.76(a)) and (1.76(c))

$$E_{xi}(x,y,z) = \frac{\delta^2}{\delta x \delta z}\phi_i^e(x,y,z) - j\omega\mu o\frac{\delta}{\delta y}\phi_i^h(x,y,z) \qquad (1.78(c))$$

From (1.76(b)) and (1.76(d))

$$H_{xi}(x,y,z) = j\omega\epsilon_i\frac{\delta\phi_i^e}{\delta y}(x,y,z) + \frac{\delta^2}{\delta x \delta z}\phi_i^h(x,y,z) \qquad (1.78(d))$$

From (1.76(a)) and (1.76(c))

$$E_{yi}(x,y,z) = \frac{\delta^2}{\delta y \delta z}\phi_i^e(x,y,z) + j\omega\mu o\frac{\delta\phi_i^h}{\delta x}(x,y,z) \qquad (1.78(e))$$

From (1.76(b)) and (1.76(d))

$$H_{yi}(x,y,z) = -j\omega\epsilon_i\frac{\delta\phi_i^e}{\delta x}(x,y,z) + \frac{d^2}{\delta y \delta z}\phi_i^h \qquad (1.78(f))$$

The simultaneous TM to Z and TE to Z condition results in $H_{zi} = 0$, $E_{zi} = 0$, therefore

$$(\nabla^2 + k_i^2)\phi_i^e = 0 \qquad (1.79(a)) \qquad \text{from } 1.78(a),(b)$$

$$(\nabla^2 + k_i^2)\ \phi_i^h = 0 \qquad (1.79(b))$$

Equation (1.79) is Helmholtz's equation.

Assuming

$$\epsilon_1 = \epsilon_o \epsilon_{r1} = \epsilon_o \qquad (1.80(a))$$

$$\epsilon_2 = \epsilon_o \epsilon_{r2} \qquad (1.80(b))$$

$$\epsilon_3 = \epsilon_o \epsilon_{r3} \qquad (1.80(c))$$

and letting the fourier transforms of the potential functions be

$$\tilde{\phi}_i^{e,h}(\alpha_n, y) = \int_{-L}^{L} \phi_i^{e,h}(x, y) \exp(j\alpha_n x)\, dx \qquad (1.81)$$

where α_n is the transform variable and

$$\alpha_n = \frac{(2n-1)\,\pi}{2L} \qquad (1.82(a))$$

when Φ_i^e is even in x, Φ_i^h is odd in x

$$\alpha_n = \frac{2n\pi}{2L} \qquad (1.82(b))$$

when Φ_i^e is odd in x and Φ_i^h is even in x. For the present case since only the even mode should be considered we use equation

(1.82(a)). For two coupled lines where both odd and even mode exists we would use both (1.82(a)) and (1.82(b)).

Then taking the fourier transforms of equation (1.78) and taking into account the Z dependence we get

$$\tilde{E}_{zi}(\alpha_n, y) = (k_i^2 - \beta^2)\,\tilde{\phi}_i^e(\alpha_n, y) \qquad (1.83(a))$$

$$\tilde{H}_{zi}(\alpha_n, y) = (k_i^2 - \beta^2)\,\tilde{\phi}_i^h(\alpha_n, y) \qquad (1.83(b))$$

$$\tilde{E}_{xi}(\alpha_n, y) = -\alpha_n \beta \tilde{\phi}_i^e(\alpha_n, y) - j\omega\mu_o \frac{d}{dy}\tilde{\phi}_i^h(\alpha_n, y) \qquad (1.83(c))$$

$$\tilde{H}_{xi}(\alpha_n, y) = j\omega\epsilon_i \frac{d}{dy}\tilde{\phi}_i^e(\alpha_n, y) - \alpha_n \beta \tilde{\phi}_i^h(\alpha_n, y) \qquad (1.83(d))$$

$$\tilde{E}_{yi}(\alpha_n, y) = j\beta \frac{d}{dy}\tilde{\phi}_i^e(\alpha_n, y) - \omega\mu_o \alpha_n \tilde{\phi}_i^h(\alpha_n, y) \qquad (1.83(e))$$

$$\tilde{H}_{yi}(\alpha_n, y) = \omega\epsilon_i \alpha_n \tilde{\phi}_i^e(\alpha_n, y) + j\beta \frac{d}{dy}\phi_i^h(\alpha_n, y) \qquad (1.83(f))$$

and

$$\left(\frac{d^2}{dy^2} - \gamma_i^2\right)\tilde{\phi}_i^{e,h}(\alpha_n, y) = 0 \qquad (1.84)$$

from (1.79), where

$$\gamma_i^2 = \alpha_n^2 + \beta^2 - k_i^2 \qquad (1.85)$$

Equations (1.84), (1.83(c)), (1.83(d)), (1.83(e)), (1.83(f)) are proven by taking the inverse transforms.

We then establish solutions for (1.84) in the different regions i.

Taking into account the boundary conditions at y = 0, y = c the general solutions of (1.84) are.

IN REGION 1

$$\tilde{\phi}_i^e(\alpha_n, y) = A^e \alpha_n \sinh \gamma_i (c-y) \qquad (1.86(a))$$

$$\tilde{\phi}_1^h(\alpha_n, y) = A^h(\alpha_n) \cosh \gamma_1 (c-y) \qquad (1.86(b))$$

IN REGION 2

$$\tilde{\phi}_2^e(\alpha_n, y) = B^e(\alpha_n) \sinh \gamma_2 (y-d) + C^e(\alpha_n) \cosh \gamma_2 (y-d) \qquad (1.87(a))$$

$$\tilde{\phi}_2^h(\alpha_n, y) = B^h(\alpha_n) \cosh \gamma_2 (y-d) + c^h(\alpha_n) \sinh \gamma_2 (y-d) \qquad (1.87(b))$$

IN REGION 3

$$\phi_3^e(\alpha_n, y) = D^e(\alpha_n) \sinh \gamma_3 y \qquad (1.88(a))$$

$$\phi_3^h(\alpha_n, y) = D^h(\alpha_n)\cosh\gamma_3 y \qquad (1.88(b))$$

where $A^{e/h}$, $B^{e/h}$, $C^{e/h}$, $D^{e/h}$ are unknown constants which are to be determined.

Using (1.86), (1.87) and (1.88) in (1.83) results in the following set of equations.

$$\tilde{E}_{x1} = -\alpha_n\beta A^e\sinh\gamma_1(c-y) + j\gamma_1\omega\mu_o A^h\sinh\gamma_1(c-y) \qquad (1.89(a))$$

$$\tilde{E}_{x2} = -\alpha_n\beta\left[B^e\sinh\gamma_2(y-d) + C^e\cosh\gamma_2(y-d)\right] - j\omega\mu_o\gamma_2\left[B^h\sinh\gamma_2(y-d) + C^h\cosh\gamma_2(y-d)\right] \qquad (1.89(b))$$

$$\tilde{E}_{x3} = -\alpha_n\beta D^e\sinh\gamma_3 y - j\omega\mu_o\gamma_3 D^h\sinh\gamma_3 y \qquad (1.89(c))$$

$$\tilde{E}_{y1} = -j\beta\gamma_1 A^e\cosh\gamma_1(c-y) - \omega\mu_o\alpha_n A^h\cosh\gamma_1(c-y) \qquad (1.89(d))$$

$$\tilde{E}_{y2} = j\beta\gamma_2\left[B^e\cosh\gamma_2(y-d) + C^e\sinh\gamma_2(y-d)\right] - \omega\mu_o\alpha_n\left[B^h\cosh\gamma_2(y-d) + C^h\sinh\gamma_2(y-d)\right] \qquad (1.89(f))$$

$$\tilde{E}_{y3} = j\beta\gamma_3 D^e\cosh y - \omega\mu_o\alpha_n D^h\cosh\gamma_3 y \qquad (1.89(g))$$

$$\tilde{E}_{z1} = (k_1^2 - \beta^2)\, A^e \sinh \gamma_1 (c-y)$$
$$\tilde{E}_{z2} = (k_2^2 - \beta^2) \left[\beta^e \sinh \gamma_2 (y-d) + C^e \cosh \gamma_2 (y-d)\right] \qquad (1.89(h))$$

$$\tilde{E}_{z3} = (k_3^2 - \beta^2)\, D^e \sinh \gamma_3 y \qquad (1.89(i))$$

$$\tilde{H}_{x1} = -j\omega\epsilon_1 A^e \gamma_1 \cosh (c-y) - \alpha_n \beta A^h \cosh \gamma_1 (c-y) \qquad (1.89(j))$$

$$\tilde{H}_{x2} = j\omega\epsilon_2 \gamma_2 \left[B^e \cosh \gamma_2 (y-d) + C^e \sinh (y-d)\right]$$
$$- \alpha\beta \left[B^h \cosh \gamma_2 (y-d) + C^h \sinh \gamma_2 (y-d)\right] \qquad (1.89(k))$$

$$\tilde{H}_{x3} = j\omega\epsilon_3 \gamma_3 \left[D^e \cosh \gamma_3 y\right] - \alpha\beta D^h \cosh \gamma_3 y \qquad (1.89(l))$$

$$\tilde{H}_{y1} = \omega\epsilon_1 \alpha_n A^e \sinh \gamma_1 (c-y) - j\beta\gamma_1 \sinh \gamma_1 (c-y) \qquad (1.89(m))$$

$$\tilde{H}_{y2} = \omega\epsilon_2 \alpha_n \left[B^e \sinh \gamma_2 (y-d) + C^e \cosh \gamma_2 (y-d)\right]$$
$$+ j\beta\gamma_2 \left[B^h \sinh \gamma_2 (y-d) + C^h \cosh \gamma_2 (y-d)\right] \qquad (1.89(n))$$

$$\tilde{H}_{y3} = \omega\epsilon_3 \alpha_n D^e \sinh \gamma_3 y + j\beta\gamma_3 D^h \sinh \gamma_3 y \qquad (1.89(o))$$

$$\tilde{H}_{z1} = (k_1^2 - \beta^2)\, A^h \cosh \gamma_1 (c-y) \qquad (1.89(p))$$

$$\tilde{H}_{z2} = (k_2^2 - \beta^2) \left[B^h \cosh \gamma_2 (y-d) + C^h \sinh \gamma_2 (y-d) \right] \qquad (1.89(q))$$

$$\tilde{H}_{z3} = (k_3^2 - \beta^2)\, D^h \cosh \gamma_3 y \qquad (1.89(r))$$

In order to solve for the unknowns $A^{e/h}$, $B^{e/h}$, $C^{e/h}$, $D^{e/h}$ the following boundary conditions are applied at y = d + t.

$$\tilde{E}_{x1} = \tilde{E}_{x2} \qquad \text{for all x}$$

$$\tilde{E}_{z1} = \tilde{E}_{z2} \qquad \text{for all x}$$

$$\tilde{H}_{x2} - \tilde{H}_{x1} = \tilde{J}_z\,, \qquad -\frac{W}{2} \le x \le \frac{W}{2} \quad \text{on the strip}$$

$$= 0\,, \qquad |x| > \frac{W}{2}$$

$$\tilde{H}_{z2} - \tilde{H}_{z1} = -\tilde{J}_x \qquad -\frac{W}{2} \le x \le \frac{W}{2} \quad \text{on the strip}$$

$$= 0 \qquad |x| > \frac{W}{2}$$

where $J_z(x)$ and $J_x(x)$ are the unknown Z-directed and transverse current densities respectively on the strip.

(Note: $J_x(x) = J_t(x)$ in section 1.3).

at y = d

$$\tilde{E}_{x2} = \tilde{E}_{x3} \quad \text{for all x}$$

$$\tilde{E}_{z2} = \tilde{E}_{z3} \quad \text{for all x}$$

$$\tilde{H}_{x2} = \tilde{H}_{x3} \quad \text{for all x(no current on the dielectric interface)}$$

$$\tilde{H}_{z2} = \tilde{H}_{z3} \quad \text{for all x(no current on the dielectric interface)}$$

After the $A^{e/h}$, $B^{e/h}$, $C^{e/h}$, $D^{e/h}$ are found, finally the general coupled equations

$$\tilde{E}_z(\alpha, d+t) = \tilde{Z}_{zz}(\alpha,\beta)\tilde{J}_z(\alpha) + \tilde{Z}_{zx}(\alpha,\beta)\tilde{J}_x(\alpha) \qquad (1.90(a))$$

$$\tilde{E}_x(\alpha, d+t) = \tilde{Z}_{xz}(\alpha,\beta)\tilde{J}_z(\alpha) + \tilde{Z}_{xx}(\alpha,\beta)\tilde{J}_x \qquad (1.90(b))$$

are obtained [1.9]

where

$$\tilde{Z}_{zz},\ \tilde{Z}_{zx},\ \tilde{Z}_{xz},\ \tilde{Z}_{xx}$$

are transforms of Green's functions which are found from the boundary conditions and (1.89). The proof is not repeated here as

it is done in section (4.2) for the quasi-TEM case, instead we repeat the analysis in [1.9] for completeness.

In (1.90) the

$$\tilde{E}_z, \tilde{E}_x, \tilde{J}_x, \tilde{J}_z \text{ are unknowns } \tilde{E}_z, \tilde{E}_x$$

can be eliminated by applying Gellerkin's method in the spectral domain in conjunction with Parseval's theorem.

To solve we start by defining the inner product [1.4]

$$\langle \tilde{\phi}_1(\alpha n), \phi_2^*(\alpha n) \rangle = \sum_{n=-\infty}^{\infty} \phi_1(\alpha n)\, \phi_2^*(\alpha n) \qquad (1.91)$$

and Parseval's Theorem which states for figure (1.5)

$$\int_{-L}^{L} \phi_1(x)\, \phi_2(x)\, dx = \frac{1}{2L} \sum_{n=-\infty}^{\infty} \phi_1(\alpha n)\, \phi_2^*(\alpha n)$$

then expand

$$\tilde{J}_z(\alpha_n), \tilde{J}_x(\alpha_n)$$

in terms of unknown basis functions J_{zm}, J_{xm} which ideally describes the physical current density conditions on the strip as closely as possible (as stated earlier in discussion of the method of moments technique)

$$\tilde{J}_z = \sum_{m=1}^{N} a_m J_{zm}, \qquad m=1...N \qquad (1.92(a))$$

$$\tilde{J}_x = \sum_{m=1}^{N} b_m J_{xm}, \qquad m=1...M \qquad (1.92(b))$$

where a_m, b_m are unknowns.

The inner product is then taken with another set of testing function J_{zk}, $J_{x\ell}$ for different values of k and ℓ where, k = 1,---N, ℓ = 1,---M. [1.9]

Applying Parseval's theorem and the condition

$$E_z(x, d+t) = 0, \; Ex(x, d+t) = 0$$

on the strip and the fact that J_{zk}, $J_{x\ell}$ are zero outside the strip, then the following equations are obtained

$$\int_{-\infty}^{\infty} \left[\tilde{J}_{zk} \tilde{Z}_{zz} \sum_{m=1}^{N} a_m \tilde{J}_{zm} + \tilde{J}_{zk} \tilde{Z}_{zx} \sum_{m=1}^{M} b_m J_{xm} \right] d\alpha = 0, \; k = 1, ---N \qquad (1.93(a))$$

$$\int_{-\infty}^{\infty} \left[\tilde{J}_{x\ell} \tilde{Z}_{xz} \sum_{m=1}^{N} a_m \tilde{J}_{zm} + \tilde{J}_{x\ell} \tilde{Z}_{xx} \sum_{m=1}^{M} b_m J_{xm} \right] d\alpha = 0, \; l = 1, ---M \qquad (1.93(b))$$

Equation (1.93) can be expressed in matrix form

$$\sum_{m=1}^{N} K_{km}^{(1,1)}\, a_m + \sum_{m=1}^{M} k_{km}^{(1,2)}\, b_m = 0 \quad k = 1,2---N \quad (1.94(a))$$

$$\sum_{m=1}^{N} K_{lm}^{(2,1)}\, a_m + \sum_{m=1}^{M} k_{lm}^{(2,2)}\, b_m = 0 \quad l = 1,---M \quad (1.94(b))$$

In order for (1.94) to have a non-trivial solution in a_m, b_m the determinant of the matrix must be zero.

and since in (1.94) [1.9]

$$K_{km}^{(1,1)} = \int_{-\infty}^{\infty} \tilde{J}_{zk}(\alpha)\, \tilde{Z}_{zz}(\alpha,\beta)\, \tilde{J}_{zm}(\alpha)\, d\alpha$$

$$K_{km}^{(1,2)} = \int_{-\infty}^{\infty} \tilde{J}_{zk}(\alpha)\, \tilde{Z}_{zx}(\alpha,\beta)\, \tilde{J}_{xm}(\alpha)\, d\alpha$$

$$K_{km}^{(2,1)} = \int_{-\infty}^{\infty} \tilde{J}_{xl}(\alpha)\, \tilde{Z}_{xz}(\alpha,\beta)\, \tilde{J}_{zm}(\alpha)\, d\alpha$$

$$K_{lm}^{(2,2)} = \int_{-\infty}^{\infty} \tilde{J}_{xl}(\alpha)\, \tilde{Z}_{xx}(\alpha,\beta)\, \tilde{J}_{xm}(\alpha)\, d\alpha$$

when M = 1, N = 1, for example, (1.94) becomes

$$\begin{bmatrix} \int_\alpha \tilde{J}_{z1}\tilde{Z}_{zz}\tilde{J}_{z1}\,d\alpha & \int_\alpha \tilde{J}_{z1}\tilde{Z}_{zx}\tilde{J}_{x1}\,d\alpha \\ \int_\alpha \tilde{J}_{x1}\tilde{Z}_{xz}\tilde{J}_{z1}\,d\alpha & \int_\alpha \tilde{J}_{x1}\tilde{Z}_{xx}\tilde{J}_{x1}\,d\alpha \end{bmatrix} \begin{bmatrix} a_1 \\ b_1 \end{bmatrix} = 0$$

the propagation constant β is found at a given frequency ω by setting the determinant of (1.94) to zero to achieve a non-trivial solution. Once β is found, a_m, b_m are found by solving (1.94). The J_x, J_z can now be found from 1.92 $\therefore$ the fields can then be calculated.

Characteristic impedance variation with frequency is found by taking the power/current definition as outlined in section 1.2

$$Z_o = \frac{2P}{II^*}, \text{where } P = \int_s ExH$$

in the Z-direction and I =

$$\int_{-\frac{w}{2}}^{\frac{w}{2}} J\,dx$$

and J is found from (1.92) since a_m, b_m are now known. In chapter 4 the technique is used to solve some complex coupled microstrip structures, however, in those cases, the approximation is made that quasi-TEM conditions apply and the scalar potentials satisfy Poisson's or Laplace's equation rather than the more general Helmholtz equation dealt within this section.

REFERENCES

[1.1] Reinmut K. Hoffmann, "Handbook of Microwave Integrated Circuits"

Artech House Inc.

[1.2] K.C. Gupta, Ramesh Garg, I.J. Bahl, "Microstrip Lines and Slotlines"

Artech House Inc.

[1.3] R.E. Eaves JNR and D.M. Bolle, "Guided Waves in Limit Cases of Microstrip"

IEEE Microwave Theory and Techniques Volume MTT-18

April, 1970 Page 231 - 232

[1.4] Bharathi Bhat and Shiban Koul, " Analysis, Design and Applications of Fin Lines"

Artech House 1987 Page 130

[1.5] Masahiro Hashimoto, "A Rigorous Solution for Dispersive Microstrip"

IEEE Microwave Theory and Techniques

Volume MTT-33, No.11 November, 1985 Page 1131-1137

[1.6] Robert S. Collin, "Foundations of Microwave Engineering"

McGraw Hill: New York, 1966 Page 32

[1.7] N.G. Alexopoulos, "Integrated Circuit Structures on Anisotropic Substrates"

IEEE Microwave Theory and Techniques Volume MTT-33

October, 1985 Page 884 - 889

[1.8] Raymond Crampagne, Magid Ahmadpanah, Jean-Louis Guiraud, "A Simple Method of Determining the Green's Function for a Large Class of MIC Lines Having Multilayered Dielectric Structures"

IEEE Transactions on Microwave Theory and Techniques

Volume MTT-26 No.2 February, 1978 Page 82 - 87

[1.9] Tatsu Itoh, "Numerical Techniques for Microwave and Millimetre Wave Passive Structures"

John Wiley and Sons New York, 1988

[1.10] Nirod K. Das and David M. Pozar, "A Generalised Spectral Domain Green's Function for Multilayer Dielectric Substrates with Application to Multilayer Transmission Lines"

IEEE Transactions on Microwave Theory and Techniques

Volume MTT-35 No. 3 March, 1987

[1.11] Eikichi Yamashita, "Variational Method for the Analysis of Microstrip Like Transmission Lines"

Planar Transmission Line Structures, Edited by T. Itoh

IEEE Press 1987 Page 3 - 9

[1.12] Roger F. Harrington, "Time Harmonic Electromagnetic Fields"

McGraw Hill: New York, 1961 Page 182

[1.13] Kiyomichi Araki and Yoshiyuki Naito, "Upper Bound Calculations on Capacitance of Microstrip Lines Using Variational Method and Spectral Domain Approach"

IEEE Transactions on Microwave Theory and Techniques

Volume MTT-26 No.7 July, 1978 Page 506 - 509

[1.14] Jeffrey B. Knorr and Ahmet Tefekciglu, "Spectral Domain Calculation of Microstrip Characteristic Impedance"

Planar Transmission Line Structures, Edited by T.Itoh,

IEEE Press 1987 Page 74 - 77

[1.15] Rolf H. Jansen, "The Spectral Domain Approach for Microwave Integrated Circuits"

IEEE Transactions on Microwave Theory and Techniques

Volume MTT-33, No.10 October, 1985

Page 1043 - 1056

CHAPTER 2

APPLICATIONS OF COUPLED MICROSTRIP LINES

2.0 INTRODUCTION

Coupled microstrip lines in anisotropic substrate configurations are used extensively in microwave/millimetre wave circuits. The more popular functions are as directional couplers, filters, delay lines and interdigital capacitor [2.1]. Less exploited functions, so far are as high impedance low loss transmission lines [2.2] and as impedance transformers in matching circuits or as phase shifters. In the above applications coupling between the microstrip lines is a desired attribute, in other applications such high density multilayer thin film interconnects used in VLSIC, VHSIC and megabit memories [2.3] interconductor coupling is a nuisance whose importance cannot be ignored as frequency increases and therefore must be understood. In this chapter the coupler, phase shifter and impedance transformation functions will be considered.

2.1 MICROSTRIP COUPLER WITH EQUAL WIDTH LINES (SYMMETRICAL)

Consider the coupled lines indicated in figure (2.1(a)), consisting of conducting strips of equal width on an isotropic dielectric of permittivity ϵ_r. If the quasi-static assumption is made the structure supports two modes, the even mode (unbalanced) and the odd mode (balanced). The field patterns of these modes are shown in

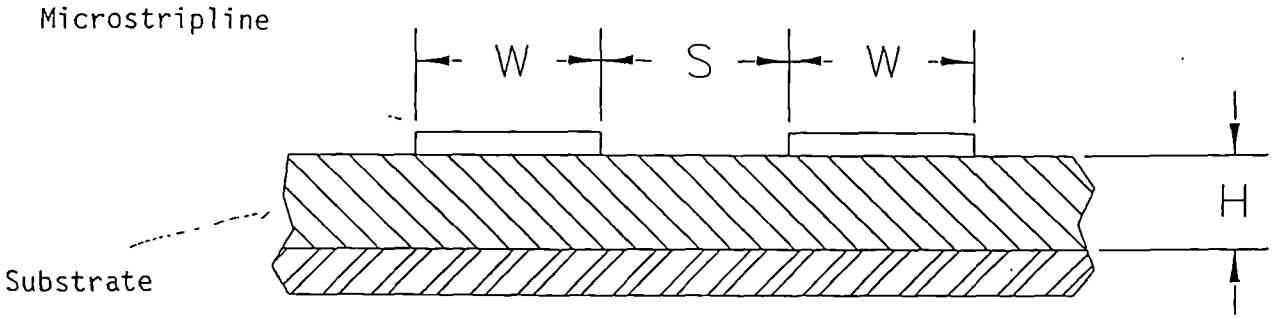

(2.1(a))

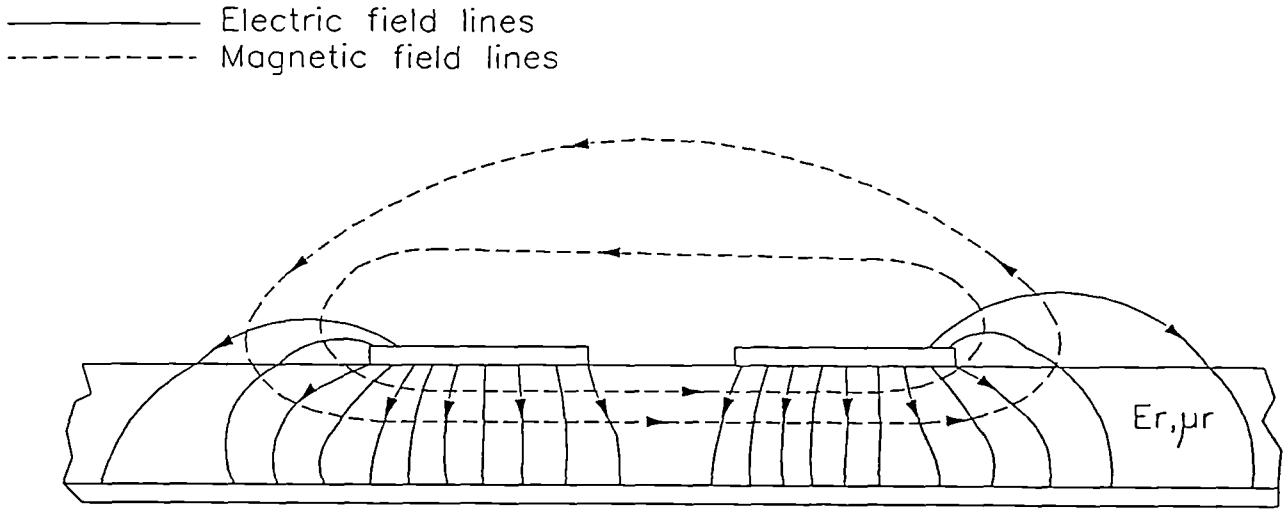

Even mode

(2.1(b))

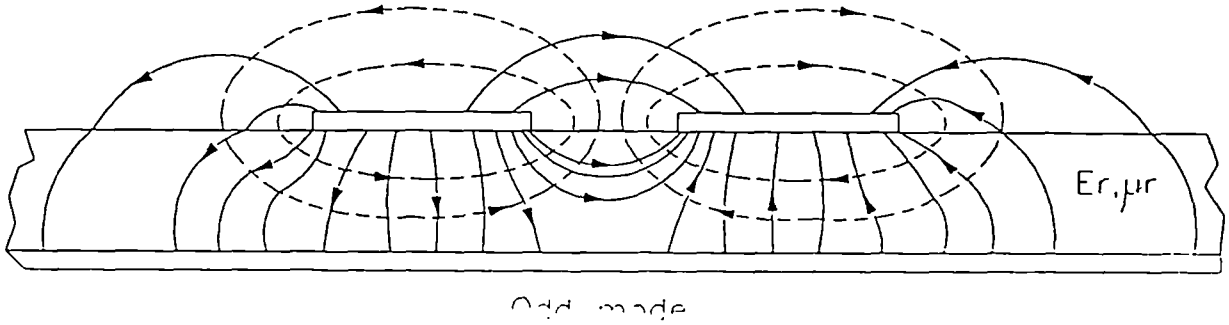

Odd mode

(2.1(c))

Figure (2.1) Field Patterns of Coupled Lines

figure 2.1(b), and 2.1(c); which indicate that in the even (unbalanced) mode the voltages on the strip are in phase ie. $V_1 = V_2$ whereas in the odd (balanced) mode they are 180° out of phase ie. $V_2 = -V_1$. Superposition of odd and even modes describe propagation in the structure. To examine the coupling behaviour of such strips consider figure 2.2 in which all four ports are of the structure are terminated by impedances Z_1, Z_2, Z_3, Z_4.

θ is the electrical length of the coupled section and voltages and currents are as shown. Z_{oo}, Z_{oe} are odd and even mode impedances.

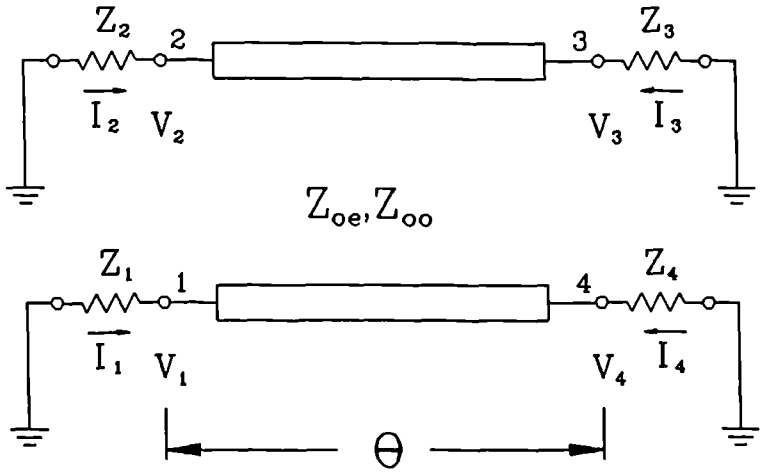

Figure 2.2 Coupled Microstrip

Considering I_1, I_2, I_3, I_4 to arise from current generators ie. infinite internal impedance it can be shown [2.3] that the impedance matrix of the coupled line four port is as follows:

$$[Z] = -j\begin{bmatrix} Z_+ctn\theta & Z_-ctn\theta & Z_-csc\theta & Z_+csc\theta \\ Z_-ctn\theta & Z_+ctn\theta & Z_+csc\theta & Z_-csc\theta \\ Z_-csc\theta & Z_+csc\theta & Z_+ctn\theta & Z_-ctn\theta \\ Z_+csc\theta & Z_-csc\theta & Z_-ctn\theta & Z_+ctn\theta \end{bmatrix} \qquad (2.1)$$

where

$$Z_+ = (Z_{oe} + Z_{oo}) / 2$$
$$Z_- = (Z_{oe} - Z_{oo}) / 2$$

for the special case $Z_1 = Z_2 = Z_3 = Z_4 = Z_0$, it is shown that by superposition of odd and even mode voltage and currents the in put impedance of the coupled line section at port 1 is

$$Z_{in} = \frac{V_{1o} + V_{1e}}{I_{1o} + I_{1e}} \qquad (2.2)$$

where o, e refer to odd and even modes

then

$$Z_{in} = \frac{\dfrac{Z_{1o}}{Z_o + Z_{1o}} + \dfrac{Z_{1e}}{Z_o + Z_{1e}}}{\dfrac{1}{Z_o + Z_{1o}} + \dfrac{1}{Z_o + Z_{1e}}} \qquad (2.3)$$

where Z_{1o}, Z_{1e} are input impedances of the system in the odd and even modes considered separately.

Using the transmission line equation

$$Z_{1o} = Z_{oo}\left[\frac{Z_o + j\,Z_{oo}\tan\theta}{Z_{oo} + j\,Z_o\tan\theta}\right] \qquad (2.4)$$

$$Z_{ie} = Z_{oe}\left[\frac{Z_o + j\,Z_{oe}\tan\theta}{Z_{oe} + j\,Z_o\tan\theta}\right] \qquad (2.5)$$

and substituting 2.4, 2.5 into 2.3 it is found that if

$$Z_o = (Z_{oo}\,.\,Z_{oe})^{\frac{1}{2}} \qquad (2.6)$$

then $Z_{in} = Z_o$ ie. the coupler is matched. When condition (2.6) holds then the scattering matrix of the coupler is

$$[S] = \begin{bmatrix} o & S_{12} & o & S_{14} \\ S_{12} & o & S_{14} & o \\ o & S_{14} & o & S_{12} \\ S_{14} & o & S_{12} & o \end{bmatrix} \qquad (2.7)$$

where

$$S_{12} = \frac{jk\sin\theta}{\sqrt{1-k^2}\cos\theta + j\sin\theta} \qquad (2.8)$$

$$S_{14} = \frac{\sqrt{1-k^2}}{\sqrt{1-k^2\cos\theta + j\sin\theta}} \qquad (2.9)$$

$$k = \frac{Z_{oe}/Z_{oo} - 1}{Z_{oe}/Z_o + 1} \qquad (2.10)$$

where k is the voltage coupling coefficient. From (2.7), (2.8) and (2.9) the following coupler characteristics can be deduced (for the unique case of

$$Z_o = \sqrt{Z_{oe}Z_{oo}}$$

1. The device is a quadrature coupler.
2. Coupling is in the backward direction (S_{12})
3. The directivity is infinite
4. Voltage coupling constant is dependent on the ratio Z_{oe}/Z_{oo}.

There are three important additional constraints on the structure which leads to conditions 2 and 3.

They are as follows:

(a) The lines are symmetrical

(b) The coupler is matched

(c) The phase velocities of the odd and even modes are assumed to be equal.

We now examine what happens when the assumptions are invalidated.

2.2 MICROSTRIP COUPLER WITH ASYMMETRIC LINES

When the lines in figure (2.2) are asymmetrical (ie. of different widths) Crystal [2.5] shows that infinite directivity is achieved if

$$G_a G_b = AB - D^2 \qquad (2.11(a))$$

There are two conditions for impedance matching

$$G_a G_b = AB - D^2 \qquad (2.11(a))$$

and

$$G_a / G_b = A/B \qquad (2.11(b))$$

where G_a, G_b are the terminating admittances of the two lines, which need not be real,

$$A = \frac{Y_{oo}^a + Y_{oe}^a}{2} \qquad (2.12(a))$$

$$B = \frac{Y_{oo}^b + Y_{oe}^b}{2} \qquad (2.12(b))$$

$$D = \frac{Y_{oo}^a - Y_{oe}^a}{2} = \frac{Y_{oo}^b - Y_{oe}^b}{2} \qquad (2.12(c))$$

where Y_{oe}^a, Y_{oo}^a are admittances measured at port 1 for an infinite section of coupled line excited in the even and odd modes respectively, with voltage sources at ports 1 and 2. Y_{oe}^b, Y_{oo}^b are corresponding even and odd mode admittances measured at port 2 with sources at ports 1 and 2. [2.5]

It can also be shown that the asymmetric coupled line acts as an impedance transformer in which the coupled signal may be transformed to a higher or lower impedance than the input signal. The coupling coefficient k, and the terminating admittances of the asymmetric coupled line are connected by the following equations:

$$k = D'/\sqrt{A'B'} \qquad (2.13(a))$$

$$G_a = \sqrt{\left(\frac{A'}{B'}\right)}\left(\sqrt{A'B' - D^2}\right) \qquad (2.13(b))$$

$$G_b = \left(\sqrt{\frac{B'}{A'}}\right)\left(\sqrt{A'B' - D^2}\right) \qquad (2.13(c))$$

and the theoretical limit of the impedance transformation ratio (between incident and coupled ports) for a given coupling value is given by

$$\frac{1}{k^2} \geq \frac{G_a}{G_b} \text{ and } \frac{G_b}{G_a} \qquad (2.13(d))$$

The asymmetric coupler can be designed from a knowledge of the symmetric coupler of equal coupling by applying the fact that an asymmetrical coupler is mathematically equivalent to a symmetric coupler where the coupled line of the symmetric coupler has impedance transformers of turns ratio

$$1 : \sqrt{B/A}$$

connected at both ends, (ie. ports 2 and 3). And Crystal [2.5] shows that the following equivalence is valid

$$A = A' \qquad (2.13(e))$$

$$N = \sqrt{B'/A'} \qquad (2.13(f))$$

$$D = D'/N \qquad (2.13(g))$$

where the primed quantities refer to the asymmetric coupler and the unprimed to the symmetric equivalent. Therefore knowing k and A for the symmetric coupler the parameters for the unsymmetric coupler can be calculated.

A frequently encountered problem of microwave system design is the requirement for a transition from 50 to 75 ohms at the IF band. The requirement for a compact transition is presently met by using a resistive divider. The resistive divider approach reduces dynamic range of the system. It is proposed here to achieve a low loss compact transition from 50 to 75 ohms at MHz frequencies by using an asymmetric spiral coupler similar to the type shown in figure (2.11), with ground plane septum, to achieve the required value of k.

From equation (2.13(d)),

$$\frac{1}{k^2} = 1.5$$

ie. k = 0.81

$$\text{and } \frac{Z_{oe}}{Z_{oo}} = 9.5$$

This ratio can be met by the ground plane septum method analyzed in chapter 4. The transformer design will be as follows: (1) for the selected substrate determine the line spacing and septum lengths which result in the required even to odd mode impedance ratio for symmetric lines (2) use equation (2.13) to determine the width of the coupled line in the asymmetric configuration.

2.3 MISMATCHED COUPLER

To address the case where the coupler is mismatched let the input impedance at port 1 be Z_{1x} where x = '0' or 'e' and let Z_o be the source/load characteristic impedance.

Then

$$\alpha_{1n} = \frac{Z_{1x}}{Z_o} = \alpha_n \left[\frac{1 + j\alpha_n \tan\theta}{\alpha n + j \tan\theta} \right]$$

and if

$$\alpha_k = \sqrt{\alpha_e \alpha_o} = \text{coupler impedance}$$

$$k = \frac{\alpha_e - \alpha_o}{\alpha_e + \alpha_o} = \text{voltage coupling coefficient}$$

$$k_1 = \sqrt{1 - k^2}$$

then from [2.5]

$$S_{1m} = j \sin\theta \left\{ \frac{(\alpha_k^2 - 1) + k(\alpha_k^2 + 1)}{2\alpha_k k_1 \cos\theta + j \sin\theta \left[(\alpha_k^2 + 1) + k(\alpha_k^2 - 1)\right]} \right. \qquad (2.14(a))$$
$$\left. \pm \frac{(\alpha_k^2 - 1) - k(\alpha_k^2 + 1)}{2\alpha_k k_1 \cos\theta + j \sin\theta \left[(\alpha_k^2 + 1) - k(\alpha_k^2 - 1)\right]} \right\}$$

where m = 1, 2 and the positive sign and negative signs in (2.14(a)) refers to S_{11} and S_{12} respectively.

Similarly

$$S_{1n} = \alpha_k k_1 \left\{ \frac{1}{2\alpha_k k_1 \cos\theta + j \sin\theta \left[(\alpha_k^2 + 1) + k(\alpha_k^2 - 1)\right]} \right. \qquad (2.14(b))$$
$$\left. \pm \frac{1}{2\alpha_k k_1 \cos\theta + j \sin\theta \left[(\alpha_k^2 + 1) - k(\alpha_k^2 + 1)\right]} \right\}$$

where n = 3,4 and the plus sign refers to S_{14} and the minus to S_{13}.

when $\alpha_k = 1$

(2.14) reduces to (2.7) the matched coupler case.

2.4 UNEVEN PHASE VELOCITY

So far equal even/odd mode phase velocities have been assumed. However, due to the dielectric inhomogeneity of the microstrip structure even and odd mode phase velocities V_{pe}, V_{po} are generally unequal

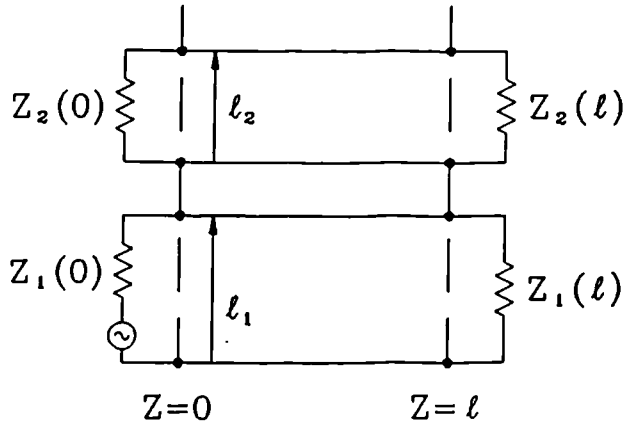

Figure 2.3(a) Coupled Microstrip

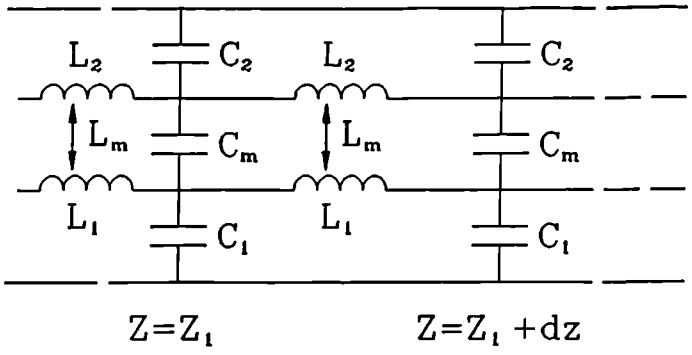

Figure 2.3(b) Equivalent Circuit

Krage and Haddad [2.7] using the notation in figure 2.3(b)), where L_j, C_j, (j = 1, 2) are equivalent self inductance and capacitance respectively per unit length of each strip j in the presence of the other line k (k = 1, 2) where j ≠ k and L_m, C_m are mutual inductance and capacitance per unit length, respectively, indicates that the behaviour of the system can be described by the following equations

$$\frac{\delta e_1}{\delta z} + L_1 \frac{\delta i_1}{\delta t} + L_m \frac{\delta i_1}{\delta t} = o \qquad (2.15(a))$$

$$\frac{\delta i}{\delta z} + C_1 \frac{\delta e_1}{\delta t} - C_m \frac{\delta e_2}{\delta t} = o \qquad (2.15(b))$$

$$\frac{\delta e_2}{\delta z} + L_2 \frac{\delta i_2}{\delta t} + L_m \frac{\delta i_1}{\delta t} = o \qquad (2.15(c))$$

$$\frac{\delta i_2}{\delta z} + C_2 \frac{\delta e_2}{\delta t} - C_m \frac{\delta e_1}{\delta t} = O \qquad (2.15(d))$$

$$L_1 = L_{10} - L_m, \quad L_2 = L_{20} - L_m, \quad C_1 = C_{10} + C_m, \quad C_2 = C_{20} + C_m$$

Assuming that the lines are lossless and that the impedances of each line is not a function of distance, Z, along the line then the propagation constant

$$\gamma = \pm j\beta_o\sqrt{1 \pm \delta} \qquad (2.16)$$

ie. four possible phase velocities if the medium is homogenous only one phase velocity is allowed and δ = o

$$\text{where} \quad \beta_o = \sqrt{\frac{\beta_1^2 + \beta_2^2}{2} - \beta_1 \beta_2 k_L k_c} \qquad (2.17)$$

and

$$\delta = \sqrt{1 - \left(\frac{\beta_1^2 \beta_2^2}{\beta_o^4}\right)(1 - k_L^2)\ (1 - k_c^2)} \qquad (2.18)$$

$$\beta_i = \omega\sqrt{L_i C_i} \quad (i = 1, 2) \qquad (2.19)$$

$$k_L = L_m / L_1 L_2 \qquad (2.20)$$

$$\text{and} \quad k_c = C_m / \sqrt{C_1 C_2} \qquad (2.21)$$

and the exp jωt time dependence is assumed.

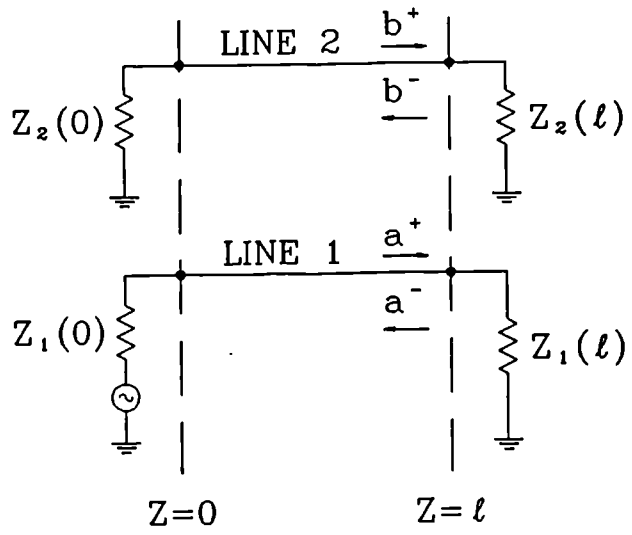

Figure 2.4 Schematic for Coupled Wave Analysis

Considering figure 2.4 in which the modes on the line are represented by a^+, a^-, b^+, b^- with directions as shown.

For a homogenous medium ie. $\delta = o$ and setting $\beta_1 = \beta_{2\,(TEM\ conditions)}$ (ie. the symmetrical condition referred to in section 2.1) and matched terminations, then $k_L = k_c = k$ or $k_L = -k_c$ (2.18)

and Krage and Haddad have shown that the reflected wave

$$\frac{a^-(o)}{a^+(o)} = o \qquad (2.22)$$

the transmitted wave

$$\frac{a^+(\ell)}{a^+(o)} = \frac{\sqrt{(1-k^2)}}{\sqrt{(1-k^2)}\cos\theta + j\sin\theta} \qquad (2.23)$$

the coupled wave

$$\frac{b^{-}(o)}{a^{+}(o)} = \frac{j k \sin\theta}{\sqrt{(1-k^2)}\cos\theta + j\sin\theta} \qquad (2.24)$$

the directivity related wave

$$\frac{b^{+}(\ell)}{a_{+}(o)} = o \qquad (2.25)$$

where

$$\theta = \frac{\omega \ell}{c} \text{ and } C = 1/\sqrt{\mu\,\epsilon}$$

μ and ϵ are permeability and permittivity of the homogenous medium respectively.

It is worthwhile to note that equation 2.24 is identical to (2.8).

Defining coupling

$$C = \sqrt{\frac{|b^{-}(o)|^2\,(1-|\rho_2(o)|^2)}{|a^{+}(o)|^2}} \qquad (2.26)$$

Directivity

$$D = \sqrt{\frac{|b^+(\ell)|^2\,(1-|\rho_2(\ell)|^2)}{|b^-(o)|^2\,(1-|\rho_2(o)|^2)}} \qquad (2.27)$$

where $\rho_i(Z)$ is voltage reflection coefficient of line i at a position Z. Then using equations (2.20), (2.21), (2.22), (2.23), (2.24) and (2.25),

$$C = \frac{\sqrt{2}\,k\sin\theta}{\sqrt{2-k^2-k^2\cos^2\theta}} \qquad (2.28)$$

$$D = o \qquad (2.29)$$

For the non-homogenous dielectric case $k_L \neq k_c$. If in this case $\beta_1 = \beta_2$ and the ports are matched

then

$$\beta_o = \beta_1\sqrt{1-k_L k_c} \qquad (2.30) \qquad \text{from} \quad (2.15)$$

and

$$\delta = (k_L - k_c)\,/\,(1-k_L k_c) \qquad (2.31)$$

and following [2.6] defining

$$\phi_1 = \sqrt{(1+k_L)\,(1-k_c)} \qquad (2.32)$$

$$\phi_2 = \sqrt{(1 - k_L)\ (1 + k_C)} \qquad (2.33)$$

$$\theta_1 = \beta_1 \phi_1 \ell \qquad (2.34)$$

$$\theta_2 = \beta_1 \phi_2 \ell \qquad (2.35)$$

$$\Delta = k_L - k_C \qquad (2.36)$$

then

$$C = \left|\frac{b^-(o)}{a^+(o)}\right| \qquad (2.37)$$

and

$$\begin{aligned}\frac{b^-(o)}{a^+(o)} = (k_L + k_C)\ \{ & [2\cos(\theta_1+\theta_2) - 2\cos(\theta_1-\theta_2)] \\ & + j\,[(\phi_1+\phi_2)\sin(\theta_1+\theta_2) + (\phi_2-\phi_1)\sin(\theta_1-\theta_2)]\} \\ & \div [4\ (1+\phi_1\phi_2) - \Delta^2]\cos(\theta_1+\theta_2) \\ & - [4\ (1-\phi_1\phi_2) - \Delta^2]\cos(\theta_1-\theta_2) \\ & + j\{[4\ (\phi_1-\phi_2) + 2\,\Delta\ (\phi_2-\phi_1)]\sin(\theta_1+\theta_2) \\ & - [4\ (\phi_1-\phi_2) - 2\,\Delta\ (\phi_1+\phi_2)]\sin(\theta_1-\theta_2)\}\end{aligned} \qquad (2.38)$$

and

$$D = \left|\frac{b^+(\ell)}{b^-(o)}\right|$$

and

$$\frac{b^+(\ell)}{b^-(o)} = \{2\,(\phi_1\phi_2)\,(\cos\theta_2 - \cos\theta_1) + j\,[2\,(\phi_1\sin\theta_2 - \phi_2\sin\theta_1) - \Delta\,(\phi_1\sin\theta_2 + \phi_2\sin\theta_1)]\} \div \{\left(\frac{k_L + k_C}{2}\right)\{2\,[\cos(\theta_1+\theta_2) - \cos(\theta_1-\theta_2)] + j\,[(\phi_1+\phi_2)\sin(\theta_1+\theta_2) + (\phi_1-\phi_2)\sin(\theta_1-\theta_2)]\}\} \qquad (2.39)$$

As Δ is increased [2.6] power coupled to the b^- mode is decreased and power coupled to the $b^{+\,mode}$ is increased which results in degraded directivity as well as co-directional behaviour if Δ is increased sufficiently.

For optimum contra-directional microstrip coupler performance it is therefore necessary to find means of making $\Delta \rightarrow o$ ie. equalising V_{po} and V_{pe}. Chapter 3 deals with techniques of achieving this condition.

2.5 COUPLER BANDWIDTH SENSITIVITY TO Z_{oe}/Z_{oo}

Ratio of power at port 2 of the coupler to input power at port 1 is given by [2.11]

$$C^2 = \frac{k^2\sin^2\theta}{1 - k^2\cos^2\theta} \qquad (2.40(a))$$

Where θ is the electrical length of the coupler

$$C^2 = k^2 \; for \; \theta = \frac{\pi}{2}$$

The value of θ for which

$$\frac{R^2}{k^2} = m$$

is given by

$$\theta_m = \sin^{-1}\left[\left(\frac{m - mk^2}{1 - mk^2}\right)^{\frac{1}{2}}\right] \qquad (2.40(b))$$

If fractional bandwidth BW is defined as

$$\frac{f_2 - f_1}{f_c}, \text{ then since } \theta_c = \frac{\pi}{2} \; and \; \frac{f}{f_c} = \frac{2\theta}{\pi}$$

Then fractional bandwidth for a given m is

$$BW = \frac{4}{\pi}\left[\frac{\pi}{2} - \sin^{-1}\left(\frac{m - mk^2}{1 - mk^2}\right)^{\frac{1}{2}}\right] \qquad (2.40(c))$$

Where fc is frequency at which m = 1.

Therefore fractional bandwidth increases as k increases and reaches a maximum of 2 when k = 1.

Since

$$k = \frac{1 - Z_{oo}/Z_{oe}}{1 + Z_{oo}/Z_{oe}}$$

bandwidth is maximised by minimising the ratio Z_{oo}/Z_{oe}. Chapter 3 examines ways of achieving this.

2.6 COUPLED MICROSTRIP LINE PHASE SHIFTER

Referring to figure 2.2 if ports 2 and 4 are short circuited then the ABCD matrix of the structure becomes [2.5].

$$A = \frac{Y_{oe}\cot\theta_e + Y_{oo}\cot\theta_o}{Y_{oe}\,\mathrm{cosec}\,\theta_e - Y_{oo}\,\mathrm{cosec}\,\theta_o} \qquad (2.41(a))$$

$$B = \frac{2j}{Y_{oe}\,\mathrm{cosec}\,\theta_e - Y_{oo}\,\mathrm{cosec}\,\theta_o} \qquad (2.41(b))$$

$$C = \frac{j}{2}\,\frac{Y_{oe}^2 + Y_{oo}^2 - 2\,Y_{oe}Y_{oo}\,(\cot\theta_e\cot\theta_o + \mathrm{cosec}\,\theta_e\,\mathrm{cosec}\,\theta_o)}{Y_{oe}\,\mathrm{cosec}\,\theta_e - Y_{oo}\,\mathrm{cosec}\,\theta_o} \qquad (2.41(c))$$

$$D = A \qquad (2.41(d))$$

and the equivalent circuit is as shown in figure 2.5.

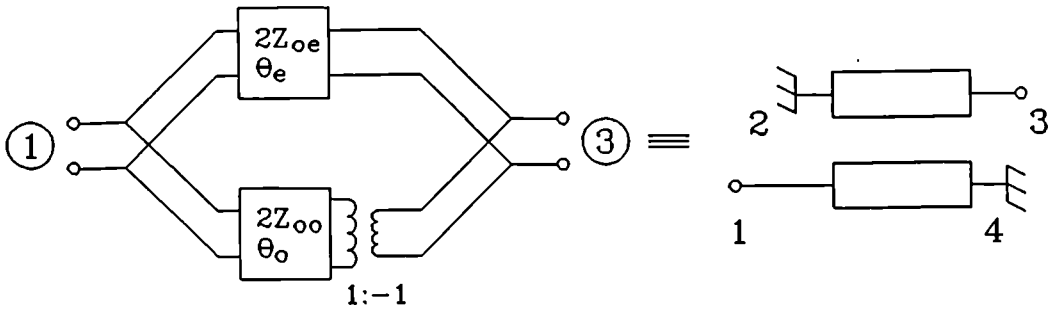

Figure 2.5 Terminated Coupled Line Equivalent Circuit

From equation (2.41) when $Z_{oe} >> Z_{oo,}$ ie. $Y_{oe} << Y_{oo}$ the ABCD matrix elements are approximately

$$A = D = -\cos\theta_o$$

$$B = -2jZ_{oo}\sin\theta_o$$

$$C = -\frac{j}{2Z_{oo}}\sin\theta_o$$

ie. the equivalent transmission matrix becomes

$$\begin{bmatrix} -1 & 0 \\ 0 & -1 \end{bmatrix} \begin{bmatrix} \cos\theta_o & j2Z_o\sin\theta_o \\ j\frac{\sin\theta_o}{2Z_{oo}} & \cos\theta_o \end{bmatrix} \qquad (2.42)$$

which represent a 180° phase shifter in series with a transmission line of length θ_o and characteristic impedance $2Z_{oo}$. This result

offers a simple technique for achieving in planar form the 180° phase shift required for broadband push-pull amplifiers and balanced mixers. As part of this exercise a 90 degree section of coupled line terminated as mentioned above was used to replace the 270 degree section of a microstrip rat race. The circuit layout is shown in figure (2.5(a)). The circuit was realised on 0.025 inch thick Epsilon 10 (ϵ_r = 10) with line spacing of 0.0017 inch and line width 0.016 inches in the coupled section, resulting in Z_{oe}/Z_{oo} ratio of 2.7. Predicted data is shown in table (2.1). Figure (2.5(b)) shows measured phase response of the path D to B versus D to C.

Measured data was as follows:

Frequency Band		7.5 to 10 GHz (28% bandwidth)
Coupling	D to B	3 ± 0.2 dB
COUPLING	D to C	3 ± 0.2 dB
COUPLING	D to A	10 dB minimum
PHASE DIFFERENCE	D to B vs. D to C	180° ± 10°

The phase response matches Aikawa's [2.9] result for Z_{oe}/Z_{oo} = M = 2.7, however measured insertion loss ripple was greater than Aikawa's, this is mainly due to source/load mismatch in our test setup as well as a poor termination at port A. In addition isolation is worse than would be expected due to the fact that (1). the quasi-static assumption is breaking down (2). phase velocities of even and odd modes are unequal.

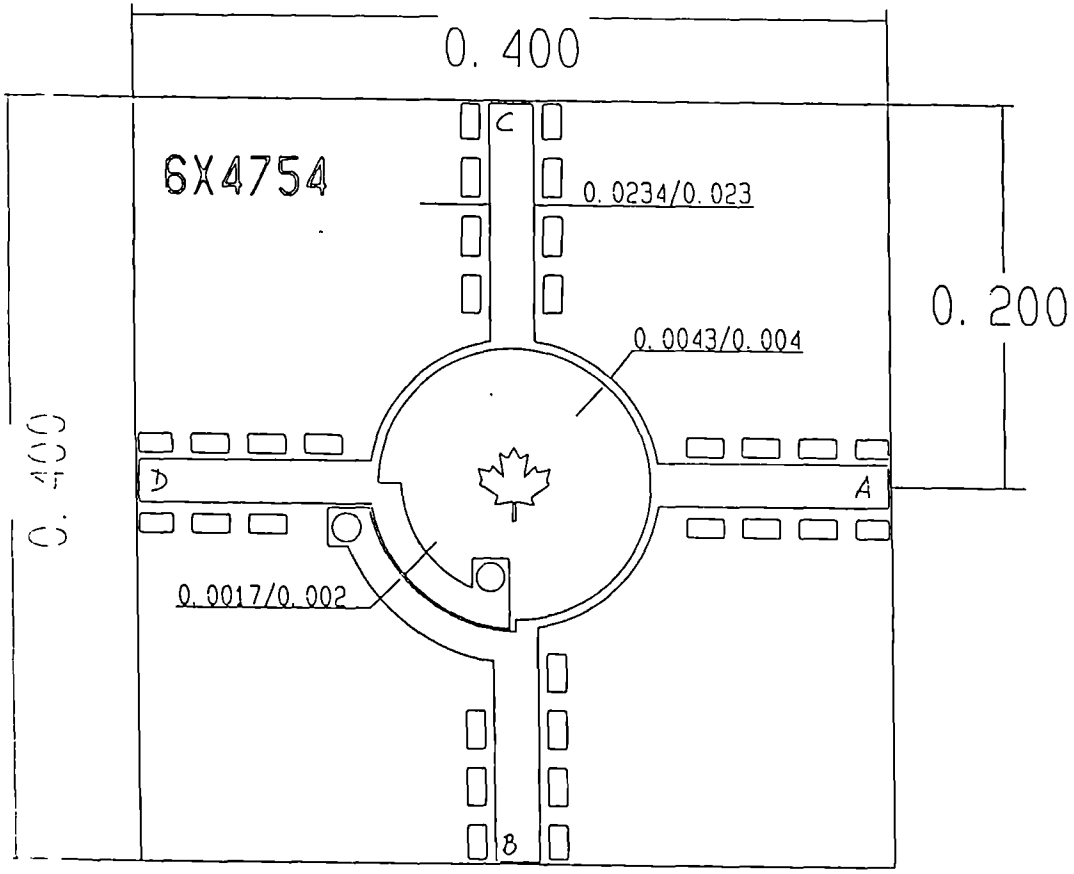

NOTES.

1. XXX/XXX REPRESENT DIMS. BEFORE/AFTER ETCHING.
2. USE 25MIL EPSILON 10 OR RT6010 (6009032-00)
3. USE MASK #67243-13
4. All dimensions in inches

Figure (2.5(a)) Layout of Optimised Magic-T

The bandwidth over which (2.42) holds is dependent on the ratio Z_{oe}/Z_{oo} = M as shown in section (2.5). In section (2.8) we propose a broadband 180° phase splitter in which very high Z_{oe}/Z_{oo} ratio is achieved by the use of the tuning septum approach which is analyzed in chapter 4.

Touchstone(TM)-Configuration (100 1600 100 17405 0651 1000 1 3294)

FREQ-GHZ	ANG[S12] HYBRID D-B	ANG[S14] HYBRID D-C	DB[S12] HYBRID D-B	DB[S14] HYBRID D-C
6.00	147.835	-45.950	-5.333	-4.672
6.50	135.834	-56.373	-4.803	-4.321
7.00	123.863	-66.735	-4.388	-4.042
7.50	111.971	-77.007	-4.073	-3.825
8.00	100.181	-87.172	-3.844	-3.660
8.50	88.490	-97.233	-3.690	-3.538
9.00	76.870	-107.211	-3.598	-3.449
9.500	65.269	-117.142	-3.561	-3.387
10.00	53.619	-127.076	-3.576	-3.347
10.50	41.838	-137.070	-3.643	-3.330
11.00	29.837	-147.186	-3.771	-3.336
11.50	17.528	-157.477	-3.972	-3.375
12.00	4.829	-167.987	-4.266	-3.457

Table (3.1) Calculated Response of Optimised Rat Race

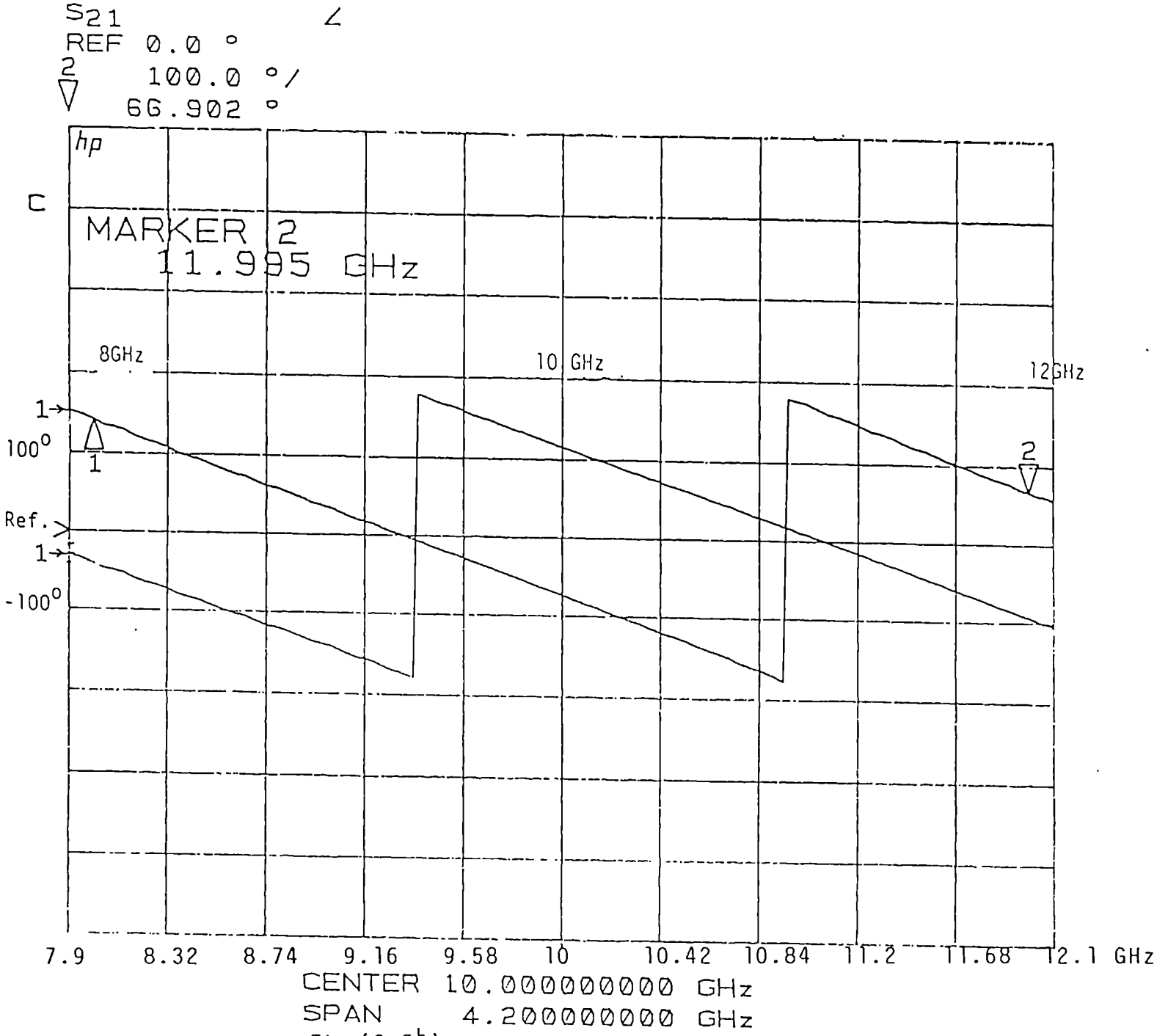

Fig.(2.56)Magic-T Relative Phase Response D to B vs D to C

2.7 SELECTIVELY TERMINATED COUPLED MICROSTRIP

2.7.1 PORT 2 SHORT CIRCUITED PORT 3 OPEN CIRCUITED

Consider figure 2.2. If port 2 is short circuited and port 3 open circuited the equivalent circuit is shown in figure 2.7 [2.10], in a non-homogenous configuration.

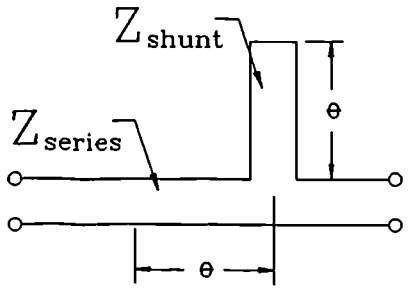

Figure 2.6 Equivalent Circuit

Where

$$Z_{series} = \frac{2 Z_{oe} Z_{oo}}{(Z_{oe} + Z_{oo})} \qquad (2.43(a))$$

$$Z_{shunt} = \frac{(Z_{oe} - Z_{oo})^2}{2 (Z_{oe} + Z_{oo})} \qquad (2.43(b))$$

when $Z_{oe} >> Z_{oo}$ (2.43) becomes

$$Z_{series} = 2\,Z_{oo}$$

$$Z_{shunt} = \frac{Z_{oe}}{2}$$

Examination of the data for most low noise MESFET up to X-band, indicates that the optimum complex noise match impedance is in the upper half of the Smith chart but with an angle which is greater at the low end of the frequency band than at the high end. To approach optimum noise match over a broadband, frequently requires the use of a shunt inductor as well as a lossy series inductor. If $Z_{oe} >> Z_{oo}$ and much greater than the terminating impedances, the coupled line could perform the same function with lower loss. To the author's knowledge this low noise match has not been used.

Another application of the equivalent circuit in figure 2.6 is its use in broadening the bandwidth of a conventional branchline coupler in a compact arrangement. The technique is based on that described by Mayer and Knochel [2.13] in which a high impedance $\lambda/2$ line is added to each port of the coupler and at the end of the $\lambda/2$ line away from the coupler a $\lambda/2$ open circuited line is attached as shown in figure (2.7(a))

Myer & Knochel

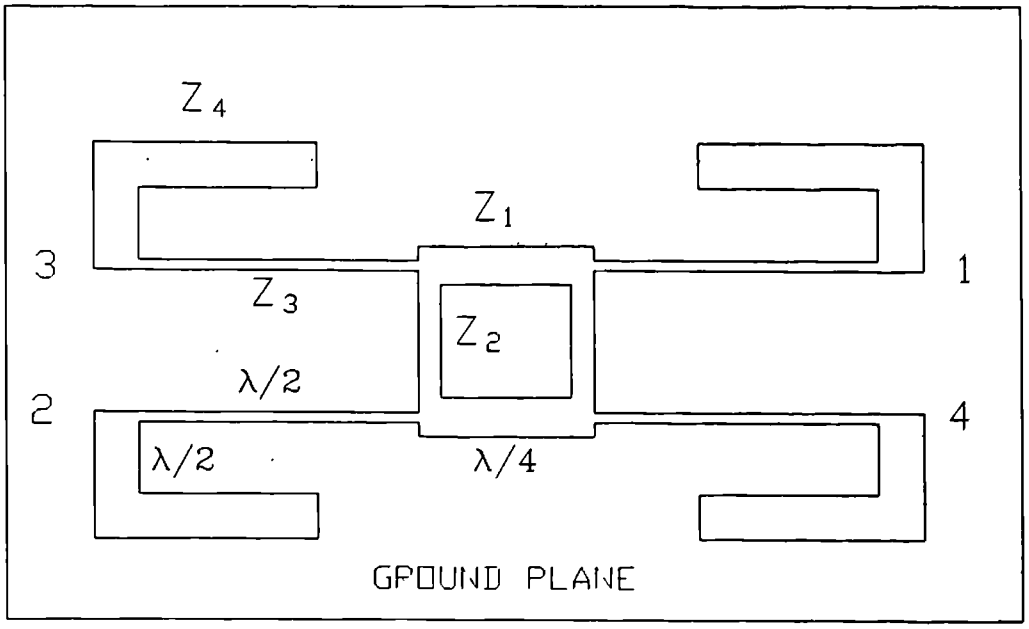

FIGURE: 2.7a

Proposed

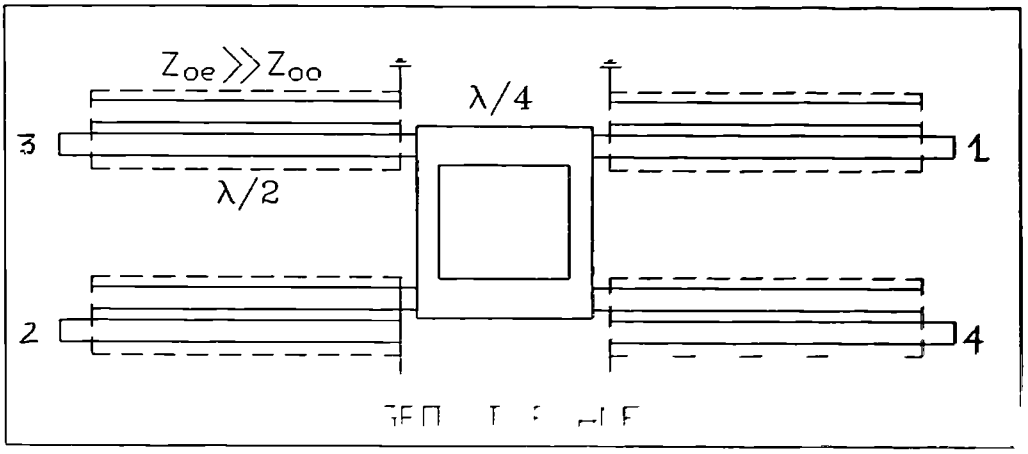

FIGURE: 2.7b

BROADBAND BRANCH LINE COUPLER

In Mayer and Knochel's circuit Z_3 = 92.7 ohms. This creates two problems, the first is radiation loss and the second is that the circuit would be of limited usefulness above 18 GHz where a thin substrate would be required. The approach suggested in this thesis circumvents both problems and results in a more compact structure. To prove the concept a branchline coupler was designed to cover the 5.9 - 6.4 GHz civil earth station transmit band using the standard technique as well as the coupled line technique shown in figure (2.7(b)).

Figures (2.7(c)) through (2.7(f)) shows predicted performance of the conventional branchline coupler. Figures (2.7(g)) through (2.7(i) shows the predicted performance of the proposed branchline coupler with a coupled section as the tuning element as shown in figure (2.7(b)).

Bandwidth, particularly of the coupled and isolated path, as well as input return loss, is improved from approximately 10% to 49%. The coupled line structure which is similar to that shown in figure 4.1 has line spacing of 0.001 inch and line width 0.012 inch realised on a substrate of ϵ_r = 2.4 and thickness 0.010 inch; with tuning septums.

Figure (2.7(c)) Transmitted Path Conventional Branchline Coupler

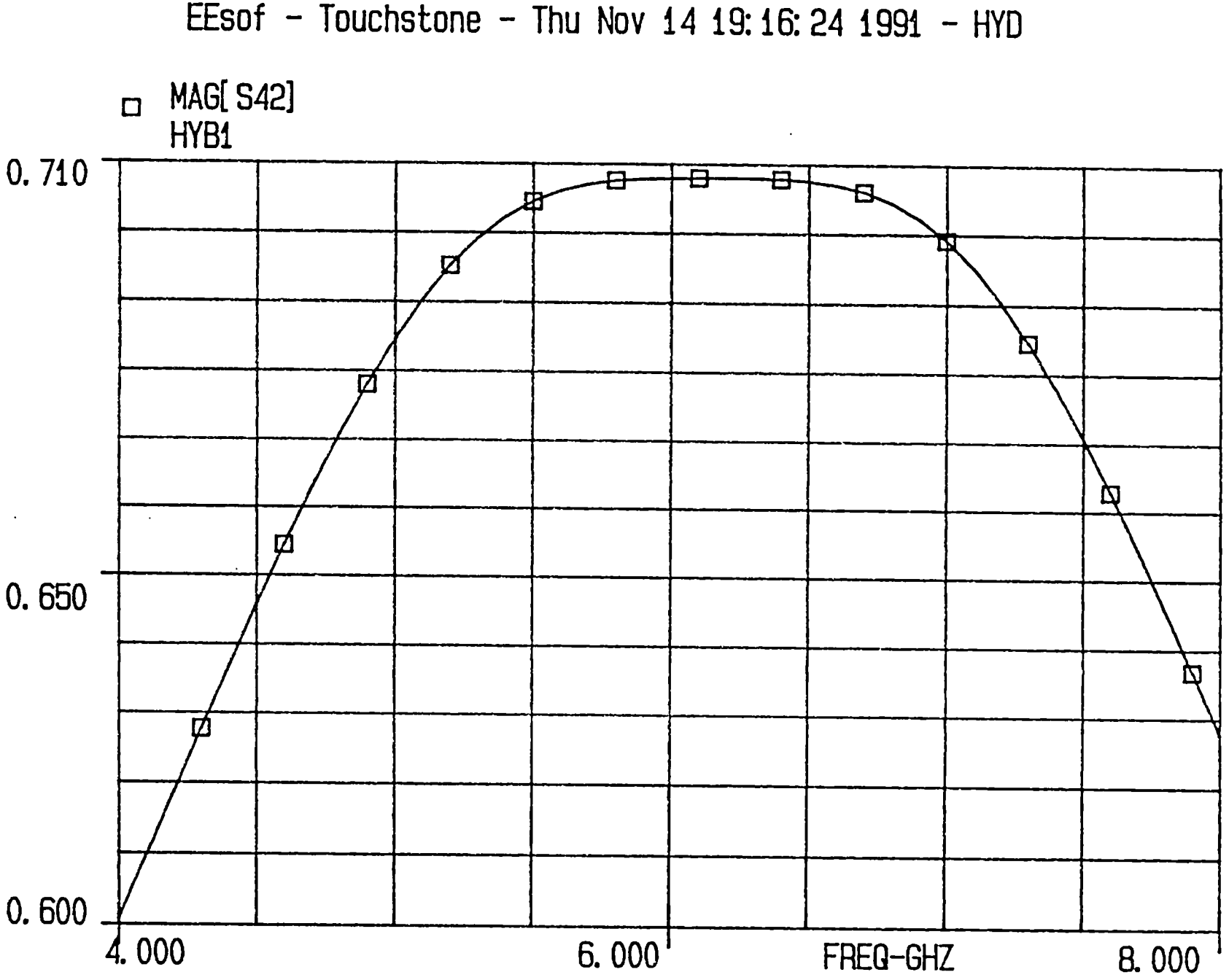

Figure (2.7(d)) Coupled Path Conventional Branchline Coupler

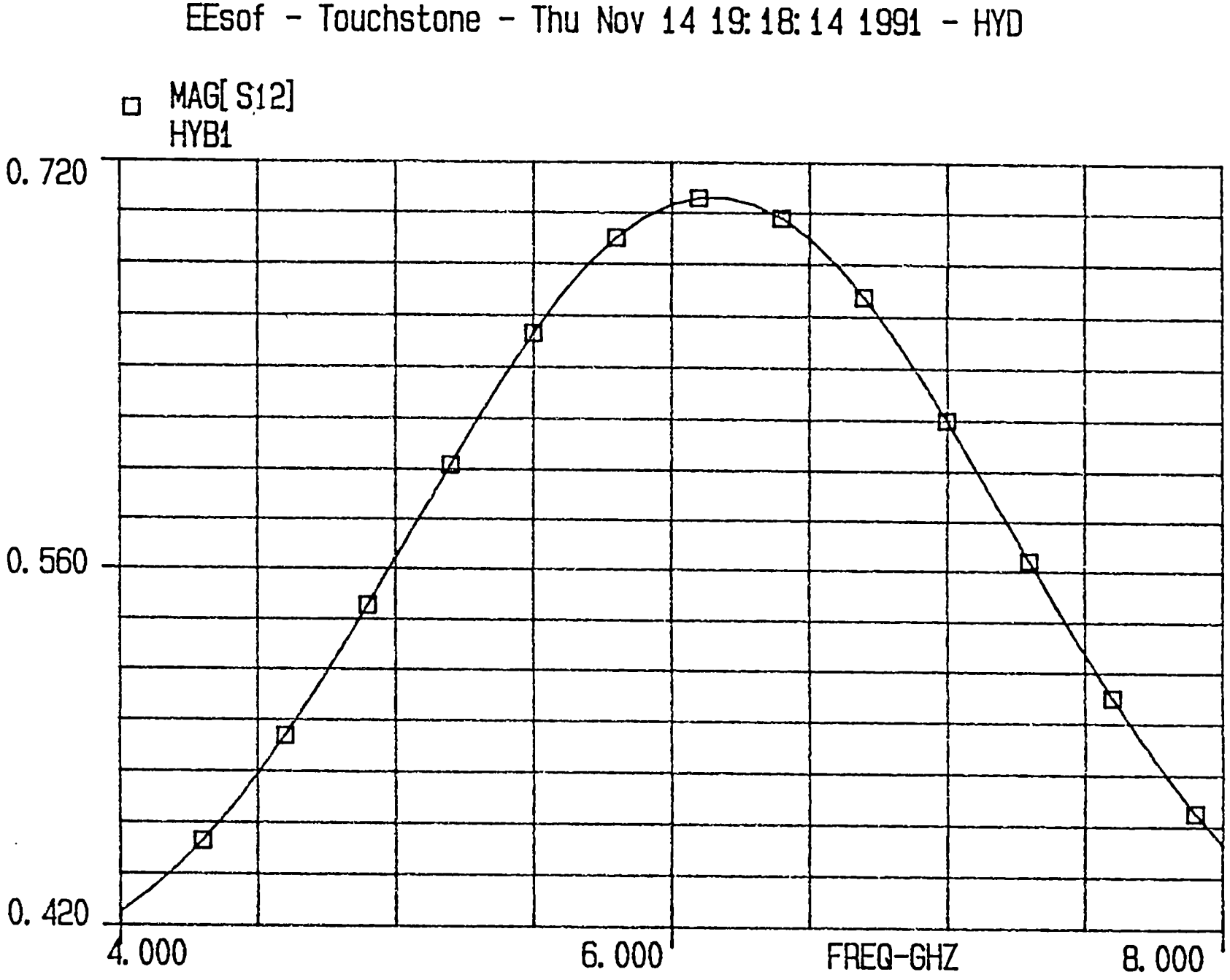

Figure (2.7(e)) Isolated Path Conventional Branchline Coupler

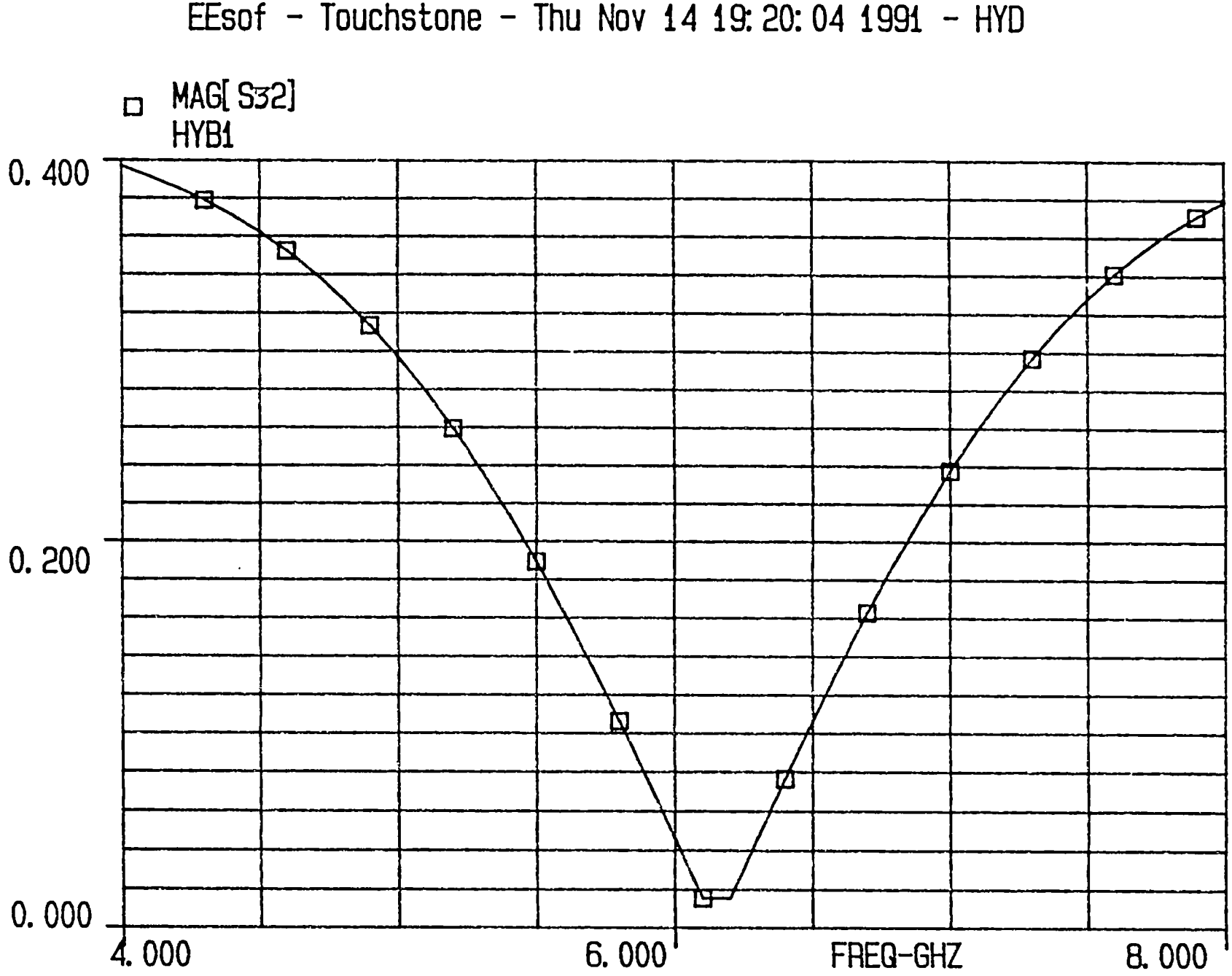

Figure (2.7(f)) Input Return Loss - Conventional Branchline Coupler

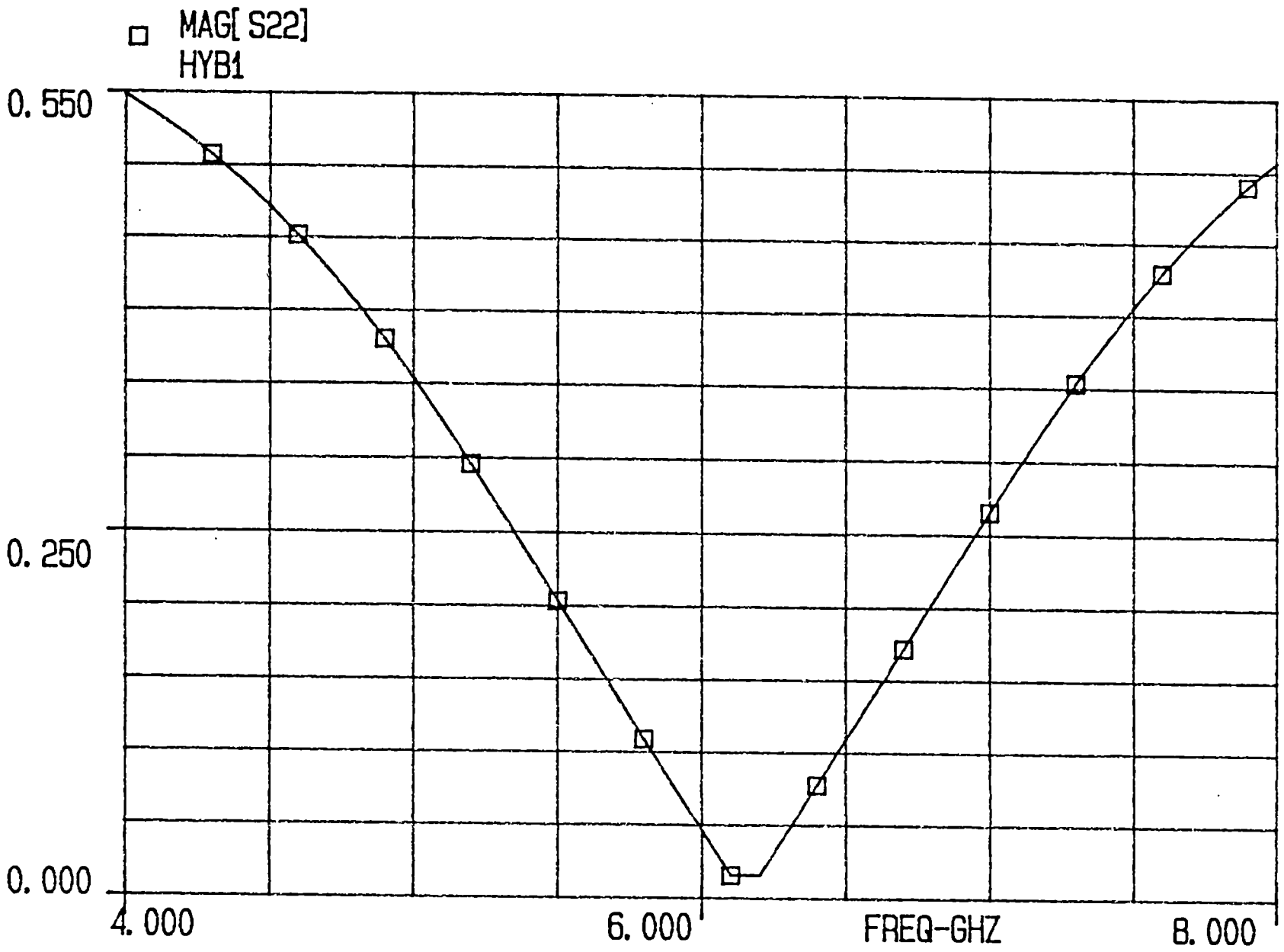

Figure (2.7(g)) Transmitted Path - Branchline Coupler with Coupled Tuning Element

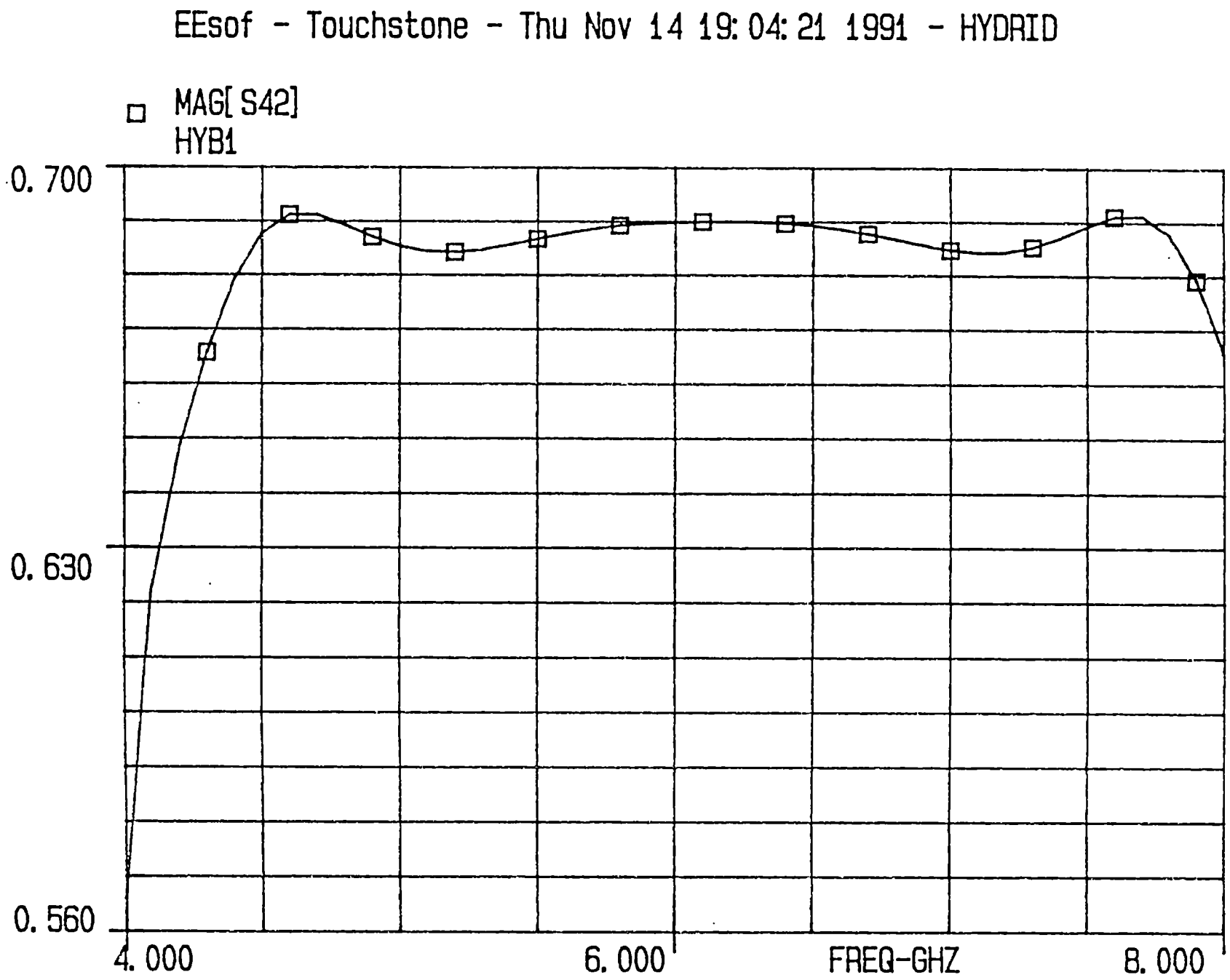

Figure (2.7(h)) Coupled Path - Branchline Coupler with Coupled Tuning Element

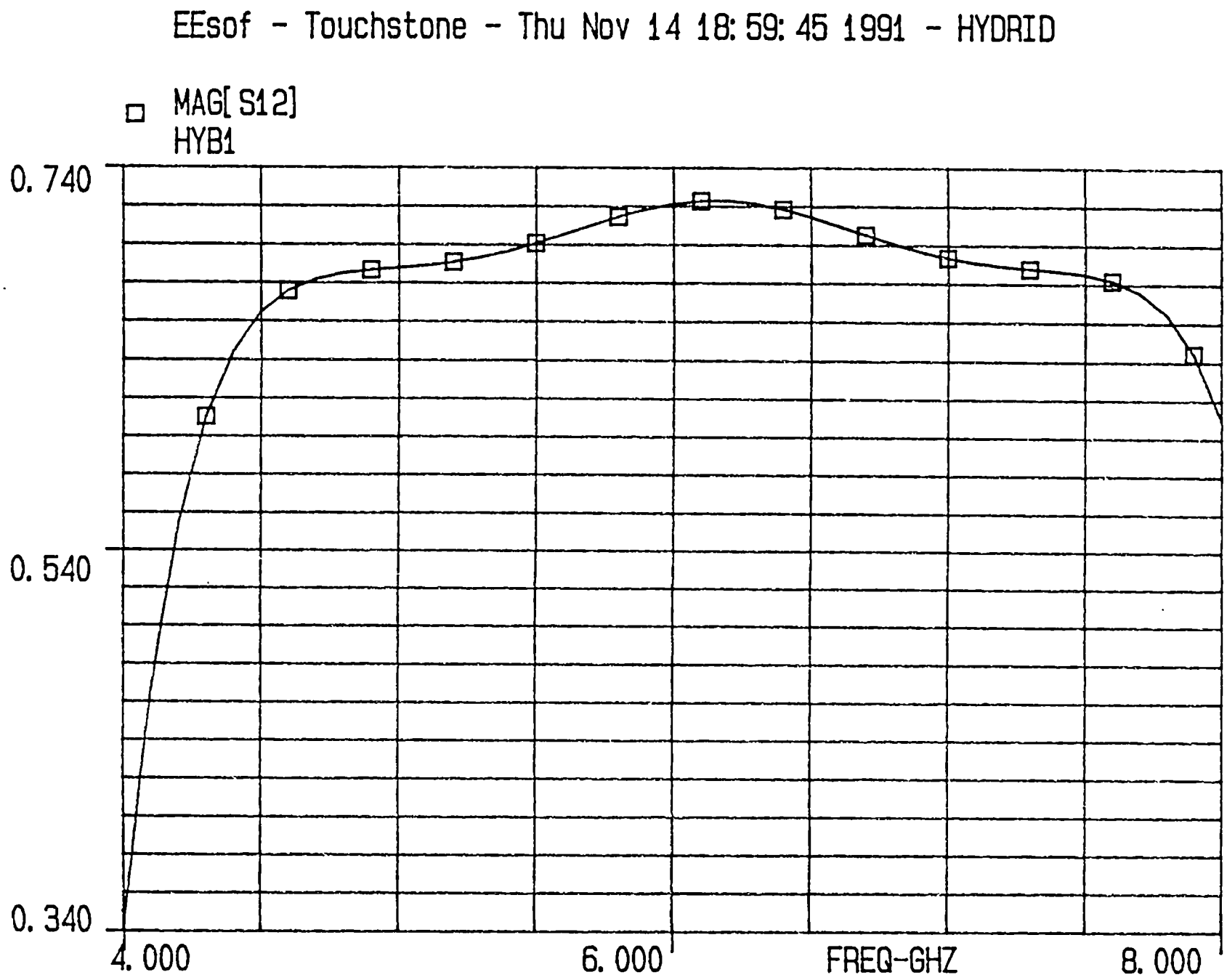

Figure (2.7(i)) Isolated Path - Branchline Coupler with Coupled Tuning Element

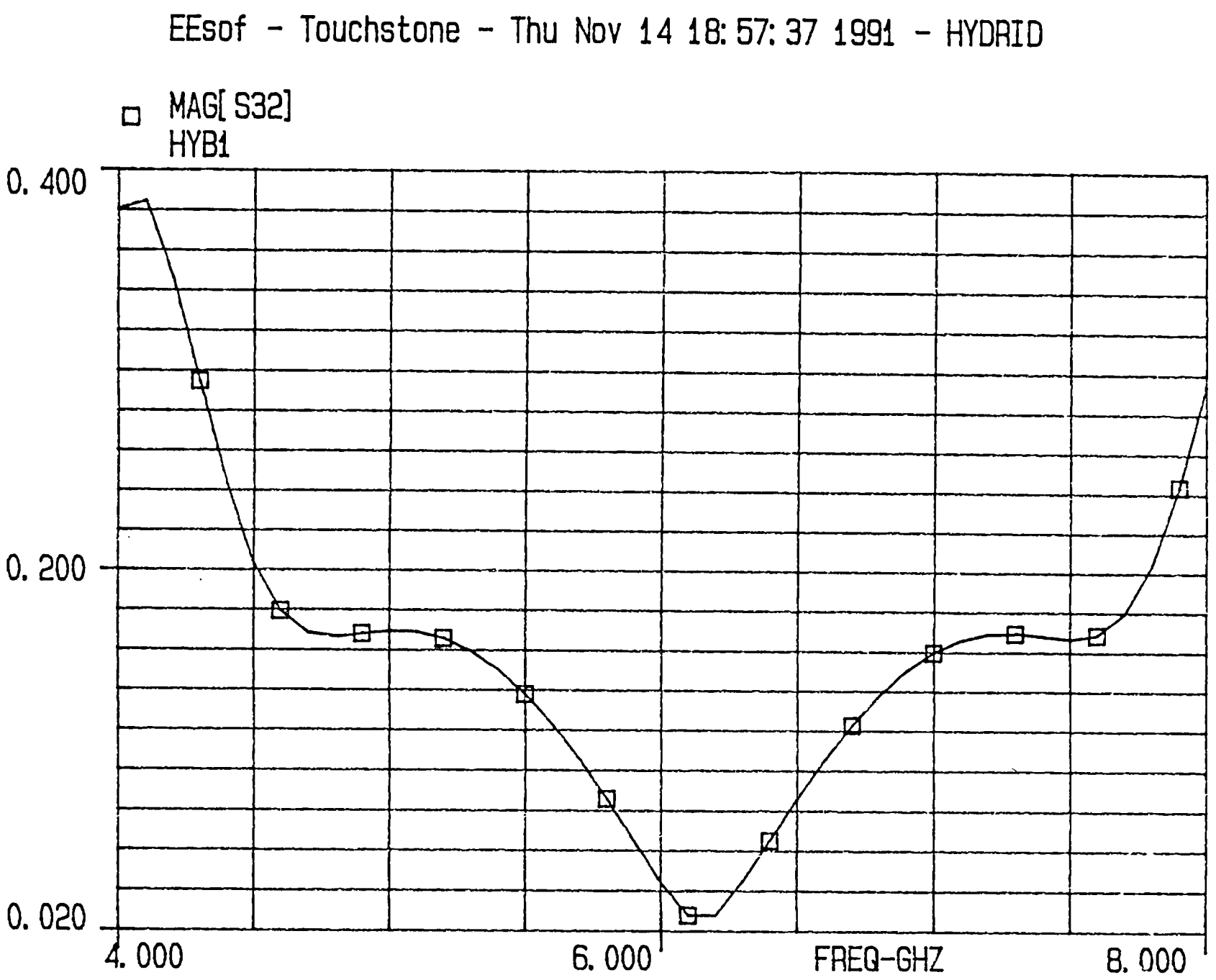

Figure (2.7(j)) Input Return Loss - Branchline Coupler with Coupled Tuning Element

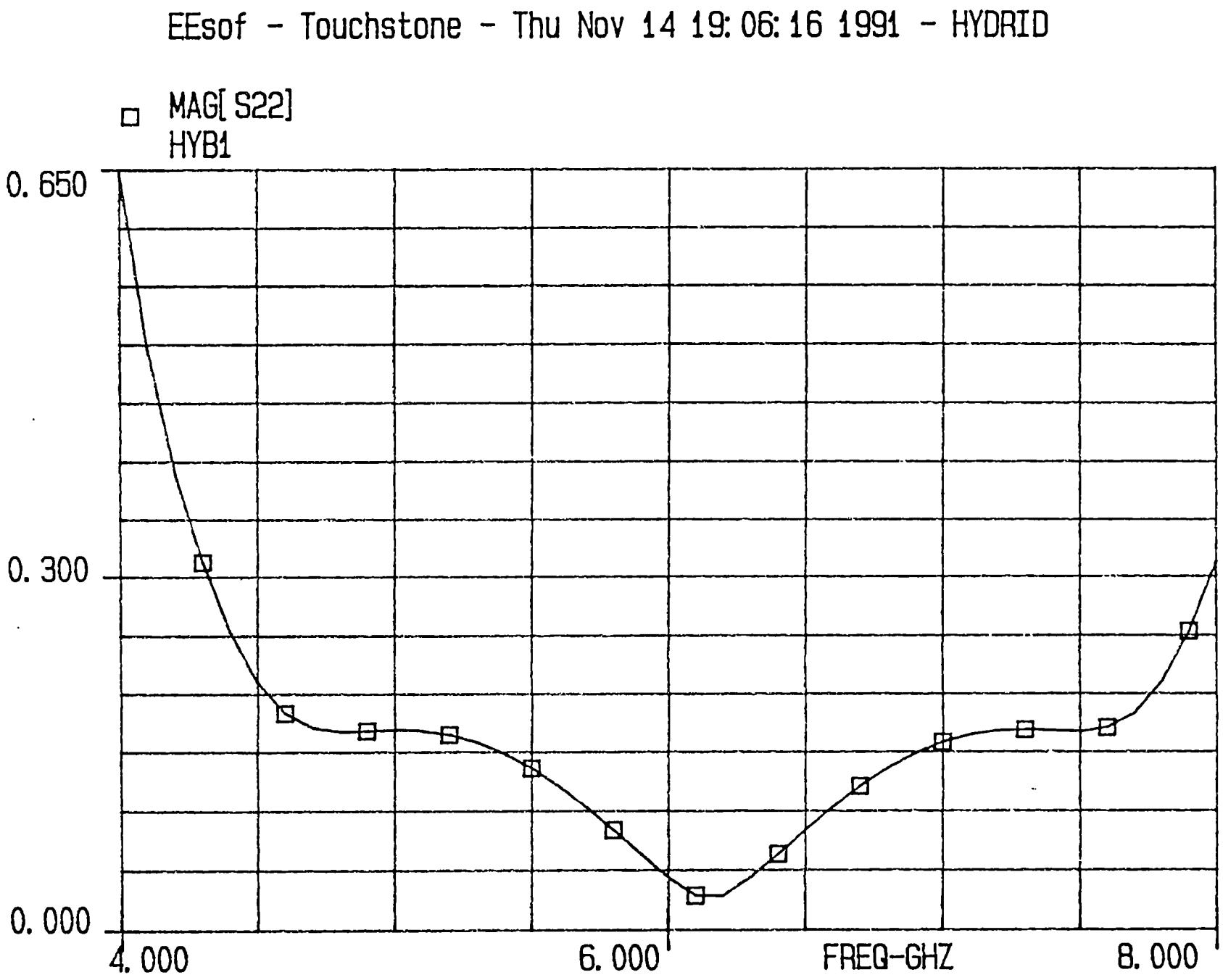

2.7.2 PORTS 2 AND 4 OPENED CIRCUITED

If in figure 2.2 ports 2 and 4 are both open circuited the equivalent circuit of the coupled line section becomes as shown in figure 2.7.

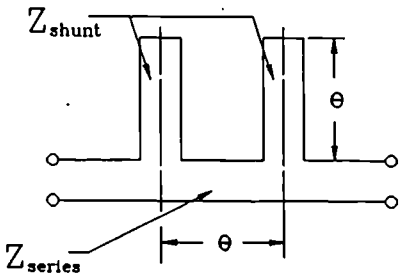

Figure 2.7 Equivalent Circuit

where

$$Z_{series} = \frac{Z_{oe} - Z_{oo}}{2} \qquad (2.47)$$

$$Z_{shunt} = Z_{oo} \qquad (2.48)$$

when $Z_{oe} > > Z_{oo}$,

$$Z_{series} = \frac{Z_{oe}}{2} \qquad (2.49)$$

and the equivalent series transmission line becomes an inductor when the terminating impedances are much lower than Z_{oe}. This is a technique of achieving impedance of greater than 250 ohms with easily manufacturable dimensions and without the excessive radiation and metal losses that would occur with a single microstrip. (The maximum manufacturable limit for single microstrip is approximately 150 ohms when $\epsilon_r = 10.$) This structure can additionally be used as a two stub tuner. When the structure in figure (2.5(a)) was cascaded with coupled lines as defined in this section the coupling band width exceeded an octave.

2.7.3 PORT 3 SHORT CIRCUITED/PORT 4 SHORT CIRCUITED

If ports 3 and 4 are both short circuited the equivalent circuit is as shown in figure 2.8

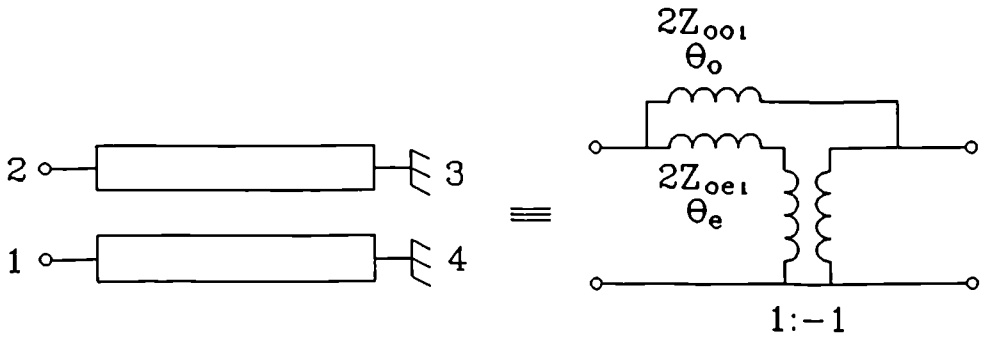

Figure 2.8 Equivalent Circuit Ports 3 and 4 Short Circuited

ABCD matrix elements are

$$A = \frac{Y_{oo}\cot\theta_o + Y_{oe}\cot\theta_e}{Y_{oo}\cot\theta_o - Y_{oe}\cot\theta_e} = D \qquad (2.50)$$

$$B = j\left[\frac{2}{Y_{oo}\cot\theta_o - Y_{oo}\cot\theta_e}\right] \qquad (2.51)$$

$$C = -j\left[\frac{2\,Y_{oo}\,Y_{oe}\cot\theta_o\cot\theta_e}{Y_{oo}\cot\theta_o - Y_{oe}\cot\theta_e}\right] \qquad (2.52)$$

when $Z_{oe} > > Z_{oo}$

$A = D = 1$

$B = j2Z_{oo}\tan\theta_o$

$C = -j2Y_{oe}\cot\theta_e$

if $Y_{oe} \rightarrow o$ then the configuration becomes a controllable low loss series inductor.

2.7.4 PORT 2 SHORT CIRCUITED/PORT 3 SHORT CIRCUITED

When ports 2 and 3 are short circuited the equivalent circuit is as shown in figure 2.10.

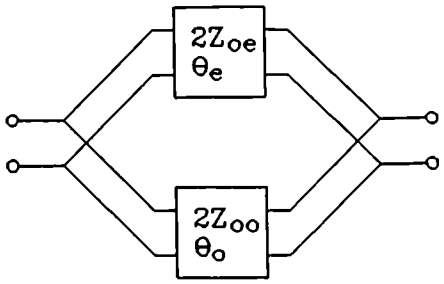

Figure 2.10 Equivalent Circuit Ports 2 and 3 Short Circuited.

ABCD matrix is

$$A = \frac{Y_{oe}\cot\theta_e + Y_{oo}\cot\theta_o}{Y_{oe}\,\mathrm{cosec}\,\theta_e + Y_{oo}\,\mathrm{cosec}\,\theta_o} = D \qquad (2.53)$$

$$B = j\left[\frac{2}{Y_{oe}\,\mathrm{cosec}\,\theta_e + Y_{oo}\,\mathrm{cosec}\,\theta_o}\right] \qquad (2.54)$$

$$C = j\frac{\left[Y_{oe}^2 + Y_{oo}^2 + 2\,Y_{oe}\,Y_{oo}\,(\mathrm{cosec}\,\theta_e\,\mathrm{cosec}\,\theta_o - \cot\theta_e\cot\theta_o)\right]}{2\left[Y_{oe}\,\mathrm{cosec}\,\theta_e + Y_{oo}\,\mathrm{cosec}\,\theta_o\right]} \qquad (2.55)$$

when $Y_{oo} > > Y_{oe}$

$A = \cos\theta = D$

$B = j2Z_{oo}\sin\theta_o$

$C = j\,\dfrac{\sin\theta_o}{2Z_{oo}}$

Using this circuit concept and multiple coupled lines such as the six strip coupled section described in chapter 4, where Z_{oo} of 12 ohms is achievable with ϵ_r = 9.8 and even lower Z_{oo} could be achieved with ϵ_r = 38 or higher, low impedance compact microwave sections can be realised. This fact should prove useful particularly in MMICs.

In addition as ϵ_r increases the physical single-strip line width below which transverse resonances occur decreases. This imposes a limit on the lowest impedance single strip line which can be realised. This limit frequently precludes the use of low enough impedance transmission lines in matching large gate periphery power GaAs FETs. In addition low impedance single lines are generally not used in GaAs MMICs due to the high substrate cost. Denlinger [1.4] has also shown that transverse current is proportional to w/λo and that the quasi-TEM approximation (J_z > > J_t) holds for

$$\frac{w}{\lambda_o} = \leq 0.1$$

where w is the width of the microstrip line and λ_o is wavelength in free space, J_z, J_t are longitudinal and transverse current densities respectively. This sets a quasi-TEM limit for microstrip width. The coupled line in figure (2.10) may be used to achieve low impedances without the disadvantages of wide single microstrip lines.

2.8 PROPOSED BROADBAND LOW FREQUENCY 180 DEGREE PHASE SPLITTER

There are several microwave applications such as push pull amplifiers and image reject mixers in which octave bandwidth 180 degree phase splitters are required at low frequencies ie. up to 6 GHz.

To date these devices have not been done in the planar distributed form which is compatible with other microwave integrated circuit components due to the prohibitively large circuit areas which would be required when conventional microstrip is used. The structure shown in figure (2.11) is proposed to fill this gap.

The structure consists of an inherently broadband input T - network feeding a pair of identical coupled spirals. Each spiral consists of two edge coupled microstrip lines. In the spiral fed by PATH 'A' the coupled lines are terminated as indicated in section 2.7.4, whereas the spiral fed by PATH 'B' is terminated as described in section 2.6

In order to achieve a very high (> 20) ratio of Z_{oe}/Z_{oo} the ground plane under the spirals is removed as shown in chapter (4).

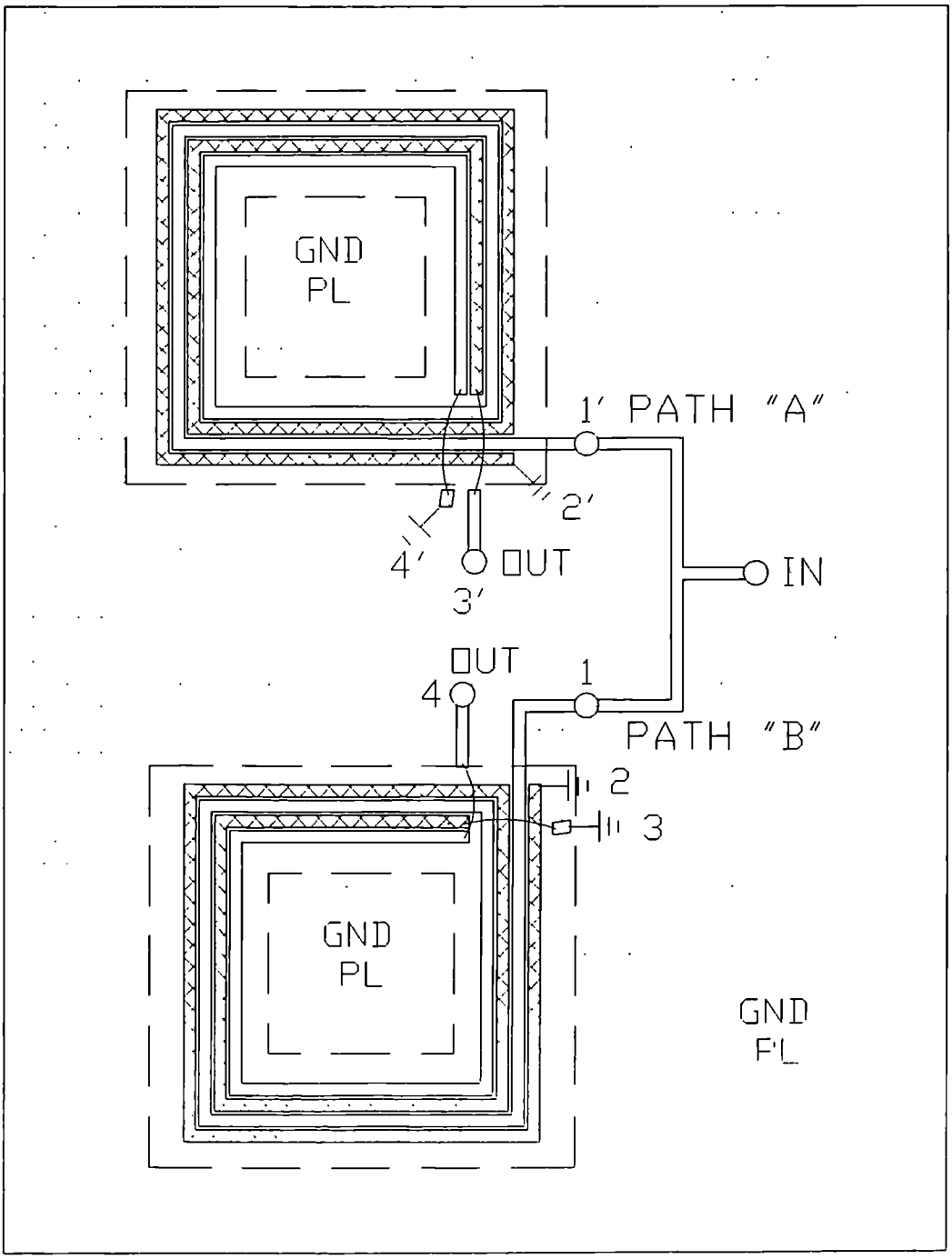

FIGURE 2.11 PROPOSED PLANER LOW FREQUENCY
180 DEGREE PHASE SPLITTER

Each spiral coupler is analyzed in the following way, assuming that quasi-static conditions hold; which is reasonable, considering the intended frequency of operation.

1. Treat the spiral as a cascade of 4 line couplers and impose the condition of current and voltage continuity between the couplers.

2. Calculate the even and odd mode capacitances of the four line structure by using the technique outlined in section (4.3).

3. Calculate the even and odd mode impedance of the four coupled lines Z_{oo}, Z_{oe} as done in section (4.3).

4. Calculate the even and odd mode admittance

$$Y_{oe} = \frac{1}{Z_{oe}}, \quad Y_{oo} = \frac{1}{Z_{oo}}$$

5. Calculate the chain matrix of each 4 strip section from the expression [2.8]

$$\begin{bmatrix} V_1 \\ V_2 \\ I_1 \\ I_2 \end{bmatrix} \begin{bmatrix} a_{11} & a_{12} & b_{11} & b_{12} \\ a_{21} & a_{22} & b_{21} & b_{22} \\ c_{11} & c_{12} & d_{11} & d_{12} \\ c_{21} & c_{12} & d_{11} & d_{12} \\ c_{21} & c_{22} & d_{21} & d_{22} \end{bmatrix} \begin{bmatrix} V_4 \\ V_3 \\ -I_4 \\ -I_3 \end{bmatrix} \qquad (2.56)$$

Where

$$a_{11} = a_{22} = d_{11} = d_{22} = \frac{1}{2} \cos(\theta_e + \cos\theta_o) \qquad (2.57(a))$$

$$a_{12} = a_{21} = d_{12} = d_{21} = \frac{1}{2} (\cos\theta_e - \cos\theta_o) \qquad (2.57(b))$$

$$b_{11} = b_{22} = \frac{j}{2} (Z_{oe}\sin\theta_e + Z_{oo}\sin\theta_o) \qquad (2.57(c))$$

$$b_{12} = b_{21} = \frac{j}{2} (Z_{oe}\sin\theta_e - Z_{oo}\sin\theta_o) \qquad (2.57(d))$$

$$c_{11} = c_{22} = \frac{j}{2} (Y_{oe}\sin\theta_e + Y_{oo}\sin\theta_o) \qquad (2.57(e))$$

$$c_{12} = c_{21} = \frac{j}{2} (Y_{oe}\sin\theta_e - Y_{oo}\sin\theta_o) \qquad (2.57(f))$$

and (2.56) is derived by considering two coupled lines as shown in figure (2.12), θ_e, θ_o are even and odd mode electrical lengths of the couplers.

6. The overall spiral performance is then calculated from the cascade matrix with the ports terminated as shown in figure (2.11)

To achieve quadrature phase shift the PATH 'B' spiral could be used alone, letting the length of the complete coupled section be

$$\theta = \frac{\pi}{2}$$

This structure should find an application in MMICs as well as in miniature hybrid microwave integrated circuits (MHMICs) in which the unit could be made very small by using high dielectric constant substrates such as $(Z_r S_n)\ T_i 0_4$, $\epsilon_r = 38$ or $BaO - Pbo - Nd_2O_3 - Ti\ O_2$, $\epsilon_r = 88$.

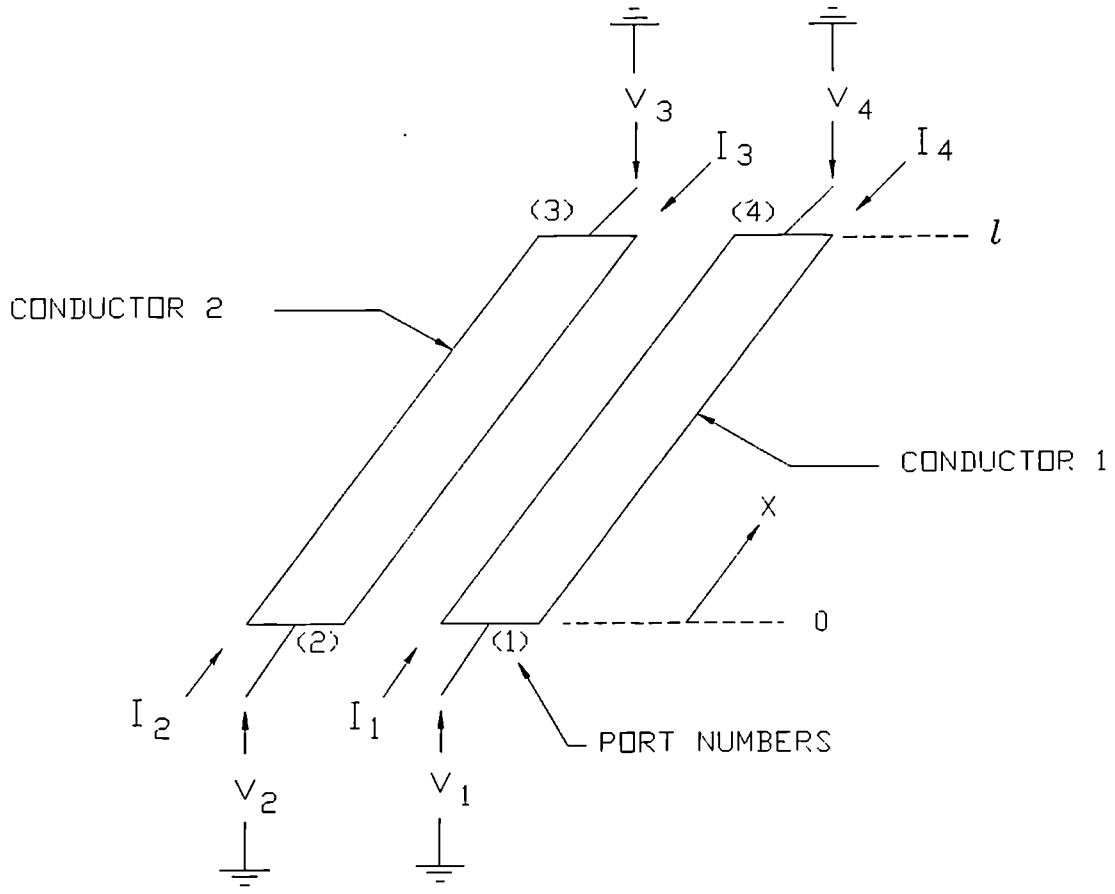

FIGURE 2.12. SCHEMATIC OF PAIP COUPLED-LINES EQUIVALENT [2.8]

REFERENCES

[2.1] John I. Hobdell, "Optimisation of Interdigital Capacitors"

IEEE Transactions on Microwave Theory and Techniques

Volume MTT-27, No. 9

September, 1979 Page 788-791

[2.2] Antonio Quaglia, "Use Coupled Lines to Achieve High Impedances in Microstrip"

Microwaves and RF October, 1983

Page 120 -127

[2.3] Lawrence Carin and Kevin J. Webb, "Isolation Effects in Single and Double Plane VLSI Interconnects"

IEEE Transactions on Microwave Theory and Techniques

Volume 28, No.4 April, 1990

Page 396 - 404

[2.4] E.M.T. Jones and J.T. Bolljohn, "Coupled-Strip Transmission Line Filters and Directional Couplers"

IRE Transactions on Microwave Theory,

Volume MTT-4 April, 1956 Page 75

[2.5] Edward G. Cristal, "Coupled Transmission-Line Directional Couplers with Coupled Lines of Unequal Characteristic Impedance"

IEEE Transactions on Microwave Theory and Techniques

Volume MTT-14, No.7 July, 19, 1966 Page 337-346

[2.6] Charles Buntchuh, "Octave Bandwidth, High Directivity Microstrip Coupler"

RADC Project # F30602-72-C-0282

[2.7] Mark K. Krage and George I. Haddad, "Characteristics of Coupled Microstrip Transmission Lines - I: Coupled-Mode Formulation of Inhomogeneous Lines"

IEEE Transactions on Microwave Theory and Techniques

Volume MTT-18, No.4 April, 1970 Page 217-222

[2.8] George I. Zysman and A. Kent Johnson, "Coupled Transmission Line Networks in an Inhomogeneous Dielectric Medium"

IEEE Transactions on Microwave Theory and Techniques

Volume, MTT-17, No. 10 October, 1989 Page 753-759

[2.9] Masayoshi Aikawa, "Wideband Stripline Reverse Phase Hybrid Ring in GHz Band"

Electronics and Communications in Japan

Volume 58B, No. 10 October, 1975 Page 521-528

[2.10] G. Matthaei, L. Young, E.M.T. Jones, "Microwave Filters, Impedance - Matching Networks and Coupling Structures"

Artech House Books Dedham, MA

[2.11] K.C. Gupta and Armjit Singh, "Microwave Integrated Circuits"

New York Wiley

1974 Page 73 - 85

[2.12] Bernd Mayer and Reinhard Knochel, "Branchline Couplers with Improved Design Flexibility and Broad Bandwidth"

IEEE MTT - Symposium Digest 1990

Page 391 - 394

CHAPTER 3

METHODS OF EVEN/ODD MODE PHASE VELOCITY EQUALISATION AND OF MAXIMISING EVEN TO ODD MODE CHARACTERISTIC IMPEDANCE RATIO

3.0 INTRODUCTION

As shown in chapter 2 equation (2.39) directivity is maximised when

$$\Delta = k_L - k_C = 0$$

for any two coupled lines.

A clearer relationship than (2.39) is obtained if we follow the approach of Napoli and Hughes [3.1] in which symmetric coupled lines are considered as this is the most commonly occurring situation.

Considering a coupling section length ℓ in which the spacing of the two lines do not vary with ℓ, then if the ports of the coupler are defined as in figure 2.2 and the further assumption is made that all ports are terminated in their characteristic impedance Zo then due to the symmetry assumption $L_1 = L_2 = L$, $C_1 = C_2 = C$. We can then write the even and odd mode wave numbers and a characteristic impedances β_{oe}, β_{oo}, Z_{oe}, Z_{oo} as follows:

$$\beta_{oe} = \omega\sqrt{LC} \qquad (3.1)$$

$$Z_{oe} = \sqrt{L/C} \qquad (3.2)$$

$$\beta_{oo} = \omega\sqrt{(L - 2M)(C + 2C_m)} \qquad (3.3)$$

$$Z_{oo} = \sqrt{(L - 2M)/(C + 2C_m)} \qquad (3.4)$$

Then assuming space variation exp ± j ϒ z, where ϒ = ± β_{oo}, ± β_{oe} indicating incident and reflected even and odd mode signals; as well as time dependence exp j ω t, then the scattering parameters of the system are given by [3.1]

$$S_{11} = \frac{\rho_e}{2}\left(1 - \frac{1 - \rho_e^2}{\exp(2j\beta_{oe}\ell) - \rho_e^2}\right) + \frac{\rho_o}{2}\left(1 - \frac{1 - \rho_o^2}{\exp(2j\beta_{oo}\ell) - \rho_o^2}\right) \qquad (3.5(a))$$

$$S_{21} = \frac{(1 - \rho_e^2)\exp(j\beta_{oe}\ell)}{2\{\exp(2j\beta_{oe}\ell) - \rho_e^2\}} + \frac{(1 - \rho_o^2)\exp(j\beta_{oo}\ell)}{2\{\exp(2j\beta_{oo}\ell) - \rho_o^2\}} \qquad (3.5(b))$$

$$S_{31} = \frac{\rho_e}{2}\left(1 - \frac{1 - \rho_e^2}{\exp(2j\beta_{oe}\ell) - \rho_e^2}\right) - \frac{\rho_o}{2}\left(1 - \frac{1 - \rho_o^2}{\exp(2j\beta_{oo}\ell) - \rho_o^2}\right) \qquad (3.5(c))$$

$$S_{41} = \frac{(1 - \rho_e^2)\exp(j\beta_{oe}\ell)}{2\{\exp(2j\beta_{oe}\ell) - \rho_e^2\}} - \frac{(1 - \rho_o^2)\exp(j\beta_{oo}\ell)}{2\{\exp(2j\beta_{oo}\ell) - \rho_o^2\}} \qquad (3.5(d))$$

Where

$$\rho_e = -\left(1 - \frac{Z_{oe}}{Z_o}\right)/\left(1 + \frac{Z_{oe}}{Z_o}\right)$$

$$\rho_o = -\left(1 - \frac{Z_{oo}}{Z_o}\right)/\left(1 + \frac{Z_{oo}}{Z_o}\right)$$

When

$$\beta_{oo}\ell = \beta_{oe}\ell = \frac{\pi}{2}$$

and the coupler is matched ie.

$$S_{11} = 0,\ Z_{oe}Z_{oo} = Z_o^2 \text{ and } \rho_e = -\rho_o = \rho$$

then equation (3.5) reduces to

$$S_{11} = \frac{\rho_e}{1 - \rho_e^2} + \frac{\rho_e}{1 + \rho_o^2} = 0 \qquad (3.6(a))$$

$$S_{21} = \frac{j}{2}\left(\frac{1 - \rho_e^2}{1 + \rho_e^2} + \frac{1 - \rho_o^2}{1 + \rho_o^2}\right) = -j\left(\frac{1 - \rho^2}{1 + \rho^2}\right) \qquad (3.6(b))$$

$$S_{31} = \frac{\rho_e}{1 + \rho_e^2} - \frac{\rho_o}{1 + \rho_o^2} = \frac{2\rho}{1 + \rho^2} \qquad (3.6(c))$$

$$S_{41} = -\frac{j}{2}\left(\frac{1 - \rho_e^2}{1 + \rho_e^2} - \frac{1 - \rho_o^2}{1 + \rho_o^2}\right) = 0 \qquad (3.6(d))$$

Therefore for these conditions, directivity of the coupler

$$= \left|\frac{S_{31}}{S_{41}}\right| \rightarrow \infty \text{ from (3.6(c)) and (3.6(d))}$$

When the phase velocities of the two modes are uneven

ie.

$$\beta_{oe} \neq \beta_{oo}$$

then

$$S_{41} \neq 0$$

Since

$$\rho_e = -\rho_o = \rho$$

continues to hold, and

$$(\beta_{oe} + \beta_{oo})\,\ell = \pi$$

then

$$S_{41} \approx \frac{\pi}{4}\left(\frac{1-\rho^2}{1+\rho^2}\right)\left(\frac{\beta_{oe}-1}{\beta_{oo}}\right) \qquad (3.7)$$

and directivity is

$$\left|\frac{S_{31}}{S_{41}}\right| \approx \left(\frac{4}{\pi\,(1-|S_{31}|^2)} \cdot \frac{|S_{31}|}{\frac{\beta_{oe}}{\beta_{oo}} - 1}\right)^2 \qquad (3.8)$$

Therefore as the ratio β_{oe}/β_{oo} increases, directivity degrades. It is also noted that when $\beta_{oo} \neq \beta_{oe}$ directivity is dependent on coupling and degrades as coupling decreases (or as the dielectric constant of the substrate is increased). Alexopoulous et al [3.5] has indicated that a 10 percent difference between β_{oo} and β_{oe} results in a directivity degradation of a 10 dB coupler to 13 dB from its theoretical directivity of infinity. β_{oo} is usually

greater than β_{oe} for edge coupled lines.

Since many practical coupler applications require loose coupling, it is therefore important to examine ways of equalising β_{oe} and β_{oo}.

3.2 TECHNIQUES OF EQUALIZING β_{oo} and β_{oe}

Among the techniques used to equalise β_{oo} and β_{oe} are the following:

1. Edge coupled lines with dielectric overlay. [3.2]
2. Edge coupled lines on more than one substrate but with no overlay. [3.2]
3. Broadside coupled lines with overlay. [3.2]
4. Broadside coupled lines on more than one substrate but with no overlay. [3.2]
5. The serpentine or wiggling approach. [3.3]
6. Overlay with floating strip. [3.4]
7. Broadside coupled strips in rectangular waveguide with air gap. [3.2]
8. The use of substrate anisotropy in conjunction with the variation of the distance of the box lid to the coupled microstrip. [3.5], [3.6]
9. Edge coupled microstrip line with tuning septum.

Methods (1) through (6) have been covered in several papers and will not be addressed further here. Methods (6), (7) and (8) have been less used and will be considered in more detail.

3.2.1 Broadside Coupled Strips in Rectangular Waveguide

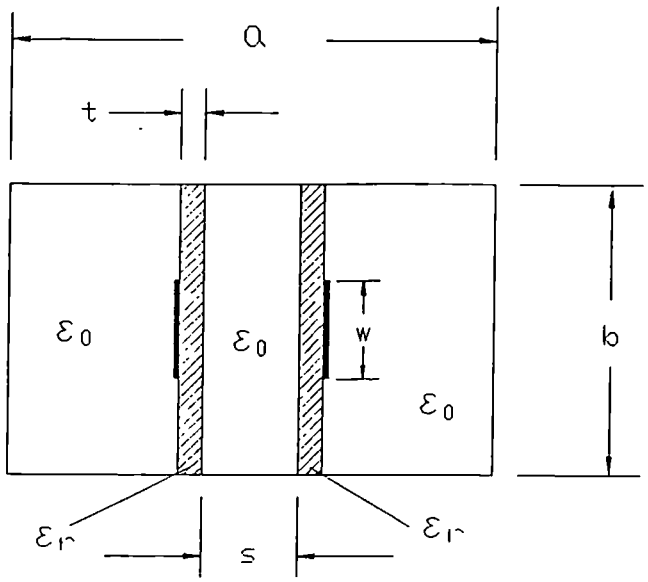

Figure (3.1) Broadside Coupled Lines in Rectangular Waveguide

As in figure (3.1) two strips on high dielectric constant substrates are mounted parallel to the E-field of the rectangular waveguide. The performance of this coupler is dependent on the degree of dielectric anisotropy of the substrate as-well-as the dimensions s and (a-s)/2; as will be shown later.

Horno and Medina [3.2] has shown by the variational technique in the spectral domain and assuming quasi-static conditions that for WR-28 waveguide (a = 7.11 mm, b = 3.56 mm) using Epsilon 10 (ϵ_x = 13.0, ϵ_y = 10.2) then $\beta_{oo} = \beta_{oe}$ at S≈ = 0.2 mm. For

Sapphire (ϵ_x = 9.4, ϵ_y = 11.6), then $\beta_{oo} = \beta_{oe}$ at S ≈ 0.42 mm. This technique of equalising β_{oo} and β_{oe} is easier to implement than other broadside techniques since the air dielectric allows easy adjustment of S.

3.2.2 Use of Substrate Anisotropy in Conjunction with Lid Height

Alexopoulous and Maas [3.5] have shown that if an anisotropic substrate supports coupled lines, then the degree of inequality between β_{oo} and β_{oe} is controllable by the substrate anisotropy and, if (ϵ_{par}) the permittivity in the direction of the ground plane is greater than (ϵ_{perp}), the perpendicular component, the odd mode phase velocity is reduced relative to the even mode. The two mode velocities are equal when $\epsilon_{par} \approx 2\ \epsilon_{perp}$ (3.9).

The condition expressed in equation (3.9) is generally not naturally occurring, however, and phase velocity equalisation is in practice realised through the use of composite anisotropic dielectrics [3.6], [3.7].

An outline of the analysis technique based on [3.6] is given below

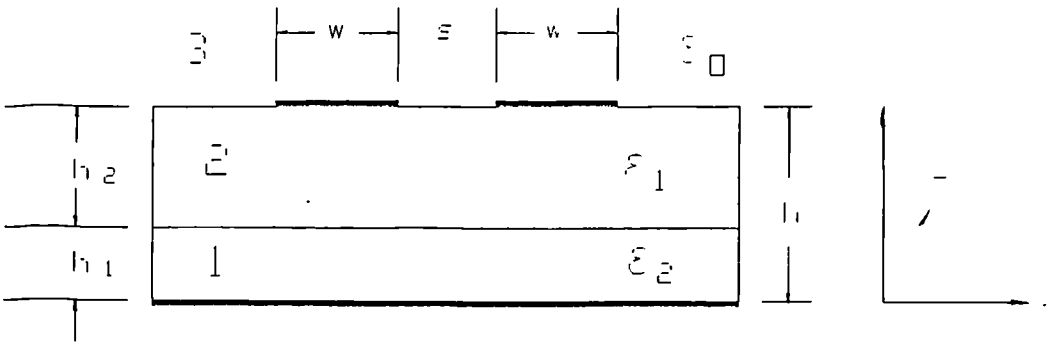

Figure (3.2) Coupled Microstrip on Double Anisotropic Substrate

Considering figure (3.2) in which the permittivity of the two regions are tensors represented by

$$\bar{\epsilon}_i = \epsilon_o \begin{bmatrix} \epsilon_i^{11} & \epsilon_i^{12} \\ \epsilon_i^{12} & \epsilon_i^{22} \end{bmatrix} \qquad (3.10)$$

where i = 1,2.

Then assuming infinitely thin strips and imposing the quasi-TEM condition the scalar potential is the solution of Laplace's equation which in this case is

$$\bar{\nabla} . (\epsilon_i \bar{\nabla} \phi_i(x,y)) \qquad (3.11)$$

The general solution of which, in the spectral domain, is [3.6]

$$\phi_i(\beta,y) = \{(A_i \sinh \beta R_i y) + B_i \cosh(\beta R_i y)\} \exp(-j\beta S_i y) \qquad (3.12)$$

where β is the transform variable and

$$R_i = \{ \epsilon_i^{11}/\epsilon_i^{22} - (\epsilon_i^{12}/\epsilon_i^{22})^2 \}^{1/2} \qquad (3.13(a))$$

$$S_i = \epsilon_i^{12}/\epsilon_i^{22} \qquad (3.13(b))$$

A_i, B_i are constants which are determined by applying the boundary conditions applicable to the system.

Horno and Medina have shown that the fourier transformed Green's function is

$$g(\beta) = \{ \beta \left(1 + \epsilon_2^m \left[\frac{\epsilon_2^m + \epsilon_1^m \coth(\beta h_i^m) \coth(\beta h_2^m)}{\epsilon_2^m \coth(\beta h_2^m) + \epsilon_1^m \coth(\beta h_i^m)} \right] \right\}^{-1} \qquad (3.14)$$

where

$$\epsilon_i^m = (\epsilon_i^{11} \epsilon_i^{22} - \epsilon_i^{12})^{1/2}$$

$$h_i^m = R_i h_i \quad i=1,2$$

Knowing the Green's function; the characteristic impedance and effective dielectric constant (leading to β_{oo}, β_{oe}) can be found by the variational method or by the spectral domain technique covered in chapters 1 and 4.

The analysis was done [3.6] for Boron Nitride in region 1 and Sapphire in region 2; where the permittivity tensor components are: for Boron Nitride

$$\epsilon_1^{11} = 5.12,\ \epsilon_1^{22} = 3.4,\ \epsilon_1^{12} = 0$$

for Sapphire

$$\epsilon_2^{11} = 9.40,\ \epsilon_2^{22} = 11.6,\ \epsilon_2^{12} = 0$$

The superscripts '11' refer to the x-axis and '22' to the y-axis. It was found that there were two values of the ratio h_2/h for which $\beta_{oe} = \beta_{oo}$ and this proves that the composite anisotropic dielectric configuration can be used for even and odd mode phase velocity compensation in edge coupled microstrip lines by using the appropriate thickness of each dielectric layer. Alexopoulous [3.5] has also shown that it is possible with a single anisotropic substrate to equalise β_{oo} and β_{oe} by appropriate choice of lid position.

3.2.3 Edge Coupled Lines with Tuning Septums

As shown in section (4.2) it is possible to equalise β_{oo} and β_{oe} for coupled lines on an isotropic substrate by optimising the dimension G in figure (4.1). This is a simple method of achieving phase velocity equalisation, the even mode impedance is however simultaneously increased by the presence of the gap in the ground plane leading to tighter coupling for a given spacing s. As stated earlier in this chapter, the need for β_{oo}, β_{oe} equalisation techniques decreases as coupling factor increases; therefore this technique would be of limited usefulness unless either wide strip spacing or wide strip widths are used. If wide strip widths are used careful attention must then be given to the possible onset of higher order modes.

3.3 Method of Increasing Z_{oe}/Z_{oo} Ratio

Referring to equation (1.29) it is clear that to maximise Z_{oe}/Z_{oo} its necessary to minimise C_s^e, maximise C_s^o or do both simultaneously.

3.3.1 Minimising C_s^e

One important technique of minimising C_s^e is the use of the configuration in figure (4.1) where Z_{oe}/Z_{oo} ratio greater than 5 is seen to be practical.

3.3.2 Maximising C_s^o

Techniques for maximising C_s^o include:

1. The use of multistrip structures such as the lange coupler [3.8].
2. The use of a second metallised substrate mounted perpendicular to the plane of the coupled strips as shown in figure (3.3) [3.9].

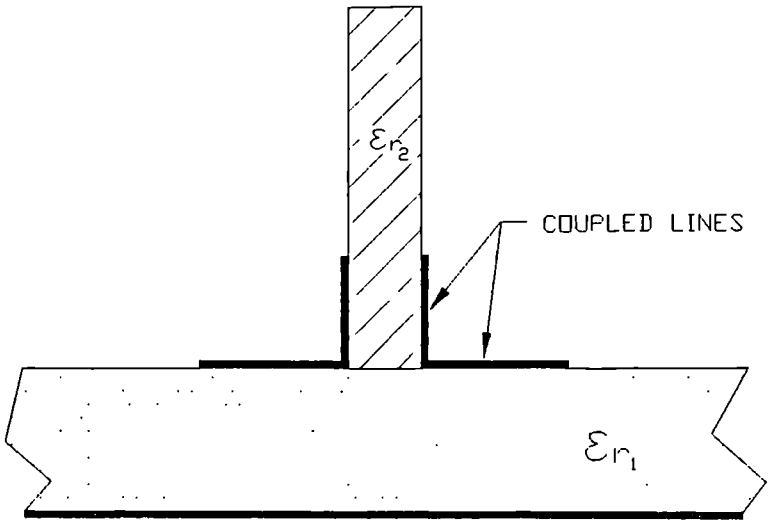

Figure (3.3) Vertically Integrated Coupler

In this configuration ϵ_{r1} determines Z_{oe} and ϵ_{r2} determines Z_{oo}. The two impedances can be changed almost independently. Z_{oe}/Z_{oo} ratios greater than 5.7 have been achieved with this technique. This structure offers the added characteristic of equalised β_{oo} and β_{oe} for correctly chosen ϵ_{r1}, ϵ_{r2} and height of the metallisation on the vertical section.

3.3.3 Decreasing C_s^e and Increasing C_s^o Simultaneously

Techniques of simultaneously decreasing C_s^e and increasing C_s^o include:

(1) The use of broadside coupled suspended microstrip. Whereas very low odd mode impedance is possible a large ratio of β_{oo} to β_{oe} can be produced unless specific precautions are taken.

(2) The use of multiple strips with tuning septums. As shown in chapter 4; Z_{oe}/Z_{oo} ratio of greater than 20 is possible with this technique.

REFERENCES

[3.1] L.S. Napoli and J.J. Hughes, " Characteristics of Coupled Microstrip Lines"

RCA Review September, 1970

Page 479 - 498

[3.2] Manuel Horno and Francisco Medina, "Multilayer Planar Structures for High Directivity Directional Coupler Design"

IEEE Transactions on Microwave Theory and Techniques

Volume MTT-34, No.12 December,1986

Page 1442-1449

[3.3] F.C. deRonde, "Wideband High Directivity in MIC Proximity Couplers by Planar Means"

Page 480 - 482

[3.4] Mark K. Krage and George I. Haddad, "Characteristics of Coupled Microstrip Transmission Lines: Sections I and II"

IEEE Transactions on Microwave Theory and Techniques

Volume, MTT-18, No.4 April, 1970

Page 217 - 228

[3.5] Nicolaos G. Alexopoulous and S.A. Maas, " Characteristics of Microstrip Directional Couplers on Anisotropic Substrates"

IEEE Transactions on Microwave Theory and Techniques

Volume MTT-30, No. 8 August, 1982

Page 1267-1270

[3.6] Manuel Horno and Ricardo Marques, "Coupled Microstrip on Double Anisotropic Layers"

IEEE Transactions on Microwave Theory and Techniques

Volume, MTT-32, No.4 April, 1984

Page 467 - 470

[3.7] Ricardo Marques, Manuel Horno and Francisco Medina, " A New Recurrence Method for Determining the Green's Function of Planar Structures with Arbitrary Anisotropic Layers"

IEEE Transactions on Microwave Theory and Techniques

Volume, MTT-33, No. 5 May, 1985

Page 424 - 428

[3.8] Vitorio Rizzoli and Alesandro Lipparini, "The Design of Interdigitated Couplers for MIC Applications"

IEEE Transactions on Microwave Theory and Techniques

Volume, MTT-26, No.1 January, 1978

Page 7 - 15

[3.9] Yoshihiro Konishi et al "A Directional Coupler of a Vertically Installed Planar Circuit Structure"

IEEE Transactions on Microwave Theory and Techniques

Volume 36, No. 6 June, 1988

Page 1057-1063

[3.10] I.J. Bahl and Prakash Bhartia, "Characteristics of Inhomogeneous Broadside Coupled Striplines"

IEEE Transactions on Microwave Theory and Techniques

Volume MTT-28, No.6 June, 1980

Page 529 - 535

CHAPTER 4

COUPLED MICROSTRIP WITH GROUND PLANE SEPTUM

4.0 INTRODUCTION

One technique of achieving high even to mode impedance ratios in planar coupled microstrip structures is shown in figure (4.1) below. The analysis technique is based on the spectral domain method by Itoh [5.1]. The major contribution of this section is to fill in the blanks left by Itoh, to express the fourier transforms of the charge distribution functions in a form, which can be processed easily on a personal computer. In addition, it is shown, by comparison with the Bryant-Weiss results that, whereas impedances using this method with two basis functions of the type described by Itoh and others, is adequate for practical coupler designs, they do not completely agree with Bryant-Weiss. The disagreement is such that the spectral domain method is likely to be the one in error, as shown later in this chapter. The method is then applied to the analysis of a six strip 0.9 dB broadband coupler. In addition it is shown that the analysis of figure (4.1) can be used to simplify the analysis of broadside coupled lines with tuning septums. So far as the author is aware these have not been done before.

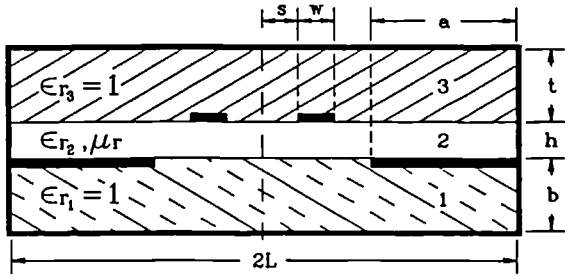

Figure 4.1 Cross-section of two coupled microstrip lines with tuning septum

4.1 THE TWO STRIP CASE

In figure 4.1 $\epsilon_{r1} = \epsilon_{r3=1}$, $\epsilon_{r2} = \epsilon r>1$, $\mu_{r=1}$. ϵ_{r2} is, in addition isotropic and purely real. The conductor strips are of infinitesimal thickness and are perfect conductors.

Due to the symmetry of the structure it can be analyzed in terms of even and odd modes with symmetry axis at x=0. The quasi-TEM approximation is assumed and Poisson's equation is solved subject to the boundary conditions applicable to the structure.

The regions of the structure are designated 1, 2, and 3 as shown bounded by a conducting enclosure. Using the designations in [5.1] the following boundary conditions are applicable:

$$\phi_1 (x,b) = \phi_2 (x,b), \; 0 < x < L \qquad (4.1(a))$$

$$\phi_1 (x,b) = 0, \; L-a < x < L \text{ (on the septum)} \qquad (4.1(b))$$

$$\phi_1 (x,b) = v(x), \; 0 < x < L-a \text{ (on the dielectric/air interface)} \qquad (4.1(c))$$

And considering the normal component of displacement to the dielectric boundary

$$\epsilon_r \frac{d}{dy}\phi_2 \Big|_{y=b} - \frac{d}{dy}\phi_1 \Big|_{y=b} = \frac{-\rho_s(x)}{\epsilon_0} \quad , L-a < x < L \text{ (on the septum)} \qquad (4.1(d))$$

$$= 0 \quad , 0 < x < L-a \text{ (on the dielectric)}$$

$$\phi_2(x, b+h) = \phi_3(x, b+h) \quad , 0 < x < L \text{ (at the region 2/3 interface)} \qquad (4.2(a))$$

$$\phi_2(x, b+h) = \phi_v(x) = V, \; S < x < S+W \text{ (on the microstrip)} \qquad (4.2(b))$$

$$= \phi_o(x) \quad , 0 < x < s \text{ and } s+w < x < L$$

$$\frac{d}{dy}\phi_3 \Big|_{y=b+h} - \epsilon_r \frac{d}{dy}\phi_2 \Big|_{y=b+h} = \frac{-\rho(x)}{\epsilon_o} \quad , (s < x < s+w) \qquad (4.2(c))$$

$$= 0 \quad , o < x < s \text{ and } s+w < x < L$$

$$\phi_i(0, y) = 0 \qquad i = 1, 2, 3 \qquad (4.3(a))$$

on the conducting walls of the enclosure. At x = o

$$\frac{d}{dx}\phi_i = 0 \text{ on the magnetic wall (Newmann Condition)} \qquad (4.3(b))$$

$$\phi_i(o, y) = 0 \qquad (4.3(c))$$

on the electric wall (Derichlet Condition) $\Phi_1(x,y)$, $\Phi_2(x,y)$, $\Phi_3(x,y)$ are scalar electric potential functions in the regions 1, 2

and 3. V is the known potential on the strip, ϵ_o permittivity of free space, $\rho(x)$, $\rho_s(x)$ are charge density distributions on the strip and the septum respectively and are unknowns, $v(x)$ and $\Phi_o(x)$ are unknown potential distributions at the dielectric interfaces between regions (1) and (2) and (2) and (3).

To determine the capacitance per unit length and therefore even and odd mode impedances and effective dielectric constants the two dimensional Poisson's equation is solved in the Fourier transform domain using the sine and cosine transform expressions listed below:

$$\tilde{\phi}(n,y) = \int_o^L \phi(x,y) \cos k_n x \, dx \qquad (4.4(a))$$

$$\text{where } k_n = \frac{n-\frac{1}{2}}{L}\pi$$

$$n = 1, 2, ---\infty$$

$$\tilde{\phi}(n,y) = \int_o^L \phi(x,y) \sin k_n x \, dx \qquad (4.4(b))$$

$$\text{where } k_n = \frac{n\pi}{L}$$

$$n = 1, 2, ---\infty$$

Equations (4.4(a)) and (4.4(b)) refer to the even and odd modes respectively and are chosen to satisfy the enclosure boundary conditions of equations (4.3(a)), (4.3(b)), (4.3(c)). Considering the general charge distribution ρ(x,y) we can write

$$\rho\,(x,y) = f(x)\,\delta\,(y-b-h) \qquad (4.5)$$

where δ(y-b-h) is the Dirac delta. The Poisson's equation for the potential distribution Φ_i is

$$\nabla^2 \phi_i\,(x,y) = \frac{-\rho}{\epsilon} \qquad (4.6(a))$$

When y ≠ b + h and y ≠ b, Laplaces equation is obtained.

$$\nabla^2 \phi_i\,(x,y) = 0 \qquad (4.6(b))$$

Taking the Fourier transform of Φ_i (x,y) we get

$$\tilde{\phi}_i[n,y] = \int_o^L \phi_i\,(x,y)\,\exp[jk_x x]dx$$

Applying this to (4.6(b)) we get

$$\frac{d^2}{dy^2}\,\tilde{\phi}_i\,(n,y) - k_n^2\,\tilde{\phi}_i\,(n,y) = 0 \qquad (4.7)$$

The solutions of equation (5.7) are:

$$\tilde{\Phi}_1(n,y) = A_n \sinh[k_n y] \qquad (4.8)$$

$$\tilde{\Phi}_2(n,y) = B_n^s \sinh[k_n (y-b)] + B_n^c \cosh[k_n (y-b)] \qquad (4.9)$$

$$\tilde{\Phi}_3(n,y) = C_n \sinh[k_n (d-y)] \qquad (4.10)$$

Taking transforms of the boundary conditions (4.1) and (4.2) gives

$$\tilde{\Phi}_1(n,b) = \tilde{\Phi}_2(n,b) \qquad (4.11(a))$$

$$\tilde{\Phi}_1(n,b) = \tilde{V}(n) \qquad (4.11(b))$$

$$\epsilon_r \frac{d}{dy}\tilde{\Phi}_2|_{y=b} - \frac{d}{dy}\tilde{\Phi}_1|_{y=b} = \frac{-\tilde{\rho}_s(n)}{\epsilon_o} \qquad (4.11(c))$$

$$\tilde{\Phi}_2(n,b+h) = \tilde{\Phi}_3(n,b+h) \qquad (4.12(a))$$

$$\tilde{\Phi}_2(n,b+h) = \tilde{\Phi}_v(n) + \tilde{\Phi}_o(n) \qquad (4.12(b))$$

$$\frac{d}{dy}\tilde{\Phi}_3|_{y=b+h} - \epsilon_r \frac{d}{dy}\tilde{\Phi}_2|_{y=b+h} = -\left[\frac{\rho(n)}{\epsilon_o}\right] \qquad (4.12(c))$$

and taking transforms of the functions

$$\tilde{V}_e(n) = \int_o^{(L-a)} V(x) \cos k_n x dx \qquad (4.13(a)) \text{ even mode}$$

$$\tilde{V}_o(n) = \int_o^{(L-a)} V(x) \sin k_n x dx \qquad (4.13(b)) \text{ odd mode}$$

$$\tilde{\rho}_s(n) = \int_{(L-a)}^{L} \rho_s(x) \cos k_n x dx \qquad (4.14(a)) \text{ even mode}$$

$$\tilde{\rho}_s(n) = \int_{L-a}^{L} \rho_s(x) \sin k_n x dx \qquad (4.14(b)) \text{ odd mode}$$

$$\tilde{\phi}_e(n) = \int_o^{s} \phi_v(x) \cdot \cos k_n x dx + \int_{s+w}^{L} \phi_o(x) \cos k_n x dx \qquad (4.15(a)) \text{ even mode}$$

$$\tilde{\phi}_o(n) = \int_o^{s} \phi_v(x) \sin k_n x dx + \int_{s+w}^{L} \phi_o(x) \sin k_n x dx \qquad (4.15(b)) \text{ odd mode}$$

$$\tilde{\rho}_e(n) = \int_s^{(s+w)} \rho(x) \cos k_n x dx \qquad (4.16(a)) \text{ even mode}$$

$$\tilde{\rho}_o(n) = \int_s^{(s+w)} \rho(x) \sin k_n x dx \qquad (4.16(b)) \text{ odd mode}$$

$$\tilde{\Phi}_v(n) = \int_s^{(s+w)} V\cos k_n x\,dx \qquad (4.17(a)) \text{ even mode}$$

$$\tilde{\Phi}_v(n) = \int_s^{(s+w)} V\sin k_n x\,dx \qquad (4.17(b)) \text{ odd mode}$$

Substituting (4.8) and (4.9) or (4.10) into (4.11(a)), (4.11(c)), (4.12(a)) and (4.12(c)) results in the following:

$$A_n \sinh k_n b = B_n^c \qquad (4.18(a))$$

$$\frac{d}{dy}\tilde{\Phi}_2 = k_n B_n^s \cosh k_n(y-b) + k_n B_n^c \sinh k_n(y-b) \qquad (4.18(b))$$

$$\frac{d}{dy}\tilde{\Phi}_1 = k_n A_n \cosh k_n y \qquad (4.18(c))$$

Substituting (4.8) and (4.9) into (4.11(c)) we get

$$\epsilon_r k_n B_n^s - k_n A_n \cosh k_n b = \frac{\tilde{\rho}_s(n)}{\epsilon_o} \qquad (4.19)$$

Substituting (4.9) and (4.10) into (4.12(a)) we get

$$B_n^s \sinh k_n h + B_n^c \cosh k_n h = c_n \sinh k_n(d-b-h) \qquad (4.20)$$

Or

$$B_n^s \sinh k_n h + B_n^c \cosh k_n h = c_n \sinh k_n (t) \qquad (4.20)$$

From (4.10)

$$\frac{d}{dy} \tilde{\Phi}_3 = -k_n C_n \cosh k_n (d-y) = -k_n C_n \cosh (k, t)|_{y=b+h} \qquad (4.21)$$

From (4.9)

$$\frac{d}{dy} \tilde{\Phi}_2 = k_n B_n^s \cosh k_n (y-b) + k_n B_n^c \sinh k_n (y-b)\,|_{y=b+h}$$

$$= k_n B_n^s \cosh k_n h + k_n B_n^c \sinh k_n h \qquad (4.22)$$

Substituting (4.8) and (4.9) into (4.12(c)) we arrive at

$$C_n \cosh k_n t + \epsilon_r B_n^s \cosh k_n h + \epsilon_r B_n^c \sinh k_n h = \frac{\tilde{\rho}(n)}{\epsilon_o k_n} \qquad (4.23)$$

therefore we have 4 equations for 4 unknowns

$$A_n \sinh k_n b - B_n^c = 0$$

$$A_n k_n \cosh k_n b - \epsilon_r k_n B_n^s = \frac{\tilde{\rho}_s(n)}{\epsilon_o}$$

$$B_n^c \cosh k_n h + B_n^s \sinh k_n h - C_n \sinh k_n t = 0$$

$$\epsilon_r B_n^c \sinh k_n(h) + \epsilon_r B_n^s \cosh k_n(h) + C_n \cosh k_n(t) = \frac{\tilde{\rho}(n)}{\epsilon_o k_n}$$

if we let

$$\alpha 1 = \sinh k_n b \qquad \alpha 2 = \sinh k_n h \qquad \alpha 3 = \sinh k_n t$$

$$\beta 1 = \cosh k_n b \qquad \beta 2 = \cosh k_n h \qquad \beta 3 = \cosh k_n t$$

we now can write:

$$\begin{bmatrix} A_n \\ B_n^c \\ B_n^s \\ C_n \end{bmatrix} \cdot \begin{bmatrix} \alpha 1 & -1 & 0 & 0 \\ k_n \beta 1 & 0 & -[k_n \epsilon_r] & 0 \\ 0 & \beta 2 & \alpha 2 & -\alpha 3 \\ 0 & \epsilon_r k_n \alpha 2 & \epsilon_r k_n \beta 2 & k_n \beta 3 \end{bmatrix} = \begin{bmatrix} 0 \\ \frac{\tilde{\rho}_s(n)}{\epsilon_o} \\ 0 \\ \frac{\tilde{\rho}(n)}{\epsilon_o} \end{bmatrix} \qquad (4.24)$$

letting the second matrix in the equation (4.24) be [A] then:

$$|A| = \alpha 1 \, k_n^2 \, [-\epsilon_r \, [\beta 2 \, \beta 3 + \epsilon_r \, \alpha 2 \, \alpha 3] + \beta 1 \, [\alpha 2 \, \beta 3 + \epsilon_r \, \beta 2 \, \alpha 3]$$

And

$$A_n = \frac{\begin{bmatrix} 0 & -1 & 0 & 0 \\ \frac{\tilde{\rho}_s(n)}{\epsilon_o} & 0 & -[k_n \epsilon_r] & 0 \\ 0 & \beta 2 & \alpha 2 & -\alpha 3 \\ \frac{\tilde{\rho}(n)}{\epsilon_o} & \epsilon_r k_n \alpha 2 & \epsilon_r k_n \beta 2 & k_n \beta 3 \end{bmatrix}}{|A|}$$

Or

$$A_n = \frac{\frac{\tilde{\rho}_s(n)}{\epsilon_o} k_n [\alpha 2\ \beta 3 + \epsilon_r \beta 2\ \alpha 3] + \epsilon_r k_n \frac{\tilde{\rho}(n)}{\epsilon_o} \alpha 3}{|A|} \qquad (4.25)$$

$$B_n^c = \frac{\begin{bmatrix} \alpha 1 & 0 & 0 & 0 \\ k_n \beta 1 & \frac{\tilde{\rho}_s(n)}{\epsilon_o} & -[k_n \epsilon_r] & 0 \\ 0 & 0 & \alpha 2 & -\alpha 3 \\ 0 & \frac{\tilde{\rho}(n)}{\epsilon_o} & \epsilon_r k_n \beta 2 & k_n \beta 3 \end{bmatrix}}{|A|}$$

$$B_n^c = \left[\frac{\tilde{\rho}_s(n)}{\epsilon_o} k_n [\alpha 2\ \beta 3 + \epsilon_r \beta 2\ \alpha 3] + \epsilon_r k_n \frac{\tilde{\rho}(n)}{\epsilon_o} \alpha 3 \right] \frac{\alpha 1}{|A|} \qquad (4.26)$$

$$B_n^s = \frac{\begin{bmatrix} \alpha 1 & -1 & 0 & 0 \\ k_n \beta 1 & 0 & \frac{\tilde{\rho}_s(n)}{\epsilon_o} & 0 \\ 0 & \beta 2 & 0 & -\alpha 3 \\ 0 & \epsilon_r k_n \alpha 2 & \frac{\tilde{\rho}(n)}{\epsilon_o} & k_n \beta 3 \end{bmatrix}}{|A|}$$

$$B_n^s = \frac{\frac{-\tilde{\rho}_s(n)}{\epsilon_o} k_n \alpha 1 \left[\beta 2\, \beta 3 + \epsilon_r \alpha 2\, \alpha 3\right] + k_n \frac{\tilde{\rho}(n)}{\epsilon_o} \beta 1\, \alpha 3}{|A|} \qquad (4.27)$$

$$C_n = \frac{\begin{bmatrix} \alpha 1 & -1 & 0 & 0 \\ k_n \beta 1 & 0 & -\epsilon_r k_n & \frac{\tilde{\rho}_s(n)}{\epsilon_o} \\ 0 & \beta 2 & \alpha 2 & 0 \\ 0 & \epsilon_r k_n \alpha 2 & \epsilon_r k_n \beta 2 & \frac{\tilde{\rho}(n)}{\epsilon_o} \end{bmatrix}}{|A|}$$

$$C_n = \frac{\epsilon_r k_n \alpha 1 \left[\beta 2 \frac{\tilde{\rho}(n)}{\epsilon_o} + \frac{\tilde{\rho}_s(n)}{\epsilon_o} \beta 1\, \beta 2\right] + k_n \frac{\tilde{\rho}(n)}{\epsilon_o} \beta 1\, \alpha 2}{|A|} \qquad (4.28)$$

Substituting (4.8) into (4.11(b))

$$A_n \sinh[k_n b] = \tilde{v}_n \qquad (4.29)$$

and substituting (4.9) into (4.12(b)), we arrive at

$$B_n^s \sinh[k_n y - b] + B_n^c \cosh[k_n (y-b)] = \tilde{\phi}_v(n) + \tilde{\phi}_o(n)$$

or

$$B_n^s \sinh[k_n h] + B_n^c \cosh[k_n h] = \phi_v(n) + \phi_o(n) \qquad (4.30)$$

and using the expressions for A_n, B_n^c, B_n^s in expressions (4.25), (4.26), (4.27) and (4.28) the following expressions are obtained:

$$\tilde{G}_{11}(n)\ \tilde{\rho}(n) + \tilde{G}_{12}(n)\ \tilde{\rho}_s(n) = \tilde{\phi}_v(n) + \tilde{\phi}_o(n) \qquad (4.13(a))$$

$$\tilde{G}_{21}(n)\ \tilde{\rho}(n) + G_{22}(n)\ \tilde{\rho}_s(n) = \tilde{v}(n) \qquad (4.31(b))$$

Where

$$G_{11} = \left[\frac{1}{\det}\right]\left[\coth[k_n h] + \left[\frac{1}{\epsilon_r}\right]\coth[k_n b]\right] \qquad (4.32(a))$$

$$\tilde{G}_{12} = \left[\frac{1}{\det}\right]\left[\frac{1}{\sinh[k_n h]}\right] = \tilde{G}_{21} \qquad (4.32(b))$$

$$\tilde{G}_{22} = \left[\frac{1}{\det}\right]\left[\coth[k_n h] + \left[\frac{1}{\epsilon_r}\right]\coth[k_n t]\right] \qquad (4.32(c))$$

$$\det = \epsilon_o k_n \left[\begin{array}{l} \epsilon_r + \coth[k_n b]\coth[k_n h] + \ldots \\ + \coth[k_n t]\left[\coth[k_n h] + \left[\frac{1}{\epsilon_r}\right]\coth[k_n b]\right] \end{array}\right]$$

To solve equation (4.32)

$$\tilde{\rho}(n), \tilde{\rho}_s(n)$$

are expressed in terms of expansion basis functions as follows:

$$\tilde{\rho}(n) = \sum_{k=1}^{K} = a_k \tilde{\rho}_k(n) \;, \kappa = 1, 2, --k \qquad (4.33(a))$$

$$\tilde{\rho}_s(n) = \sum_{m=1}^{M} b_m \tilde{\rho}_{sm}(n) \;, m = 1, 2, ---m \qquad (4.33(b))$$

where a_k, b_m are unknown coefficients to be evaluated. The $\tilde{\rho}_k(n)$, $\tilde{\rho}_{sm}(n)$ being chosen such that the inverse transforms $\rho_k(x)$, $\rho_{sm}(x)$ satisfy the non-zero charge conditions on the strip and the septum only as well as the edge singularity conditions.

Substituting (4.33) into (4.31) gives:

$$\tilde{G}_{11}(n)\sum_{k=1}^{K} a_k \tilde{\rho}_k(n) + \tilde{G}_{12}(n)\sum_{m=1}^{M} b_m \tilde{\rho}_{sm}(n) = \tilde{\phi}_v(n) + \phi_o(n) \qquad (4.34(a))$$

$$\tilde{G}_{21}(n)\sum_{k=1}^{K} a_k \tilde{\rho}_k(n) + \tilde{G}_{22}(n)\sum_{m=1}^{M} b_m \tilde{\rho}_{sm}(n) = \tilde{v}(n) \qquad (4.34(b))$$

taking the inner products of terms in both (4.34(a)) and (4.34(b)) with ρ_i, ρ_{sj} seperately where, ρ_i, ρ_{sj} are the same set of known (testing) basis functions (Gelerkin)

i = 1, 2, . . . K j = 1, 2, . . . M n = 1, 2, ... ∞

we get

$$\sum_{n=1}^{\infty} \tilde{\rho}_i \quad \tilde{G}_{11} \quad \sum_{k=1}^{k} a_k \tilde{\rho}_k(n) \quad + \sum_{n=1}^{\infty} \tilde{\rho}_i \quad \tilde{G}_{12}(n) \quad \sum_{m=1}^{M} b_m \tilde{\rho}_{sm}(n) \quad =$$

$$\sum_{n=1}^{\infty} \left[\tilde{\rho}_i(n)\phi_v(n) + \tilde{\phi}_o(n)\tilde{\rho}_i(n)\right] \qquad (4.35(a))$$

$$\sum_{n=1}^{\infty} \tilde{\rho}_{sj}\tilde{G}_{11}\sum_{k=1}^{k} a_k \tilde{\rho}_k(n) + \sum_{n=1}^{\infty} \tilde{\rho}_{sj}\tilde{G}_{12}(n)\sum_{m=1}^{M} b_m \tilde{\rho}_{sm}(n) =$$

$$\sum_{n=1}^{\infty} \left[\tilde{\rho}_{sj}(n)\phi_v(n) + \tilde{\phi}_o(n)\tilde{\rho}_{sj}\right] \qquad (4.35(b))$$

$$\sum_{n=1}^{\infty} \tilde{\rho}_{sj}\tilde{G}_{21}\sum_{k=1}^{k} a_k \tilde{\rho}_k(n) + \sum_{n=1}^{\infty} \tilde{\rho}_{sj} \quad \tilde{G}_{22}(n) \quad \sum_{m=1}^{M} b_m \tilde{\rho}_{sm}(n) =$$

$$\sum_{n=1}^{\infty} \left[\tilde{\rho}_{sj}\tilde{v}(n)\right] \qquad (4.35(c))$$

$$\sum_{n=1}^{\infty} \tilde{\rho}_i \, \tilde{G}_{21} m \sum_{k=1}^{k} a_k \tilde{\rho}_k(n) + \sum_{n=1}^{\infty} \tilde{\rho}_i \, \tilde{G}_{22}(n) \sum_{m=1}^{M} b_m \tilde{\rho}_{sm}(n) =$$

$$\sum_{n=1}^{\infty} \tilde{\rho}_i(n) \, \tilde{v}(n) \qquad (4.35(d))$$

Taking (4.35(a)), (4.35(c)) and using the following substitutes

$$K_{11ik} = \sum_{n=1}^{\infty} \tilde{\rho}_i(n) \, \tilde{G}_{11}(n) \, \tilde{\rho}_k(n) \qquad (4.36(a))$$

$$K_{12im} = \sum_{n=1}^{\infty} \tilde{\rho}_i(n) \, \tilde{G}_{12}(n) \, \tilde{\rho}_{sm}(n) \qquad (4.36(b))$$

$$K_{21jk} = \sum_{n=1}^{\infty} \tilde{\rho}_{sj}(n) \, \tilde{G}_{21}(n) \, \tilde{\rho}_k(n) \qquad (4.36(c))$$

$$K_{22jm} = \sum_{n=1}^{\infty} \tilde{\rho}_{sj}(n) \, \tilde{G}_{22}(n) \, \tilde{\rho}_{sm}(n) \qquad (4.36(d))$$

Setting

$$P_i = \sum_{n=1}^{\infty} \left[\tilde{\rho}_i(n)\ \tilde{\Phi}_v(n) + \tilde{\rho}_i(n)\ \tilde{\Phi}_o(n) \right] \qquad (4.36(e))$$

Then

$$\sum_{k=1}^{k} K_{11ik}\, a_k + \sum_{m=1}^{M} K_{12im}\, b_m = P_i \qquad (4.37(a))$$

$$\sum_{k=1}^{k} K_{21jk}\, a_k + \sum_{m=1}^{M} K_{22jm}\, b_m = \sum_{n=1}^{\infty} \tilde{\rho}_i(n)\ \tilde{v}_n = 0 \qquad (4.37(b))$$

$$P_i = \sum_{n=1}^{\infty} \left[\tilde{\rho}_i(n)\ \tilde{\Phi}_v(n) + \tilde{\rho}_i(n)\ \tilde{\Phi}_o(n) \right] = \left[\frac{L}{2} \right] \int_o^L \rho_i(x)\, v\, dx$$

$$= \left[L \frac{v}{2} \right] \int_s^{(S+W)} \rho_i(x)\ dx \qquad (4.38)$$

$$\text{as} \quad \sum_n \rho_i(n)\ \phi_o(n) = 0$$

See section 1 of this thesis for an explanation of (4.37(b)), (4.38).

The a_k, b_m are then found by substituting the computed values of P_1 in (4.37) and solving the simultaneous equations. Using the

variational principle (or minimum energy principle) for line capacitance C (lower bound)

$$\left[\frac{1}{C}\right] = \left[\frac{1}{Q^2}\right] \int_s \rho(x,y)\, \phi(x,y)\, dl \qquad (4.39)$$

Where

$$Q = \int_s \rho(x,y)\, dl$$

and $\rho(x,y)$ is the charge distribution on the strip $\Phi(x,y)$ is the potential distribution; and the integral are taken on all the surfaces over which the $\rho(x,y)$ exists, then by setting $\Phi(x,y) = v(x) = 1$ the line capacitance of the structure in figure 1 is

$$C = \int_S^{(S+W)} \rho(x)\, dx \qquad (4.40)$$

$$= \sum_{k=1}^{k} \int_S^{(S+W)} a_k \rho_k(x)\, dx = \left[\frac{2}{L}\right] \sum_k a_k P_k$$

from (4.33) and (4.38). Since (4.39) has a stationery nature [4.10] an approximate trial function $\rho(x)$ results in only a second order error in (4.40). And as pointed out in chapter 1 the best choice of the $\rho(x)$, $\rho_s(x)$ basis functions are those which maximise C. Itoh [4.1] has indicated that an accurate solution of C can be found by setting K = M = 2 in (4.37) resulting in the following equations:

$$K_{1111}\,a_1 + K_{1112}\,a_2 + K_{1211}\,b1 + K_{1212}\,b_2 = P_1 \qquad (4.37(a)) \qquad i=1$$

$$K_{1121}a_1 + K_{1122}\,a_2 + K_{1221}\,b1 + K_{1222}\,b_2 = P_2 \qquad (4.37(a)) \qquad i=2$$

$$K_{2111}\,a_1 + K_{2112}\,a_2 = K_{2211}\,b1 + K_{2212}\,b_2 = 0 \qquad (4.37(b)) \qquad j=1$$

$$K_{2121}\,a_1 + K_{2122}\,a_2 + K_{2221}\,b1 + K_{2222}\,b_2 = 0 \qquad (4.37(b)) \qquad j=2$$

resulting in the 4 X 4 matrix equation,

$$\begin{bmatrix} K_{1111} & K_{1112} & K_{1211} & K_{1212} \\ K_{1121} & K_{1122} & K_{1221} & K_{1222} \\ K_{2111} & K_{2112} & K_{2211} & K_{2212} \\ K_{2121} & K_{2122} & K_{2221} & K_{2222} \end{bmatrix} \begin{bmatrix} a_1 \\ a_2 \\ b_1 \\ b_2 \end{bmatrix} = \begin{bmatrix} P_1 \\ P_2 \\ 0 \\ 0 \end{bmatrix} \qquad (4.41)$$

using the following charge distribution functions

$$\rho_1(x) = \left[\frac{4}{5w}\right]\left[1 + \left[\left[\frac{2}{w}\right]\left[x - s - \frac{w}{2}\right]\right]^3\right] \qquad \text{at} \quad s<x<s+w \qquad (4.42)$$

$$= 0, \text{otherwise.}$$

$$\rho_2(x) = \frac{1}{\pi\sqrt{\left[\frac{w}{2}\right]^2 - \left[x - s - \frac{w}{2}\right]^2}} \qquad \text{at} \quad s < x < s+w \qquad (4.43)$$

$$= 0, \text{otherwise}$$

$$\rho_{s1}(x) = \left[\frac{4}{a^4}\right] (L-x)^3 \qquad L-a < x < L \qquad (4.44)$$

$$\rho_{s2}(x) = \left[\frac{1}{2a}\right] \frac{L-x}{\sqrt{a^2-(L-x)^2}} \qquad L-a < x < L \qquad (4.45)$$

$$= 0, \text{otherwise}$$

In the above, the charge distribution expressions (4.43) and (4.45) reflect charge singularities at the edges of the strip and the septum respectively. Taking the Fourier transforms we arrive at, by setting

$$k_{en} = \frac{2n-1}{2L}\pi \qquad \text{even mode} \qquad (4.46)$$

$$k_{on} = \frac{n\pi}{L} \qquad \text{odd mode} \qquad (4.47)$$

$$\tilde{\rho}_{1e}(n) = \left[\frac{4}{5w}\right]\int_s^{(s+w)}\left[1+\left[\frac{2}{w}\left[x-s-\frac{w}{2}\right]\right]^3\right]\cos[k_{en}x]dx \qquad \text{even mode} \qquad (4.48(a))$$

$$\tilde{\rho}_{10} = \left[\frac{4}{5w}\right]\int_s^{(s+w)}\left[1+\left[\frac{2}{w}\left[x-s-\frac{w}{2}\right]\right]^3\right]\sin[k_{on}x]dx \qquad \text{odd mode} \qquad (4.48(b))$$

$$\tilde{\rho}_{2e}(n) = \left[\frac{1}{\pi}\right]\int_{s}^{(s+w)} \frac{\cos[k_{en}x]}{\sqrt{\left[\frac{w}{2}\right]^2 - \left[x-s-\left[\frac{w}{2}\right]\right]^2}}\,dx \qquad \text{even mode} \qquad (4.49(a))$$

$$\tilde{\rho}_{2o}(n) = \left[\frac{1}{\pi}\right]\int_{s}^{(s+w)} \frac{\sin[k_{on}x]}{\sqrt{\left[\frac{w}{2}\right]^2 - \left[x-s-\left[\frac{w}{2}\right]\right]^2}}\,dx \qquad \text{odd mode} \qquad (4.49(b))$$

$$\tilde{\rho}_{s1e}(n) = \left[\frac{4}{a^4}\right]\int_{(L-a)}^{L} (L-x)^3 \cos[k_{en}x]\,dx \qquad \text{even mode} \qquad (4.50(a))$$

$$\tilde{\rho}_{s1o}(n) = \left[\frac{4}{a^4}\right]\int_{(L-a)}^{L} (L-x)^3 \sin[k_{on}x]\,dx \qquad \text{odd mode} \qquad (4.50(b))$$

$$\tilde{\rho}_{s2e}(n) = \left[\frac{1}{2a}\right]\int_{(L-a)}^{L} \frac{(L-x)\cos[k_{en}x]}{\sqrt{a^2-(L-x)^2}}\,dx \qquad \text{even mode} \qquad (4.51(a))$$

$$\tilde{\rho}_{s2o}(n) = \left[\frac{1}{2a}\right]\int_{(L-a)}^{L} \frac{(L-x)\sin[k_{on}x]}{\sqrt{a^2-(L-x)^2}}\,dx \qquad \text{odd mode} \qquad (4.51(b))$$

The expressions in equations (4.48) through (4.51) can be expressed in a form which considerably reduces computing time by the following technique.

Consider equation (4.48(a)) and setting $\rho_e(n) = I_1$, we then have

$$I_1 = \left[\frac{4}{5w}\right]\int_s^{(s+w)}\left[1 + \left[\frac{2}{w}\left[x-s-\frac{w}{2}\right]\right]^3\right]\cos\left[k_{en}x\right]dx \qquad (4.52)$$

$$\text{let } (x-s-w/2) = z; \qquad (4.53)$$

$$\text{then} x = z + s + w/2 = z + s' \text{ where, } s' = s+\frac{w}{2} \qquad (4.54(a))$$

$$\text{and } dx = dz \qquad (4.54(b))$$

and the limits s and s + w for the x variable are

$$-w/2 \text{ and } w/2 \text{ respectively for the z - variable} \qquad (4.54(c))$$

therefore substituting equation (4.54) into (4.52) we arrive at

$$I_1 = \left[\frac{4}{5w}\right]\int_{-\frac{w}{2}}^{\frac{w}{2}}\left[1 + \left[\frac{2z}{w}\right]^3\right]\cos\left[k_{en}\,(z+s')\right]dz \qquad (4.55)$$

$$= \left[\frac{4}{5w}\right]\int_{-\frac{w}{2}}^{\frac{w}{2}}\left[1 + \left[\frac{2z}{w}\right]^3\right]\left[\begin{matrix}\cos\left[k_{en}z\right]\cos\left[k_{en}s'\right] \cdots \\ + \sin\left[k_{en}z\right]\sin\left[k_{en}s'\right]\end{matrix}\right]dz \qquad (4.56)$$

But

$$\int_{-\frac{w}{2}}^{\frac{w}{2}} \sin[k_{en}z]\sin[k_{en}s']\,dz = 0$$

Therefore

$$I_1 = \left[\frac{8}{5w}\right]\int_{-\frac{w}{2}}^{\frac{w}{2}}\left[1+\left[\frac{2z}{w}\right]^3\right]\cos[k_{en}z]\cos[k_{en}s']\,dz$$

$$=\left[\frac{8}{5w}\right]\cos[k_{en}s']\left[\frac{\sin\left[k_{en}\frac{w}{2}\right]}{k_{en}}+\left[\frac{8}{w^3}\right]\int_o^{\frac{w}{2}} z^3\cos[k_{en}z]dz\right] \qquad (4.57)$$

$$\text{let } k_{en}\,z = \theta$$

Then

$$\int_o^{\frac{w}{2}} z^3\cos[k_{en}z]\,dz = \int_o^{\left[k_{en}\frac{w}{2}\right]}\left[\frac{\theta^3}{k_{en}^4}\right]\cos(\theta)\,d\theta = F(\theta)$$

$$= \left[\frac{1}{k_{en}^4}\right][\sin\theta\,(\theta^3-6\theta)+\cos\theta\,(3\theta^2-6)] \qquad (4.58)$$

$$= \left[\frac{1}{k_{en}^4}\right]\left[F\left[k_{en}\frac{w}{2}\right]-F(0)\right]$$

$$\text{and by setting } k_{en}\frac{w}{2} = \alpha_n$$

$$I_1 = \left[\frac{8}{5w}\right]\cos\left[k_{en}\, s'\right]\left[\frac{1}{k_{en}}\right]\sin\left[\alpha_n\right] + \left[\frac{1}{\alpha_n^3}\right]\left[F\left[\alpha_n\right] - F(0)\right] \qquad (4.59)$$

Similarly it can be shown that if

$$I_2 = \tilde{\rho}_{10}(n) \qquad I_3 = \tilde{\rho}_{2e}(n) \qquad I_4 = \tilde{\rho}_{20}(n)$$

$$I_5 = \tilde{\rho}_{s1e}(n) \qquad I_6 = \tilde{\rho}_{s1o}(n) \qquad I_7 = \tilde{\rho}_{s2e}(n)$$

$$\text{and } I_8 = \tilde{\rho}_{s20}(n) \qquad (4.60)$$

$$I_2 = \left[\frac{4}{5w}\right]\int_s^{(s+w)}\left[1 + \left[\frac{2}{w}\left[x - s - \frac{w}{2}\right]\right]^3\right]\sin\left[k_{on}x\right]dx \qquad (4.61)$$

substituting equation (4.53) into (4.61) we arrive at

$$I_2 = \left[\frac{4}{5w}\right]\int_{-\frac{w}{2}}^{\frac{w}{2}}\left[1 + \left[2\frac{z}{w}\right]^3\right]\sin\left[k_{on}(z+s')\right]dz$$

$$= \left[\frac{4}{5w}\right]\int_{-\frac{w}{2}}^{\frac{w}{2}}\left[1 + \left[\frac{2z}{w}\right]^3\right]\left[\begin{matrix}\sin\left[k_{on}z\right]\cos\left[k_{on}s'\right] \cdots \\ + \cos\left[k_{on}z\right]\sin\left[k_{on}s'\right]\end{matrix}\right]dz = 0 \qquad (4.62)$$

but

$$\int_{-\frac{w}{2}}^{\frac{w}{2}}\sin\left[k_{on}\, z\right]\cos\left[k_{on}\, s'\right]dz = 0$$

Therefore

$$I_2 = \left[\frac{8}{5w}\right]\int_{-\frac{w}{2}}^{\frac{w}{2}}\left[1+\left[2\frac{z}{w}\right]^3\right]\cos\left[k_{on}z\right]\sin\left[k_{on}s'\right]dz \qquad (4.63)$$

$$\text{and setting} \qquad \alpha_n = k_{on}\frac{w}{2}$$

$$\text{and by setting} k_{on}\frac{w}{2} = \alpha_n$$

$$I_2 = \left[\frac{8}{5w}\right]\sin\left[k_{on}s'\right]\left[\frac{1}{k_{on}}\right]\sin\left[\alpha_n\right] + \left[\frac{1}{\alpha_n^3}\right]\left[F\left[\alpha_n\right]-F(0)\right] \qquad (4.64)$$

Similarly

$$I_3 = \left[\frac{1}{\pi}\right]\int_{-\frac{w}{2}}^{\frac{w}{2}}\frac{\cos\left[k_{en}\,(z+s')\right]}{\sqrt{\left[\frac{w}{2}\right]^2 - z^2}}dz \qquad (4.65)$$

and since

$$\int_{-\frac{w}{2}}^{\frac{w}{2}}\frac{\cos\left[k_{en}z\right]\cos\left[k_{en}s'\right]-\sin\left[k_{en}z\right]\sin\left[k_{en}s'\right]}{\sqrt{\left[\frac{w}{2}\right]^2 - z^2}} \qquad (4.66)$$

$$\int_{-\frac{W}{2}}^{\frac{W}{2}} \frac{\sin[k_{en}z]\sin[k_{en}s']}{\sqrt{\left[\frac{W}{2}\right]^2 - z^2}}\,dz = 0$$

$$I_3 = \left[\frac{1}{\pi}\right]\int_{-\frac{W}{2}}^{\frac{W}{2}} \frac{\cos[k_{en}s']\cos[k_{en}z]}{\sqrt{\left[\frac{W}{2}\right]^2 - z^2}}\,dz \qquad (4.67)$$

using the standard result

$$\int_o^2 [a^2 - x^2]^{\eta-\frac{1}{2}} \cos(xy)\,dx = 2^{\eta-1}\,\Gamma\left[\eta + \frac{1}{2}\right]\sqrt{\pi}\,a^{\eta}\,y^{-\eta}\,J_{\eta}(ay)$$

(4.67) can be written with $\eta=0$

$$\begin{aligned} I_3 &= 2\cos\left[k_{en}\,s'\right]\frac{1}{2}\,\Gamma\left[\frac{1}{2}\right]\sqrt{\pi}\left[\frac{W}{2}\right]^0 y^0\,J_0\left[\frac{W}{2}k_{en}\right] \\ &= \cos[k_{en}\,s']\,J_0\left[k_{en}\frac{W}{2}\right] \qquad (4.68) \\ &= \cos\left[k_{en}\left[s+\frac{W}{2}\right]\right]J_0\left[k_{en}\frac{W}{2}\right] \end{aligned}$$

similarly it can be shown that

$$\begin{aligned} I_4 &= \sin\left[k_{on}\,s'\right]J_0\left[k_{on}\,\frac{W}{2}\right] \\ &= \sin\left[k_{on}\left[s+\frac{W}{2}\right]\right]J_0\left[k_{on}\,\frac{W}{2}\right] \end{aligned} \qquad (4.69)$$

$$I_5 = \left[\frac{4}{a^4}\right]\int_{(L-a)}^{L} (L-x)^3 \cos[k_{en}x]dx \qquad (4.70)$$

now letting L - x = z

$$I_5 = \left[\frac{4}{a^4}\right]\int_0^a (z)^3 \cos[k_{en}(L-z)]dx$$

$$= \left[\frac{4}{a^4}\right]\int_0^a (z)^3 [\cos[k_{en}L]\cos[k_{en}z] + \sin[k_{en}L]\sin[k_{en}z]]\, dz \qquad (4.71)$$

But

$$\cos[k_{en}L] = \cos\left[(2n-1)\frac{\pi}{2}\right] = 0 \text{ for all n; see equation} \qquad (4.46)$$

Therefore

$$I_5 = \left[\frac{4}{a^4}\right]\int_0^a (z)^3 \sin[k_{en}L]\sin[k_{en}z]\, dx \qquad (4.73)$$

$$= \frac{4\sin[k_{en}L]}{a^4}\left[\frac{1}{k_{en}^4}\right]\phi[k_{en}a]$$

Where

$$\phi[k_{en}a] = \sin[k_{en}a]\left[3[k_{en}a]^2 - 6\right] - \cos[k_{en}a]\left[[k_{en}a]^3 - 6k_{en}a\right] \qquad (4.75)$$

Similarly

$$I_6 = \frac{4\cos[k_{on}L]}{a^4 k_{on}^4}\,\phi[k_{on}a] \qquad (4.76)$$

$$I_7 = \left[\frac{1}{2a}\right]\int_{(L-a)}^{L} \frac{L-x}{\sqrt{a^2-(L-x)^2}}\cos[k_{en}x]dx \qquad (4.77)$$

letting L - x = z

$$I_7 = \left[\frac{1}{2a}\right]\int_0^a \frac{z}{\sqrt{a^2-z^2}}\cos[k_{en}(L-z)]dz$$

$$= \left[\frac{1}{2a}\right]\int_0^a \frac{z}{\sqrt{a^2-z^2}}\begin{bmatrix}\cos[k_{en}L]\cos[k_{en}z]\ldots\\ +\sin[k_{en}L]\sin[k_{en}z]\end{bmatrix}dz \qquad (4.78)$$

Since

$$\cos[k_{en}L] = \cos\left[\frac{n-\frac{1}{2}}{L}\pi L\right] = 0, \text{ for all n see} \qquad (4.4(a))$$

$$I_7 = \left[\frac{1}{2a}\right]\int_0^a \frac{z}{\sqrt{a^2-z^2}}\sin[k_{en}L]\sin[k_{en}z]dz$$

$$= \sin\frac{[k_{en}L]}{2a}\int_0^a \frac{z}{\sqrt{a^2-z^2}}\sin[k_{en}z]dz \qquad (4.79)$$

using the standard result

$$\int_0^a [a^2 - x^2]^{\eta - \frac{1}{2}} \sin(xy)\, dx = 2^{\eta-1}\, \Gamma\left[\eta + \frac{1}{2}\right] \sqrt{\pi}\, a^{\eta+1}\, y^{-\eta}\, J_{\eta\eta}(ay)$$

where $\eta\eta = \eta + 1$ (4.80)

for $\eta = 0$ equation (4.80) becomes

$$= \frac{\pi}{2}\, a\, J_1(ay) \qquad (4.81)$$

using (4.81) in (4.79) yields

$$I_7 = \left[\frac{\pi}{4}\right] \sin[k_{en} L]\, J_1[k_{en} a] \qquad (4.82)$$

$$I_8 = \left[\frac{1}{2a}\right] \int_{(L-a)}^{L} \frac{L - x}{\sqrt{a^2 - (L-x)^2}} \sin[k_{on} x]\, dx \qquad (4.83)$$

letting L - x = z

$$I_8 = \left[\frac{1}{2a}\right] \int_0^a \frac{z}{\sqrt{a^2 - z^2}} \sin[k_{on}(L-z)]\, dz$$

$$= \left[\frac{1}{2a}\right] \int_0^a \frac{z}{\sqrt{a^2 - z^2}} \begin{bmatrix} \sin[k_{on}L]\cos[k_{on}z]\ldots \\ -\cos[k_{on}L]\sin[k_{on}z] \end{bmatrix} dz \qquad (4.84)$$

since

$$\sin[k_{on} L] = \sin\left[n \frac{\pi}{L} L\right] \quad 0, \text{ for all integer n}$$

$$I_8 = \left[\frac{1}{2a}\right] \int_0^a \frac{z}{\sqrt{a^2 - z^2}} [-\cos[k_{on} L]] \sin[k_{on} z]\, dz$$

$$= \frac{-\cos(n\pi)}{2a} \int_0^a \frac{z}{\sqrt{a^2 - z^2}} \sin[k_{on} z]\, dz \qquad (4.85)$$

$$I_8 = -\cos(n\pi)\, J_1[a_{k_{on}}] \qquad (4.86)$$

Using this analysis technique, even and odd mode characteristic impedances Z_{oe}, Z_{oo} with corresponding effective dielectric constants were calculated for different values of ϵ_r and 'a' for the following fixed conditions h= 0.010 inch, w = 1.2 h, L= 10 h, t = 10 h, s = 0.1 h, b = 10 h. using commercially available software MATHCAD run on a personal computer. A detailed program listing for the case ϵ_r = 38 is given in Appendix 1.

Convergence was confirmed by comparing results for n = 50 to 1000. A comparison of results was made with those from the commercially available software Touchstone for the case a = L with ϵ_r = 15.4.

As shown in table (4.1(a)) the discrepancy does not exceed 1.5 percent for even mode impedance and 2.2 percent for odd mode impedance when n = 1000. Figure (4.1(a)) displays the data graphically. As shown on page 279 of REF [1.12] equation (4.39) should result in an upper bound of characteristic impedance. Since, as figure (4.1(a)) shows, the calculated impedances are lower than the Bryant-Weiss results, this indicates that the basis functions chosen were not optimum for the order of the matrix considered. It is therefore necessary to (1) increase the number of basis functions used or (2) choose basis functions which more closely represent the physical charge conditions on the strip/septum (ie. modify 4.42 and 4.44 to reflect the singularity) to ensure complete equivalence between the two calculations. Since Z_{oo} shows the greater discrepancy the greater error is in $\rho(x)$. More accurate results may be achieved if (4.42) were changed to

$$\rho_1(x) = \frac{1}{w} + \alpha_1\left[\frac{1}{\sqrt{\frac{x-s}{w}}} - 2\right] + \alpha_2\left[\frac{1}{\sqrt{\frac{s+w-x}{w}}} - 2\right], \qquad s<x,\ s+w$$

and (4.44) were changed to

$$\rho_{s1}(x) = \frac{2}{L-a} + \alpha_1\left[\frac{1}{\sqrt{\frac{L-a-x}{L-a}}} - 1\right], \qquad L-a<x<L$$

In addition functions of the type $(\cos x)^{\eta-1}$ could be used where $\eta = \frac{1}{2}$ and where x is appropriately chosen as x-S, s+w-x etc. and α_1, α_2 are variational constants [3.2].

The results of the calculation are however quite adequate for practical applications.

Summation Number	Calculated Using this Thesis		Calculated From EEsof (Bryant-Weiss)		Percent Variation	
n	Z_{oe} ohm	Z_{oo} ohm	Z_{oe} ohm	Z_{oo} ohm	Z_{oe}	Z_{oo}
50	4.6	2.21				
150	41.60	15.07				
300	46.34	32.33				
450	51.38	36.70				
600	52.63	36.84				
800	52.97	37.63				
1000	53.51	37.90	54.35	38.76	1.5	2.2

Table (4.1(a)) Variation of calculated Z_{oe}, Z_{oo} with summation number 'n' for microstrip without septum using analysis technique outlined in thesis and comparison to commercially available program results. h = 0.005; w = 0.7 h; L = 0.650; t = 0.646; s = 0.42 h; b = 0 (ie. no septum)

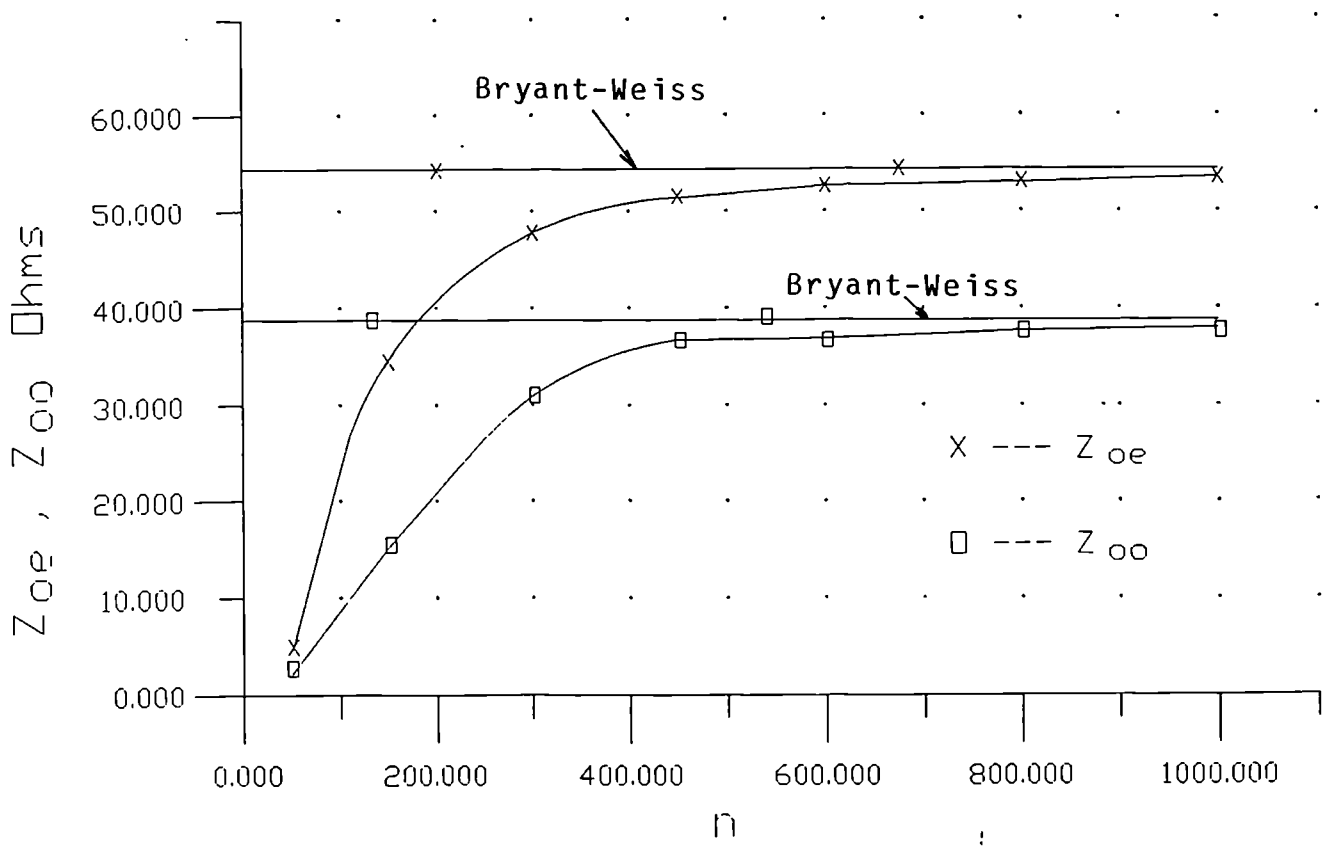

Figure (4.1(a)) Variation of Calculated Zoe, Zoo, with Summation Number 'n' Microstrip without Septum

4.1.1 CALCULATED DATA

Table (4.1(b)) through (f) display calculated data for different parameter variations in the structure shown in figure (4.1). Figures (4.2) through (4.4) display the data graphically. The data in table (4.1(c)) shows that for all other parameters fixed there is a value of 'a' at which $\epsilon_{effo} = \epsilon_{effe}$, ie. is phase velocities of the two modes are equalised as can be seen in figure (4.2).

It is noted that the crossover points occur at decreasing values of 'a' for decreasing values of ϵ_r. This is expected since as ϵ_{r2} approaches ϵ_{r1} the effects of changing 'a' are reduced.

Table (4.1(d)) shows that for all other parameters fixed the ratio Z_{oe}/Z_{oo} increases with increasing ϵ_r. As expected figure (4.4) shows that the value of Z_{oe}/Z_{oo} should coincide at a = L for all ϵ_r, ie. the case of standard coupled microstrip with no septum gap. It is also observed from figure (4.4(a)) that variation of Z_{oe}/Z_{oo} is approximately linear with variation in 'a' over the range a = 0.095 to a = 0.078 for ϵ_r = 2.2 and over the range a = 0.095 to a = .075 for ϵ_r = 9.8. For ϵ_r = 38 approximate linearity is displayed over most of the curve. For practical tuning applications where a predictable ratio is desirable a high ϵ_r is therefore to be preferred.

Table (4.1(e)) shows variation of Z_{oe}, Z_{oo}, ϵ_{effe}, ϵ_{effo} with 's' and 'a'. It is observed from this table that ϵ_{effe} and ϵ_{effo} is close to being equalised for a = 0.640 and that this does not appear to be heavily dependent on ,S, the strip spacing. This is an important result since it implies that high directivity couplers of different coupling values can be made for a fixed value of 'a'. This result simplifies considerably the processing of cascaded couplers using tuning septums since only a single septum width is required, reducing coupler discontinuities. Figure (4.4(a)) shows that the values at which $\epsilon_{effe} = \epsilon_{effo}$ are closely spaced for different values of S. It is also observed from figure (4.4(a)) that ϵ_{effe} can be equalised for different values of S using the same value of a; this also reduces the number of masks and substrate carriers required for couplers using septums. In addition this characteristic could be used to equal β_{oe} and β_{oo} for tapered edge coupled microstrip line ultrabroadband directional couplers.

Table (4.1(f)) displays data for the important case S = 0 which is the microstrip-slot coupler [4.6].

The ratio $\frac{Z_{oe}/2 - Z_o}{Z_o}$ indicates the percentage variation of the characteristic impedance of the line when a < L (ie. with septum) and when a = L (ie. standard microstrip). At a = 0.640 (ie. G/h = 0.8) the results of this analysis agrees with that of Hoffmann et al [4.6] to within 2 percent. Hoffmann's analysis was

based on the method of lines. To the author's knowledge data has not been published for lower values of 'a' ie. higher values of G, as has been done in this thesis.

	ϵ_r=2.4		ϵ_r=9.8		ϵ_r=38	
'a'inch	Zoe ohm	Zoo ohm	Zoe ohm	Zoo ohm	Zoe ohm	Zoo ohm
0.095	122.1	56.4	69.4	32.0	36.8	16.8
0.090	139.3	57.2	81.7	32.6	43.7	17.0
0.085	162.2	58.8	98.5	33.7	53.4	17.7
0.080	185.7	60.7	116.5	35.7	63.9	18.6
0.075	206.8	62.2	133.3	36.3	74.1	19.2
0.070	224.8	63.2	148.4	37.2	83.5	19.7
0.065	240.01	63.9	161.7	37.8	92.1	20.1
0.060	253.0	64.4	173.6	38.2	100.0	20.4
0.055	264.0	64.8	184.1	38.5	107.3	20.6
0.050	273.4	65.0	193.5	38.8	114.0	20.7

Table (4.1(b)) Even and odd mode characteristic impedance (ohms) Zoe, Zoo, versus 'a'.

(h = 0.010 inch, b = 10 h, w = 1.2 h, L = 10 h, t = 10 h, s=0.1 h)

	ϵ_r=2.4		ϵ_r=9.8		ϵ_r=38	
'a' inch	ϵ_{effe}	ϵ_{effo}	ϵ_{effe}	ϵ_{effo}	ϵ_{effe}	ϵ_{effo}
0.095	1.84	1.73	5.7	5.4	20.3	19.6
0.090	1.73	1.72	5.0	5.3	17.5	19.2
0.085	1.62	1.69	4.4	5.1	14.9	18.6
0.080	1.53	1.66	3.9	4.9	12.9	17.7
0.075	1.47	1.64	3.5	4.8	11.4	17.1
0.070	1.42	1.63	3.3	4.7	10.2	16.7
0.065	1.39	1.62	3.0	4.6	9.4	16.4
0.060	1.36	1.61	2.9	4.5	8.6	16.0
0.055	1.33	1.60	2.7	4.5	8.0	15.8
0.050	1.31	1.60	2.6	4.5	7.6	15.7

Table (4.1(c)) Even and odd mode effective dielectric constant ϵ_{effe}, ϵ_{effo}, Versus 'a'.

(h = 0.010 inch, w = 1.2 h, L = 10 h, t = 10 h, S = 0.1 h, b=10 h)

	ϵ_r=2.4	ϵ_r=9.8	ϵ_r=38
'a' inch	Zoe/Zoo	Zoe/Zoo	Zoe/Zoo
0.095	2.16	2.16	2.19
0.090	2.44	2.50	2.57
0.085	2.76	2.92	3.02
0.080	3.05	3.26	3.43
0.075	3.32	3.67	3.85
0.070	3.56	3.98	4.23
0.065	3.76	4.28	4.51
0.060	3.93	4.54	4.90
0.055	4.07	4.78	5.2
0.050	4.20	4.98	5.5

Table (4.1(d)) Ratio to Z_{oe}/Z_{oo} versus 'a'.

(h = 0.010 inch, w = 1.2 h, L = 10 h, t = 10 h, S = 0.1 h, b=10 h)

s inch	a inch	Zoe ohm	ϵeffe	Z_{oo} ohm	ϵ_{effo}
0.001	0.640	87.80	5.06		
	0.615	116.32	4.19		
	0.590	149.88	3.49		
0.005	0.640	80.92	5.01	40.39	5.02
	0.615	105.71	4.21	40.32	5.09
	0.590	138.96	3.47	42.69	4.87
0.010	0.640	76.19	4.94	42.69	4.87
	0.615	95.88	4.28	46.36	5.04
	0.590	128.46	3.49	49.91	4.76
0.015	0.640	73.60	4.86	51.62	4.78
	0.615	88.06	4.39	50.26	4.99
	0.590	119.36	3.55	54.87	4.68

Table (4.1(e)) Variation of characteristic impedance and effective dielectric constant for structure in Figure (4.1) with 's' and 'a' varied.

(h = 0.025; L = 0.650; w = 0.025; b = 0.100; t = 0.646; ϵr = 9.8)

G=2(L-a) inch	$\frac{G}{h}$	a	Zoe ohm	ϵeffe	$\frac{Z_{oe}/2-Z_o}{Z_o}$ %
0.020	0.8	0.640	90.5	5.08	6.2
0.070	2.8	0.615	120.0	4.19	25
0.120	4.8	0.590	153.7	3.50	59.4
0.170	6.8	0.565	179.2	3.08	86.5
0.220	8.8	0.540	198.1	2.80	106.0
0.270	10.8	0.515	212.1	2.61	120.0
0.320	12.8	0.490	222.5	2.47	131.0
0.370	14.8	0.465	230.4	2.37	139.6
0.420	16.8	0.440	236.3	2.29	145.8
0.470	18.8	0.415	240.8	2.23	150.8
0.520	20.8	0.390	244.3	2.19	154.4
0.570	22.8	0.365	246.9	2.16	157.1
0.620	24.8	0.340	248.9	2.13	158.3
0.670	26.8	0.315	250.4	2.11	160.4
0.720	28.8	0.290	251.6	2.09	161.4
0.770	30.8	0.265	252.6	2.09	161.4
0.820	32.8	0.240	253.3	2.08	163.8
0.870	34.8	0.215	253.8	2.06	164.4

Table (4.1(f)) Structure in figure (4.1) with S = 0 and with ground plane septum length 'a' varied.

(h = 0.025; w = 0.025; L = 0.650; t = 0.646; b = 0.100; ϵr = 9.8)

(h = 0.010 inch, w = 1.2 h, L = 10 h, t = 10 h, s = 0.1 h, b = 10 h)

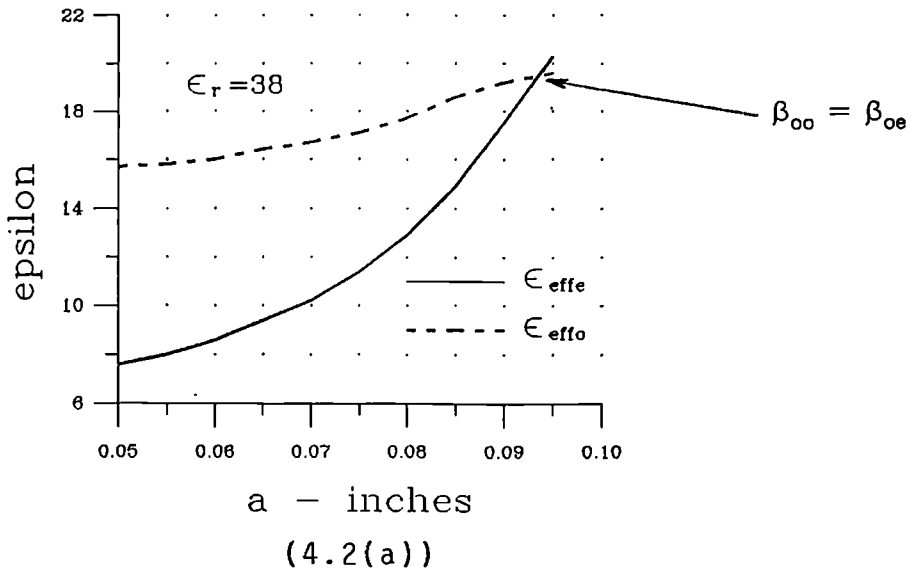

(4.2(a))

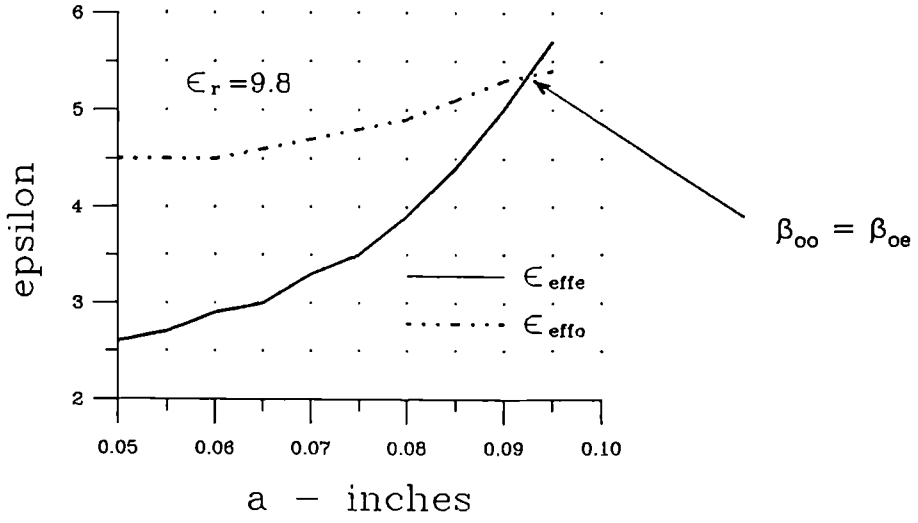

(4.2(b))

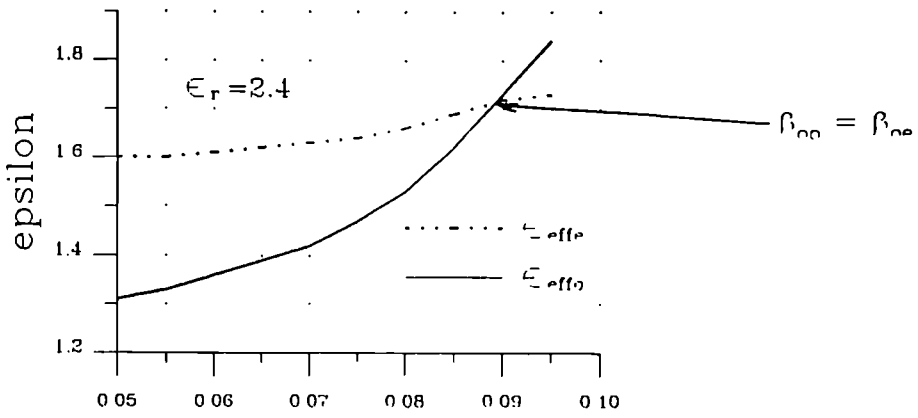

(4.2(c))

Figure 4.2 Effective Dielectric Constant versus Septum Length 'a'.

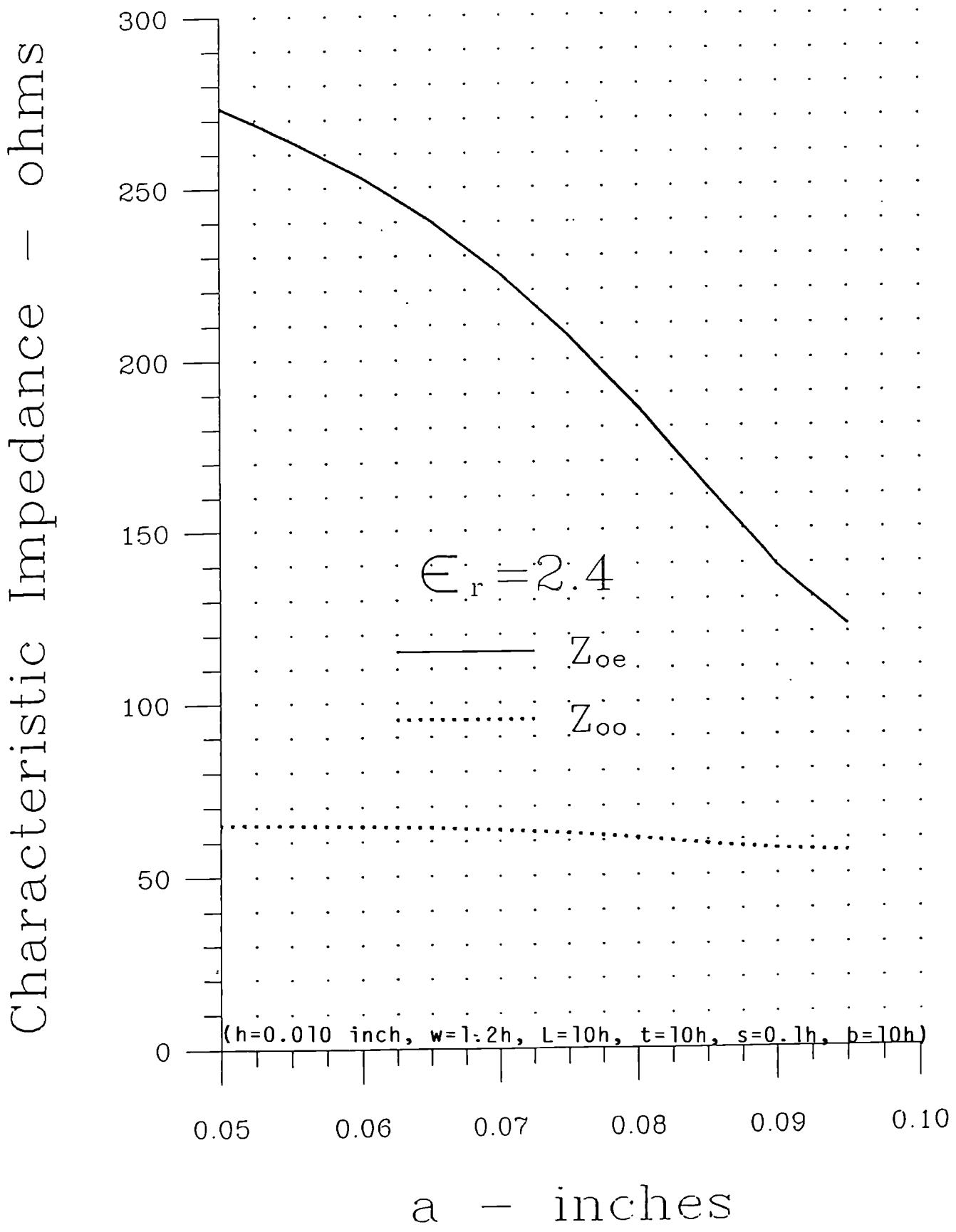

Figure (4.3(a)) Zoe, Zoo versus 'a'.

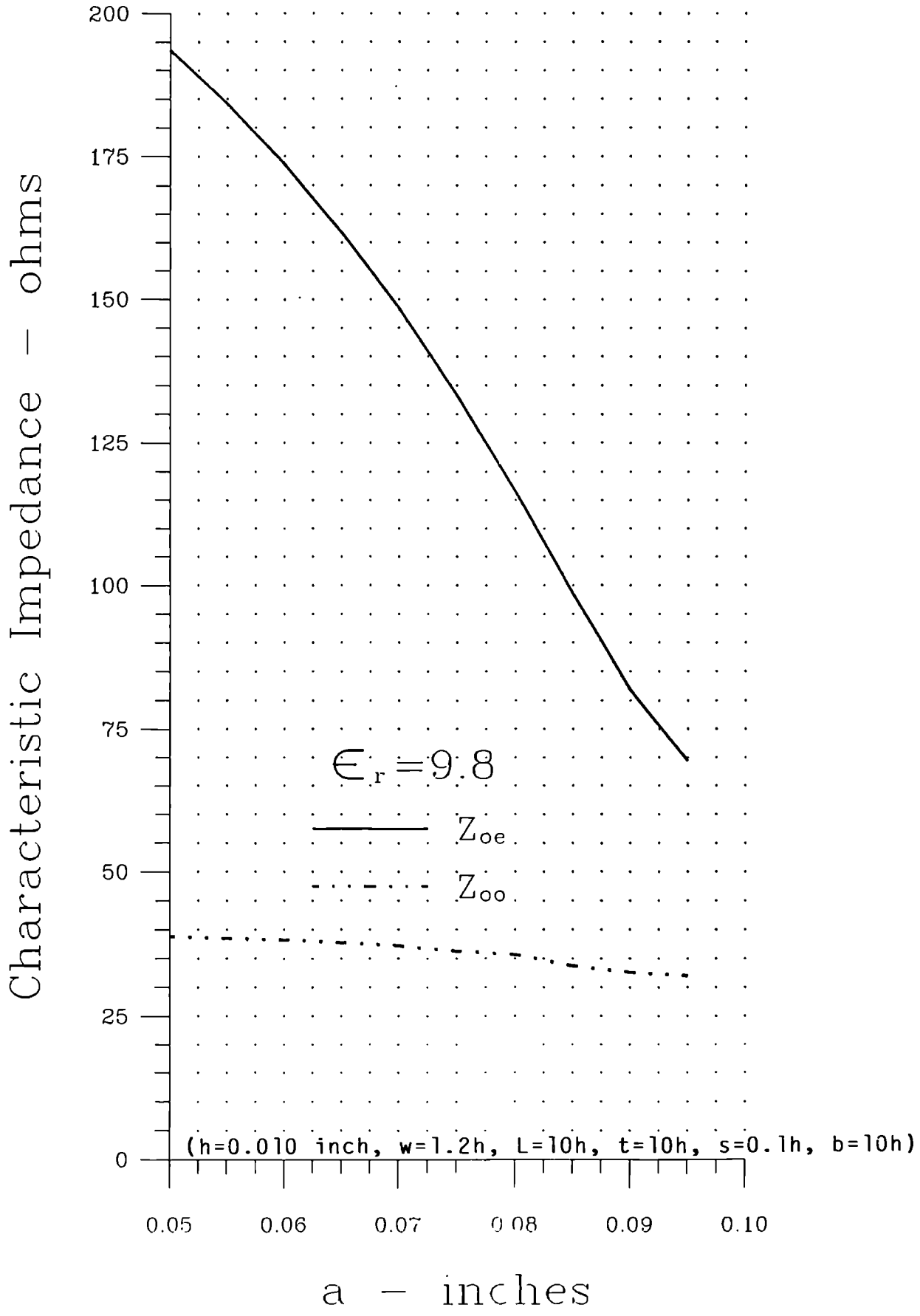

Figure (4.3(b)) Zoe, Zoo versus 'a'.

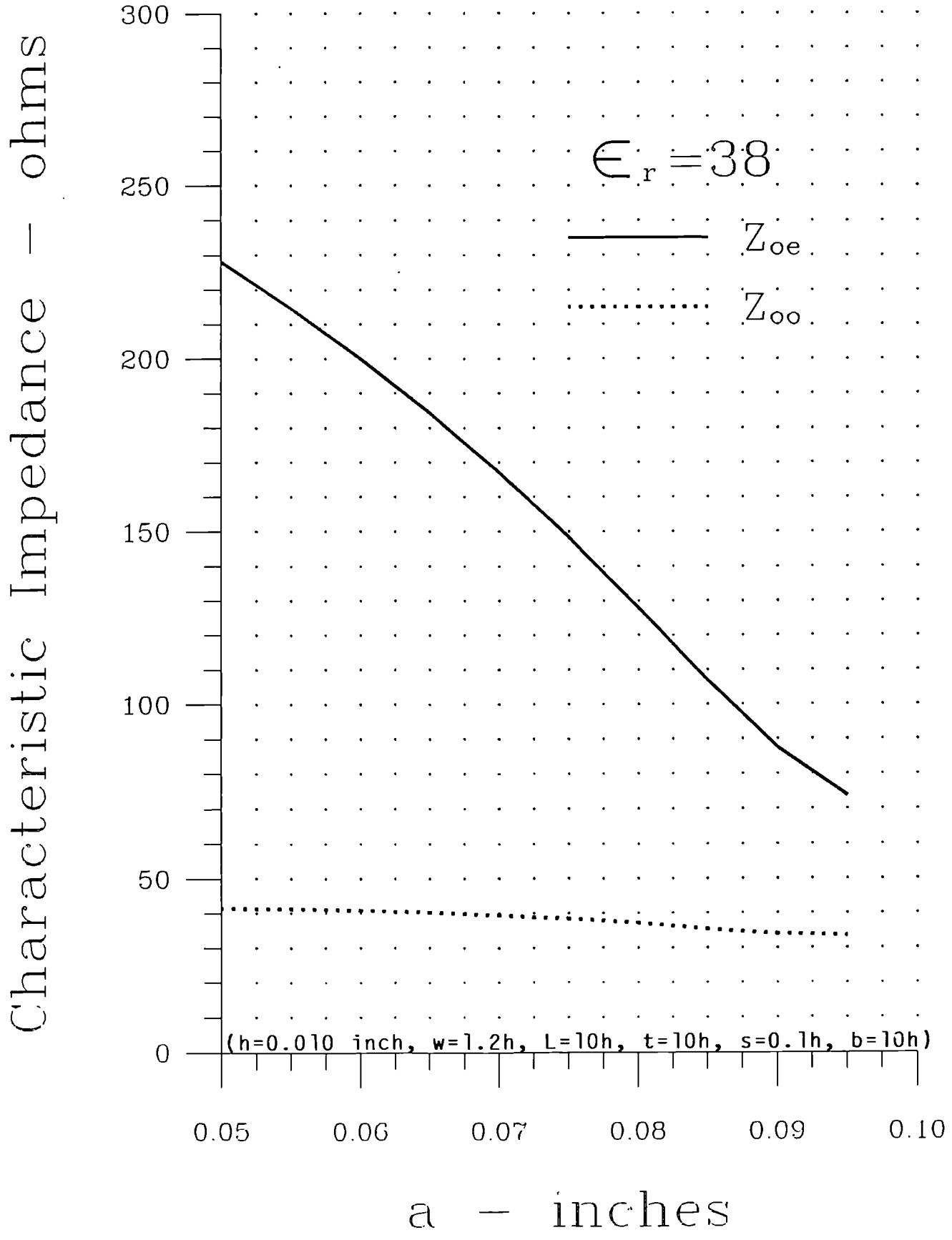

Figure (4.3(c)) Zoe, Zoo versus 'a'.

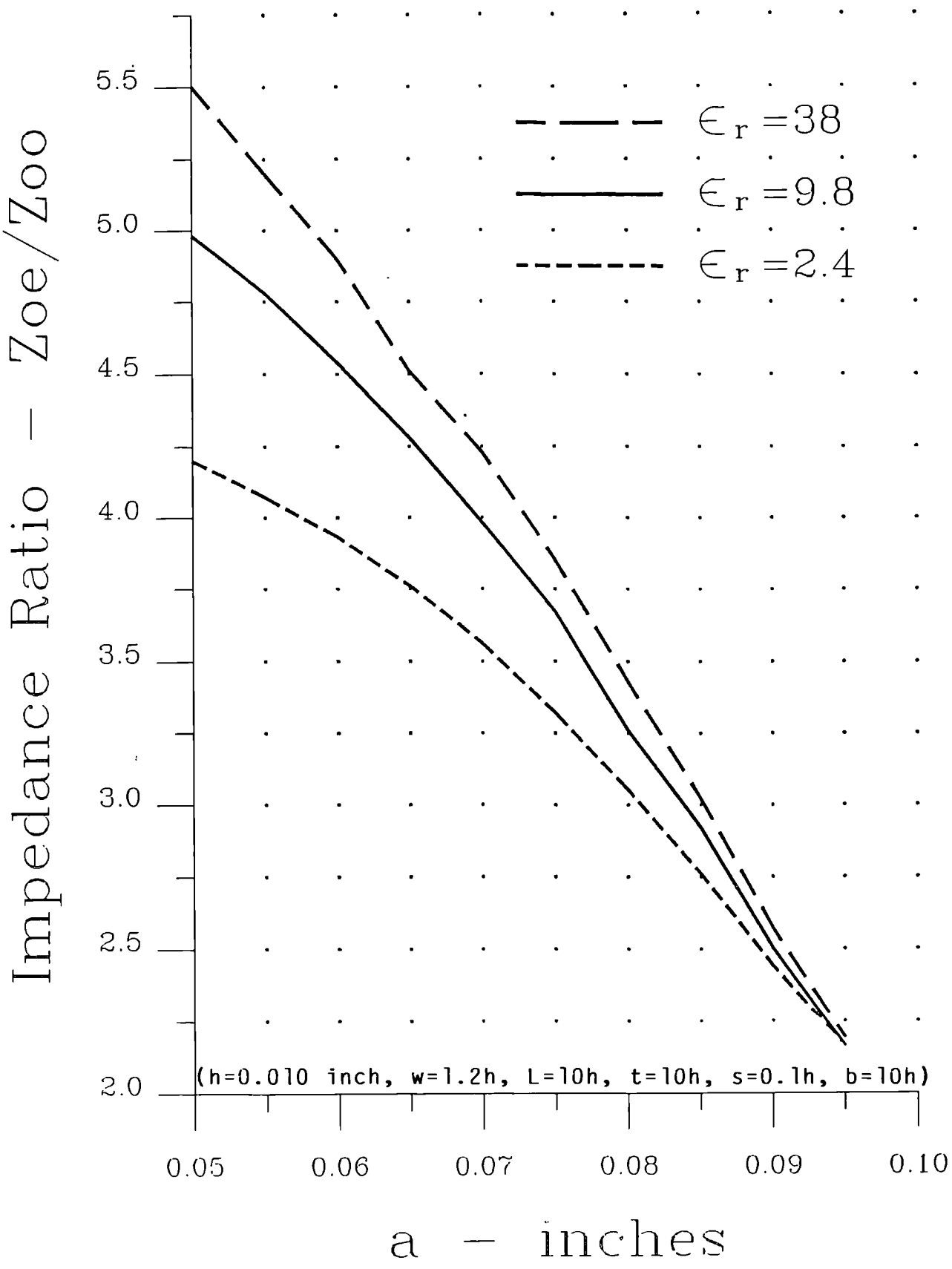

Figure 4.4 Impedance Ratio versus 'a'.

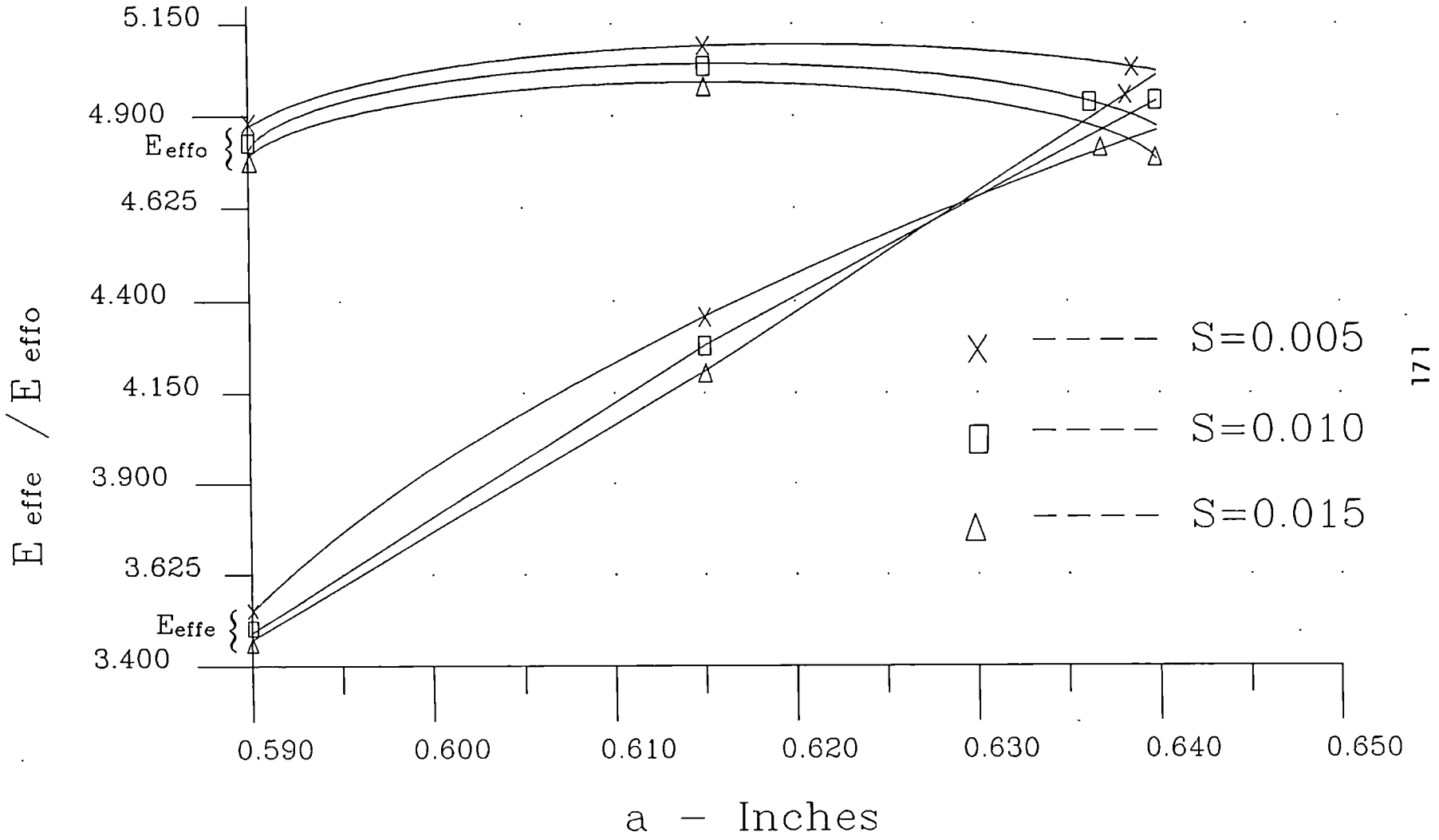

FIGURE: (4.4(a)). Variation of Eeffe, Eeffo with "a" and "s" (Er = 9.8)

4.2 THE SIX STRIP CASE

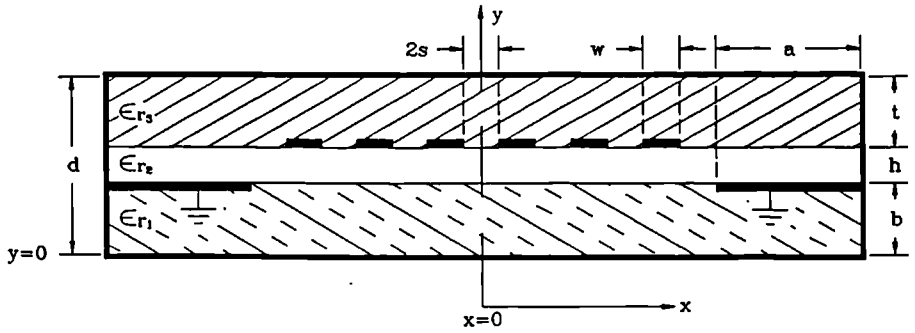

Figure (4.5) SIX STRIP CONFIGURATION

Refer to figure (4.5) in which are six strips of equal width. Taking advantage of the symmetry axis at x=0 only three strips in one half space needs to be considered. The odd and even mode concept is applied to the system by assuming equal potential on the three strip for the even case and opposite potentials on adjacent strips for the odd case.

The assumptions are identical to those for the two strip case with the additional constraint that any coupling between non-adjacent strips can be ignored.

Before proceeding to the method of calculation of the characteristic impedances and effective dielectric constants of the system, the method of expressing even and odd mode capacitances for a general six strip configuration will be examined.

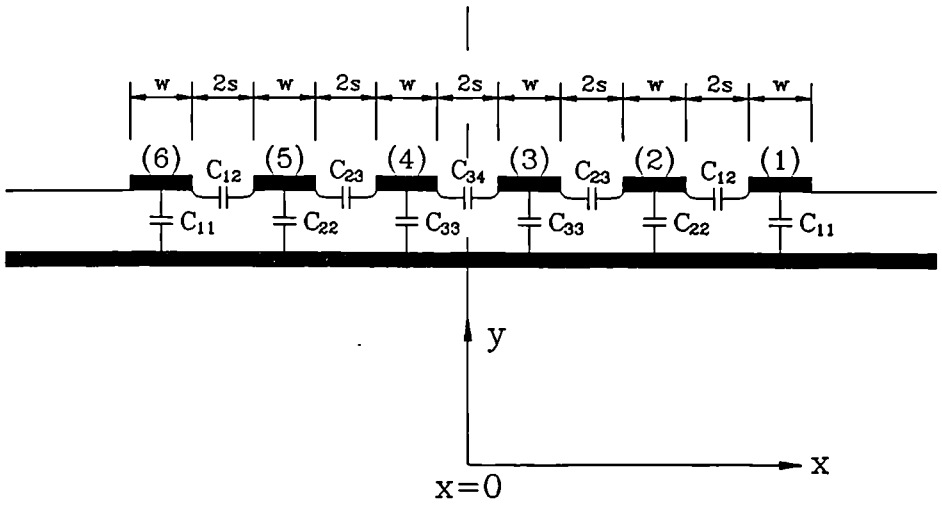

Figure 4.6 Capacitance model for 6 strip coupler.

In figure (4.6) we assume [4.3] that the coupling capacitance C_{12}, C_{23}, C_{34} are the same as that for a two strip system with the same spacing s and width w. The even and odd mode capacitance of each two strip cell are C_{qe} and C_{qo}. The self capacitances of the two outer strips are C_{11} and includes any fringing capacitance, the self-capacitance of the inner strips are $C_{22} = C_{33}$.

We can then write the following equations for the even mode calculation of the system.

$$C_{11} = C_{1e} \qquad (4.87(a))$$

$$C_{22} = C_{2e} \qquad (4.87(b))$$

$$C_{33} = C_{3e} \qquad (4.87(c))$$

The even mode capacitance of the system is then

$$Ce = (C_{1e} + C_{2e} + C_{3e}) \qquad (4.88)$$

which is half the total capacitance to ground of all the strips. The odd mode capacitance of the system is calculated similarly but with electric walls between the two strips of each two strip cell. We can then write

$$C_{10} = 2C_{12} + C_{11} = 2C_{12} + C_{1e} \qquad ie.\ C_{12} = \frac{C_{10} - C_{1e}}{2} \qquad (4.89(a))$$

$$C_{20} = C_{22} + 2C_{12} + 2C_{23} \quad ie.\ C_{23} = \frac{(C_{20} - C_{2e})}{2} - \frac{(C_{10} - C_{1e})}{2} \qquad (4.89(b))$$

$$\begin{aligned} C_{30} &= C_{33} + 2_{23} + 2C_{34} \\ &= C_{3e} + 2C_{23} + 2C_{34} \end{aligned}$$

$$\text{ie.}\ C_{34} = \frac{(C_{30} - C_{3e})}{2} - \frac{(C_{20} - C_{2e})}{2} + \frac{C_{10} - C_{1e}}{2} \qquad (4.89(c))$$

The odd mode capacitance of the system C_o is then

$$\begin{aligned} C_o &= C_{1e} + C_{2e} + C_{3e} + 4C_{12} + 4C_{23} + 2C_{34} \\ &= C_e + 4C_{12} + 4C_{23} + 2C_{34} \qquad (4.90) \end{aligned}$$

Substituting (4.89(a), (4.89(b)), (4.89(c)) into equation (4.90) we arrive at

$$C_o = C_e + [(C_{10} - C_{1e}) + (C_{20} - C_{2e}) + (C_{30} - C_{3e})] \qquad (4.91)$$

Returning to figure 4.5

The boundary conditions are

$$\phi_1 (x,b) = \phi_2 (x,b) \ , \ 0 < x < L \qquad (4.92(a))$$

$$\phi_1 (x,b) = V(x) \ , \ 0 < x < L - a \qquad (4.92(b))$$

$$\phi_1 (x,b) = 0 \ , L - a < x < L \qquad (4.92(c))$$

$$\epsilon_r \frac{\delta \phi_2}{\delta y}\Big|_{y=b} - \frac{\delta \phi_1}{\delta y}\Big|_{y=b} = \frac{\rho_s (x)}{\epsilon_o} \ , \ L - a < x < L$$

$$= 0 \ o < x < L - a \qquad (4.93(a))$$

$$\phi_2 (x, b+h) = \phi_3 (x, b+h) \ \ o < x < L \qquad (4.94(a))$$

$$\phi_2 (x, b+h) = \phi_v (x) = |v| \qquad (4.94(b))$$

for $s < x < s+w$, $3s + w < x < 3s + 2w$, $5s + 2s < x < 5s + 3w$

$$\phi_2 (x_1 b + h) = \phi_o(x) \qquad (4.94(c))$$

for $o < x < s$, $s+w < x < 3s + w$, $3s +2w < x < 5s +2w$, $5s + 3w < x < L$

$$\frac{\delta \phi_3}{\delta x}\Big|_{y=b+h} - \epsilon_r \frac{\delta \phi_2}{\delta y} = \frac{-\rho_q}{\epsilon_o}(x) \qquad (4.95(a))$$

for $s < x < s+w$, $3s + w < x < 3s + 2w$, $5s + 2w < x < 5s +3w$

$$\frac{\delta \phi_3}{\delta x}\Big|_{y=b+h} - \epsilon_r \frac{\delta \phi_2}{\delta y} = 0$$

for $o < x < s$, $s+w < x < 3s+w$, $3s +2w < x < 5s + 2w$, $5s + 3w < x < L$

$\rho_q(x)$ is the charge distribution on strips 1, 2 and 3 and q = 1, 2, 3.

Equations (4.33(a)), (4.33(b)) can be rewritten

$$\tilde{\rho}_q(n) = \sum_{k=1}^{N} \sum_{q=1}^{3} a_k \tilde{\rho}_{qk} \qquad (4.96)$$

where k = 1, 2 - - - N

$$\tilde{\rho}_s(n) = \sum_{m=1}^{H} b_m \tilde{\rho}_{sm}(n) \qquad (4.97)$$

where m = 1, - - - H

Equations (4.34(a)), (4.34(b)) can be rewritten

$$\tilde{G}_{11}(n) \sum_{k=1}^{N} \sum_{q=1}^{3} a_{qk} \tilde{\rho}_{qk}(n) + \tilde{G}_{12}(n) \sum_{m=1}^{H} b_m \tilde{\rho}_{sm}(n) = \tilde{\phi}_v(n) + \tilde{\phi}_o(n) \qquad (4.98)$$

$$\tilde{G}_{21}(n) \sum_{k=1}^{N} \sum_{q=1}^{3} a_{qk} \tilde{\rho}_{qk}(n) + \tilde{G}_{22}(n) \sum_{m=1}^{H} b_m \tilde{\rho}_{sm}(n) = \tilde{V}_n \qquad (4.99)$$

Taking the inner product with

$$\tilde{\rho}_{pi}(n) \text{ and } \tilde{\rho}_{sj}(n)$$

where p = 1, 2, 3, i = 1, 2, ---N, j= 1, 2, -- H

we arrive at

$$\sum_{k=1}^{N} \sum_{q=1}^{3} \sum_{n=1}^{\infty} \tilde{\rho}_{pi}(n)\, \tilde{G}_{11}(n)\, a_{qk} \tilde{\rho}_{qk}(n) + \sum_{n=1}^{\infty} \sum_{m}^{H} \tilde{\rho}_{pi}(n)\, \tilde{G}_{12}\, b_m \tilde{\rho}_{sm}(n)$$

$$= \sum_{n=1}^{\infty} \left[\tilde{\rho}_{pi}(n)\, \tilde{\phi}_v(n) + \tilde{\rho}_{pi}(n)\, \tilde{\phi}_o(n) \right] = \sum_{n=1}^{\infty} \tilde{\rho}_{pi}(n)\, \tilde{\phi}_v(n) \qquad (4.100)$$

since

$$\sum \tilde{\rho}_{pi}(n)\ \tilde{\phi}_o(n) = 0$$

and

$$\sum_{k=1}^{N}\sum_{q=1}^{3}\sum_{n=1}^{\infty} \tilde{\rho}_{sj}(n)\ \tilde{G}_{21}(n)\ a_{qk}\tilde{\rho}_{qk}(n) + \sum_{n=1}^{\infty}\sum_{m=1}^{H} \tilde{\rho}_{sj}(n)\ \tilde{G}_{22}(n)\ b_m\tilde{\rho}_{sm}(n)$$

$$= \sum_{n=1}^{\infty} \tilde{\rho}_{sj}(n)\ \tilde{V}_n \qquad (4.101)$$

N, H are the number of basis functions chosen per strip and septum respectively. As indicated earlier in this the thesis and references [4.1], [4.5] N = H = 2 results in accurate results. Equation (4.99) becomes

$$\sum_{n=1}^{\infty}\sum_{k=1}^{2} \tilde{\rho}_{pi}(n)\ \tilde{G}_{11}(n)\ a_{1k}\tilde{\rho}_{1k}(n) + \sum_{n=1}^{\infty}\sum_{k=1}^{2} \tilde{\rho}_{pi}(n)\ \tilde{G}_{11}\ a_{2k}\tilde{\rho}_{2k}(n)$$

$$+ \sum_{n=1}^{\infty}\sum_{k=1}^{2} \tilde{\rho}_{pi}(n)\ \tilde{G}_{11}(n)\ a_{3k}\tilde{\rho}_{3k} + \sum_{n=1}^{\infty}\sum_{m}^{2} \tilde{\rho}_{pi}\tilde{G}_{12}(n)\, b_m\tilde{\rho}_{sm}$$

$$= \sum_{n=1}^{\infty} \tilde{\rho}_{pi}(n)\ \tilde{\phi}_v(n) \qquad (4.102(a))$$

with further expansion we get

$$\sum_{n=1}^{\infty} \tilde{\rho}_{pi}(n)\, \tilde{G}_{11}(n)\, a_{11}\, \tilde{\rho}_{11}(n) + \sum_{n=1}^{\infty} \tilde{\rho}_{pi}(n)\, \tilde{G}_{11}\, a_{12}\, \tilde{\rho}_{12}(n) + \sum_{n=1}^{\infty} \tilde{\rho}_{pi}(n)\, \tilde{G}_{11}\, a_{21}\, \tilde{\rho}_{21}$$

$$+ \sum_{n=1}^{\infty} \tilde{\rho}_{pi}(n)\, \tilde{G}_{11}(n)\, a_{22}\, \tilde{\rho}_{22}(n) + \sum_{n=1}^{\infty} \tilde{\rho}_{pi}\, \tilde{G}_{11}(n)\, a_{31}\, \tilde{\rho}_{31}(n)$$

$$+ \sum_{n=1}^{\infty} \tilde{\rho}_{pi}(n)\, \tilde{G}_{11}\, a_{32}\, \tilde{\rho}_{32}(n) + \sum_{n=1}^{\infty} \tilde{\rho}_{pi}(n)\, \tilde{G}_{12}\, b_1\, \tilde{\rho}_{s1}(n)$$

$$+ \sum_{n=1}^{\infty} \tilde{\rho}_{pi}(n)\, \tilde{G}_{12}(n)\, b_2\, \tilde{\rho}_{s2}(n) = \sum_{n=1}^{\infty} \tilde{\rho}_{pi}(n)\, \tilde{\phi}_v(n) \qquad (4.102(b))$$

$$\sum_{n=1}^{\infty} \tilde{\rho}_{sj}(n)\, \tilde{G}_{21}(n)\, a_{11}\, \tilde{\rho}_{11}(n) + \sum_{n=1}^{\infty} \tilde{\rho}_{sj}(n)\, \tilde{G}_{21}(n)\, a_{12}\, \tilde{\rho}_{12}(n)$$

$$+ \sum_{n=1}^{\infty} \tilde{\rho}_{sj}(n)\, \tilde{G}_{21}(n)\, a_{21}\, \tilde{\rho}_{21}(n) + \sum_{n=1}^{\infty} \tilde{\rho}_{sj}(n)\, \tilde{G}_{21}(n)\, a_{22}(n)\, \tilde{\rho}_{22}(n)$$

$$+ \sum_{n=1}^{\infty} \tilde{\rho}_{sj}(n)\, \tilde{G}_{21}(n)\, a_{31}\, \tilde{\rho}_{31}(n) + \sum_{n=1}^{\infty} \tilde{\rho}_{sj}(n)\, \tilde{G}_{21}(n)\, a_{32}\, \tilde{\rho}_{32}(n)$$

$$+ \sum_{n=1}^{\infty} \tilde{\rho}_{sj}(n)\, \tilde{G}_{22}(n)\, b_1\, \tilde{\rho}_{s1}(n) + \sum_{n=1}^{\infty} \tilde{\rho}_{sj}(n)\, \tilde{G}_{22}(n)\, b_2\, \tilde{\rho}_{s2}(n) = 0 \qquad (4.103)$$

Again

$$\sum_{n=1}^{\infty} \tilde{\rho}_{pi}(n)\, \tilde{\phi}_v(n) = \frac{L}{2} \int_o^L \tilde{\rho}_{pi}(x)\, V dx$$

$$= P_{pi} \qquad (4.104)$$

Now the charge expansion basis functions are taken as

$$\rho_{11} = \frac{1}{\pi\sqrt{\left(\frac{w}{2}\right)^2 - \left(x - 5S - \frac{5}{2}w\right)^2}} \qquad (4.105(a))$$

$$\rho_{12} = \frac{4}{5w}\left\{1\left[\frac{+2\left(x - 5S - \frac{5}{2}w\right)}{w}\right]^3\right\} \qquad (4.105(b))$$

(4.105) holds for 5S + 2w < x < 5S + 3w and is zero elsewhere

$$\rho_{21} = \frac{1}{\pi\sqrt{\left(\frac{w}{2}\right)^2 - \left(x - 3S - \frac{3}{2}w\right)^2}} \qquad (4.106(a))$$

$$\rho_{22} = \frac{4}{5w}\left\{1 + \left[\frac{2\left(x - 3S - \frac{3}{2}w\right)}{w}\right]^3\right\}$$

(4.106) holds for 3S + w < x < 3S + 2w and is 0 elsewhere

$$\rho_{31} = \frac{1}{\pi\sqrt{\left(\frac{w}{2}\right)^2 - \left(x - S - \frac{3}{2}w\right)^2}} \qquad (4.107(a))$$

$$\rho_{32} = \frac{4}{5w}\left\{1 + \left[\frac{2\left(x - S - \frac{3}{2}w\right)}{w}\right]^3\right\} \qquad (4.107(b))$$

(4.107) holds for S < x < s + w and is zero elsewhere

$$\rho_{s1} = \frac{4}{a^4}(L-x)^3 \qquad (4.108(a))$$

for L - a < x < L

ρ_{s1} = 0 elsewhere

$$\rho_{s2} = \frac{1}{2a}\frac{L-x}{\sqrt{a^2-(L-x)^2}} \qquad (4.108(b))$$

(4.108) holds for L - a < x < L and is zero elsewhere

Substituting (4.105), (4.106), (4.107) into (4.104) we get for the even mode when V = 1 on all strips

$$P_{11e} = \frac{L}{2}\int_{5s+2w}^{5s+3w}\rho_{11}(x)\,dx$$

$$P_{12e} = \frac{L}{2}\int_{5s+2w}^{5s+3w}\rho_{12}(x)\,dx$$

$$P_{21e} = \frac{L}{2}\int_{3s+w}^{3s+2w}\rho_{21}(x)\,dx$$

$$P_{22e} = \frac{L}{2}\int_{3s+w}^{3s+2w}\rho_{22}(x)\,dx$$

$$P_{31e} = \frac{L}{2}\int_{s}^{s+w}\rho_{31}(x)\,dx$$

$$P_{32e} = \frac{L}{2} \int_{s}^{s+w} \rho_{32}(x)\, dx$$

For the odd mode

$$P_{11o} = -\rho_{11e}$$

$$P_{12o} = -\rho_{12e}$$

$$P_{21o} = \rho_{21e}$$

$$P_{22o} = \rho_{22e}$$

$$P_{31o} = -\rho_{31e}$$

$$P_{32o} = -\rho_{32e}$$

We can now rewrite (4.102), (4.103) as follows (equation 4.109)

$$\begin{bmatrix}
\sum \tilde{G}_{11}\tilde{\rho}_{11}^{2} & \sum \tilde{G}_{11}\tilde{\rho}_{11}\tilde{\rho}_{12} & \sum \tilde{G}_{11}\tilde{\rho}_{11}\tilde{\rho}_{21} & \sum \tilde{G}_{11}\tilde{\rho}_{11}\tilde{\rho}_{22} & \sum \tilde{G}_{11}\tilde{\rho}_{11}\tilde{\rho}_{31} & \sum \tilde{G}_{11}\tilde{\rho}_{11}\tilde{\rho}_{32} & \sum \tilde{G}_{12}\tilde{\rho}_{11}\tilde{\rho}_{s1} & \sum \tilde{G}_{12}\tilde{\rho}_{11}\tilde{\rho}_{s2} \\
\sum \tilde{G}_{11}\tilde{\rho}_{12}\tilde{\rho}_{11} & \sum \tilde{G}_{11}\tilde{\rho}_{12}^{2} & \sum \tilde{G}_{11}\tilde{\rho}_{12}\tilde{\rho}_{21} & \sum \tilde{G}_{11}\tilde{\rho}_{12}\tilde{\rho}_{22} & \sum \tilde{G}_{11}\tilde{\rho}_{12}\tilde{\rho}_{31} & \sum \tilde{G}_{11}\tilde{\rho}_{12}\tilde{\rho}_{32} & \sum \tilde{G}_{12}\tilde{\rho}_{12}\tilde{\rho}_{s1} & \sum \tilde{G}_{12}\tilde{\rho}_{12}\tilde{\rho}_{s2} \\
\sum \tilde{G}_{11}\tilde{\rho}_{21}\tilde{\rho}_{11} & \sum \tilde{G}_{11}\tilde{\rho}_{21}\tilde{\rho}_{12} & \sum \tilde{G}_{11}\tilde{\rho}_{21}^{2} & \sum \tilde{G}_{11}\tilde{\rho}_{21}\tilde{\rho}_{22} & \sum \tilde{G}_{11}\tilde{\rho}_{21}\tilde{\rho}_{31} & \sum \tilde{G}_{11}\tilde{\rho}_{21}\tilde{\rho}_{32} & \sum \tilde{G}_{12}\tilde{\rho}_{21}\tilde{\rho}_{s1} & \sum \tilde{G}_{12}\tilde{\rho}_{21}\tilde{\rho}_{s2} \\
\sum \tilde{G}_{11}\tilde{\rho}_{22}\tilde{\rho}_{11} & \sum \tilde{G}_{11}\tilde{\rho}_{22}\tilde{\rho}_{12} & \sum \tilde{G}_{11}\tilde{\rho}_{22}\tilde{\rho}_{21} & \sum \tilde{G}_{11}\tilde{\rho}_{22}^{2} & \sum \tilde{G}_{11}\tilde{\rho}_{22}\tilde{\rho}_{31} & \sum \tilde{G}_{11}\tilde{\rho}_{22}\tilde{\rho}_{32} & \sum \tilde{G}_{12}\tilde{\rho}_{22}\tilde{\rho}_{s1} & \sum \tilde{G}_{12}\tilde{\rho}_{22}\tilde{\rho}_{s2} \\
\sum \tilde{G}_{11}\tilde{\rho}_{31}\tilde{\rho}_{11} & \sum \tilde{G}_{11}\tilde{\rho}_{31}\tilde{\rho}_{12} & \sum \tilde{G}_{11}\tilde{\rho}_{31}\tilde{\rho}_{21} & \sum \tilde{G}_{11}\tilde{\rho}_{31}\tilde{\rho}_{22} & \sum \tilde{G}_{11}\tilde{\rho}_{31}^{2} & \sum \tilde{G}_{11}\tilde{\rho}_{31}\tilde{\rho}_{32} & \sum \tilde{G}_{12}\tilde{\rho}_{31}\tilde{\rho}_{s1} & \sum \tilde{G}_{12}\tilde{\rho}_{31}\tilde{\rho}_{s2} \\
\sum \tilde{G}_{11}\tilde{\rho}_{32}\tilde{\rho}_{11} & \sum \tilde{G}_{11}\tilde{\rho}_{32}\tilde{\rho}_{12} & \sum \tilde{G}_{11}\tilde{\rho}_{32}\tilde{\rho}_{21} & \sum \tilde{G}_{11}\tilde{\rho}_{32}\tilde{\rho}_{22} & \sum \tilde{G}_{11}\tilde{\rho}_{32}\tilde{\rho}_{31} & \sum \tilde{G}_{11}\tilde{\rho}_{32}^{2} & \sum \tilde{G}_{12}\tilde{\rho}_{32}\tilde{\rho}_{s1} & \sum \tilde{G}_{12}\tilde{\rho}_{32}\tilde{\rho}_{s2} \\
\sum \tilde{G}_{21}\tilde{\rho}_{s1}\tilde{\rho}_{11} & \sum \tilde{G}_{21}\tilde{\rho}_{s1}\tilde{\rho}_{12} & \sum \tilde{G}_{21}\tilde{\rho}_{s1}\tilde{\rho}_{21} & \sum \tilde{G}_{21}\tilde{\rho}_{s1}\tilde{\rho}_{22} & \sum \tilde{G}_{21}\tilde{\rho}_{s1}\tilde{\rho}_{31} & \sum \tilde{G}_{21}\tilde{\rho}_{s1}\tilde{\rho}_{32} & \sum \tilde{G}_{22}\tilde{\rho}_{s1}^{2} & \sum \tilde{G}_{22}\tilde{\rho}_{s1}\tilde{\rho}_{s2} \\
\sum \tilde{G}_{21}\tilde{\rho}_{s2}\tilde{\rho}_{11} & \sum \tilde{G}_{21}\tilde{\rho}_{s2}\tilde{\rho}_{12} & \sum \tilde{G}_{21}\tilde{\rho}_{s2}\tilde{\rho}_{21} & \sum \tilde{G}_{21}\tilde{\rho}_{s2}\tilde{\rho}_{22} & \sum \tilde{G}_{21}\tilde{\rho}_{s2}\tilde{\rho}_{31} & \sum \tilde{G}_{21}\tilde{\rho}_{s2}\tilde{\rho}_{32} & \sum \tilde{G}_{22}\tilde{\rho}_{s2}\tilde{\rho}_{s1} & \sum \tilde{G}_{22}\tilde{\rho}_{s2}^{2}
\end{bmatrix}
\begin{bmatrix} a_{11} \\ a_{12} \\ a_{21} \\ a_{22} \\ a_{31} \\ a_{32} \\ b_1 \\ b_2 \end{bmatrix}
=
\begin{bmatrix} P_{11} \\ P_{12} \\ P_{21} \\ P_{22} \\ P_{31} \\ P_{32} \\ 0 \\ 0 \end{bmatrix}$$

The summation is over n=1 → ∞ and all terms in the matrix on the left are fourier transforms.

The a_{qk}, b_n are found from the above set of simultaneous equations. The even and odd mode capacitance of each strip is found from:

$$\frac{C_{q(o/e)}}{\epsilon_o} = \sum_{k=1}^{K} a_{qk}\rho_{qk(o/e)}$$

Using the following expressions

$$k_{en} = \frac{n - 0.5}{L}\pi \ , \ k_{on} = \frac{n}{L}\pi \ , \ \alpha_n = k_{en}\frac{w}{2}$$

$$\beta_n = k_{on}\frac{w}{2} \ , \ s_1 = 5\ (s+\frac{w}{2}) \ , \ s_2 = 3\ (s+\frac{w}{2}) \ , \ s_3 = (s+\frac{w}{2})$$

and

$$f(\theta) = \sin\theta[\theta^3 - 6\theta] + \cos\theta[3\theta^2 - 6]$$

and following the approach in section 4.1 the $\tilde{\rho}_{qk}$ can be expressed in the following way:

$$\tilde{\rho}_{11e} = J_o(\alpha n)\cos k_{en} s_1 \qquad (4.110(a))$$

$$\tilde{\rho}_{11o} = J_o(\beta n)\sin k_{on} s_1 \qquad (4.110(b))$$

$$\tilde{\rho}_{21e} = J_o(\alpha_n)\cos k_{en} s_2 \qquad (4.110(c))$$

$$\tilde{\rho}_{21o} = J_o(\beta_n)\sin k_{on} s_2 \qquad (4.110(d))$$

$$\tilde{\rho}_{31e} = J_o(\alpha_n)\cos k_{en} s_3 \qquad (4.110(e))$$

$$\tilde{\rho}_{31o} = J_o(\beta_n) \sin k_{on} s_3 \qquad (4.110(f))$$

$$\tilde{\rho}_{12e} = \left(\frac{8}{5w}\right) (\cos k_{en} s_1) \left(\frac{1}{k_{en}}\right)\left[\sin \alpha_n + \frac{1}{\alpha_n^3} (f(\alpha_n) + 6)\right] \qquad (4.111(a))$$

$$\tilde{\rho}_{12o} = \left(\frac{8}{5w}\right) (\sin k_{on} s_1) \left(\frac{1}{k_{on}}\right)\left[\sin \beta_n + \frac{1}{\beta_n^3} (f(\beta_n) + 6)\right] \qquad (4.111(b))$$

$$\tilde{\rho}_{22e} = \left(\frac{8}{5w}\right) \cos(k_{en} s_2) \left(\frac{1}{k_{en}}\right)\left[\sin \alpha_n + \frac{1}{\alpha_n^3} (f(\alpha_n) + 6)\right] \qquad (4.111(c))$$

$$\tilde{\rho}_{22o} = \frac{8}{5w} \sin(k_{on} s_2) \left(\frac{1}{k_{on}}\right)\left[\sin \beta_n + \frac{1}{\beta_n^3} (f(\beta_n) + 6)\right] \qquad (4.111(d))$$

$$\tilde{\rho}_{32e} = \left(\frac{8}{5w}\right) \cos(k_{en} s_3) \left(\frac{1}{k_{en}}\right)\left[\sin \alpha_n + \frac{1}{\alpha_n^3} (f(\alpha_n) + 6)\right] \qquad (4.111(e))$$

$$\rho_{32o} = \frac{8}{5w} \sin(k_{on} s_3) \left(\frac{1}{k_{on}}\right)\left[\sin \beta_n + \frac{1}{\beta_n^3} (f(\beta_n) + 6)\right] \qquad (4.111(f))$$

Numerical evaluation proves that (see Appendix 3)

$$\tilde{\rho}_{11e} \approx \tilde{\rho}_{12e} \qquad (4.112(a))$$

$$\tilde{\rho}_{21e} \approx \tilde{\rho}_{22e} \qquad (4.112(b))$$

$$\tilde{\rho}_{31e} \approx \tilde{\rho}_{32e} \qquad (4.112(c))$$

$$\tilde{\rho}_{11o} \approx \tilde{\rho}_{12o} \qquad (4.112(d))$$

$$\tilde{\rho}_{21o} \approx \tilde{\rho}_{22o} \qquad (4.112(e))$$

$$\tilde{\rho}_{31o} \approx \tilde{\rho}_{32o} \qquad (4.112(f))$$

Therefore only three even and three odd terms need to be taken into account in equation (4.109).

A MATHCAD program for calculating the even and odd mode impedance of each strip was prepared using equation (4.88) and (4.91) the even and odd mode impedance Z_e, Z_o of the system of six strip was calculated. The program is given in Appendix 2. The evaluation was done with n = 1 --- 500 and checked for convergence with n = 1 --- 1000.

The method of solution is as follows:

1. Calculate the P_{qk} terms
2. Calculate the a_{qk}, b_m terms
3. Use the a_{qk}, P_{qk} to calculate $C_{qe,}$ where C_{qe} is the even mode capacitance of the qth strip.
4. Use the C_{qe} to calculate C_e with and without dielectric ie. the even mode capacitance of the system of lines using equation (4.88).
5. Follow steps (1) through (4) above to calculate C_{qo} the odd mode capacitance off each strip.
6. Use the C_{qe} and C_{qo} along with equation (4.90) to calculate C_o, odd mode capacitance of the system.
7. Use C_e, C_o to calculate Z_e, Z_o, ϵ_{effe}, $\epsilon_{effo.}$
8. Calculate $Z_{oe}/Z_{oo} = m$
9. Calculate coupling factor = $(M - 1)/(M + 1)$

Where Z_e, Z_o, ϵ_{effe}, ϵ_{effo} are even mode impedance, odd mode impedance, even mode effective dielectric constant and odd mode effective dielectric constant respectively.

Table 4.2 shows variation of calculated Z_{oe}, Z_{oo} ϵ_{effe}, ϵ_{effo} and coupling factor for different values of 'a' with ϵ_r= 9.8 and all other parameters in figure (4.5) fixed.

a	Z_{oe}	Zoo	Z_{oe}/Z_{oo}	Coupling	ϵ_{effe}	ϵ_{effo}
inch	ohm	ohm		dB		
0.600	217.14	12.07	17.97	0.966	3.48	4.33
0.550	243.22	12.07	20.15	0.863	2.94	4.00
0.500	249.44	12.07	20.66	0.841	2.82	3.90
0.450	251.09	12.07	20.80	0.836	2.79	3.88
0.400	251.59	12.07	20.84	0.834	2.78	3.87
0.350	251.75	12.07	20.86	0.833	2.78	3.87
0.300	251.82	12.07	20.86	0.833	2.78	3.87
0.250	251.84	12.07	20.86	0.833	2.78	3.87
0.200	251.86	12.07	20.86	0.833	2.78	3.87
0.150	251.86	12.07	20.86	0.833	2.78	3.87
0.100	251.86	12.07	20.86	0.833	2.78	3.87

Table (4.2) Variation of Z_{oe}, Zoo, ϵ_{effe}, ϵ_{effo} with 'a' for the structure in figure (4.5). (Six Strip Coupler)

(h = 0.015; w = 0.001; s = 0.00035; L = 0.65; t = 0.65; b = 0.025; ϵr = 9.8)

Figure (4.7) displays the data in table (4.2) graphically. It is observed that for the values of 'a' examined Z_{oo} is only weakly dependent on 'a'. This is as expected by examining equation (4.90). As $C_e \rightarrow 0$, C_o becomes the dependent on the interstrip capacitances only; thus the effect of the septum becomes less pronounced. It therefore follows that Z_{oe} could be made to vary almost independently of Z_{oo} if enough strips are used in the coupler.

It is observed that Z_{oe}, ϵ_{effe}, ϵ_{effo} are slowly varying functions of 'a' for the six strip case for the given cavity dimensions when a < . 500 (ie. 0.77 L). When a > 0.500 inch rate of change of the above mentioned functions with 'a' is much greater. Therefore for practical applications it would be desirable to keep the $\frac{a}{L}$ ratio below a given value in order to minimize the effects of manufacturing tolerances. It is also observed that, for the ranges of dimensions used, Z_{oo} is fixed with respect to $\frac{a}{L}$ and by comparison with the two strip data it is seen that Z_{oo} for the six strip is much less a function of 'a' than it is for the two strip case. This is due to the fact that in the six strip case more of the odd mode electric field is in region 3, (air). This is an important observation which implies that for properly chosen enclosure dimensions the performance of the broadband hybrid proposed in section (2.8) would be dependent only line spacing, line width and substrate thickness. This would also be true for other structures whose performance is mainly dependent on Z_{oo}.

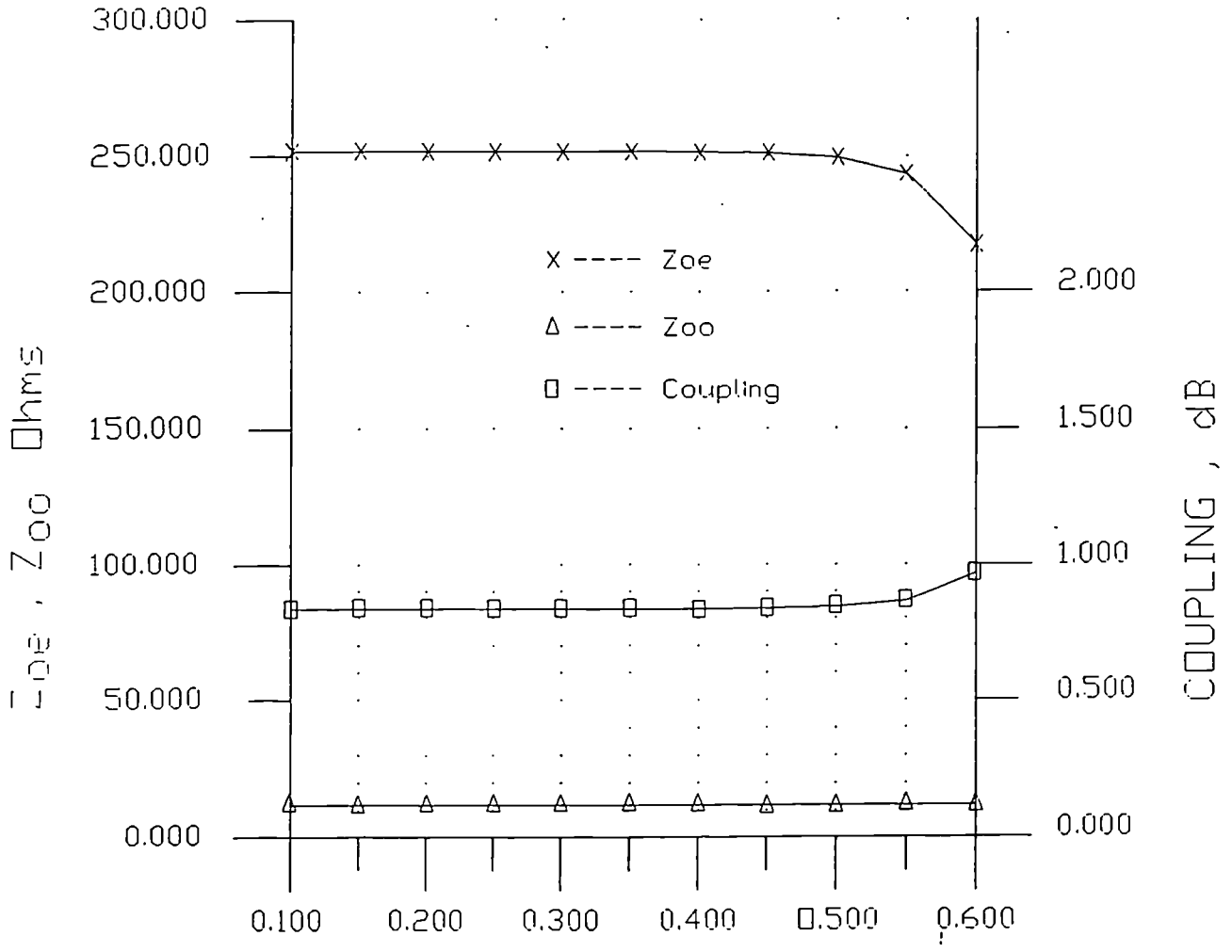

Figure (4.7) Variation of Zoe, Zoo with 'a' for the Structure in Figure (4.5)

4.3 BROADSIDE COUPLED MICROSTRIP WITH NON-UNIFORM SEPTUM SPACING

Yamamoto et al [4.7] has shown that for asymmetrical coupled lines, where the asymmetry indicates an exponential variation in the even and odd mode impedance of the coupler along its length, then referring to figure (4.8), the coupled response approaches an asymptotic value as frequency increases. That is, the coupler is theoretically a high pass network that does not suffer from the spurious response associated with uniform coupled lines. The above mentioned high pass characteristic is dependent on three conditions:

1. The coupler being terminated as shown in figure (4.8) with the characteristic impedance of the system.

2. The coupling k(o) = 0 at z = 0 where

$$k(z) = \frac{Z_{oe}(z) - Z_{oo}(z)}{Z_{oe}(z) + Z_{oo}(z)} \qquad (4.113)$$

   where $Z_{oe}(z)$, $Z_{oo}(z)$ are even and odd mode characteristic impedances at a point Z along the coupler.

3. The condition $Z_{oe}(z)\ Z_{oo}(z) = Z_o^2$ has to be maintained along the length of the coupler where Z_o is the terminating impedance at ports 1 through 4.

Conditions (1) and (3) can be met with edge coupled asymmetric lines as shown in figure (4.8) [4.7], however, condition (2) would require lines with infinite separation at Z = 0.

Structures which could meet condition (2) have been reported [4.8] [4.9], however these realisations used either coupled rods or coupled striplines neither of which is compatible with miniature microwave integrated circuitry.

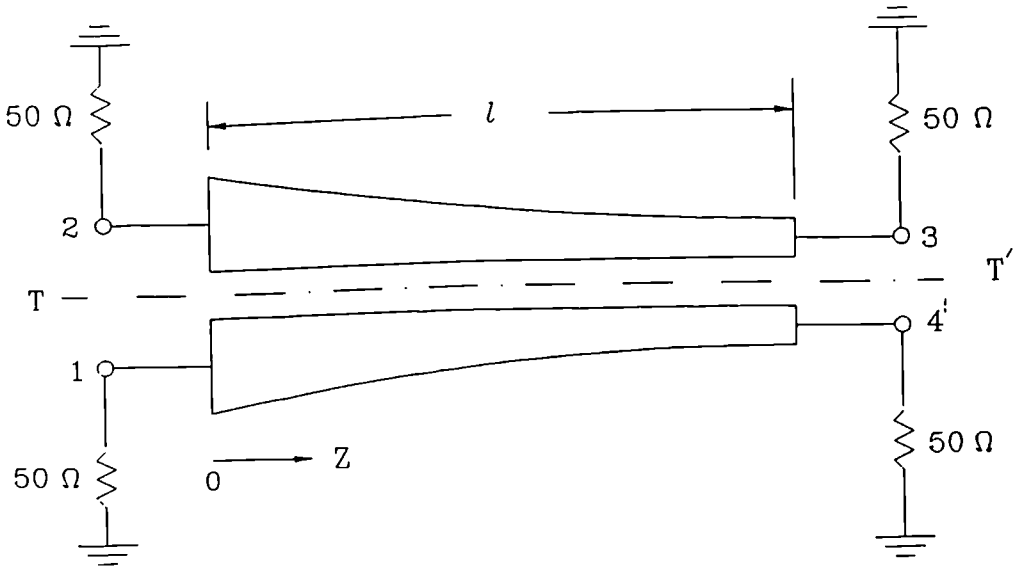

FIGURE: 4 8. Coupled nonuniform transmission-line directional coupler

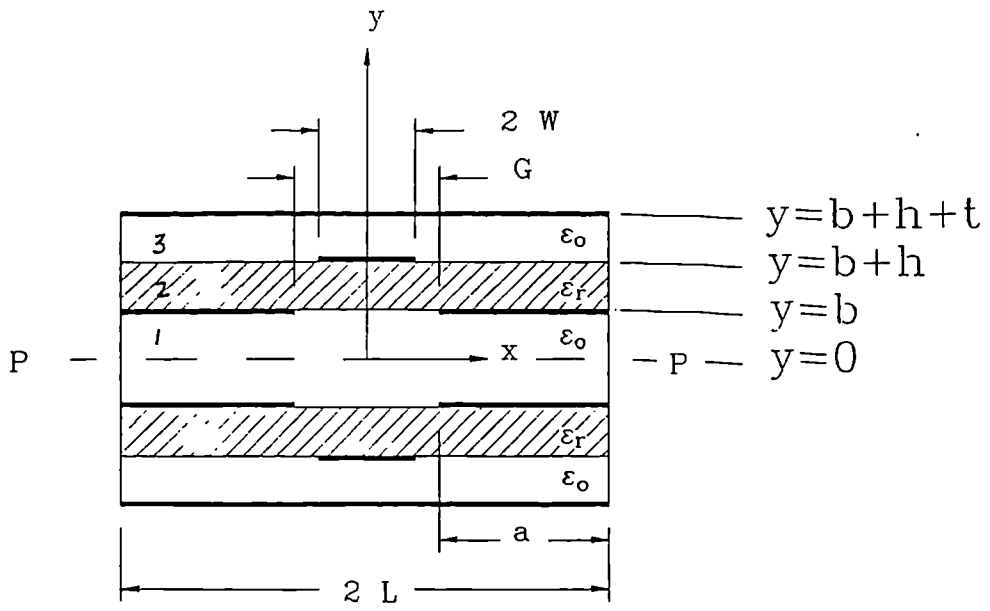

FIGURE: 4.9. Broadside Coupled Microstrip with Tuning Septum

In figure (4.9) broadside coupled microstrips with printed tuning septums are proposed to meet condition 2. The broadside coupled lines are of uniform width and the spacing of the septum is varied exponentially along the length ℓ of the coupler in the Z direction. As indicated in [4.7] the steps required to design the couple are, in order,

1. From the coupling value (C dB) required, calculate the product $\mu\ell$, where μ is taper rate of G along Z and ℓ is coupler length as shown in figure (4.8), using equation (54) of reference [4.7].
2. Determine ℓ from the lower band edge of the frequency range required as well as coupling ripple allowable.
3. Determine μ.

The problem is therefore to determine the even and odd mode characteristic impedance for the structure shown in cross section in figure (4.9). The spectral domain technique is used. Due to the symmetry of the structure it can be divided into two parts by a line at y = 0; and its performance can be analyzed as a superposition of even and odd modes by considering only the top half of the structure in which three regions 1, 2, 3 are defined, as shown, with relative dielectric constants of unity in regions 1 and 3 and ϵ_r in region 2.

For the odd mode an electric wall can be drawn along P - P^1; therefore the calculation of odd mode impedance in figure (4.9) is reduced to the calculation of even mode characteristic impedance of the coupled microstrip structure in figure (4.1), with s = 0. The actual odd capacitance is then twice that calculated ie. the odd mode impedance of figure (4.9) is a half of the even mode impedance in figure (4.1) with s = o, when other corresponding physical conditions in the structures are made equal. Low odd mode impedance can be achieved by letting b tend to zero and reducing h.

When the even mode field conditions in figure (4.9) are examined it is clear that a magnetic wall can be placed along the line P - P^1 ie. at (x,o). In addition a magnetic wall can be placed along the line (o,y).

To calculate the even mode impedance we divide the strip at x = o into two strips with equal voltages, V_1 and carrying equal currents with spacing 2S between them. The structure is then analyzed identically to the even mode calculation for figure (4.1) by letting s → o; and placing magnetic walls at (o,y) and at (x,o). The actual even mode impedance is then one half of the calculated value.

The boundary conditions to be satisfied in the space domain in the regions i = 1, 2, 3 of the upper half section of figure (4.9) are then

$$\frac{\delta \phi_i}{\delta x}(o,y) = 0 \qquad \text{magnetic wall} \qquad (4.114(a))$$

$$\frac{d\phi_i}{dy}(x,o) = 0 \qquad \text{magnetic wall} \qquad (4.114(b))$$

At y = b

$$\phi_1(x,b) = \phi_2(x,b) \qquad (4.114(c))$$

$$\phi_1(x,b) = V(x) \ , \ 0 < x < L-a \qquad (4.114(d))$$

$$\phi_1(x,b) = 0 \ , \ < L-a < x < L \text{ on the septum} \qquad (4.114(e))$$

$$\epsilon_r \frac{d\phi_2(x,y)}{dy}\Big|_{y=b} - \frac{d\phi_1}{dy}(x,y)\Big|_{y=b} = \frac{-\rho_s(x)}{\epsilon_o} \quad L-a < x < L \qquad (4.114(f))$$
$$= 0 \quad 0 < x < L-a$$

At y = b+h

$$\phi_2(x, b+h) = \phi_3(x, b+h) \qquad (4.114(g))$$

$$\phi_2(x, b+h) = \phi_v(x) = V, \; s < x < s+w \quad (s \to o) \qquad (4.114(h))$$

$$\phi_2(x, b+h) = \phi_o(x), \; o < x < s, \; s+w < x < L \qquad (4.114(i))$$

$$\frac{d}{dy}\phi_3(x,y)\Big|_{y=b+h} - \epsilon_r \frac{d}{dy}\phi_2(x,y)\Big|_{y=b+h} = \frac{-\rho(x)}{\epsilon_o}, \; s < x < s+w \; (s \to o) \qquad (4.114(j))$$
$$= 0, \; o < x < s, \; s+w < x < L \; (s \to o)$$

where $\rho(x)$, $\rho_s(x)$ are charge density functions on the strip and on the septum respectively.

The fourier transforms of the boundary conditions are then taken. The balance of the analysis is the same as that in section (4.1) with the following exceptions:

1. Only the even mode is considered, therefore the fourier transform used is

$$\phi_i(n,y) = \int_o^L \phi_i(x,y) \cos k_n x \, dx \qquad (4.114(k))$$

$$\text{where } k = (n - \frac{1}{2}) \frac{\pi}{L}, \; n = 1, 2---$$

2. The general solution of Laplace's equation in the fourier transform domain considering region 1 is

$$\tilde{\phi}_1(n,y) = A_n \cosh k_n y \qquad (4.114(l))$$

Apart from the ability to realise a high pass coupler in microstrip form, the structure in figure (4.9) can be used to overcome the large variation between even and odd mode phase velocities which is a characteristic of broadside coupled microstrip lines; by using varying septum length 'a'. When a = o we have the broadside coupled suspended strips of Homo and Medina. [3.2]

In addition, because of the septums are printed, the characteristic parameters of the structure can be well controlled and is easily mounted in a mechanically stable fashion.

Alternatively the structure in figure (4.9) can be analyzed without considering its structural symmetry. The structure is divided into regions i, starting at the lower air dielectric region. ie. i = 1,2--,M, where M=6 and dielectric (interfaces, j, where j = 1,2--,

N, where N=4. The discussion will be restricted to the TEM assumption, and only the Poisson equation needs to be solved. Dispersion analysis could also be done by using the wave equation.

Considering figure (4.9) (ie. a cross section of the actual coupler) assume the fourier transform of the potential function anywhere in the structure is

$$\tilde{\phi}(n,y) = \int_o^L \phi(x,y)\, e^{j\beta x}\, dx \qquad (4.115)$$

$$\text{where} \quad \beta = \frac{n\pi}{2L} \qquad n = 1, 2 - - - \infty$$

Poisson's equation in the transform domain is then

$$\left(\frac{d^2}{dy^2} - \beta^2\right)\tilde{\phi}\,(n,y) = o \qquad (4.116)$$

The general solution of (4.116) in the i^{th} layer is

$$\tilde{\phi}_i(n,y) = C_i(n)\, Sinh\,\beta y + D_i(n)\cosh\beta y \qquad (4.117)$$

The transform of the potential function at boundaries between the regions satisfies the following equations:

$$\tilde{\phi}_i(n,y_j) = \phi_{i+1}(n,y_j) \qquad (4.118(a))$$

$$\tilde{\Phi}_j(n, y_j) = \tilde{\Phi}_{vj} + \tilde{\Phi}_{dj} \qquad (4.118(b))$$

at the j^{th} interface where there are strips, where $\tilde{\Phi}_{vj}$ is the transform of the known potential on the conductors at the j^{th} interface and $\tilde{\Phi}_{dj}$ is the transform of the unknown potential on the j^{th} interface outside the conductors and

$$\epsilon_{i+1} \frac{d\tilde{\Phi}_{i+1}}{dy}\Big|_{y=y_j} - \epsilon_i \frac{d\tilde{\Phi}_i}{dy}\Big|_{y=y_j} = \frac{-\tilde{\rho}_j(n)}{\epsilon_o} \qquad (4.118(c))$$

where $\tilde{\rho}_j(n)$ is the transform of the unknown charge distributions at the j^{th} interface.

To solve for C_i, D_i (4.117) is substituted into (4.118) and coupled equations of the form

$$\sum_{j=1}^{N} \tilde{G}_{ij}\, \tilde{\rho}_j(n) = \tilde{\Phi}_{vi} + \tilde{\Phi}_{di} \qquad i = 1, --N \qquad (4.119)$$

where $\tilde{G}_{ij}$ is the transform of the Greens function associated with unit charge at the j^{th} interface and determines the potential at the i^{th} region.

$\tilde{\rho}_j$ is then expanded as discussed earlier to get

$$\tilde{\rho}_j = \sum_{m=1}^{M_j} \sum_{q=1}^{Q_j} C_{jq}^m \tilde{\rho}_{jq}^m \quad (4.120) \quad m = 1, 2, --M_j,\ q = 1, 2---Q_j$$

where M is the number of conductors at the j^{th} interface and Q_j is the number of known basis function chosen for use at the j^{th} interface. $\tilde{\rho}_{jg}^{m}$ is transform of the charge basis function and C_{jq}^{m} are constants.

(4.119) then becomes

$$\sum_{j=1}^{N} \tilde{G}_{ij} \sum_{m=1}^{Mj} \sum_{q=1}^{Qj} C_{jq}^{m} \tilde{\rho}_{jq}^{m} = (\tilde{\Phi}_{vi} + \tilde{\Phi}_{di}) \qquad i = 1,2\text{--}N \quad (4.121)$$

Taking the inner product with another set of different known basis functions

ρ_{ir}^{R}, $\quad R = 1,2\text{---}M_j$

$\quad r = 1,2\text{---}Q_j$

$\quad i = 1,2\text{---}N$

we arrive at the matrix

$$\sum_{n=1}^{\infty} \sum_{j=1}^{N} \sum_{m=1}^{Mj} \sum_{q=1}^{Qj} \tilde{\rho}_{ir}^{R}(n)\, \tilde{G}_{ij}(n)\, C_{jq}^{m} \tilde{\rho}_{jq}^{m}(n) = \sum_{n=1}^{\infty} \tilde{\rho}_{ir}^{R}(n)\, [\tilde{\Phi}_{vi}(n) + \tilde{\Phi}_{di}(n)] = \sum_{n=1}^{\infty} \tilde{\rho}_{ir}^{R}(n)\, \tilde{\Phi}_{vi}(n) \quad (4.122)$$

[4.10] after applying Parsevals theorem. (4.122) is then solved for C_{jq}^{m}. After C_{jq}^{m} is found, $\rho_j(x)$ the total charge at the j^{th} interface is found from the expression

$$\rho_j(x) = \sum_{m=1}^{Mj} \sum_{q=1}^{Qj} C_{jq}^{m}\, \rho_{qj}^{m}(x)$$

The capacitance is then found from $\rho_j(x)$ and from the capacitance characteristic impedance and effective dielectric constant is calculated. In the ease of figure (4.9) $M_j = 4$.

The charge basis functions would be the same as those used in section (4.1) and (4.2).

REFERENCES

[4.1] Tatsuo Itoh, "A Generalised Spectral Domain Analysis for Coupled Suspended Microstrip Lines with Tuning Septums"

IEEE Transactions on Microwave Theory and Techniques

Volume MTT-26, No. 10 October, 1978

[4.2] Masayoshi Aikawa, "Microstrip Line Directional Coupler with Tight Coupling and High Density"

Electronics and Communications in Japan

Volume J60-B,No.4 Page 253-259 April, 1977

[4.3] Darko Kajfez, Zoha Paunouic and Stane Paulin, "Simplified Design of Large Coupler"

IEEE Transactions on Microwave Theory and Techniques

Volume MTT-26, No.10 October, 1978 Page 806 - 808

[4.4] Ramesh Garg and I.J. Bahl, "Characteristics of Coupler Microstrip Lines"

IEEE Transactions of Microwave Theory and Techniques

Volume MT-27, No.7 July, 1979 Page 700 - 705

[4.5] Koji Shibata, Kozo Hatori, Yasuyuki Tokumitsu, Hidemitsu Komizo, "Microstrip Spiral Directional Coupler"

IEEE Transactions on Microwave Theory and Techniques

Volume 29, No. 7 July, 1981 Page 680 - 689

[4.6] Reinmut K. Hoffmann and Johann Siegl, "Microstrip - Slot Coupler Design. Parts I and II"

IEEE Transactions on Microwave Theory and Techniques

Volume MTT-30, No. 8 August, 1982 Page 1205-1217

[4.7] Sadahiko Yamamoto, Takashi Azakami, Kiyoyasu Itakura, "Coupled Non-Uniform Transmission Line and Its Applications"

IEEE Transactions on Microwave Theory and Techniques

Volume, MTT-15, No.4 April, 1987 Page 220 - 231

[4.8] Joel D. Bickford, "Ultra-Broadband High-Directivity Directional Coupler Design"

[4.9] J.L. Ekstrom, "The Z-Matrix Parameters of Tapered Transmission Lines"

IRE Transactions on Circuit Theory

Volume, CT-9 June, 1962 Page 132 - 135

[4.10] Robert E. Collin, "Field Theory of Guided Waves"

IEEE Press, New York, 1990 Second Edition

Page 273 - 279

[4.11] Tatsuo Itoh "Generalized Spectral Domain Method for Multiconductor Pointed Lines and Its Application to Tunable Suspended Microstrips"

IEEE Transactions on Microwave Theory and Techniques,

Volume MTT-26, No.12 December, 1978

Page 983-987

CHAPTER 5.0

5.1 APPLICATION OF THE SIX-STRIP COUPLED MICROSTRIP LINE TO A 2-18 GHz 3 dB COUPLER DESIGN AND 2 - 18 GHZ MEDIUM POWER GaAs FET AMPLIFIER REALIZATION

In order to check the validity of the analysis of the six strip coupler discussed in chapter 4, the technique was used to design a three section cascaded broadband 3 dB coupler using the six-strip structure as the tightly coupled centre section. Couplers were realised on both 0.015 inch and 0.025 inch thick alumina substrate with the following thin film metallization scheme: Titanium - Tungsten, tantalum nitride, gold. The thickness of the Titanium - Tungsten, tantalum nitride layers were approximately 2000 angstroms. The gold layer was 4 microns; dielectric constant of the substrate was 9.8.

The dimensions of the two six strip configurations were, referring to figure 4.5,

coupler #(1): h = 0.015, w= 0.001, s = 0.00035, L = 0.65, t = 0.65, b = 0.025, a = 0.575, ϵ_r = 9.8

coupler #(2): h = 0.025, w = 0.001, b = 0.025, a = 0.575, L = 0.65, t = 0.65, s = 0.00035, ϵ_r = 9.8

From appendix 2 the following parameters were calculated for the six strip section

1. Six-Strip Section #1

Z_{oe} = 234.8, Z_{oo} = 12.1 ϵ_{effe} = 3.11, ϵ_{effo} = 4.1 Z_{oe}/Z_{oo} = 19.40

2. Six-Strip Section #2

Z_{oe} = 228.0 ohms, Z_{oo} = 11.3 ohm, ϵ_{effe} = 3.80, ϵ_{effo} = 5.40, Z_{oe}/Z_{oo} = 20.18

5.2 CASCADED COUPLER DESIGN

The cascaded coupler concept is well documented [5.1], [5.2], [5.3], [5.4]

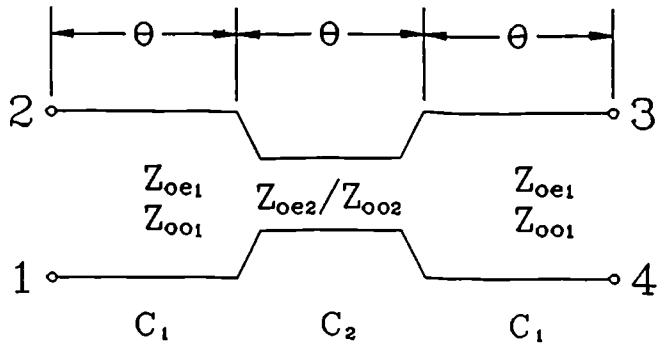

Figure 5.1 3 - Section Coupler Schematic

Figure 5.1 shows a three section cascaded coupler schematic in which all ports are assumed terminated in the characteristic impedance Z_o. Following the approach in [5.4] θ is the electric length of each section and

$$\theta = \frac{\pi}{4},$$

C_1, C_2 are the coupling factor in each section. The coupler can be specified by its mid-band coupled response C_o and another parameter V_1 [5.4 page 783] which determines the shape of the coupling response versus frequency. An equal ripple response was chosen,

the design procedure was as follows:

1. C_o was calculated from

$$20 \log C_o = -3.3 \qquad (5.1)$$

$$\therefore C_o = 0.684$$

2. Fractional bandwidth

$$w = \frac{f_2 - f_1}{f_o} = 2\frac{(f_2 - f_1)}{(f_2 + f_1)} = \quad 1.6$$

where f_1 = 2.0 GHz, f_2 = 18 GHz; and f_1, f_2 are the 0.3 dB equal ripple band edges.

3.

$$R = \frac{1 + C_o}{1 - C_o}$$

$$= 5.32 \qquad (5.2)$$

4.

$$V_2 = V_1 \sqrt{R} \qquad (5.3)$$

V_1 is found from V_{1MF} using figure 13.03 - 2 and using the upper extrapolated curve of figure 13.03 - 3 in reference [5.4].
We arrive at

$$\frac{V_1 - 1}{V_{1MF} - 1} \cong 3.8 \qquad (5.4)$$

From figure 13.03 - 2 [6.4] $V_{1MF} = 1.1$

$\therefore V_1 = 1.38$

$$V_2 = 1.38\sqrt{5.32}$$

$$= 3.18$$

and $Z_1 = V_1$ $Z_2 = V_1 V_2 = (1.38)(3.18) = 4.39$

$$C_1 = \frac{Z_1^2 - 1}{Z_2^2 + 1} = 0.31 \qquad (5.5)$$

and 20 log C_1 = -10.2 dB

$$C_2 = \frac{Z_2^2 - 1}{Z_2^2 + 1} = 0.90 \qquad (5.6)$$

and 20 log C_2 = -0.91 dB

Thus using this design approach, the two outer sections of the three section coupler should have a coupling factor 10.2 dB and the

central section 0.9 dB. 0.9 dB coupling is not achievable by standard microstrip techniques, assuming one coupling section is used.

The even and odd mode impedance of coupled line sections are found by using the following expression

$$\text{Coupling Factor } C = \frac{Z_{oe} - Z_{oo}}{Z_{oe} + Z_{oo}} = \frac{\frac{Z_{oe}}{Z_{oo}} - 1}{\frac{Z_{oe}}{Z_{oo}} + 1} \qquad (5.7)$$

And the condition

$$\sqrt{Z_{oe} Z_{oo}} = Z_o \qquad (5.8)$$

which ensures that the coupler is perfectly matched to its terminating impedance. Setting

$$Z_o = 50 \text{ and } C_2 = 0.9$$

$$Z_{oo2} = 11.5 \text{ ohms and } Z_{oe2} = 220 \text{ ohms}$$

$$Z_{oo1} = 36.3 \text{ ohms } \textit{and } Z_{oe1} = 68.9 \text{ ohms}$$

The structure was then inputted to Eesoff's Touchstone program with

the dimensions of the centre section fixed to the dimensions given earlier in this chapter ie. for h= 0.015 with Z_{oe} = 234.8 ohms, Z_{oo} = 12.1 ohms and for h = 0.025 inch Z_{oe} = 228 ohms, Z_{oo} = 11.3 ohms.

As will be shown later in this chapter these impedances values are achievable with line spacings and line widths which are well within the capability of most thin film facilities. The design was then optimised for bandwidth by varying the parameters of the outer sections of the coupler. Tables 5.1(a)(b) and 5.2(a)(b) are program listings and output data for both couplers.

The couplers were realised at the Lucas Aerospace Quasi-MMIC facility in Mississauga, Canada. Features included plated via holes, thin film resistive terminations and airbridge connections between alternate fingers. Figure (5.2(a)), (b) shows the coupler circuit layout for the 0.015 and 0.025 thick substrates respectively. Figure (5.3) shows the substrate carrier details.

As shown in figures (5.2(a)), (5.2(b)) the etched substrate line width and spacing for the h = .015 inch case were 0.001 and 0.0007 inch respectively. In the h= 0.025 inch case line spacing and width were 0.001 and 0.0006 inch. Figure 5.3 shows the carrier to which the substrates were mounted for testing. The substrate were brazed to the carrier with a gold Germanium eutectic perform so that the dimension 'a' in figure 4.1 would be well defined. The carrier material was chosen for close match in thermal coefficient

of expansion with the substrate to prevent cracking in the heat-up cool-down cycle of the eutectic reflow process. This is particularly critical for the = 0.015 inch thick case.

Figure (5.4(a)) shows plots of calculated and measured coupling factor and figure (5.4(b)) shows calculated and measured return loss for h = 0.015 inch. Figure (5.5(a)) and (5.5(b)) show the same data for h = 0.025 inch.

It is observed that in both the 0.015 and 0.025 case the measured direct port response shows excellent agreement with the calculated result; up to 20 GHz in the 0.015 inch case and up to 14 GHz in the 0.025 inch case. One primary reason for the poorer performance of the 0.025 inch coupler is the greater radiation loss for thicker substrate, a condition which worsens as frequency increases. In both the 0.015 and 0.025 inch cases there is a considerable variation between measured and predicted coupling response over the 11 to 17 GHz frequency band as well as a lower than predicted coupling value over most of the measured frequency band. One contributor to this is the quality of the termination on the 'isolated' port.

The second is the fact that the design was based an quasi-static analysis, ie. only the longitudinal current component was considered. However, as shown in chapter (1), the characteristic impedances, on which coupling calculations were based, is very dependent on the transverse current component at higher frequencies. Therefore some coupling deviation from calculated values should not unexpected as frequency is increased. Also characteristic impedance becomes more frequency dependent as strip with decreases ie. $\frac{H}{\lambda}$ increases for fixed λ ie. related to the Z_{22} term in section 1.2.

The third reason is finite directivity due to unequal even and odd mode phase velocities, particularly in sections 1 of the cascaded coupler where coupling is lowest (ie. 10.2 dB). Alexopoulous et al [3.5] has shown that for a 10 dB coupler which is uncompensated for even and odd mode phase velocity the directivity can be as low as 13 dB, this would partially account for the generally lower value of coupled power measured relative to calculated value. In this regard the performance of the coupler could be improved by using technique number 9 listed in section 3.2 for the 10.2 dB coupled section.
The fourth is the effect of the air-bridges which was not taken into account in the calculation and which should be properly modelled. It is also observed that it is the coupled power which would be most affected by the presence of the airbridges.

The fifth, Wei-Xu Huang [5.11] has reported the existence of complex modes (ie. modes where $\gamma = \alpha \pm j\,\beta$) in the 11.6 to 17.75 GHz range for dielectric constant $\epsilon_r = 8.875$ to $\epsilon_r = 20$. These evanescent modes may be contributing to the coupled response over the 11 to 17 GHz band.

The sixth possible contribution is higher order modes particularly in sections 1 of the coupler in which modes other than the fundamental (quasi-TEM) mode are expected to propagate above 11 GHz for $\epsilon_r = 9.8$ [5.11]. It is reasonable to conclude from the data, however, that the six strip analysis is adequate for most practical applications. It is the author's intent to, as a separate exercise, (1) measure the response of the 6-strip section only (2) to attempt a full wave analysis of the structure.

The seventh reason is that the effect of losses (dielectric, ohmic and radiation) were not taken into account in the analysis. As shown in chapter 6 these losses are frequency dependent and become more pronounced as frequency increases.

```
DIM
      FREQ GHZ
      RES OH
      IND NH
      CAP PF
      LNG MIL
      TIMES PS
      COND/OH
      ANG DEG
VAR
 W1=12
 S1=5
 L1=88
CKT
 MSUB      ER-9.8     H=15 T=0.15     RHO=1      RGH=0.0
 MCLIN     2     4     6     8     W W 1      S S1       L L1
 CLIN            8     6     10    12    ZE=234.93 Z0=12.07  E=90 F=12.5
 MCLIN     12    10    14    16    W W1 S S1  L L1
 RES       4     0                 R=50
 DEF3P     16    2     14          NET

net        1     2     3
net        4     3     2
def2p            1     4          back

FREQ
 SWEEP     2     22    1

OUT
 NET DB[S12]    GR1
 NET DC[S13]    GR1
 NET DB[S11]    GR2
 back      db[s12]    gr1
GRID
 RANGE     2     22    1
 GR1       -6    0     1

OPT
```

Table (5.1(a)) Touchstone Program for Cascaded Coupler (h = 0.015 inch)

FREQ-GHZ	DB[S12] NET	DB[S13] NET	DB[S11] NET
2.00000	-1.538	-5.363	-28.515
3.00000	-2.660	-3.474	-27.277
4.00000	-3.567	-2.591	-26.560
5.00000	-4.176	-2.168	-25.711
6.00000	-4.489	-1.994	-24.556
7.00000	-4.543	-1.985	-23.124
8.00000	-4.395	-2.102	-21.534
9.00000	-4.118	-2.326	-19.931
10.0000	-3.795	-2.631	-18.443
11.0000	-3.509	-2.967	-17.148
12.0000	-3.329	-3.259	-16.045
13.0000	-3.290	-3.434	-15.083
14.0000	-3.394	-3.454	-14.233
15.0000	-3.611	-3.339	-13.538
16.0000	-3.883	-3.147	-13.060
17.0000	-4.145	-2.945	-12.824
18.0000	-4.325	-2.792	-12.802
19.0000	-4.357	-2.736	-12.939
20.0000	-4.180	-2.834	-13.178
21.0000	-3.749	-3.179	-13.488
22.0000	-3.049	-3.972	-13.923

Table (5.1(b)) Touchstone Program Data for Cascaded Coupler (h = 0.015 inch)

```
DIM
      FREQ GHZ
      RES OH
      IND NH
      CAP PF
      LNG MIL
      TIME PS
      COND/OH
      ANG DEG
VAR
 W1=21
 S1=8
 L1=88
CKT
 MSUB      ER-9.8     H=25 T=0.15     RHO=1      RGH=0.0
 MCLIN     2     4     6     8     W W 1      S S1       L L1
 CLIN            8     6     10    12    ZE=228     Z0=11.27  E=90 F=12.5
 MCLIN     12    10    14    16    W W1 S S1  L L1
 RES       4     0                 R=50
 DEF3P     16    2     14          NET

net        1     2     3
net        4     3     2
def2p            1     4          back

FREQ
 SWEEP     2     22    1

OUT
 NET DB[S12]    GR1
 NET DB[S13]    GR1
 back      db[s12]    GR1
GRID
 RANGE     2     22    1
 GR1       -6    0     1

OPT
```

Table (5.2(a)) Touchstone Program for Cascaded Coupler (h = 0.025 inch)

FREQ-GHZ	DB[S12] NET	DB[S13] NET	DB[S11] NET	DB[S12] BACK
2.00000	-1.568	-5.234	-35.254	-0.777
3.00000	-2.719	-3.366	-30.959	-0.060
4.00000	-3.647	-2.502	-27.896	-0.135
5.00000	-4.268	-2.093	-25.402	-0.354
6.00000	-4.587	-1.993	-23.216	-0.499
7.00000	-4.644	-1.935	-21.245	-0.518
8.00000	-4.498	-2.064	-19.469	-0.455
9.00000	-4.226	-2.298	-17.909	-0.416
10.0000	-3.911	-2.609	-16.593	-0.474
11.0000	-3.638	-2.945	-15.523	-0.581
12.0000	-3.473	-3.229	-14.647	-0.705
13.0000	-3.451	-3.387	-13.893	-0.892
14.0000	-3.571	-3.386	-13.234	-1.084
15.0000	-3.803	-3.248	-12.711	-1.200
16.0000	-4.090	-3.036	-12.374	-1.172
17.0000	-4.365	-2.821	-12.232	-0.953
18.0000	-4.553	-2.664	-12.242	-0.722
19.0000	-4.583	-2.617	-12.342	-0.756
20.0000	-4.389	-2.737	-12.473	-0.993
21.0000	-3.922	-3.128	-12.620	-1.150
22.0000	-3.178	-4.018	-12.868	-1.088

Table (5.2(b)) Touchstone Program Data for Cascaded Coupler (h = 0.025 inches)

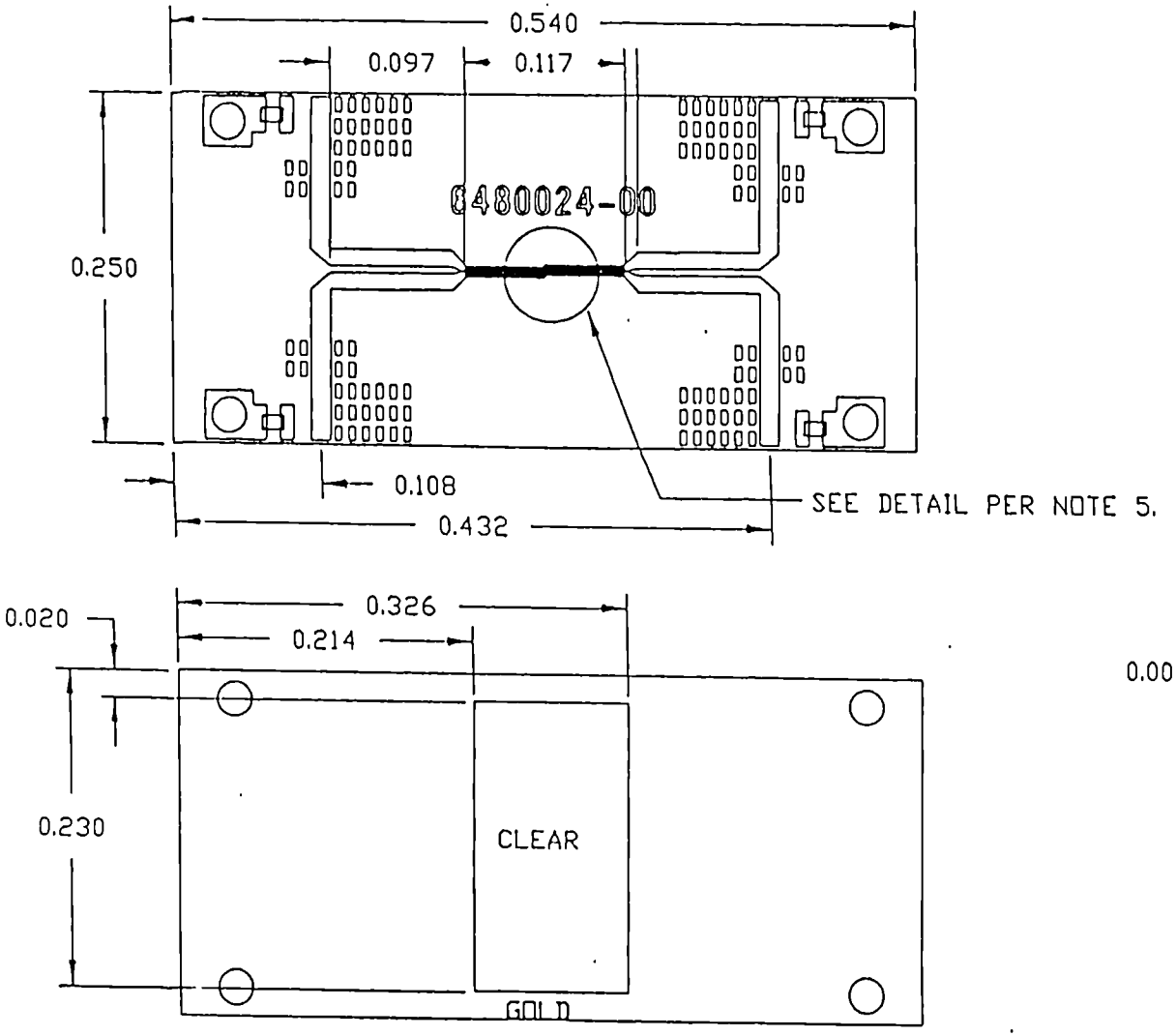

NOTES:

1. MATERIAL: ALUMINA
   TYPE: POLISHED
   THICKNESS: .015"
   P/NO: 6380016-LO
2. DEBURR AFTER DICING
3. USE MASK NO: 67557-13, 67556 67557-
4. DIM TOLERANCES:
   FOR SUB. +/_ 0.002
   FOR MASK +/_ 0.002
5. COUPLER DIMS:

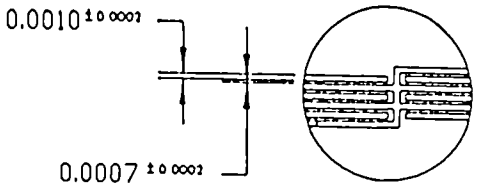

6. PLATE UP PROCESS ONLY.
7. SELECTIVE TANTALUM NITRIDE PROCESSING ONLY.
8. PLATED THRU HOLES INCLUDING SiN_4 LAYER QTY 4

Figure (5.2(a)) Cascaded Coupler Substrate

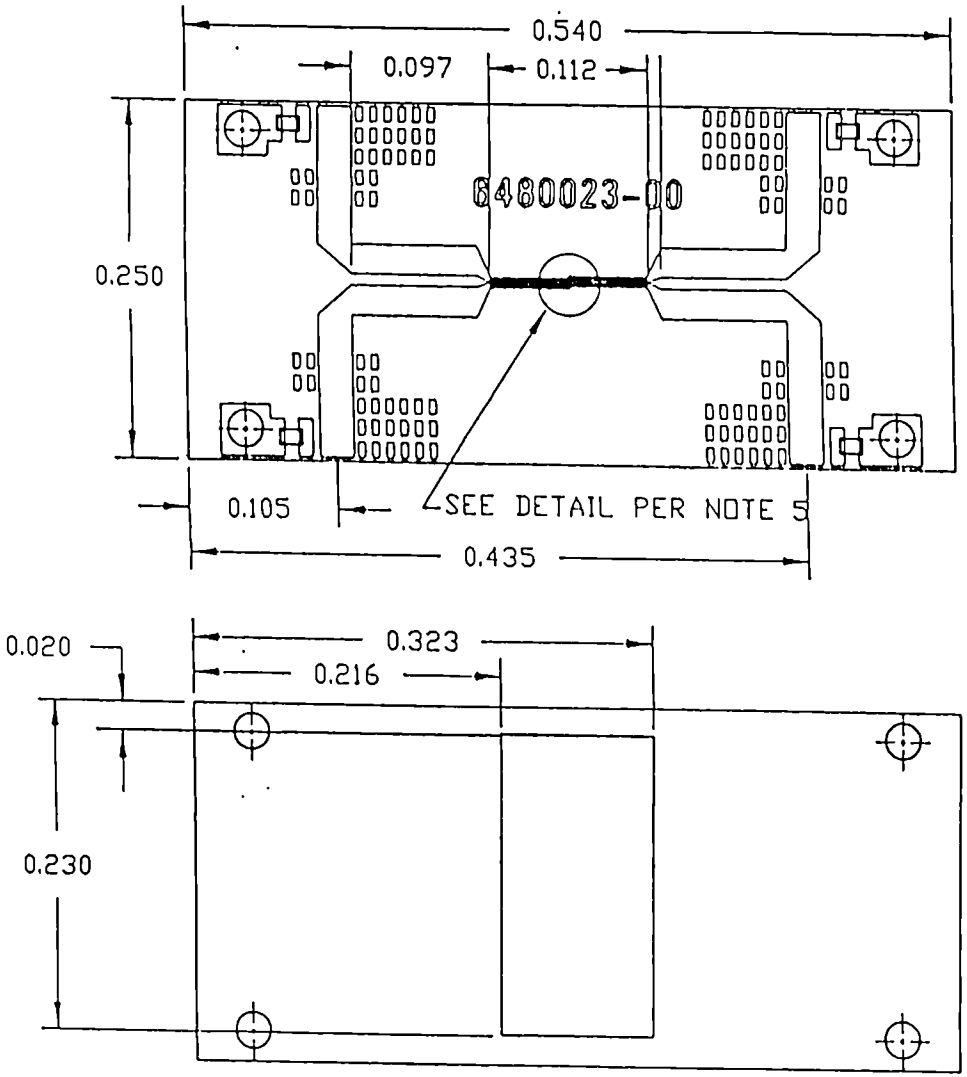

NOTES:

1. MATERIAL: ALUMINA
   TYPE: POLISHED
   THICKNESS: .025"
   P/NO: 6380015-LO
2. DEBURR AFTER DICING
3. USE MASK NO: 67556-13, 67556-2
   67556-5
4. DIM TOLERANCES:
   FOR SUB. +/_ 0.002
   FOR MASK +/_ 0.002
5. COUPLER DIMS.

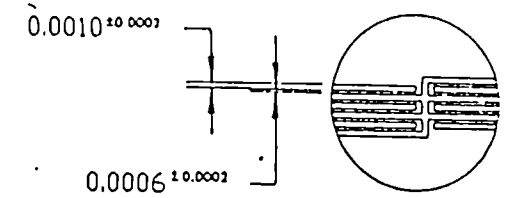

6. PLATE UP PROCESS .
7. SELECTIVE TANTALUM NITRIDE PROCESSING ONLY.
8. PLATED THRU HOLES INCLUDING SiN_4 LAYER QTY 4.

Figure (5.2(b)) Cascaded Coupler Substrate

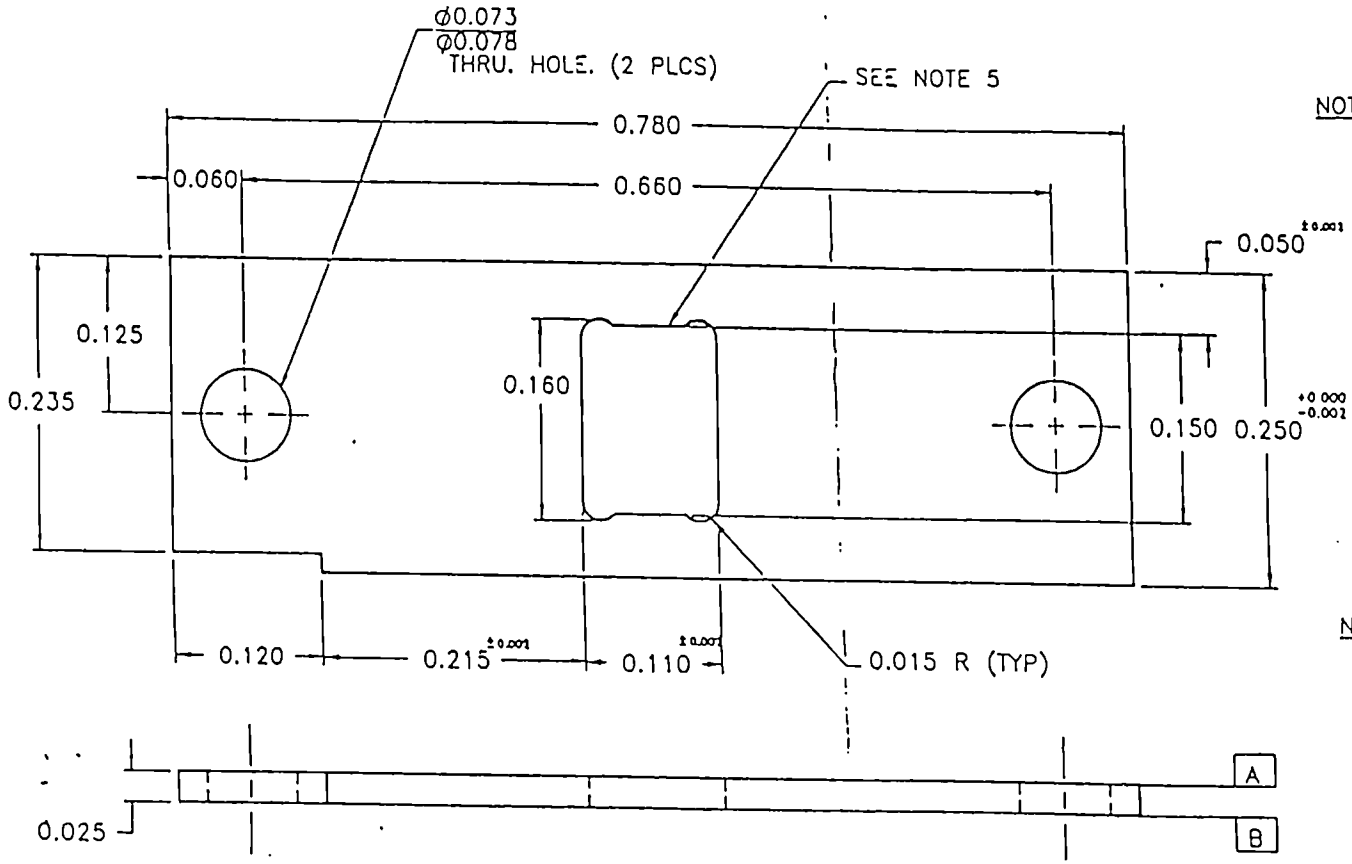

NOTES:

1. MATERIAL: KOVAR
2. REMOVE ALL BURRS. DO NOT CHAMFER.
3. GRIND OR LAP SURFACES "A", "B" TO FLATNESS OF 0.001 MAX
4. COATING: ELECTROLESS NICKEL COAT 0.0001 – 0.0002 THK. THEN GOLD PLATE PER MIL-G-445024, TYPE III CLASS 2, .000075-.000150 THK. MUST PASS 380C BLISTER TEST. MUST BE SOLDERABLE WITH 88/12 GOLD GERMANIUM ALLOY.

NOTE ON HEAT TEST BEFORE COATING

1. TEST ALL DIMENSIONALLY ACCEPTED CARRIERS ON A HOT PLATE (OR IN OVEN) AT 380C FOR 3 MINUTES.
2. COOL AT ROOM TEMP.
3. CHECK FOR FLATNESS ON ALL HEAT TESTED CARRIERS.

-01	UNCOATED PART
-02	COATED PER NOTE 4

Figure (5.3) Cascade Coupler Substrate Carrier

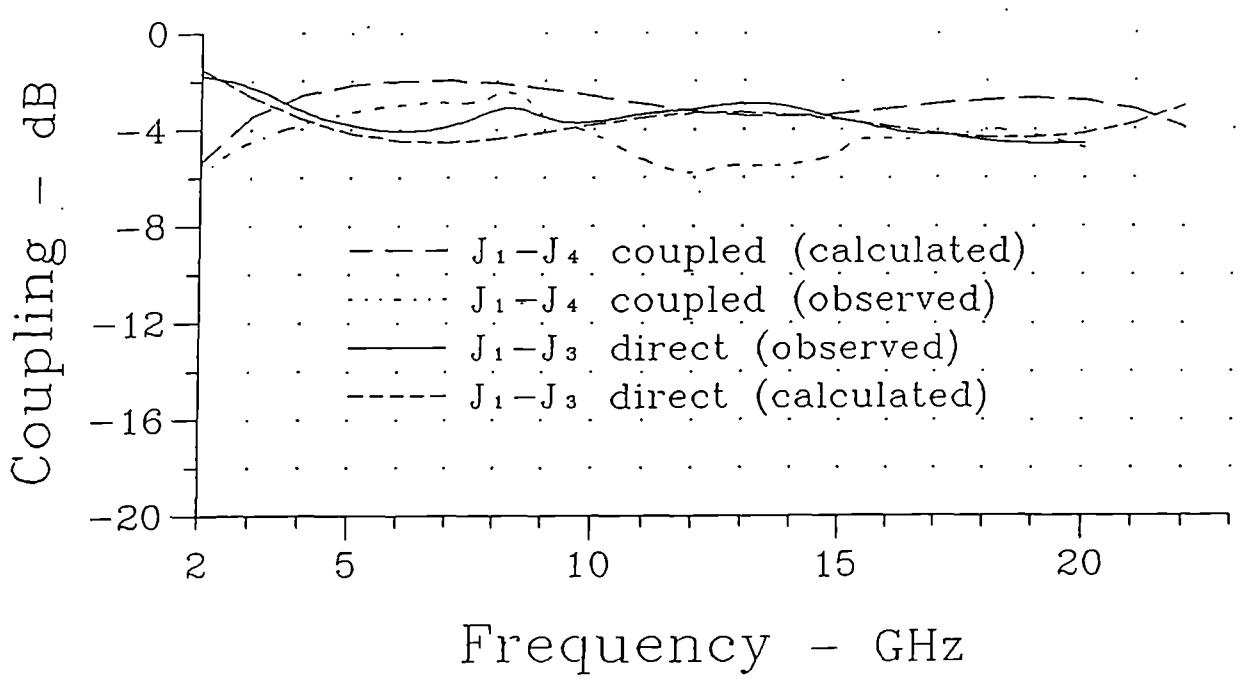

Figure (5.4(a)) Coupling versus Frequency (h = 0.015 inch)

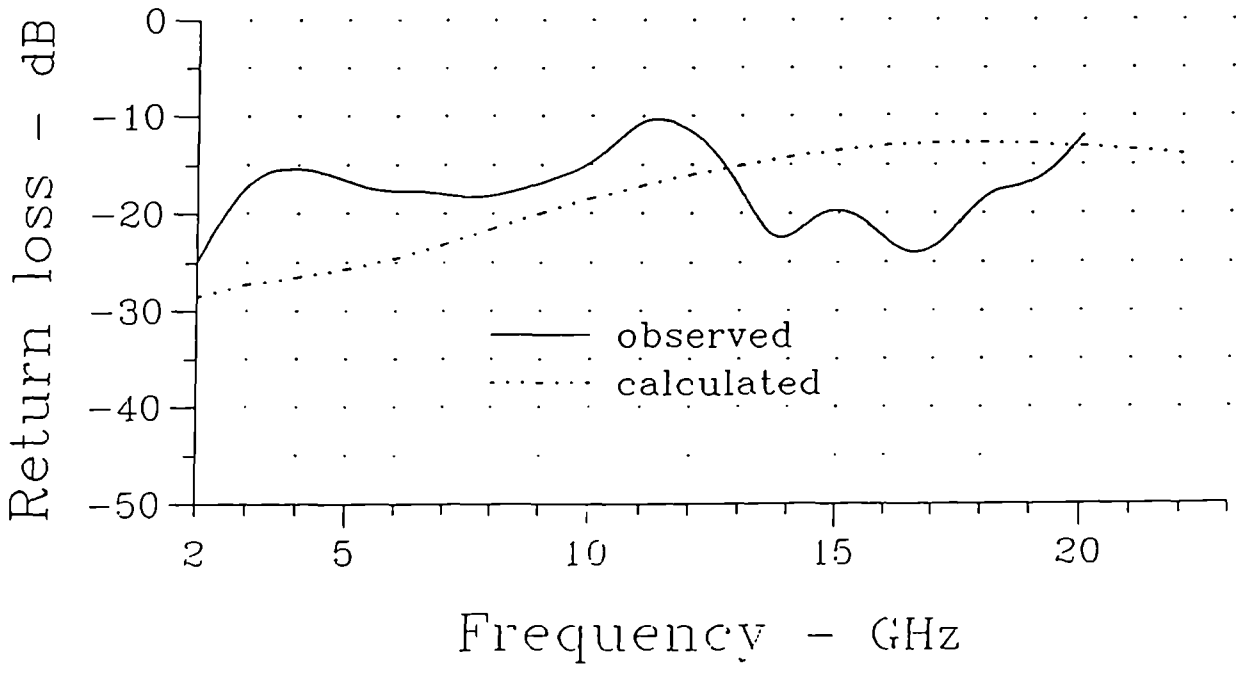

Figure (5.4(b)) Input Return Loss versus Frequency (h = 0.015 inch)

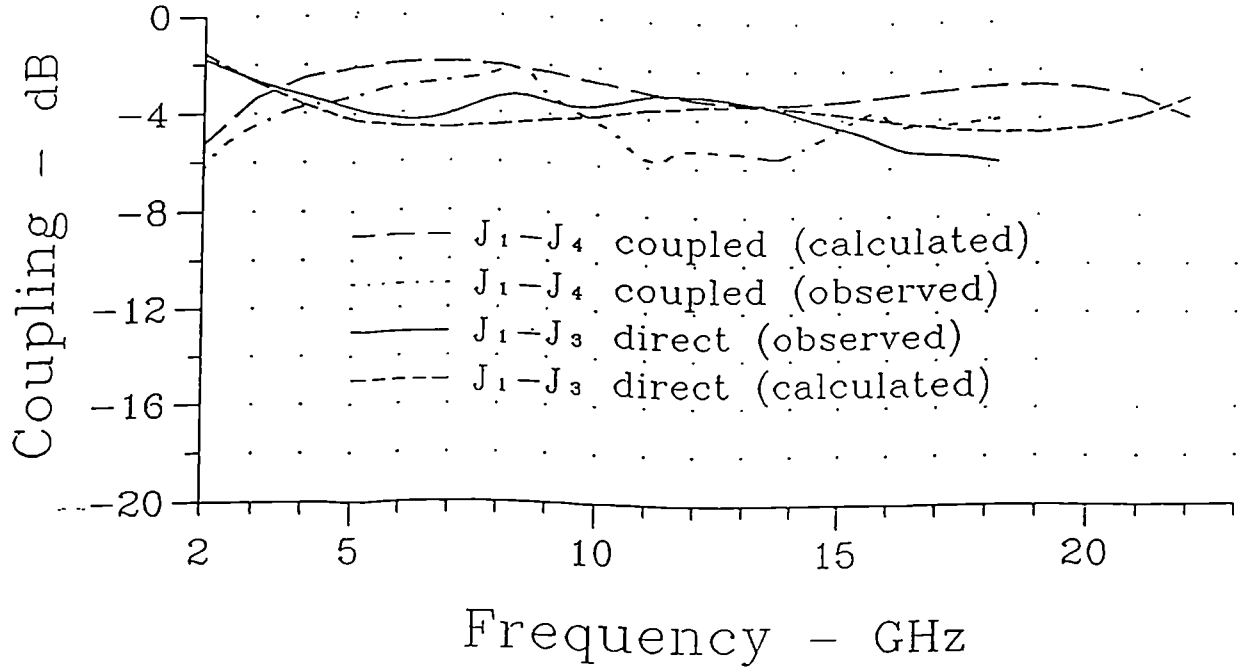

Figure (5.5(a)) Coupling versus Frequency (h = 0.025 inch)

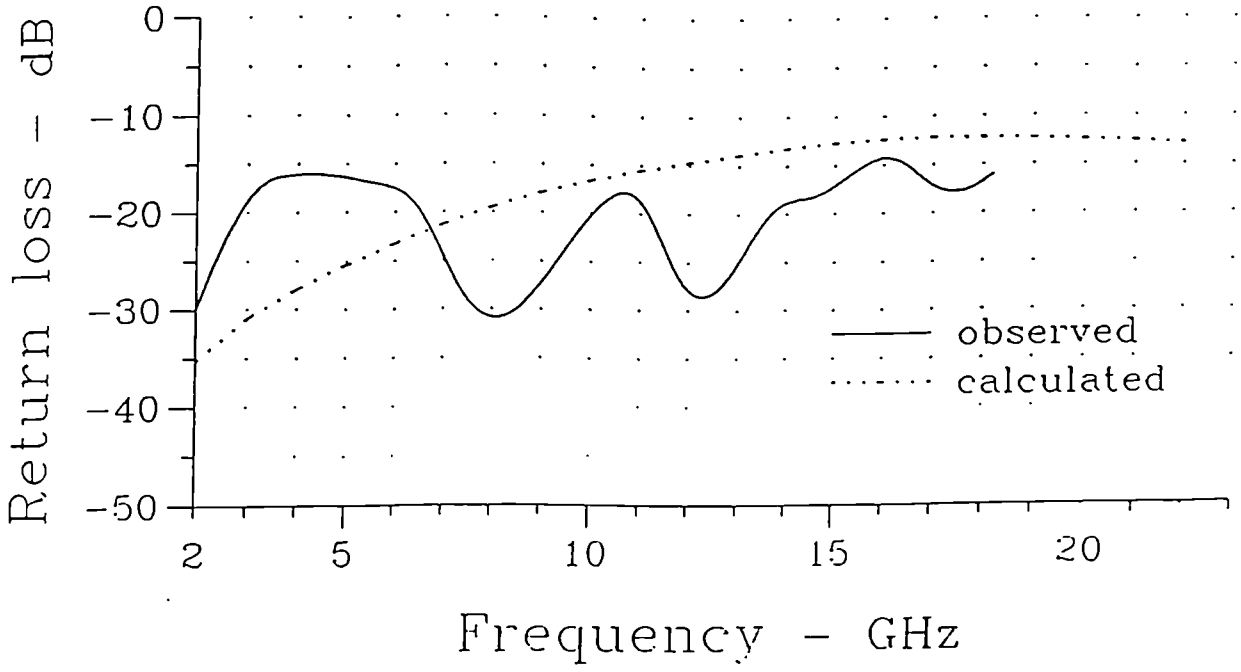

Figure (5.5(b)) Return Loss versus Frequency (h = 0.025 inch)

5.3 APPLICATION OF CASCADED COUPLER TO 2 - 18 GHz REACTIVELY MATCHED POWER AMPLIFIER

A number of techniques have been implemented to achieve multi-octave bandwidth in microwave amplifiers in which the important design parameters are gain, gain flatness, noise figure, output power (linearity) input and output VSWR and DC power consumption (ie. power added efficiency). Among the most used multi-octave designs are:

- negative feedback [5.5]
- distributed [5.6]
- lossy matched [5.7]
- balanced reactive matched [5.8]

5.3.1 Negative Feedback Amplifier

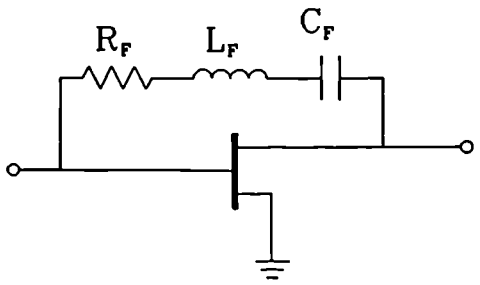

Figure 5.6 Feedback GaAs FET Amplifier Schematic

The feedback amplifier layout is shown in figure (5.6). Whereas this design approach has the advantage of reducing intermodulation distortion, as frequency increases it becomes difficult to achieve flat broadband response since uniform negative feedback with frequency cannot be achieved due to dispersion in the feedback circuit. In addition the thermal noise associated R_F considerably degrades the noise figure of the feedback amplifier with respect to the optimum noise figure of the active device used. Over a broadband the feedback amplifier generally exhibits input VSWR of the order of 4:1 which limits its application in a multistage high gain application. It is also the author's experience that this configuration results in output power which is 4 to 6 dB below output power capability of the active device for a given load match.

5.3.2 Distributed Amplifier

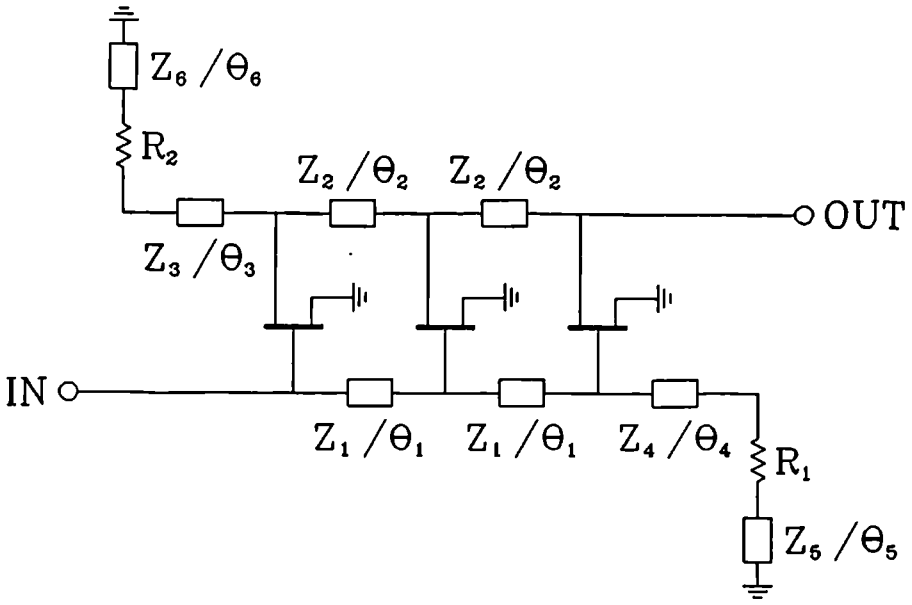

Figure 5.7 Distributed Amplifier Schematic

In figure (5.7) Z and θ represent characteristic impedance and electrical lengths of transmission line respectively. Z_1, Z_2 are typically high impedance in this configuration. The distributed amplifier is capable of very broadband performance to 20 GHz in hybrid form and above 20 GHz in monolithic form. In addition, this design approach offers a high stability factor, low gain ripple and low input/output VSWR. The disadvantages are high noise figure, relative to other single ended designs, low power added efficiency due to the number of active devices used as well as gate/drain line attenuation. The power handling capability of the distributed amplifier can be enhanced by capacitively coupling the individual devices to the gate line [5.6] so that the equivalent gate

capacitance

$$C_q = \frac{C_1 C_{gs}}{C_1 + C_{gs}}$$

where C_1, Cg_s are the coupling capacitance and gate source capacitance of the intrinsic device respectively.
The voltage drop across the gate junction is then

$$V_q = \frac{C_1}{C_1 + C_{gs}} V_{1n}$$

where V_{1n} = input voltage. It is also possible to improve output power characteristics by proportional loading of the drains of the devices. However, the distributed amplifier is still not optimum for ultra broadband wide dynamic range applications due to the noise figure limitation. Another obvious disadvantage of the distributed amplifier is increased cost and reduced reliability due to the number of active devices required.

5.3.3 LOSSY MATCH AMPLIFIER

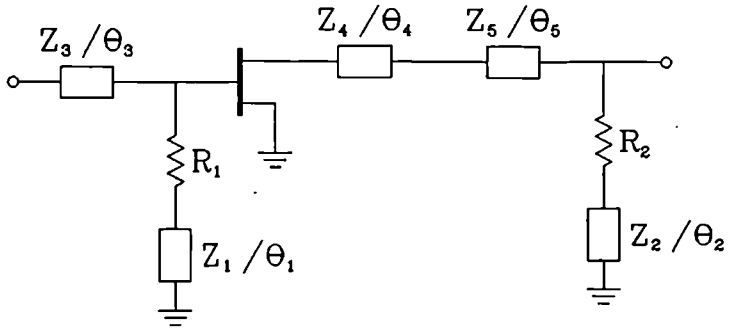

Figure 5.8 Lossy Match Amplifier Schematic

Figure 5.8 shows a loss matched amplifier schematic.

To achieve usable high frequency gain the lossy match amplifier requires a high transconductance transistor. To meet this requirement it is frequently necessary to operate two devices in parallel resulting in a low effective gate-source resistance R_{gs}. Due to the large ratio of R_{gs} to the system source impedance (typically 50 ohms) input VSWR of the amplifier will typically exceed 3:1 for multi-octave operation to 18 GHz.

In addition the noise figure and maximum output power are adversely

affected by R_1, R_2.

5.3.4 BROADBAND REACTIVE MATCHED AMPLIFIER

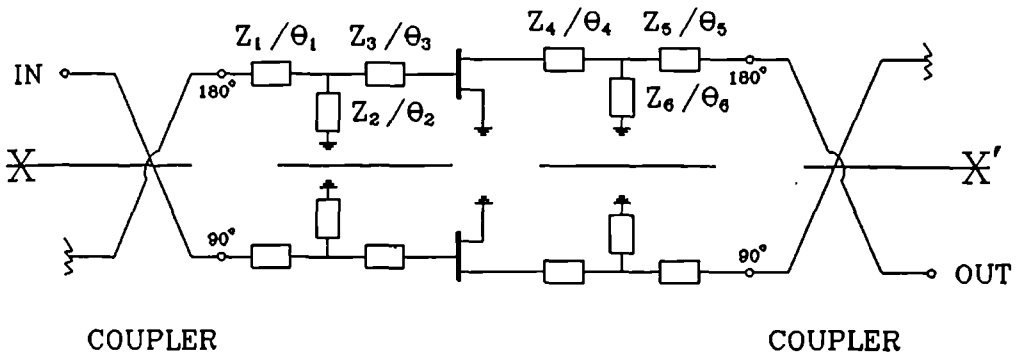

Figure 5.9 Balanced Reactive Match Amplifier Schematic

Figure 5.9 shows a balanced reactive matched amplifier schematic. Since the input and output matching circuits of the configuration is (theoretically) lossless and input output VSWR of each side of the balanced amplifier arrangement is not a critical consideration, it is possible to match the devices simultaneously for optimized noise and output power performance.

However, when two signals are combined the resultant amplitude depends on the phase and amplitude balance between the inputs, therefore it is necessary to consider the effect of phase and amplitude imbalance between the two halves of circuit considered relative to the line XX'. This imbalance may be due to a combination of effects involving the couplers, the active devices and the matching circuit. Niclas [5.10] has shown that if we consider the top half of the circuit to be section 1 and the bottom half section 2 and assume a deviation from complete phase match of

$$\Delta\phi_1 \text{ and } \Delta\phi_2 \text{ andif } |\Delta\phi_1| - |\Delta\phi_2| < 20^{o} \text{degrees}$$

then gain of the amplifier varies by 0.7 dB from optimum when

$$\Delta\phi_1, \Delta\phi_2$$

are introduced at the input of the active devices. The effect increases slightly when

$$\Delta\phi_1, \Delta\phi_2$$

occur at the output of each device.

If the parameters of the two halves of the circuit can be equalised, by selecting devices, bias optimisation and careful splitter/combiner design, the balanced amplifier offers the best overall choice for multi-octave wide dynamic range amplification. The greatest limitation to date in designing such an amplifier has been the quadrature couplers.

Several techniques have been used to configure quadrature broadband couplers including tandem microstrip configurations [5.11] and asymmetrically coupled strip line [5.12]. The tandem coupler is large and lossy and the asymmetrical stripline cannot be conveniently integrated with planar amplifier modules.

Thus there has been a real demand for compact multi-octave bandwidth microstrip coupler along with a reliable design procedure. The coupler described in section 5.2 satisfies this need.

To demonstrate the utility of the coupler described in section 5.2, a four-way balanced medium power amplifier module was designed, fabricated and tested over the 2 - 18 GHz frequency band using the coupler design.

The schematic of the module which was realised on 0.015 thick alumina substrate, ϵ_r = 9.8, is shown in figure 5.10. Figure 5.11 shows the realised circuit of one half of the structure including matching and bias circuitry. The size is 0.422 X 0.790 inches.

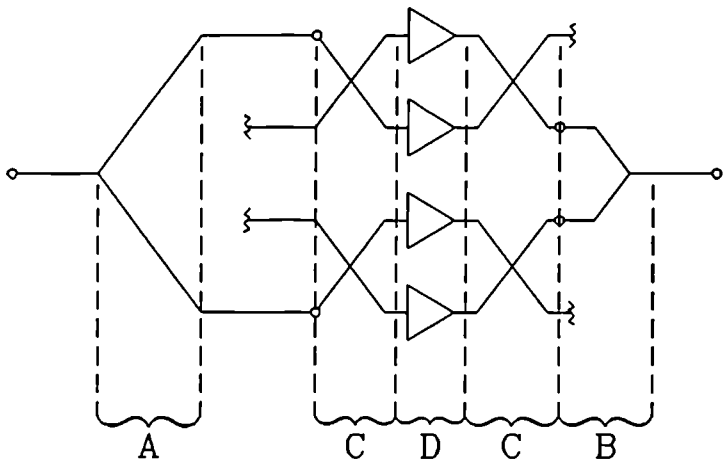

Figure 5.10 2 - 18 GHz Medium Power Amplifier Module Schematic

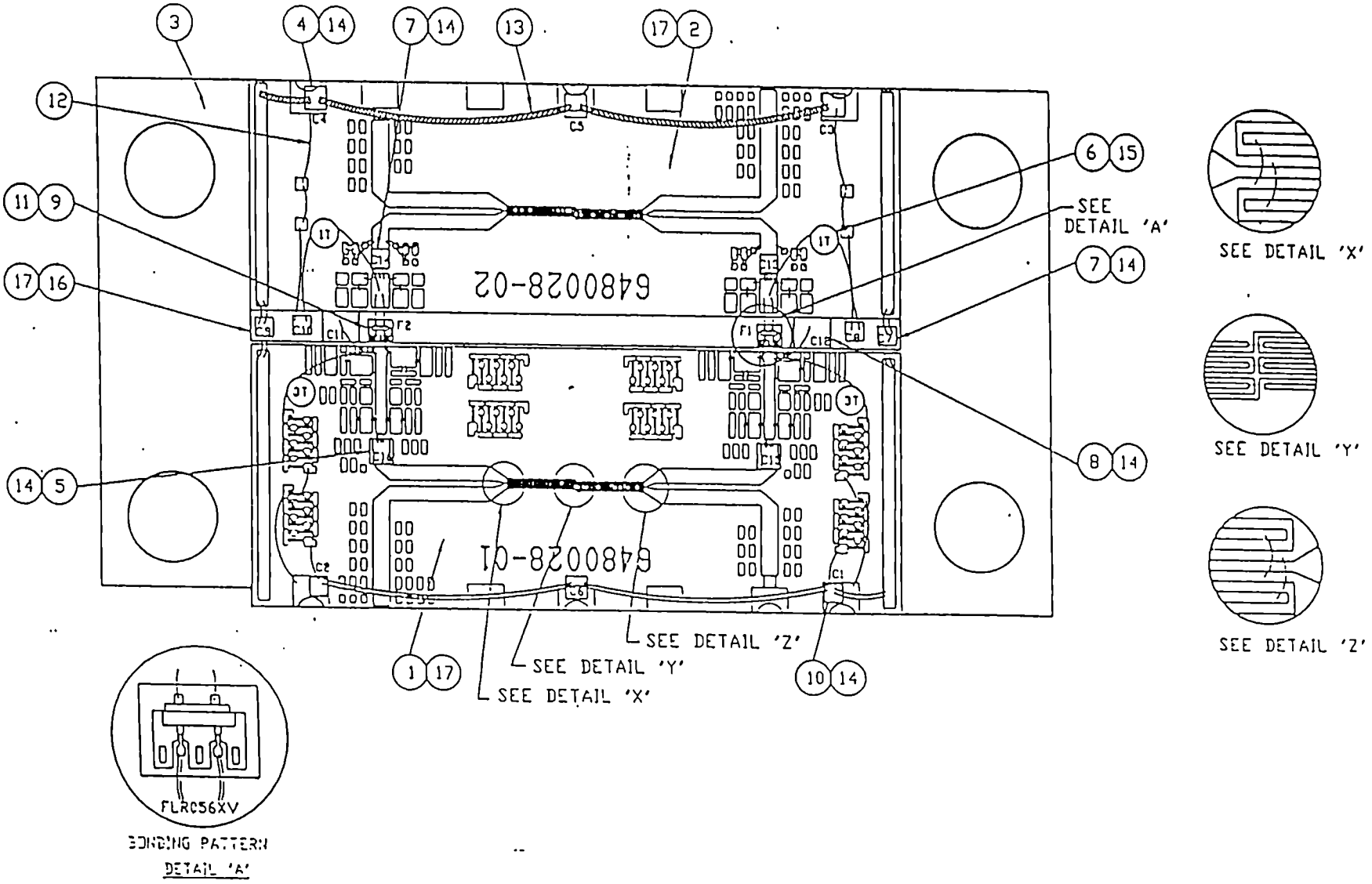

Figure (5.11) Medium Power Balanced Module Assembly

The components in 5.10 are as follows:

- 'A' Broadband in phase symmetrical divider
- 'B' Broadband in phase symmetrical combiner
- 'C' Cascaded coupler described in section 6.1 with h = 0.015 inch
- 'D' Reactively matched medium power GaAs FET.

The in-phase combiner/divider were Wilkinson Type realised on 0.009 inch thick duroid 5880, ϵ_r = 2.2.

The MESFET device chosen was the Fujitsu FLR056XV manufacturer's specifications of which are given in table (5.3). Gate length of the device was 0.3 micron. In order to minimise the junction temperature of the device (ie. maximise output power and reliability) the chip was mounted to the carrier with a gold-tin eutectic perform. The FLR056XV was chosen both for its high transconductance as well as the fact that the sources were ground through via holes, thus eliminating the need for source bond wires whose inductance would degrade high frequency gain and output power. 0.001 inch diameter gold bond wires were used for all thermo-compression bonded connections.

Item	Symbol	Test Condition	Limit Min.	Typ.	Max.	Item Unit
Drain Current	I_{DSS}	V_{DS} = 5V, V_{GS}	-	240	0	mA
Transconductance	gm	V_{DS} = 5V, 1_{DS} = 10mA	-	100	-	mS
Pinch-off Voltage	V_P	V_{DS} = 5V, I_{DS} = 10mA	-1.0	-2.0	-3.5	V
Gate-Source Breakdown Voltage	VGSO	IGS = -10μA	-3	-	-	V
Output Power at 1dB G.C.P.	P1dB	VDS = 8V	25	26	-	dBm
Power Gain at 1dB G.C.P.	G1dB	IDS = 0.61DSS (Typ)	7.0	8.0	-	dB
Power-added Efficiency	Nadd	f = 18 GHz	-	29	0	%
Thermal Resistance	Rth	Channel to Case	-	-	40	deg.C/W

Table 5.3: Electrical Characteristics FLR056XV at 25°C Ambient Temperature.

Although biased for large signal conditions, the device was reactively matched using small signal S-parameters, since large signal parameters were not available from the manufacturer and accurate load pull measurements over the 2 - 18 GHz band was considered prohibitively tedious. The module was therefore empirically tuned at the outputs of the devices after fabrication to optimise output power. Figure 5.12 shows output power at 1 dB gain compression and at saturation measured at a base plate temperature of +60 degrees centigrade.

The theoretical output power at 18 GHz is +32 dBm (typical) at 1 dB gain compression and at 25°C ambient temperature assuming no circuit losses. The measured value was 29 dBm.

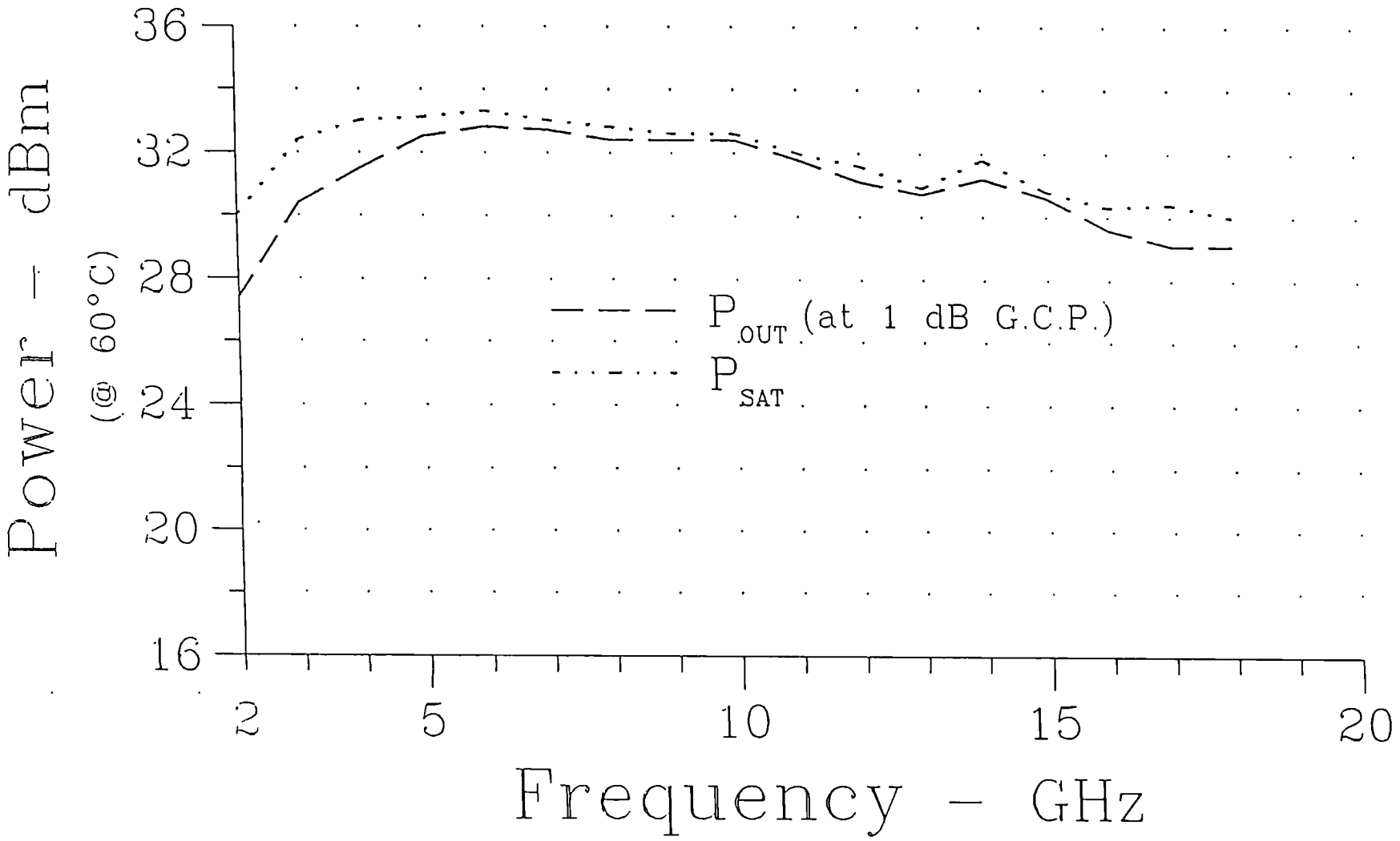

Figure (5.12) Output Power versus Frequency Medium Power 2 - 18 GHz Module

The discrepancy between theoretical and measured values is accounted for as follows:

1. TEMPERATURE DIFFERENCE

   The differences in temperature between that at which the theoretical data would be valid and the actual measurement temperature is 25°C. Assuming a 15° degree positive differential between ambient and base plate temperature, this accounts for an approximate reduction in output power of (35 X 0.01) = 0.35 dBm

2. INSERTION LOSS OF THE IN PHASE COMBINER AND OUTPUT CONNECTOR

   This was measured at 1.25 dB

3. INSERTION LOSS OF THE CASCADED QUADRATURE COUPLER

   From figure (5.4(a)) this is approximately 1.4 dB. By adding these losses to the measured data it is obvious from the above data that the device is operative close to manufacturer's specification and is proof of the utility of the broadband multistrip coupler design.

To the author's knowledge a reactively matched balanced amplifier module with this level of output power and bandwidth has not been reported before.

REFERENCES

[5.1] B.M. Oliver, "Directional Electromagnetic Couplers"

Proceeding IRE, Volume 42 November, 1954

Page 1686 - 1962

[5.2] J.K. Shimizu and E.M.T. Jones, "Coupled Transmission Line Directional Couplers"

IRE Transactions on Microwave Theory and Techniques

Vol. MTT-6 October, 1958 Page 403 - 410

[5.3] E.G. Cristal and L. Young, "Theory and Tables of Optimum Asymmetrical TEM-Mode Coupled Transmission Line Directional Couplers"

IEEE Transactions on Microwave Theory and Techniques

September, 1965 Page 544 - 553

[5.4] G. Matthaei, L. Young, E. M.T. Jones, "Microwave Filters, Impedance Matching Networks, and Coupling Structure"

McGraw-Hill, 1964 Chapter 13

[5.5] Anthony M. Pavio Jr., "A Network Modelling and Design Method for a 2 - 18 GHz Feedback Amplifier"

IEEE Transactions on Microwave Theory and Techniques

Vol. MT-30 No.12 December, 1982 Page 2212 - 2216

[5.6] Yalcin Ayasli, Steven W. Miller, Robert Mazzi, Larry K. Hanes, "Capacitively Coupled Travelling - Wave Power Amplifier"

IEEE Transactions on *Microwave Theory and Techniques*

Vol. MTT-32 No. 12 December, 1984 Page 1704 - 1709

[5.7] Kazuhiko Honjo and Yoichiro Takayama, "GaAs FET Ultra Broadband Amplifiers for G bit/S Data Rate Systems"

IEEE Transactions on Microwave Theory and Techniques

Vol. MTT-291, No.7 July, 1981

[5.8] Edward C. Niehenke, Rick D. Hess, Jed S. Rosen, Lawrence Dickens, and Joseph A. Faulkner Jr., "A Compact Broad-Band Multifunction ECM MIC Module"

IEEE Transactions on Microwave Theory and Techniques

Vol. MTT-30, No.12 December, 1982 Page 2194 - 3000

[5.9] Guillermo Gonzalez, "Microwave Transistors Amplifiers, Analysis and Design"

Prentice - Hall Inc. Englewood Cliffs

New Jersey, 1984

[5.10] Karl B. Niclas, "Planar Power Combining for Medium Power GaAs FET Amplifiers in X/Ku-Bands"

Microwave Journal June, 1979 Page 79 - 84

[5.11] Wei-Xu Huang and Tatsuo Itoh, "Complex Modes in Lossless Shielded Microstrip Lines"

IEEE Transactions on Microwave Theory and Techniques

Volume 36, No. 1 January, 1988 Page 163 - 165

CHAPTER 6

EFFECTS OF LOSS ON MICROSTRIP EDGE COUPLED STRUCTURES

The analysis in the preceding chapters have not taken into account losses. In this chapter practical aspects of loss in edge coupled structures are addressed [6.1]. Referring to figure (2.1(a)), the odd and even mode attenuation constants due to ohmic (metallic) losses for two coupled lines α_{om} and α_{em} are given by

$$\alpha_{om} = \frac{R_s}{2Z_{oo}\eta} \cdot \frac{\delta}{\delta n}(\epsilon_{oo}Z_{oo}) \text{ nepers/unit length} \quad (6.1(a))$$

where

$$\frac{\delta(\epsilon_{oo}Z_{oo})}{\delta n} = \frac{2}{H}\left[1 - \frac{S}{2H}\right]\frac{\delta(\epsilon_{oo}Z_{oo})}{\delta(S/H)} - \left[1 + \frac{T}{2H}\right]\frac{\delta\epsilon_{oo}Z_{oo}}{\delta(T/H)} - \left[1 + \frac{W}{2H}\right]\frac{\delta(\epsilon_{oo}Z_{oo})}{\delta(W/H)} \quad (6.1(b))$$

$$\alpha_{em} = \frac{R_s}{2Z_{oe}\eta} \cdot \frac{\delta\epsilon_{ee}Z_{oe}}{\delta n} \text{ (nepers/unit length)} \quad (6.2(a))$$

where

$$\frac{\delta(\epsilon_{ee}Z_{oe})}{\delta n} = \frac{2}{H}\left[1 - \frac{S}{2H}\right]\frac{\delta(\epsilon_{ee}Z_{oe})}{\delta(S/H)} - \left[1 + \frac{T}{2H}\right]\frac{\delta(\epsilon_{oo}Z_{oe})}{\delta(T/H)}$$

$$- \left[1 + \frac{W}{2H}\right]\frac{\delta(\epsilon_{ee}Z_{oe})}{\delta\left[\frac{W}{H}\right]} \qquad (6.2(b))$$

where T = thickness of the strip, η = 377 ohms, impedance of free space, S = strip spacing, W = strip width, H is thickness of the dielectric, ϵ_{oo}, ϵ_{ee} are odd and even mode effective dielectric constants; Z_{oo}, Z_{oe} are odd and even mode characteristic impedances.

$$R_s = \frac{8.26\,x\,10^{-3}}{\sqrt{f}} \qquad (6.2(c))$$

where f is frequency in gigahertz. The partial derivatives of Z_{oo}, Z_{oe} with respect to $\frac{S}{H}$, $\frac{T}{H}$ and $\frac{W}{H}$ are calculated as stated in [6.1].

It can be shown that α_{om} is always higher than α_{em} and that α_{om} is more sensitive to S/H than α_{em}. This is to be expected if the odd and even mode field patterns are considered.

The odd and even mode dielectric attenuation constants are give by

$$\alpha_{OD} = 91.0\,\frac{\epsilon_r}{\sqrt{\epsilon_{oo}}}\left(\frac{\epsilon_{oo} - 1}{\epsilon_r - 1}\right) f \tan\delta \qquad (6.3(a))$$

$$\alpha_{\epsilon D} = 91.0 \frac{\epsilon_r}{\sqrt{\epsilon_{oe}}} \left(\frac{\epsilon_{oe} - 1}{\epsilon_r - 1} \right) f \tan\delta \qquad (6.3(b))$$

where ϵ_r is the isotropic relative permittivity of the substrate, tan δ is the loss tangent of the substrate material and the total attenuation expressions are then

$$\alpha_{ee} = \alpha_{em} + \alpha_{eD} + \alpha_{eR} \qquad (6.4(a))$$

$$\alpha_{oo} = \alpha_{om} + \alpha_{oD} + \alpha_{V} \qquad (6.4(b))$$

where α_{eR}, α_{oR} are related to radiation effects. Coupler odd and even mode characteristic impedances Z_{Lo}, Z_{LE} can then be defined for coupled lossy lines

$$Z_{Lo} = Z_{oo} \left[1 - j \frac{\alpha_{om}}{\beta o} + j \frac{\alpha_{oD}}{\beta_o} \right] \qquad (6.5(a))$$

$$Z_{Le} = Z_{oe} \left[1 - j \frac{\alpha_{em}}{\beta_e} + j \frac{\alpha_{ED}}{\beta_e} \right] \qquad (6.5(b))$$

where β_o, β_e are odd and even mode propagation constants and Z_{oo}, Z_{oe} are odd and even mode characteristic impedances for the lossless case.

RAO [6.1] has shown that for loosely coupled lines the preceding expressions are accurate to within 5 percent when compared to measured results. The effect of loss on coupling factor, isolation and directivity has been shown to be most pronounced at the centre of the design band. For a 10 dB coupler designed at 8 GHz centre frequency using Bryant and Weiss's M-strip program, which does not take into account loss (or dispersion), compared to predicted results taking into account metallic and dielectric losses the following results are reported at 8 GHz.

	Parameter Calculated Bryant Weiss (M-Strip Program) (Without Losses)	Parameter Calculated with Losses Considered
Coupling	10.2 dB	10.3 dB
Directivity	22.5	21.4
Isolation	22.2 dB	21.4

Similar consideration may be applied to microstrip filters.

REFERENCES

[6.1] B. Rama Rao, "Effects of Loss and Frequency Dispersion on the Performance of Microstrip Directional Couplers and Coupled Line Filters" IEEE Transactions on Microwave Theory and Techniques July, 1974 Page 747 - 750

CONCLUSION

In-depth methods of coupled microstrip line analysis, including the importance of such considerations as transverse current distribution, dielectric anisotropy and losses, are presented in a form which should be usable by most practising microwave engineers.

Detailed analysis, including computer program listings and extensive tabular and graphical design data, is presented for multiconductor suspended coupled lines; using the spectral domain technique.

Coupled microstrip offers several degrees of freedom above single microstrip lines. However, in the past, coupled lines have been used primarily for power sampling, filtering and to a lesser extent phase shifting. This thesis presents and analyses other novel applications of both symmetric and asymmetric coupled microstrip. Examples being broadband low loss matching for low noise amplifiers and broadbanding of previously narrowband structures such as the branchline coupler which has previously been limited to 15 percent usable bandwidth. 45 percent band width for a branchline coupler is demonstrated by analysis. Previously this band width would require the use of interdigital structures, which in turn would necessitate access to expensive thermocompression or ultrasonic bonding equipment. The proposed quadrature coupler requires no bond wires or cross-overs.

Detailed analysis of tunable multiconductor couplers or couplers with metallisation at several dielectric interfaces previously required access to powerful computing facilities. By considerable algebraic preprocessing, it is demonstrated that such complex structures can be analyzed using a personal computer only. A six finger coupler in suspended microstrip, with tuning septum, in which even to odd mode impedance ratio of 20:1 was achieved with low loss, was analyzed and measured as part of a compact 2 - 18 GHz three section coupler. In the analysis, based on the spectral domain technique it is shown that, where as the use of a single charge basis function which reflects singularity

at the edges of the septum is adequate for practical coupler design, this is inadequate for more accurate analysis and additional basis functions are proposed.

Two numerical methods of analysis are presented for a novel high pass structure with multioctave performance capability realised with broadside coupled microstrips and a variable ground plane gap between the strips. One method depends on the symmetry of the structure, the other is completely general.

A compact spiral 180 degree planar coupler which is manufacturable both in MMIC and MHMIC, is proposed based on the cascade matrix analysis of multiple coupled lines. The structure is applicable down to L-band where planar structures have not been used traditionally.

As a demonstration of the accuracy of the theoretical prediction, two low loss 2 - 18 GHz quadrature cascaded couplers were designed and tested on 0.015 and .025 thick alumina. The 0.9 dB coupling factor of the centre section was realised with a six finger structure in which the ground plane was partially removed. Discrepancy between the quasi-static theoretical analysis and measurement above 11 GHz were examined and explained. The importance of dispersion, higher order mode propagation and the inequality of even and odd mode phase velocity in the design of such broadband structures is demonstrated.

Multioctave bandwidth medium power microwave amplifiers are required for military applications. To date these devices have achieved satisfactory performance over the 2 - 18 GHz band only by using a distributed approach in MMIC technology. The more economical HMIC approach has not been successfully used due to the difficulty associated with acquiring identical active discrete devices, as well as maintaining phase relationship of the gate and drain lines. By using coupled multiconductor suspended line techniques, a balanced reactively matched medium power amplifier module was realised over the 2 - 18 GHz frequency band. Output power of +29 dBm minimum was achieved

across the band, as predicted.

Fabrication cost is approximately 10 percent of that of the equivalent MMIC design.

To the author's knowledge this performance has not been approached before in HMIC technology.

The inequality between even and odd mode phase velocities of edge coupled and broadside coupled microstrip lines, which is a result of the inherent dielectric discontinuity of the configurations, causes degraded directivity in couplers. In filters the effects are frequency response asymmetry, ie. lower rejection at the high frequency, as well as a parasitic pass band at twice the centre frequency. The thesis presents methods of equalising odd and even mode velocities. The design technique and extensive data presented for the suspended coupled microstrip case can be used to improve both coupler and filter performance up to millimeter waves.

APPENDIX 1

Mathcad Program for Z_{oe}, Z_{oo} for $\epsilon_r = 38$

$h := 0.02$

$W := 1.2 \cdot h$

$L := 10 \cdot h$

$t := 10 \cdot h$

$S := 0.1 \cdot h$

$b := 10 \cdot h$

$$\epsilon_0 := \frac{8.842}{40} \cdot 10^{-12}$$

$$c := 3 \cdot 40 \cdot 10^{8}$$

$$\epsilon_{r_0} := 1$$

$$\epsilon_{r_1} := 38$$

$J := 0 \,..1$ $\quad MM := 10$

$M := 1 \,..MM$

$$a_M := L - \frac{h}{2} \cdot M$$

$$P_1 := \frac{L}{2 \cdot \pi} \cdot \int_S^{S+W} \frac{1}{\sqrt{\left[\frac{W}{2}\right]^2 - \left[x - S - \frac{W}{2}\right]^2}} \, dx$$

$P_1 = 0.05$

$N := 1 \,..150$

$$K_{e_N} := \frac{N - 0.5}{L} \cdot \pi$$

$$\rho_{1c_N} := J0\left[K_{e_N} \cdot \left[\frac{W}{2}\right]\right] \cdot \cos\left[K_{e_N} \cdot \left[S + \frac{W}{2}\right]\right]$$

$$\delta_{M,N} := K_{e_N} \cdot a_M \qquad \tau_N := K_{e_N} \cdot L$$

$$\rho_{slc_{M,N}} := \left[\frac{\pi}{4}\right] \cdot \sin[\tau_N] \cdot J1[\delta_{M,N}]$$

$$P_2 := \int_S^{S+W} \frac{L \cdot 4}{2 \cdot 5 \cdot W} \cdot \left[1 + \left[\left|2 \cdot \frac{x - S - 0.5 \cdot W}{W}\right|\right]^3\right] dx$$

$$P_2 = 0.05$$

$$ss := S + \frac{W}{2} \qquad \alpha_N := K_{e_N} \cdot \frac{W}{2}$$

$$f(\theta) := \sin(\theta) \cdot \left[\theta^3 - 6 \cdot \theta\right] + \cos(\theta) \cdot \left[3 \cdot \theta^2 - 6\right]$$

$$\rho_{2c_N} := \left[\frac{8}{5 \cdot W} \cdot \cos\left[K_{e_N} \cdot ss\right]\right] \cdot \left[\frac{1}{K_{e_N}}\right] \cdot \left[\sin[\alpha_N] + \left[\frac{1}{\alpha_N^3}\right] \cdot \left[f[\alpha_N] - f(0)\right]\right]$$

$$\Phi(\theta) := \sin(\theta) \cdot \left[3 \cdot \theta^2 - 6\right] - \cos(\theta) \cdot \left[\theta^3 - 6 \cdot \theta\right]$$

$$\rho_{s2c_{M,N}} := \left[\frac{4}{4}\right] \cdot \sin\left[\tau_{N}\right] \cdot \Phi\left[\delta_{M,N}\right]$$

$$\coth(x) := \frac{1}{\tanh(x)}$$

$$uvw_{N,J} := \left[\epsilon_{r_J} + \coth\left[K_{e_N} \cdot h\right] \cdot \coth\left[K_{e_N} \cdot b\right]\right]$$

$$xyz_{N,J} := \coth\left[K_{e_N} \cdot t\right] \cdot \left[\coth\left[K_{e_N} \cdot h\right] + \frac{1}{\epsilon_{r_J}} \cdot \coth\left[K_{e_N} \cdot b\right]\right]$$

$$det_{e_{N,J}} := \epsilon_0 \cdot K_{e_N} \cdot \left[uvw_{N,J} + xyz_{N,J}\right]$$

$$G_{e11_{N,J}} := \frac{1}{det_{e_{N,J}}} \cdot \left[\coth\left[K_{e_N} \cdot h\right] + \frac{1}{\epsilon_{r_J}} \cdot \coth\left[K_{e_N} \cdot b\right]\right]$$

$$G_{e12_{N,J}} := \frac{1}{det_{e_{N,J}} \cdot \sinh\left[K_{e_N} \cdot h\right]}$$

$$G_{e21_{N,J}} := G_{e12_{N,J}}$$

$$G_{e22_{N,J}} := \frac{1}{det_{e_{N,J}}} \cdot \left[\coth\left[K_{e_N} \cdot h\right] + \frac{1}{\epsilon_{r_J}} \cdot \coth\left[K_{e_N} \cdot t\right]\right]$$

$$K_{1111,J} := \sum_{N} G_{e11_{N,J}} \cdot \rho_{1c_N}^{2}$$

$$K_{1112,J} := \sum_{N} G_{e11_{N,J}} \cdot \rho_{1c_N} \cdot \rho_{2c_N} \qquad K_{1121,J} := K_{1112,J}$$

$$K_{1122,J} := \sum_{N} G_{e11_{N,J}} \cdot \rho_{2c_N}^{2}$$

$$K_{1211,M,J} := \sum_{N} G_{e12_{N,J}} \cdot \rho_{1c_N} \cdot \rho_{s1c_{M,N}} \qquad K_{2111,M,J} := K_{1211,M,J}$$

$$K_{1212,M,J} := \sum_{N} G_{e12_{N,J}} \cdot \rho_{1c_N} \cdot \rho_{s2c_{M,N}} \qquad K_{2121,M,J} := K_{1212,M,J}$$

$$K_{1221,M,J} := \sum_{N} G_{e12_{N,J}} \cdot \rho_{2c_N} \cdot \rho_{s1c_{M,N}} \qquad K_{2112,M,J} := K_{1221,M,J}$$

$$K_{1222,M,J} := \sum_{N} G_{e12_{N,J}} \cdot \rho_{2c_N} \cdot \rho_{s2c_{M,N}} \qquad K_{2122,M,J} := K_{1222,M,J}$$

$$K_{2211,M,J} := \sum_{N} G_{e22_{N,J}} \cdot \rho_{s1c_{M,N}}^{2}$$

$$K_{2212,M,J} := \sum_{N} G_{e22_{N,J}} \cdot \rho_{s1c_{M,N}} \cdot \rho_{s2c_{M,N}} \qquad K_{2221,M,J} := K_{2212,M,J}$$

$$K_{2222_{M,J}} := \sum_{N} G_{e22_{N,J}} \cdot \rho_{s2c_{M,N}}^{2}$$

a1x := 1 a2x := 1 b1x := 0.5 b2x := 0.5

Given

$K1 \cdot a1x + K2 \cdot a2x + K3 \cdot b1x + K4 \cdot b2x \approx P_1$

$K2 \cdot a1x + K5 \cdot a2x + K6 \cdot b1x + K7 \cdot b2x \approx P_2$

$K3 \cdot a1x + K6 \cdot a2x + K8 \cdot b1x + K9 \cdot b2x \approx 0$

$K4 \cdot a1x + K7 \cdot a2x + K9 \cdot b1x + K10 \cdot b2x \approx 0$

func(K1,K2,K3,K4,K5,K6,K7,K8,K9,K10) := find(a1x,a2x,b1x,b2x)

M := 1 ..MM $K1_J := K_{1111_J}$ $K2_J := K_{1112_J}$ $K5_J := K_{1122_J}$

$K6_{M,J} := K_{1221_{M,J}}$ $K3_{M,J} := K_{1211_{M,J}}$ $K4_{M,J} := K_{1212_{M,J}}$

$K10_{M,J} := K_{2222_{M,J}}$ $K9_{M,J} := K_{2212_{M,J}}$ $K7_{M,J} := K_{1222_{M,J}}$

$K8_{M,J} := K_{2211_{M,J}}$

$$\begin{bmatrix} ak1_{M,J} \\ ak2_{M,J} \\ bk1_{M,J} \\ bk2_{M,J} \end{bmatrix} := func\left[K1_J, K2_J, K3_{M,J}, K4_{M,J}, K5_J, K6_{M,J}, K7_{M,J}, K8_{M,J}, K9_{M,J}, K10_{M,J}\right]$$

$P_1 = 0.05 \qquad P_2 = 0.05$

$$a = \begin{bmatrix} 0 \\ 0.095 \\ 0.09 \\ 0.085 \\ 0.08 \\ 0.075 \\ 0.07 \\ 0.065 \\ 0.06 \\ 0.055 \\ 0.05 \end{bmatrix}$$

$$ak1 \cdot 10^{12} = \begin{bmatrix} 0 & 0 \\ 0.378 & 8.078 \\ 0.365 & 7.302 \\ 0.352 & 6.895 \\ 0.324 & 5.867 \\ 0.295 & 4.858 \\ 0.273 & 4.098 \\ 0.257 & 3.542 \\ 0.244 & 3.124 \\ 0.235 & 2.801 \\ 0.228 & 2.543 \end{bmatrix}$$

$$ak2 \cdot 10^{12} = \begin{bmatrix} 0 & 0 \\ 0.125 & 2.111 \\ 0.09 & 0.673 \\ 0.052 & -0.866 \\ 0.039 & -1.188 \\ 0.037 & -1.06 \\ 0.038 & -0.898 \\ 0.038 & -0.768 \\ 0.038 & -0.669 \\ 0.038 & -0.593 \\ 0.038 & -0.533 \end{bmatrix}$$

cap. in pico farads

$$C_{oe_{M,J}} := \begin{bmatrix} 2 \\ - \\ L \end{bmatrix} \cdot \left[ak1_{M,J} \cdot P_1 + ak2_{M,J} \cdot P_2\right] \cdot 10^{12}$$

$$Z_{oe_M} := \frac{10^{12}}{c \cdot \sqrt{C_{oe_{M,0}} \cdot C_{oe_{M,1}}}}$$

$$C_{oe} = \begin{bmatrix} 0 & 0 \\ 0.503 & 10.189 \\ 0.454 & 7.975 \\ 0.404 & 6.029 \\ 0.363 & 4.679 \\ 0.333 & 3.798 \\ 0.311 & 3.201 \\ 0.295 & 2.774 \\ 0.283 & 2.455 \\ 0.273 & 2.208 \\ 0.266 & 2.011 \end{bmatrix}$$

$$\epsilon_{eeff_M} := \frac{C_{oe_{M,1}}}{C_{oe_{M,0}}}$$

M
1
2
3
4
5
6
7
8
9
10

$$a = \begin{bmatrix} 0 \\ 0.095 \\ 0.09 \\ 0.085 \\ 0.08 \\ 0.075 \\ 0.07 \\ 0.065 \\ 0.06 \\ 0.055 \\ 0.05 \end{bmatrix} \qquad \epsilon_{eeff} = \begin{bmatrix} 0 \\ 20.268 \\ 17.549 \\ 14.939 \\ 12.907 \\ 11.417 \\ 10.291 \\ 9.404 \\ 8.682 \\ 8.079 \\ 7.566 \end{bmatrix} \qquad Z_{oe} = \begin{bmatrix} 0 \\ 36.822 \\ 43.774 \\ 53.422 \\ 63.986 \\ 74.144 \\ 83.525 \\ 92.125 \\ 100.024 \\ 107.295 \\ 114.007 \end{bmatrix}$$

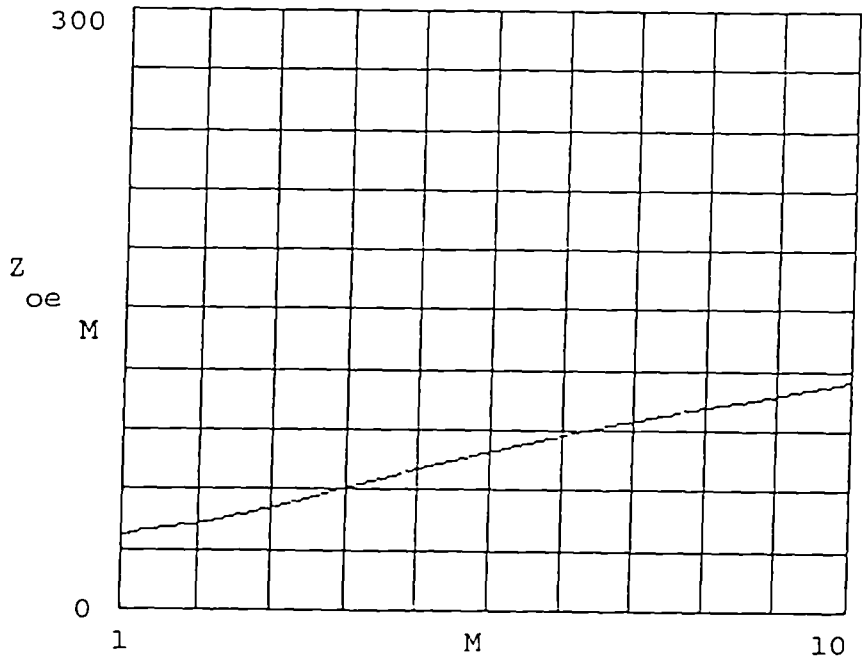

$h := 0.01$

$W := 1.2 \cdot h$

$L := 10 \cdot h$

$t := 10 \cdot h$

$S := 0.1 \cdot h$

$b := 10 \cdot h$

$$\epsilon_0 := \frac{8.842}{40} \cdot 10^{-12}$$

$$c := 3 \cdot 40 \cdot 10^{8}$$

$$\epsilon_{r_0} := 1$$

$$\epsilon_{r_1} := 38$$

$J := 0 \,..\, 1$ $\quad MM := 10$

$M := 0 \,..\, MM$

$$a_M := L - \frac{h}{2} \cdot M$$

$$P_1 := \frac{L}{2 \cdot \pi} \cdot \int_S^{S + W} \frac{1}{\sqrt{\left[\frac{W}{2}\right]^2 - \left[x - S - \frac{W}{2}\right]^2}} \, dx$$

$P_1 = 0.05$

$N := 1 \,..\, 150$ $\quad K_{o_N} := \frac{N}{L} \cdot \pi$

$$\rho_{1s_N} := J0\left[K_{o_N} \cdot \left[\frac{W}{2}\right]\right] \cdot \sin\left[K_{o_N} \cdot \left[S + \frac{W}{2}\right]\right]$$

$$\delta_{M,N} := K_{o_N} \cdot a_M \qquad \tau_N := K_{o_N} \cdot L$$

$$\rho_{sls_{M,N}} := (-1) \cdot \left[\frac{\pi}{4}\right] \cdot \cos\left[\tau_N\right] \cdot J1\left[\delta_{M,N}\right]$$

$$P_2 := \int_S^{S+W} \frac{L \cdot 4}{2 \cdot 5 \cdot W} \cdot \left[1 + \left[\left|2 \cdot \frac{x - S - 0.5 \cdot W}{W}\right|\right]^3\right] dx$$

$$P_2 = 0.05$$

$$ss := S + \frac{W}{2} \qquad \alpha_N := K_{o_N} \cdot \frac{W}{2}$$

$$f(\theta) := \sin(\theta) \cdot \left[\theta^3 - 6 \cdot \theta\right] + \cos(\theta) \cdot \left[3 \cdot \theta^2 - 6\right]$$

$$\rho_{2s_N} := \left[\frac{8}{5 \cdot W} \cdot \sin\left[K_{o_N} \cdot ss\right]\right] \cdot \left[\frac{1}{K_{o_N}}\right] \cdot \left[\sin\left[\alpha_N\right] + \left[\frac{1}{\alpha_N^3}\right] \cdot \left[f\left[\alpha_N\right] - f(0)\right]\right]$$

$$\Phi(\theta) := \sin(\theta) \cdot \left[3 \cdot \theta^2 - 6\right] - \cos(\theta) \cdot \left[\theta^3 - 6 \cdot \theta\right]$$

$$\rho_{s2s_{M,N}} := \left[\frac{4}{4 - \delta_{M,N}}\right] \cdot \left[-\cos\left[\tau_{N}\right] \cdot \Phi\left[\delta_{M,N}\right]\right]$$

$$\coth(x) := \frac{1}{\tanh(x)}$$

$$uvw_{N,J} := \left[\epsilon_{r_J} + \coth\left[K_{o_N} \cdot h\right] \cdot \coth\left[K_{o_N} \cdot b\right]\right]$$

$$xyz_{N,J} := \coth\left[K_{o_N} \cdot t\right] \cdot \left[\coth\left[K_{o_N} \cdot h\right] + \frac{1}{\epsilon_{r_J}} \cdot \coth\left[K_{o_N} \cdot b\right]\right]$$

$$det_{o_{N,J}} := \epsilon_{0} \cdot K_{o_N} \cdot \left[uvw_{N,J} + xyz_{N,J}\right]$$

$$G_{o11_{N,J}} := \frac{1}{det_{o_{N,J}}} \cdot \left[\coth\left[K_{o_N} \cdot h\right] + \frac{1}{\epsilon_{r_J}} \cdot \coth\left[K_{o_N} \cdot b\right]\right]$$

$$G_{o12_{N,J}} := \frac{1}{det_{o_{N,J}} \cdot \sinh\left[K_{o_N} \cdot h\right]}$$

$$G_{o21_{N,J}} := G_{o12_{N,J}}$$

$$G_{o22_{N,J}} := \frac{1}{det_{o_{N,J}}} \cdot \left[\coth\left[K_{o_N} \cdot h\right] + \frac{1}{\epsilon_{r_J}} \cdot \coth\left[K_{o_N} \cdot t\right]\right]$$

$$K_{1111_J} := \sum_N G_{o11_{N,J}} \cdot \rho^2_{1s_N}$$

$$K_{1112_J} := \sum_N G_{o11_{N,J}} \cdot \rho_{1s_N} \cdot \rho_{2s_N} \qquad K_{1121_J} := K_{1112_J}$$

$$K_{1122_J} := \sum_N G_{o11_{N,J}} \cdot \rho^2_{2s_N}$$

$$K_{1211_{M,J}} := \sum_N G_{o12_{N,J}} \cdot \rho_{1s_N} \cdot \rho_{s1s_{M,N}} \qquad K_{2111_{M,J}} := K_{1211_{M,J}}$$

$$K_{1212_{M,J}} := \sum_N G_{o12_{N,J}} \cdot \rho_{1s_N} \cdot \rho_{s2s_{M,N}} \qquad K_{2121_{M,J}} := K_{1212_{M,J}}$$

$$K_{1221_{M,J}} := \sum_N G_{o12_{N,J}} \cdot \rho_{2s_N} \cdot \rho_{s1s_{M,N}} \qquad K_{2112_{M,J}} := K_{1221_{M,J}}$$

$$K_{1222_{M,J}} := \sum_N G_{o12_{N,J}} \cdot \rho_{2s_N} \cdot \rho_{s2s_{M,N}} \qquad K_{2122_{M,J}} := K_{1222_{M,J}}$$

$$K_{2211_{M,J}} := \sum_N G_{o22_{N,J}} \cdot \rho^2_{s1s_{M,N}}$$

$$K_{2212_{M,J}} := \sum_N G_{o22_{N,J}} \cdot \rho_{s1s_{M,N}} \cdot \rho_{s2s_{M,N}} \qquad K_{2221_{M,J}} := K_{2212_{M,J}}$$

$$K_{2222_{M,J}} := \sum_{N} G_{o22_{N,J}} \cdot \rho^{2}_{s2s_{M,N}}$$

a1x := 1 a2x := 1 b1x := 0.5 b2x := 0.5

Given

$$K1 \cdot a1x + K2 \cdot a2x + K3 \cdot b1x + K4 \cdot b2x \approx P_1$$

$$K2 \cdot a1x + K5 \cdot a2x + K6 \cdot b1x + K7 \cdot b2x \approx P_2$$

$$K3 \cdot a1x + K6 \cdot a2x + K8 \cdot b1x + K9 \cdot b2x \approx 0$$

$$K4 \cdot a1x + K7 \cdot a2x + K9 \cdot b1x + K10 \cdot b2x \approx 0$$

func(K1,K2,K3,K4,K5,K6,K7,K8,K9,K10) := find(a1x,a2x,b1x,b2x)

M := 0 ..MM $K1_J := K_{1111_{J,J}}$ $K2_J := K_{1112_{J,J}}$ $K5_J := K_{1122_{J,J}}$

$K6_{M,J} := K_{1221_{M,J}}$ $K3_{M,J} := K_{1211_{M,J}}$ $K4_{M,J} := K_{1212_{M,J}}$

$K10_{M,J} := K_{2222_{M,J}}$ $K9_{M,J} := K_{2212_{M,J}}$ $K7_{M,J} := K_{1222_{M,J}}$

$K8_{M,J} := K_{2211_{M,J}}$

$$\begin{bmatrix} ak1_{M,J} \\ ak2_{M,J} \\ bk1_{M,J} \\ bk2_{M,J} \end{bmatrix} := func\left[K1_J, K2_J, K3_{M,J}, K4_{M,J}, K5_J, K6_{M,J}, K7_{M,J}, K8_{M,J}, K9_{M,J}, K10_{M,J}\right]$$

$P_1 = 0.05 \qquad P_2 = 0.05$

$$a = \begin{bmatrix} 0.1 \\ 0.095 \\ 0.09 \\ 0.085 \\ 0.08 \\ 0.075 \\ 0.07 \\ 0.065 \\ 0.06 \\ 0.055 \\ 0.05 \end{bmatrix} \qquad ak1 \cdot 10^{12} = \begin{bmatrix} 1.786 & 36.618 \\ 1.782 & 35.71 \\ 1.781 & 35.25 \\ 1.771 & 34.806 \\ 1.742 & 33.266 \\ 1.712 & 31.676 \\ 1.691 & 30.476 \\ 1.677 & 29.604 \\ 1.667 & 28.956 \\ 1.66 & 28.459 \\ 1.655 & 28.068 \end{bmatrix} \qquad ak1 \cdot 10^{12} = \begin{bmatrix} 1.786 & 36.618 \\ 1.782 & 35.71 \\ 1.781 & 35.25 \\ 1.771 & 34.806 \\ 1.742 & 33.266 \\ 1.712 & 31.676 \\ 1.691 & 30.476 \\ 1.677 & 29.604 \\ 1.667 & 28.956 \\ 1.66 & 28.459 \\ 1.655 & 28.068 \end{bmatrix}$$

cap. in pico farads

$$C_{oo_{M,J}} := \begin{bmatrix} 2 \\ - \\ L \end{bmatrix} \cdot \left[ak1_{M,J} \cdot P_1 + ak2_{M,J} \cdot P_2\right] \cdot 10^{12}$$

$$Z_{oo_M} := \frac{10^{12}}{c \cdot \sqrt{C_{oo_{M,0}} \cdot C_{oo_{M,1}}}}$$

$$C_{oo} = \begin{bmatrix} 1.128 & 22.767 \\ 1.123 & 22.005 \\ 1.112 & 21.399 \\ 1.09 & 20.24 \\ 1.065 & 18.947 \\ 1.046 & 17.957 \\ 1.034 & 17.265 \\ 1.026 & 16.771 \\ 1.02 & 16.405 \\ 1.016 & 16.125 \\ 1.013 & 15.905 \end{bmatrix}$$

$$\epsilon_{ooff_M} := \frac{C_{oo_{M,1}}}{C_{oo_{M,0}}}$$

M
0
1
2
3
4
5
6
7
8
9
10

$$a = \begin{bmatrix} 0.1 \\ 0.095 \\ 0.09 \\ 0.085 \\ 0.08 \\ 0.075 \\ 0.07 \\ 0.065 \\ 0.06 \\ 0.055 \\ 0.05 \end{bmatrix} \qquad \epsilon_{ooff} = \begin{bmatrix} 20.179 \\ 19.592 \\ 19.236 \\ 18.57 \\ 17.788 \\ 17.159 \\ 16.697 \\ 16.352 \\ 16.086 \\ 15.874 \\ 15.703 \end{bmatrix} \qquad Z_{oo} = \begin{bmatrix} 16.443 \\ 16.763 \\ 17.08 \\ 17.743 \\ 18.55 \\ 19.223 \\ 19.723 \\ 20.093 \\ 20.373 \\ 20.59 \\ 20.763 \end{bmatrix}$$

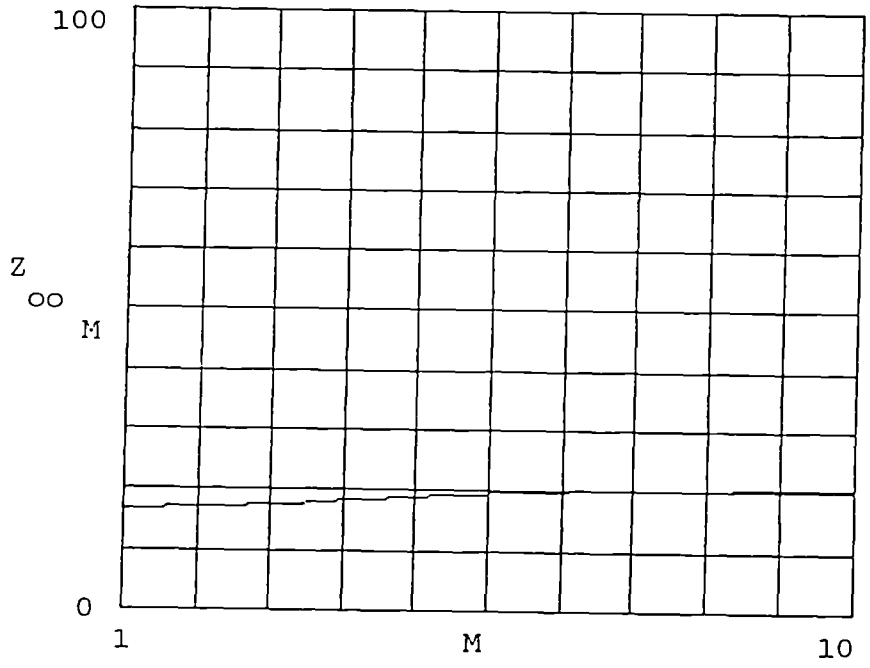

APPENDIX 2

Even mode analysis for 6 finger microstrip coupler with septum,

h = 0.015 w = 0.001 s = 0.00035

ℓ = 0.65 t = 0.65 b = 0.025 a_0 = 0.575 nn = 500 mm = 0

$$c = 3.40.10^{8} \quad \epsilon_o = \frac{8.842}{40}.10^{-12} \quad \epsilon_{p0} = 1 \quad \epsilon_{p1} = 9.8 \quad \coth(x) = \frac{1}{\tanh(x)}$$

j = 0..1 m = 0..mm $a_{m+1} = a_m - 0.010$

$$P_1 = \frac{L}{2} \quad P_2 = \frac{L}{2} \quad P_3 = \frac{L}{2}$$

$$n = 1..nn \quad k_{en} = (n - 0.5).\frac{\pi}{L} \quad s' = s + \frac{w}{2}$$

$$\rho_{1\chi(n)} = J0\left[k_{en}\left[\frac{w}{2}\right]\right]\cos\left[k_{en}.5.s'\right] \quad \rho_{2\chi n} = J0\left[k_{en}\left[\frac{w}{2}\right]\right]\cos\left[k_{en}.3.s'\right]$$

$$\rho_{3\chi n} = J0\left[k_{en}\left[\frac{w}{2}\right]\right]\cos\left[k_{en}.s'\right] \quad \rho_{\sigma 1\chi m,n} = \left[\frac{\pi}{4}\right].\sin\left[k_{en}.L\right].J1\left[k_{en}.a_m\right]$$

$$\Phi(\theta) = \sin(\theta) \cdot [3 \cdot \theta^2 - 6] - \cos(\theta) \cdot [\theta^3 - 6 \cdot \theta]$$

$$\rho_{\sigma 2\chi m,n} = \left[\frac{4}{[k_{en} \cdot a_m]^4}\right] \sin[k_{en} \cdot L] \Phi[k_{en} \cdot a_m]$$

$$uvw_{n,j} = [\epsilon_{pj} + \coth[k_{en} \cdot h] \cdot \coth[k_{en} \cdot b]]$$

$$xyz_{n,j} = \coth[k_{en} \cdot t] \left[\coth[k_{en} \cdot h] + \frac{1}{\epsilon_{pj}} \cdot \coth[k_{en} \cdot b]\right]$$

$$\det_{en,j} = k_{en} \cdot [uvw_{n,j} + xyz_{n,j}]$$

$$G_{e11n,j} = \frac{1}{\det_{en,j}} \cdot \left[\coth[k_{en} \cdot h] + \frac{1}{\epsilon_{pj}} \cdot \coth[k_{en} \cdot b]\right],$$

$$G_{e12n,j} = \frac{1}{\det_{en,j} \cdot \sinh[k_{en.h} \cdot L]}$$

$$G_{e22n,j} = \frac{1}{\det_{en,j}} \cdot \left[\coth[k_{en} \cdot h] + \frac{1}{\epsilon_{pj}} \cdot \coth[k_{en} \cdot t]\right]$$

$$k_{1j} = \sum_n G_{e11n,j} \cdot [\rho_{1\chi n}]^2 \qquad k_{2j} = \sum_n G_{e11n,j} \cdot \rho_{1\chi n} \cdot \rho_{2\chi n}$$

$$k_{3j} = \sum_{n} G_{e11n,j} \cdot \rho_{1\chi n} \cdot \rho_{3\chi n} \qquad k_{4m,j} = \sum_{n} G_{e12n,j} \cdot \rho_{1\chi n} \cdot \rho_{\sigma 1\chi m,n}$$

$$k_{5m,j} = \sum_{n} G_{e12n,j} \cdot \rho_{1\chi n} \cdot \rho_{a2\chi m,n} \qquad k_{6j} = \sum_{n} G_{e11n,j} \cdot [\rho_{2\chi n}]^2$$

$$k_{7j} = \sum_{n} G_{e11n,j} \cdot \rho_{2\chi n} \cdot \rho_{3\chi n} \qquad k_{8m,j} = \sum_{n} G_{e12n,j} \cdot \rho_{2\chi n} \cdot \rho_{\sigma 1\chi m,n}$$

$$k_{9m,j} = \sum_{n} G_{e12n,j} \cdot \rho_{2\chi n} \cdot \rho_{\sigma 2\chi m,n} \qquad FO_j = \sum_{n} G_{e11n,j} \cdot [\rho_{3\chi n}]^2$$

$$F_{1m,j} = \sum_{n} G_{e12n,j} \cdot \rho_{3\chi n} \cdot \rho_{\sigma 1\chi m,n} \qquad F2_{m,j} = \sum_{n} G_{e12n,j} \cdot \rho_{3\chi n} \cdot \rho_{\sigma 2\chi m,n}$$

$$F3_{m,j} = \sum_{n} G_{e22n,j} \cdot [\rho_{\sigma 1\chi m,n}]^2 \qquad F4_{m,j} = \sum_{n} G_{e22n,j} \cdot \rho_{\sigma 1\chi m,n} \cdot \rho_{\sigma 2\chi m,n}$$

$$F5_{m,j} = \sum_{n} Ge22_{n,j} \cdot [\rho\alpha 2\chi_{m,n}]^2$$

A = 300 B = -320 C = 280 D = -290 E = 400 F = -420 b1 = 30 b2 = 25

Given

L. A + L. B + M . C + M . D + N . E + N . F + P . b1 + Q . b2 = P_1

L. A + L . B + M . C + M . D + N . E + N . F + P . b1 + Q . b2 = P_1

M. A + M . B + R . C + R . D + S . E + S . F + T . b1 + U . b2 = P_2

M. A + M . B + R . C + R . D + S . E + S . F + T . b1 + U . b2 = P_2

N. A + N . B + S . C + S . D + V . E + V . F + W . b1 + X . b2 = P_3

N. A + N . B + S . C + S . D + V . E + V . F + W . b1 + X . b2 = P_3

P. A + P . B + T . C + T . D + W . E + W . F + Y . b1 + Z . b2 = 0

Q. A + Q . B + U . C + U . D + X . E + X . F + Z .b1 + $f5$. b2 = 0

f(L,M,N,P,Q,R,S,T,U,V,W,X,Y,Z,$f5$) = find (A, B, C, D, E, F, b1, b2)

m = 0..mm Lj = k1j Mj = K2j Qm,j = k5m,j Rj = k6j Nj = k3j

Pm,j = k4m,j Sj = k7j Xm,j = F2m,j Vj = F0j Um,j = K9m,j

Tm,j = k8m,j Wm,j = F1m,j Ym,j = F3m,j Zm,j = F4m,j f5m,j = F5m,j

Lj	**Mj**	**Qm,j**	**Rj**	**Nj**	**Pm,j**	**Vj**
0.4025	0.3268	0.00873	0.42695	0.30801	0.00533	0.48534
0.13754	0.12371	0.01304	0.14246	0.12033	0.00769	0.15348

Um,j	**Sj**	**Tm,j**	**Wm,j**	**Xm,j**	**Ym,j**	**Zm,j**
0.00871	0.3664	0.00532	0.00531	0.0087	0.00635	0.01171
0.01302	0.13135	0.00768	0.00768	0.01301	0.005	0.01003

$f5$m,j
0.02525
0.0217

$$\begin{bmatrix} A_{m,j} \\ B_{m,j} \\ C_{m,j} \\ D_{m,j} \\ E_{m,j} \\ F_{m,j} \\ \Gamma_{m,j} \\ \lambda_{m,j} \end{bmatrix} = f[L_j, M_j, N_j, P_{m,j}, Q_{m,j}, R_j, S_j, T_{m,j}, U_{m,j}, V_j, W_{m,j}, X_{m,j}, Y_{m,j}, Z_{m,j}, f5_{m,j}]$$

$$a=\begin{bmatrix} 0.575 \\ 0.565 \end{bmatrix} \qquad A=(-161.46192\ 3528.24334)$$

Am,j	Bm,j	Cm,j	Dm,j
-161.46192	161.93339	-2323.14893	2323.39018
3528.24334	-3526.75336	-30925.90307	30926.6463

Em,j	Fm,j
-64014.07375	64014.271
38005.09262	-38004.493

$$\alpha 1_{m,j}=[A_{m,j}+B_{m,j}]\cdot\epsilon_0\cdot 10^{12}\ \alpha 2_{m,j}=[C_{m,j}+D_{m,j}]\cdot\epsilon_0\cdot 10^{12}\ \alpha_{3_{m,j}}=[E_{m,j}+F_{m,j}]\cdot\epsilon_0\cdot 10^{12}$$

$\alpha 1=(0.10422\ 0.32936)$ $\alpha 2=(0.05333\ 0.16429)$ $\alpha 3=(0.0436\ 0.13255)$

capacitance in pico farads

$$C1e_{m,j}=\alpha 1_{m,j} \qquad C2e_{m,j}=\alpha 2m,j \qquad C3e_{m,j}=\alpha 3_{m,j}$$

$C_{1e}=(0.10422\ 0.32936)$ $C_{2e}=(0.05333\ 0.16429)$ $C_{3e}=(0.0436\ 0.13255)$

$$\epsilon_{\epsilon\phi\phi 1\epsilon m} = \frac{C1e_{m,1}}{C1e_{m,0}} \qquad \epsilon_{\epsilon\phi\phi 2\epsilon m} = \frac{C2e_{m,1}}{C2e_{m,0}} \qquad \epsilon_{\epsilon\phi\phi 3\epsilon m} = \frac{C3e_{m,1}}{C3e_{m,0}}$$

$$\epsilon_{\epsilon\phi\phi 1\epsilon} = 3.16026 \qquad \epsilon_{\epsilon\phi\phi 2\epsilon} = 3.08084 \qquad \epsilon_{\epsilon\phi\phi 3\epsilon} = 3.03984$$

$$Z_{o1em} = \frac{10^{12}}{c \cdot \sqrt{C_{1em,0} \cdot C_{1em,1}}} \qquad Z_{o2em} = \frac{10^{12}}{c \cdot \sqrt{C_{2em,0} \cdot C_{2em,1}}} \qquad Z_{o3em} = \frac{10^{12}}{c \cdot \sqrt{C_{3em,0} \cdot C_{3em,1}}}$$

b = 0.025 h = 0.015 a_0 = 0.575 nn = 500 2.s = 0.0007

w = 0.001

$$Z_{o1em} = 449.79049 \qquad Z_{o2em} = 890.30406 \qquad Z_{o3em} = 1096.17553$$

system capacitance calc.

$$C_{ej} = C_{1eo,j} + C_{2eo,j} + C_{3eo,j} \quad C_{ej} , \frac{0.020115}{0.6262}$$

$$Z_{oe} = \frac{10^{12}}{c \cdot \sqrt{C_{eo} \cdot C_{e1}}} \qquad \epsilon_{\epsilon\epsilon\phi\phi} = \frac{C_{e1}}{C_{e0}}$$

$$Z_{oe} = 234.80382 \qquad \epsilon_{\epsilon\epsilon\phi\phi} = 3.1131$$

Odd mode analysis for 6 finger microstrip coupler pgm. with septum

h = 0.015 w = 0.001 s = 0.00035

ℓ = 0.65 t = 0.650 b = 0.025 a_0 = 0.575 nn = 500 mm = 0

$$c = 3.40.10^{8} \qquad \epsilon_0 = \frac{8.842}{40} . 10^{-12} \qquad \epsilon_{\rho 1} = 9.8 \qquad \epsilon_{\rho 0} = 1$$

$$i = 0..1 \qquad m = 0..mm \qquad a_m + 1 = a_m - 0.010 \qquad \coth(x) = \frac{1}{\tanh(x)}$$

$$P_1 = \frac{\ell}{2} \qquad P_2 = \frac{\ell}{2} \qquad P_3 = \frac{\ell}{2}$$

$$n = 1..nn \qquad k_{on} = n . \frac{\pi}{\ell} \qquad s' = s + \frac{w}{2}$$

$$\rho 1_{on} = J0\left[k_{on} . \left[\frac{w}{2}\right]\right] . \sin\left[k_{on} . 5 . s'\right] \qquad \rho 2_{on} = J0\left[k_{on} . \left[\frac{w}{2}\right]\right] . \sin\left[k_{on} . 3 . s'\right]$$

$$\rho 3_{on} = J0\left[k_{on} . \left[\frac{w}{2}\right]\right] . \sin\left[k_{on} . s'\right] \qquad \rho_{o1om,n} = -\left[\frac{\pi}{4}\right] . \cos(n . \pi) . J1\left[k_{on} . a_m\right]$$

$$\Phi(\theta) = \sin(\theta) \cdot [3 \cdot \theta^2 - 6] - \cos(\theta) \cdot [\theta^3 - 6 \cdot \theta]$$

$$\rho_{\sigma 2 \alpha m, n} = -\left[\frac{4}{[k_{on} \cdot a_m]^4}\right] \cdot \cos(n \cdot \pi) \cdot \Phi[k_{on} \cdot a_m]$$

$$uvw_{n,j} = [\epsilon_{\rho j} + \coth[k_{on} \cdot h] \cdot \coth[k_{on} \cdot b]]$$

$$xyz_{n,j} = \coth[k_{on} \cdot t] \cdot \left[\coth[k_{on} \cdot h] + \frac{1}{\epsilon_{pj}} \cdot \coth[k_{on} \cdot b]\right]$$

$$\det_{on,j} = k_{on} \cdot [uvw_{n,j} + xyz_{n,j}]$$

$$G_{o11n,j} = \frac{1}{\det_{on,j}} \cdot \left[\coth[k_{on} \cdot h] + \frac{1}{\epsilon_{\rho j}} \cdot \coth[k_{on} \cdot b]\right]$$

$$G_{o12n,j} = \frac{1}{\det_{on,j}} \cdot \sinh[k_{on} \cdot h]$$

$$G_{o22n,j} = \frac{1}{\det_{on,j}} \cdot \left[\coth[k_{on} \cdot h] + \frac{1}{\epsilon_{\rho j}} \cdot \coth[k_{on} \cdot t]\right]$$

$$k1_j = \sum_n G_{o11n,j} \cdot [\rho_{1\sigma n}]^2 \qquad k2_j = \sum_n G_{o11n,j} \cdot \rho_{1\sigma n} \cdot \rho_{2\sigma n}$$

$$k3_j = \sum_n G_{o11n,j} \cdot \rho_{1\sigma n} \cdot \rho_{3\sigma n} \qquad k4_{m,j} = \sum_n G_{o12n,j} \cdot \rho_{1\sigma n} \cdot \rho_{\sigma 1\sigma m,n}$$

$$k5_{m,j} = \sum_n G_{o12n,j} \cdot \rho_{1\sigma n} \cdot \rho_{\sigma 2\sigma m,n} \qquad k6_j = \sum_n G_{o11n,j} \cdot [\rho_{2\sigma n}]^2$$

$$k7_j = \sum_n G_{o11n,j} \cdot \rho_{2\sigma n} \cdot \rho_{3\sigma n} \qquad k8_{m,j} = \sum_n G_{o12n,j} \cdot \rho_{2\sigma n} \cdot \rho_{\sigma 1\sigma m,n}$$

$$k9_{m,j} = \sum_n G_{o12n,j} \cdot \rho_{2\sigma n} \cdot \rho_{\sigma 2\sigma m,n} \qquad FO_j = \sum_n G_{o11n,j} \cdot [\rho_{3\sigma n}]^2$$

$$F1_{m,j} = \sum_n G_{o12n,j} \cdot \rho_{3\sigma n} \cdot \rho_{\sigma 1\sigma m,n} \qquad F2_{m,j} = \sum_n G_{o12n,j} \cdot \rho_{3\sigma n} \cdot \rho_{\sigma 2\sigma m,n}$$

$$F3_{m,j} = \sum_n G_{o22n,j} \cdot [\rho_{\sigma 1\sigma m,n}]^2 \qquad F4_{m,j} = \sum_n G_{o22n,j} \cdot \rho_{\sigma 1\sigma m,n} \cdot \rho_{\sigma 2\sigma m,n}$$

$$F5_{m,j} = \sum_n G_{o22n,j} \cdot [\rho_{\sigma 2\sigma m,n}]^2$$

A = 300 B = -320 C = 280 D = -290 E = 400 F = -420 b1 = 30 b2 = 25

Given

L. A + L. B + M . C + M . D + N . E + N . F + P . b1 + Q. b2 = $-P_1$

L. A + L . B + M . C + M . D + N . E + N . F + P . b1 + Q. b2 = $-P_1$

M. A + M . B + R . C + R . D + S . E + S . F + T . b1 + U . b2 = P_2

M. A + M . B + R . C + R . D + S . E + S . F + T . b1 + U . b2 = P_2

N. A + N . B + S . C + S . D + V . E + V . F + W. b1 + X. b2 = $-P_3$

N. A + N . B + S . C + S . D + V . E + V . F + W . b1 + X. b2 = $-P_3$

P. A + P . B + T . C + T . D + W . E + W . F + Y . b1 + Z . b2 = 0

Q. A + Q . B + U . C + U . D + X . E + X . F + Z .b1 + $f5$. b2 = 0

f(L,M,N,P,Q,R,S,T,U,V,W,X,Y,Z,$f5$) = find (A, B, C, D, E, F, b1, b2)

m = 0..mm Lj = k1j Mj = k2j Qm,j = k5m,j Rj = k6j Nj = k3j

Pm,j = k4m,j Sj = k7j Xm,j = F2m,j Vj = F0j Um,j = K9m,j

Tm,j = k8m,j Wm,j = F1m,j Ym,j = F3m,j Zm,j = F4m,j $f5$m,j = F5m,j

Lj	**Mj**	**Qm,j**	**Rj**	**Nj**	**Pm,j**	**Vj**
0.1682	0.0732	0	0.1437	0.0248	0.0004	0.0854
0.0318	0.0139	0	0.0268	0.0047	0.0004	0.0158

Um,j	**Sj**	**Tm,j**	**Wm,j**	**Xm,j**	**Ym,j**	**Zm,j**
0	0.0336	0.0002	0.0001	0	0.006	0.0005
0	0.0063	0.0003	0.0001	0	0.0043	0.0004

$f5$m,j
0.0001
0.0001

$$a=\left[\frac{0.575}{0.565}\right] \qquad A=(-8898.5445 \;\; 10104.9471)$$

$$\begin{bmatrix} A_{m,j} \\ B_{m,j} \\ C_{m,j} \\ D_{m,j} \\ E_{m,j} \\ F_{m,j} \\ \Gamma_{m,j} \\ \lambda_{m,j} \end{bmatrix} = f\left[L_j, M_j, N_j, P_{m,j}, Q_{m,j}, R_j, S_j, T_{m,j}, U_{m,j}, V_j, W_{m,j}, X_{m,j}, Y_{m,j}, Z_{m,j}, f5_{m,j}\right]$$

Am,j	Bm,j	Cm,j	Dm,j
-8898.5445	8895.0799	12336.2159	-12331.0612
10104.9471	-10123.5414	-41652.6024	41680.4697

Em,j	Fm,j
-75446.6108	75441.7804
-48908.6543	48882.5761

$$\alpha 1_{m,j} = \left[A_{m,j} + B_{m,j}\right] \cdot \epsilon_0 \cdot 10^{12} \qquad \alpha 2_{m,j} = \left[C_{m,j} + D_{m,j}\right] \cdot \epsilon_0 \cdot 10^{12}$$

$$\alpha 3_{m.j} = \left[E_{m,j} + F_{m,j}\right] \cdot \epsilon_0 \cdot 10^{12}$$

$\alpha 1 = (-0.7659 - -4.1103) \qquad \alpha 2 = (1.1394\ 6.1601) \qquad \alpha 3 = (-1.0678\ -5.7646)$

capacitance in pico farads

$$C1o_{m,j} = \alpha 1_{m,j} \qquad C2o_{m,j} = \alpha 2_{m,j} \qquad C3o_{m,j} = \alpha 3_{m,j}$$

C_{1o} = (-0.7659 -4.1103) C_{2o} = (1.1394 6.1601) C_{3o} = (-1.0678 -5.7646)

$$\epsilon_{\epsilon\phi\phi 1om} = \frac{C1o_{m,1}}{C1o_{m,0}} \qquad \epsilon_{\epsilon\phi\phi 2om} = \frac{C2o_{m,1}}{C2o_{m,0}} \qquad \epsilon_{\epsilon\phi\phi 3om} = \frac{C3o_{m,1}}{C3o_{m,0}}$$

$\epsilon_{\epsilon\phi\phi 1o} = 5.3669$ $\epsilon_{\epsilon\phi\phi 2o} = 5.4063$ $\epsilon_{\epsilon\phi\phi 3o} = 5.3988$

$$Z_{o1om} = \frac{10^{12}}{c \cdot \sqrt{C_{1om,0} \cdot C_{1om,1}}} \qquad Z_{o2om} = \frac{10^{12}}{c \cdot \sqrt{C_{2om,0} \cdot C_{2om,1}}} \qquad Z_{o3om} = \frac{10^{12}}{c \cdot \sqrt{C_{3om,0} \cdot C_{3om,1}}}$$

b = 0.025 h = 0.015 a_0 = 0.575 nn = 500 2.s = 0.0007

w = 0.001

Z_{o1om} = 46.969 Z_{o2om} = 31.4544 Z_{o3om} = 33.5891

C_{ej} =	$C_{1e0,j}$ =	$C_{2e0,j}$ =	$C_{3e0,j}$ =
0.021	0.104	0.053	0.044
0.626	0.329	0.164	0.133

$C_{1oo,j} = |C_{1oo,j}|$ $C_{2oo,j} = |C_{2oo,j}|$ $C_{3oo,j} = |C_{3oo,j}|$

$$C_{oj} = C_{ej} + [C_{1oo,j} - C_{1eo,j} + C_{2oo,j} - C_{2eo,j} + C_{3oo,j} - C_{3eo,j}]$$

$$\frac{C_{oj}}{\frac{2.973}{16.0349}}$$

$$Z_{oe} = \frac{10^{12}}{c \cdot \sqrt{C_{o0} \cdot C_{o1}}} \qquad Z_{oe} = \frac{10^{12}}{c \cdot \sqrt{C_{eo} \cdot C_{e1}}} \qquad ratio = \frac{Z_{oe}}{Z_{oo}}$$

$Z_{oo} = 12.0694$ $Z_{oe} = 234.9273$ ratio = 19.4648

$coupling = 20 \cdot \log\left[\frac{ratio-1}{ratio+1}\right]$ $coupling = -0.8933$ $C_{e1} = 0.626$ $C_{e0} = 0.$

$$\epsilon_{o\epsilon\phi\phi} = \frac{C_{o1}}{C_{o0}} \qquad \epsilon_{o\epsilon\phi\phi} = 5.3934 \qquad \epsilon_{\epsilon\epsilon\phi\phi} = \frac{C_{e1}}{C_{e0}} \qquad \epsilon_{\epsilon\epsilon\phi\phi} = 3.1144$$

$$\epsilon_{\epsilon\phi\phi} = \sqrt{\epsilon_{\epsilon\epsilon\phi\phi} \cdot \epsilon_{o\epsilon\phi\phi}} \qquad \epsilon_{\epsilon\phi\phi} = 4.0985 \qquad \frac{1}{\sqrt{\epsilon_{\epsilon\phi\phi}}} = 0.494$$

EVEN mode analysis for 6 finger microstrip coupler with pgm. with septum,

h = 0.025 w = 0.001 s = 0.0003

ℓ = 0.65 t = 0.65 b = 0.025 a_0 = 0.575 nn = 500 mm = 0

$$c = 3.40.10^8 \quad \epsilon_0 = \frac{8.842}{40}.10^{-12} \quad \epsilon_{\rho 0} = 1 \quad \epsilon_{\rho 1} = 9.8 \quad \coth(x) = \frac{1}{\tanh(x)}$$

j = 0..1 m = 0..mm $a_{m+1} = a_m - 0.010$

$$P_1 = \frac{L}{2} \quad P_2 = \frac{L}{2} \quad P_3 = \frac{L}{2}$$

$$n = 1..nn \quad k_{en} = (n - 0.5).\frac{\pi}{L} \quad s' = s + \frac{w}{2}$$

$$\rho_{1\chi n} = JO\left[k_{en}.\left[\frac{w}{2}\right]\right].\cos\left[k_{en}.5.s'\right] \quad \rho_{2\chi n} = JO\left[k_{en}.\left[\frac{w}{2}\right]\right].\cos\left[k_{en}.3.s'\right]$$

$$\rho_{3\chi n} = JO\left[k_{en}.\left[\frac{w}{2}\right]\right].\cos\left[k_{en}.s'\right] \quad \rho_{\sigma 1\chi m,n} = \left[\frac{\pi}{4}\right].\sin\left[k_{en}.L\right].J1\left[k_{en}.a_m\right]$$

$$\Phi(\theta) = \sin(\theta).[3.\theta^2 - 6] - \cos(\theta).[\theta^3 - 6.\theta]$$

$$\rho_{\sigma 2\chi m,n} = \left[\frac{4}{[k_{en}\cdot a_m]^4}\right] \cdot \sin[k_{en}\cdot L] \cdot \Phi[k_{en}\cdot a_m]$$

$$uvw_{n,j} = [\epsilon_{\rho j} + \coth[k_{en}\cdot h] \cdot \coth[k_{en}\cdot b]]$$

$$xyz_{n,j} = \coth[k_{en}\cdot t] \cdot \left[\coth[k_{en}\cdot h] + \frac{1}{\epsilon_{pj}} \cdot \coth[k_{en}\cdot b]\right]$$

$$\det_{en,j} = k_{en} \cdot [uvw_{n,j} + xyz_{n,j}]$$

$$G_{e11n,j} = \frac{1}{\det_{en,j}} \cdot \left[\coth[k_{en}\cdot h] + \frac{1}{\epsilon_{\rho j}} \cdot \coth[k_{en}\cdot b]\right],$$

$$G_{e12n,j} = \frac{1}{\det_{en,j}\cdot \sinh[k_{en.h}]}$$

$$G_{e22n,j} = \frac{1}{\det_{en,j}} \cdot \left[\coth[k_{en}\cdot h] + \frac{1}{\epsilon_{pj}} \cdot \coth[k_{en}\cdot t]\right]$$

$$k1_j = \sum_n G_{e11n,j} \cdot [\rho_{1\chi n}]^2 \qquad k2_j = \sum_n G_{e11n,j} \cdot \rho_{1\chi n} \cdot \rho_{2\chi n}$$

$$k3_j = \sum_n G_{e11n,j} \cdot \rho_{1\chi n} \cdot \rho_{3\chi n} \qquad k4_{m,j} = \sum_n G_{e12n,j} \cdot \rho_{1\chi n} \cdot \rho_{\sigma 1\chi m,n}$$

$$k5_{m,j} = \sum_n G_{e12n,j} \cdot \rho_{1\chi n} \cdot \rho_{\sigma 2\chi m,n} \qquad k6_j = \sum_n G_{e11n,j} \cdot [\rho_{2\chi n}]^2$$

$$k7_j = \sum_n G_{e11n,j} \cdot \rho_{2\chi n} \cdot \rho_{3\chi n} \qquad k8_{m,j} = \sum_n G_{e12n,j} \cdot \rho_{2\chi n} \cdot \rho_{\sigma 1\chi m,n}$$

$$k9_{m,j} = \sum_n G_{e12n,j} \cdot \rho_{2\chi n} \cdot \rho_{\sigma 2\chi m,n} \qquad FO_j = \sum_n G_{e11n,j} \cdot [\rho_{3\chi n}]^2$$

$$F1_{m,j} = \sum_n G_{e12n,j} \cdot \rho_{3\chi n} \cdot \rho_{\sigma 1\chi m,n} \qquad F2_{m,j} = \sum_n G_{e12n,j} \cdot \rho_{3\chi n} \cdot \rho_{\sigma 2\chi m,n}$$

$$F3_{m,j} = \sum_n G_{e22n,j} \cdot [\rho_{\sigma 1\chi m,n}]^2 \qquad F4_{m,j} = \sum_n G_{e22n,j} \cdot \rho_{\sigma 1\chi m,n} \cdot \rho_{\sigma 2\chi m,n}$$

$$F5_{m,j} = \sum_n G_{e22n,j} \cdot [\rho\sigma 2\chi_{m,n}]^2$$

A = 300 B = -320 C = 280 D = -290 E = 400 F = -420 b1 = 30 b2 = 25

Given

L. A + L. B + M . C + M . D + N . E + N . F + P . b1 + Q . b2 = P_1

L. A + L . B + M . C + M . D + N . E + N . F + P . b1 + Q . b2 = P_1

M. A + M . B + R . C + R . D + S . E + S . F + T . b1 + U . b2 = P_2

M. A + M . B + R . C + R . D + S . E + S . F + T . b1 + U . b2 = P_2

N. A + N . B + S . C + S . D + V . E + V . F + W . b1 + X . b2 = P_3

N. A + N . B + S . C + S . D + V . E + V . F + W . b1 + X . b2 = P_3

P. A + P . B + T . C + T . D + W . E + W . F + Y . b1 + Z . b2 = 0

Q. A + Q . B + U . C + U . D + X . E + X . F + Z .b1 + f5 . b2 = 0

f(L,M,N,P,Q,R,S,T,U,V,W,X,Y,Z,f5) = find (A, B, C, D, E, F, b1, b2)

m = 0..mm Lj = k1j Mj = K2j Qm,j = k5m,j Rj = k6j Nj = k3j

Pm,j = k4m,j Sj = k7j Xm,j = F2m,j Vj = F0j Um,j = K9m,j

Tm,j = k8m,j Wm,j = F1m,j Ym,j = F3m,j Zm,j = F4m,j

$f5_{m,j}$ = F5m,j

Lj	**Mj**	**Qm,j**	**Rj**	**Nj**	**Pm,j**	**Vj**
0.42756	0.35892	0.01029	0.45184	0.33593	0.00619	0.51305
0.12585	0.1132	0.01494	0.13047	0.10897	0.00849	0.14187

Um,j	**Sj**	**Tm,j**	**Wm,j**	**Xm,j**	**Ym,j**	**Zm,j**
0.01027	0.39714	0.00618	0.00617	0.01027	0.00635	0.01171
0.01493	0.12037	0.00848	0.00848	0.01493	0.0048	0.00967

f5m,j
0.02525
0.02078

$$\begin{bmatrix} A_{m,j} \\ B_{m,j} \\ C_{m,j} \\ D_{m,j} \\ E_{m,j} \\ F_{m,j} \\ \Gamma_{m,j} \\ \lambda_{m,j} \end{bmatrix} = f[L_j, M_j, N_j, P_{m,j}, Q_{m,j}, R_j, S_j, T_{m,j}, U_{m,j}, V_j, W_{m,j}, X_{m,j}, Y_{m,j}, Z_{m,j}, f5_{m,j}]$$

$$a = \begin{bmatrix} 0.575 \\ 0.565 \end{bmatrix} \qquad A = (9970.96215\ 13326.90248)$$

Am,j	Bm,j	Cm,j	Dm,j
9970.96215	-9970.5121	-2262.95097	2263.15965
13326.90248	-13325.17582	11246.3353	-11245.54244

Em,j	Fm,j
57426.672495	-57426.48477
-45334.50803	45335.21904

$$\alpha 1_{m,j} = \left[A_{m,j} + B_{m,j}\right] \cdot \epsilon_0 \cdot 10^{12} \quad \alpha 2_{m,j} = \left[C_{m,j} + D_{m,j}\right] \cdot \epsilon_0 \cdot 10^{12} \quad \alpha 3_{m,j} = \left[E_{m,j} + F_{m,j}\right] \cdot \epsilon_0 \cdot 10^{1}$$

$\alpha 1 = (0.09948\ 0.38168)$ $\alpha 2 = (0.04613\ 0.17526)$ $\alpha 3 = (0.0415\ 0.15717)$

capacitance in pico farads

$$C1e_{m,j} = \alpha 1_{m,j} \qquad C2e_{m,j} = \alpha 2_{m,j} \qquad C3e_{m,j} = \alpha 3_{m,j}$$

$C_{1e} = (0.10422\ 0.32936)$ $C_{2e} = (0.05333\ 0.16429)$ $C_{3e} = (0.0436\ 0.13255)$

$$\epsilon_{\epsilon\phi\phi 1\epsilon m} = \frac{C1e_{m,1}}{C1e_{m,0}} \qquad \epsilon_{\epsilon\phi\phi 2\epsilon m} = \frac{C2e_{m,1}}{C2e_{m,0}} \qquad \epsilon_{\epsilon\phi\phi 3\epsilon m} = \frac{C3e_{m,1}}{C3e_{m,0}}$$

$$\epsilon_{\epsilon\phi\phi 1\epsilon} = 3.83654 \qquad \epsilon_{\epsilon\phi\phi 2\epsilon} = 3.79948 \qquad \epsilon_{\epsilon\phi\phi 3\epsilon} = 3.78759$$

$$Z_{o1em} = \frac{10^{12}}{c \cdot \sqrt{C_{1em,0} \cdot C_{1em,1}}} \quad Z_{o2em} = \frac{10^{12}}{c \cdot \sqrt{C_{2em,0} \cdot C_{2em,1}}} \quad Z_{o3em} = \frac{10^{12}}{c \cdot \sqrt{C_{3em,0} \cdot C_{3em,1}}}$$

b = 0.025 h = 0.025 a_0 = 0.575 nn = 500 2.s = 0.0006

w = 0.001

$$Z_{o1em} = 427.65423 \quad Z_{o2em} = 926.80992 \quad Z_{o3em} = 1031.88393$$

system capacitance calc.

$$C_{ej} = C_{1eo,j} + C_{2eo,j} + C_{3eo,j} \quad \frac{C_{ej}}{\frac{0.18711}{0.71411}}$$

$$Z_{oe} = \frac{10^{12}}{c \cdot \sqrt{C_{eo} \cdot C_{e1}}} \qquad \epsilon_{\epsilon\epsilon\phi\phi} = \frac{C_{e1}}{C_{e0}}$$

$$Z_{oe} = 227.97601 \qquad \epsilon_{\epsilon\epsilon\phi\phi} = 3.81655$$

Odd mode analysis for 6 finger microstrip coupler pgm. with septum

h = 0.025 w = 0.001 s = 0.0003

L = 0.65 t = 0.650 b = 0.025 a_0 = 0.575 nn = 500 mm = 0

$$c = 3.40.10^{8} \qquad \epsilon_0 = \frac{8.842}{40} . 10^{-12} \qquad \epsilon_{\rho 1} = 9.8 \qquad \epsilon_{\rho 0} = 1$$

$$i = 0..1 \qquad m = 0..mm \qquad a_m + 1 = a_m - 0.010 \qquad \coth(x) = \frac{1}{\tanh(x)}$$

$$P_1 = \frac{L}{2} \qquad P_2 = \frac{L}{2} \qquad P_3 = \frac{L}{2}$$

$$n = 1..nn \qquad k_{on} = n . \frac{\pi}{L} \qquad s' = s + \frac{w}{2}$$

$$\rho_{1on} = J0\left[k_{on} . \left[\frac{w}{2}\right]\right] . \sin\left[k_{on} . 5 . s'\right] \qquad \rho_{2on} = J0\left[k_{on} . \left[\frac{w}{2}\right]\right] . \sin\left[k_{on} . 3 . s'\right]$$

$$\rho_{3on} = J0\left[k_{on} . \left[\frac{w}{2}\right]\right] . \sin\left[k_{on} . s'\right] \qquad \rho_{o1om,n} = -\left[\frac{\pi}{4}\right] . \cos(n . \pi) . J1\left[k_{on} . a_m\right]$$

$$\Phi(\theta) = \sin(\theta) \cdot [3 \cdot \theta^2 - 6] - \cos(\theta) \cdot [\theta^3 - 6 \cdot \theta]$$

$$\rho_{\sigma 2 \alpha m, n} = -\left[\frac{4}{[k_{on} \cdot a_m]^4}\right] \cdot \cos(n \cdot \pi) \cdot \Phi[k_{on} \cdot a_m]$$

$$uvw_{n,j} = [\epsilon_{\rho j} + \coth[k_{on} \cdot h] \cdot \coth[k_{on} \cdot b]]$$

$$xyz_{n,j} = \coth[k_{on} \cdot t] \cdot \left[\coth[k_{on} \cdot h] + \frac{1}{\epsilon_{pj}} \cdot \coth[k_{on} \cdot b]\right]$$

$$\det_{on,j} = k_{on} \cdot [uvw_{n,j} + xyz_{n,j}]$$

$$G_{o11n,j} = \frac{1}{\det_{on,j}} \cdot \left[\coth[k_{on} \cdot h] + \frac{1}{\epsilon_{\rho j}} \cdot \coth[k_{on} \cdot b]\right]$$

$$G_{o12n,j} = \frac{1}{\det_{on,j} \cdot \sinh[k_{on} \cdot h]}$$

$$G_{o22n,j} = \frac{1}{\det_{on,j}} \cdot \left[\coth[k_{on} \cdot h] + \frac{1}{\epsilon_{\rho j}} \cdot \coth[k_{on} \cdot t]\right]$$

$$k1_j = \sum_n G_{o11n,j} \cdot [\rho_{1\sigma n}]^2 \qquad k2_j = \sum_n G_{o11n,j} \cdot \rho_{1\sigma n} \cdot \rho_{z\sigma n}$$

$$k3_j = \sum_n G_{o11n,j} \cdot \rho_{1\sigma n} \cdot \rho_{3\sigma n} \qquad k4_{m,j} = \sum_n G_{o12n,j} \cdot \rho_{1\sigma n} \cdot \rho_{\sigma 1\sigma m,n}$$

$$k5_{m,j} = \sum_n G_{o12n,j} \cdot \rho_{1\sigma n} \cdot \rho_{\sigma 2\sigma m,n} \qquad k6_j = \sum_n G_{o11n,j} \cdot [\rho_{2\sigma n}]^2$$

$$k7_j = \sum_n G_{o11n,j} \cdot \rho_{2\sigma n} \cdot \rho_{3\sigma n} \qquad k8_{m,j} = \sum_n G_{o12n,j} \cdot \rho_{2\sigma n} \cdot \rho_{\sigma 1\sigma m,n}$$

$$k9_{m,j} = \sum_n G_{o12n,j} \cdot \rho_{2\sigma n} \cdot \rho_{\sigma 2\sigma m,n} \qquad FO_j = \sum_n G_{o11n,j} \cdot [\rho_{3\sigma n}]^2$$

$$F1_{m,j} = \sum_n G_{o12n,j} \cdot \rho_{3\sigma n} \cdot \rho_{\sigma 1\sigma m,n} \qquad F2_{m,j} = \sum_n G_{o12n,j} \cdot \rho_{3\sigma n} \cdot \rho_{\sigma 2\sigma m,n}$$

$$F3_{m,j} = \sum_n G_{o22n,j} \cdot [\rho_{\sigma 1\sigma m,n}]^2 \qquad F4_{m,j} = \sum_n G_{o22n,j} \cdot \rho_{\sigma 1\sigma m,n} \cdot \rho_{\sigma 2\sigma m,n}$$

$$F5_{m,j} = \sum_n G_{o22n,j} \cdot [\rho_{\sigma 2\sigma m,n}]^2$$

A = 300 B = -320 C = 280 D = -290 E = 400 F = -420 b1 = 30 b2 = 25

Given

L. A + L. B + M . C + M . D + N . E + N . F + P . b1 + Q. b2 = $-P_1$

L. A + L . B + M . C + M . D + N . E + N . F + P . b1 + Q. b2 = $-P_1$

M. A + M . B + R . C + R . D + S . E + S . F + T . b1 + U . b2 = P_2

M. A + M . B + R . C + R . D + S . E + S . F + T . b1 + U . b2 = P_2

N. A + N . B + S . C + S . D + V . E + V . F + W. b1 + X. b2 = $-P_3$

N. A + N . B + S . C + S . D + V . E + V . F + W . b1 + X. b2 = $-P_3$

P. A + P . B + T . C + T . D + W . E + W . F + Y . b1 + Z . b2 = 0

Q. A + Q . B + U . C + U . D + X . E + X . F + Z .b1 + $f5$. b2 = 0

f(L,M,N,P,Q,R,S,T,U,V,W,X,Y,Z,$f5$) = find (A, B, C, D, E, F, b1, b2)

m = 0..mm Lj = k1j Mj = k2j Qm,j = k5m,j Rj = k6j Nj = k3j

Pm,j = k4m,j Sj = k7j Xm,j = F2m,j Vj = F0j Um,j = K9m,j

Tm,j = k8m,j Wm,j = F1m,j Ym,j = F3m,j Zm,j = F4m,j

$f5$m,j = F5m,j

Lj	**Mj**	**Qm,j**	**Rj**	**Nj**	**Pm,j**	**Vj**
0.1659	0.0737	0	0.1416	0.0257	0.0004	0.0804
0.0309	0.0138	0	0.0263	0.0048	0.0004	0.0149

Um,j	**Sj**	**Tm,j**	**Wm,j**	**Xm,j**	**Ym,j**	**Zm,j**
0	0.0355	0.0002	0.0001	0	0.006	0.0005
0	0.0066	0.0002	0.0001	0	0.0039	0.0004

$f5$m,j
0.0001
0.0001

$$\begin{bmatrix} A_{m,j} \\ B_{m,j} \\ C_{m,j} \\ D_{m,j} \\ E_{m,j} \\ F_{m,j} \\ \Gamma_{m,j} \\ \lambda_{m,j} \end{bmatrix} = f[L_j, M_j, N_j, P_{m,j}, Q_{m,j}, R_j, S_j, T_{m,j}, U_{m,j}, V_j, W_{m,j}, X_{m,j}, Y_{m,j}, Z_{m,j}, f5_{m,j}]$$

$$a=\left[\frac{0.575}{0.565}\right] \qquad A=(61246.1823 \ -10304.0841)$$

Am,j	Bm,j	Cm,j	Dm,j
61246.1823	-61249.7593	44789.1836	-44783.6914
-10304.0841	10284.8006	13179.8255	-13150.1589

Em,j	Fm,j
222766.6628	-222771.9861
51471.3125	-51500.0575

$$\alpha 1_{m,j}=\left[A_{m,j}+B_{m,j}\right]\cdot\epsilon_0\cdot 10^{12} \qquad \alpha 2_{m,j}=\left[C_{m,j}+D_{m,j}\right]\cdot\epsilon_0\cdot 10^{12}$$

$$\alpha 3_{m,j}=\left[E_{m,j}+F_{m,j}\right]\cdot\epsilon_0\cdot 10^{12}$$

$\alpha 1=(-0.7907 \ -4.2626)$ $\alpha 2=(1.2141 \ 6.5578)$ $\alpha 3=(-1.1767 \ -6.3541)$

capacitance in pico farads

$$C1o_{m,j}=\alpha 1_{m,j} \qquad C2o_{m,j}=\alpha 2_{m,j} \qquad C3o_{m,j}=\alpha 3_{m,j}$$

$C_{1o}=(-0.7907 \ -4.2626)$ $C_{2o}=(1.2141 \ 6.5578)$ $C_{3o}=(-1.1767 \ -6.3541)$

$$\epsilon_{\epsilon\phi\phi 1om}=\frac{C1o_{m,1}}{C1o_{m,0}} \qquad \epsilon_{\epsilon\phi\phi 2om}=\frac{C2o_{m,1}}{C2o_{m,0}} \qquad \epsilon_{\epsilon\phi\phi 3om}=\frac{C3o_{m,1}}{C3o_{m,0}}$$

$$\epsilon_{\epsilon\phi\phi 1o} = 5.3909 \qquad \epsilon_{\epsilon\phi\phi 2o} = 5.4016 \qquad \epsilon_{\epsilon\phi\phi 3o} = 5.3998$$

$$Z_{o1om} = \frac{10^{12}}{c \cdot \sqrt{C_{1om,0} \cdot C_{1om,1}}} \qquad Z_{o2om} = \frac{10^{12}}{c \cdot \sqrt{C_{2om,0} \cdot C_{2om,1}}} \qquad Z_{o3om} = \frac{10^{12}}{c \cdot \sqrt{C_{3om,0} \cdot C_{3om,1}}}$$

b = 0.025 h = 0.025 a_0 = 0.575 nn = 500 2.s = 0.0006

w = 0.001

$$Z_{o1om} = 45.3917 \qquad Z_{o2om} = 29.5338 \qquad Z_{o3om} = 30.4758$$

C_{ej} =	$C_{1e0,j}$ =	$C_{2e0,j}$ =	$C_{3e0,j}$ =
0.187	0.099	0.046	0.042
0.714	0.382	0.175	0.157

$$C_{1oo,j} = |C_{1oo,j}| \qquad C_{2oo,j} = |C_{2oo,j}| \qquad C_{3oo,j} = |C_{3oo,j}|$$

$$C_{oj} = C_{ej} + [C_{1oo,j} - C_{1eo,j} + C_{2oo,j} - C_{2eo,j} + C_{3oo,j} - C_{3eo,j}],$$

$$\begin{array}{c} C_{oj} \\ \hline 3.1815 \\ \hline 17.1745 \end{array}$$

$$Z_{oo} = \frac{10^{12}}{c \cdot \sqrt{C_{oo} \cdot C_{o1}}} \qquad Z_{oe} = \frac{10^{12}}{c \cdot \sqrt{C_{e0} \cdot C_{e1}}} \qquad ratio = \frac{Z_{oe}}{Z_{oo}}$$

$Z_{oo} = 11.2736$ $Z_{oe} = 228.0599$ ratio = 20.2296

$coupling = 20 . \log\left[\frac{ratio-1}{ratio+1}\right]$ $coupling = -0.8594$ $C_{e1} = 0.714$ $C_{e0} = 0.$

$\epsilon_{o\epsilon\phi\phi} = \frac{C_{o1}}{C_{o0}}$ $\epsilon_{o\epsilon\phi\phi} = 5.3983$ $\epsilon_{\epsilon\epsilon\phi\phi} = \frac{C_{e1}}{C_{e0}}$ $\epsilon_{\epsilon\epsilon\phi\phi} = 3.8182$

$\epsilon_{\epsilon\phi\phi} = \sqrt{\epsilon_{\epsilon\epsilon\phi\phi} \cdot \epsilon_{o\epsilon\phi\phi}}$ $\epsilon_{\epsilon\phi\phi} = 4.54$ $\frac{1}{\sqrt{\epsilon_{\epsilon\phi\phi}}} = 0.4693$

APPENDIX 3

EVALUATION OF ρ_{qk}

L = 0.2 w = 0.0013 s = 0.0013

n = 1.. 100

$$ke_n = \frac{n - 0.5}{L} \cdot \pi \quad ko_n = \frac{n}{L} \cdot \pi \quad \alpha_n = ke_n \cdot \frac{w}{2} \quad \rho_n = ko_n \cdot \frac{w}{2}$$

$$s3 = s + \frac{w}{2} \quad s2 = 3 \cdot \left[s + \frac{w}{2}\right] \quad s1 = 5 \cdot \left[s + \frac{w}{2}\right]$$

$$f(\theta) = \sin(\theta) \cdot [\theta^3 - 6 \cdot \theta] + \cos(\theta) \cdot [3 \cdot \theta^2 - 6]$$

$$f(0) = -6$$

$$\rho 11c_n = JQ[\alpha_n] \cdot \cos[ke_n \cdot s1] \quad \rho 11s_n = JO[\beta_n] \cdot \sin[ko_n \cdot s1]$$

$$\rho 21c_n = JQ[\alpha_n] \cdot \cos[ke_n \cdot s2] \quad \rho 21s_n = JQ[\beta_n] \cdot \sin[ko_n \cdot s2]$$

$$\rho 31c_n = JQ[\alpha_n] \cdot \cos[ke_n \cdot s3] \quad \rho 31s_n = JQ[\beta_n] \cdot \sin[ko_n \cdot s3]$$

$$\rho 12c_n = \left[\frac{8}{5 \cdot w}\right] \cdot \cos[ke_n \cdot s1] \cdot \left[\frac{1}{ke_n}\right] \cdot \left[\sin[\alpha_n] + \left[\frac{1}{\alpha_n^3}\right] \cdot [f[\alpha_n] + 6]\right]$$

$$\rho 12s_n = \left[\frac{8}{5.w}\right] . \sin\left[ko_n . s1\right] . \left[\frac{1}{ko_n}\right] . \left[\sin\left[\beta_n\right] + \left[\frac{1}{\beta_n^3}\right] . \left[f\left[\beta_n\right] + 6\right]\right]$$

$$\rho 22c_n = \left[\frac{8}{5.w}\right] . \cos\left[ke_n . s2\right] . \left[\frac{1}{ke_n}\right] . \left[\sin\left[\alpha_n\right] + \left[\frac{1}{\alpha_n^3}\right] . \left[f\left[\alpha_n\right] + 6\right]\right]$$

$$\rho 22s_n = \left[\frac{8}{5.w}\right] . \sin\left[ko_n . s2\right] . \left[\frac{1}{ko_n}\right] . \left[\sin\left[\beta_n\right] + \left[\frac{1}{\beta_n^3}\right] . \left[f\left[\beta_n\right] + 6\right]\right]$$

$$\rho 32c_n = \left[\frac{8}{5.w}\right] . \cos\left[ke_n . s3\right] . \left[\frac{1}{ke_n}\right] . \left[\sin\left[\alpha_n\right] + \left[\frac{1}{\alpha_n^3}\right] . \left[f\left[\alpha_n\right] + 6\right]\right]$$

$$\rho 32s_n = \left[\frac{8}{5.w}\right] . \sin\left[ko_n . s3\right] . \left[\frac{1}{ko_n}\right] . \left[\sin\left[\beta_n\right] + \left[\frac{1}{\beta_n^3}\right] . \left[f\left[\beta_n\right] + 6\right]\right]$$

$\rho 31c_n$	$\rho 31s_n$	$\rho 32c_n$	$\rho 32s_n$
0.999	0.061	0.999	0.061
0.997	0.092	0.997	0.092
0.994	0.122	0.994	0.122
0.99	0.152	0.99	0.152
0.985	0.183	0.985	0.183
0.979	0.213	0.979	0.213
0.972	0.242	0.973	0.242
0.964	0.272	0.965	0.272
0.956	0.301	0.956	0.301
0.946	0.33	0.947	0.33
0.935	0.358	0.936	0.358
0.924	0.386	0.925	0.386
0.911	0.414	0.912	0.414
0.898	0.441	0.899	0.441
0.884	0.468	0.885	0.468
0.869	0.494	0.87	0.495
0.853	0.519	0.854	0.52
0.836	0.545	0.838	0.546
0.819	0.569	0.82	0.57
0.8	0.593	0.802	0.594
0.781	0.616	0.783	0.618
0.762	0.639	0.764	0.641
0.741	0.661	0.743	0.663
0.72	0.682	0.722	0.684
0.698	0.702	0.701	0.705
0.676	0.722	0.678	0.725
0.653	0.741	0.655	0.744
0.629	0.759	0.632	0.762

$\rho 31c_n$	$\rho 31s_n$	$\rho 32c_n$	$\rho 32s_n$
0.605	0.776	0.608	0.78
0.58	0.793	0.583	0.797
0.555	0.809	0.558	0.813
0.529	0.823	0.532	0.828
0.503	0.837	0.506	0.842
0.477	0.85	0.48	0.856
0.45	0.863	0.453	0.868
0.422	0.874	0.425	0.88
0.395	0.884	0.398	0.891
0.367	0.894	0.37	0.901
0.339	0.902	0.342	0.91
0.311	0.91	0.313	0.918
0.282	0.916	0.285	0.925
0.253	0.922	0.256	0.931
0.225	0.927	0.227	0.936
0.196	0.93	0.198	0.941
0.167	0.933	0.169	0.944
0.138	0.935	0.139	0.946
0.109	0.936	0.11	0.948
0.08	0.936	0.081	0.948
0.051	0.935	0.052	0.948

$\rho 21c_n$	$\rho 21s_n$	$\rho 22c_n$	$\rho 22s_n$
0.999	0.092	0.999	0.092
0.99	0.183	0.99	0.183
0.974	0.272	0.974	0.272
0.948	0.359	0.948	0.359
0.915	0.443	0.915	0.443
0.874	0.523	0.874	0.523
0.826	0.599	0.826	0.599
0.771	0.67	0.771	0.67
0.709	0.734	0.709	0.735
0.641	0.793	0.641	0.793
0.568	0.845	0.568	0.845
0.49	0.889	0.49	0.89
0.408	0.926	0.408	0.927
0.323	0.955	0.323	0.956
0.235	0.976	0.235	0.977
0.145	0.988	0.145	0.99
0.054	0.992	0.054	0.994
-0.037	0.988	-0.037	0.99
-0.128	0.975	-0.128	0.977
-0.217	0.955	-0.218	0.957
-0.305	0.926	-0.305	0.928
-0.389	0.889	-0.39	0.891
-0.47	0.845	-0.472	0.847
-0.547	0.793	-0.549	0.796
-0.619	0.735	-0.621	0.738
-0.686	0.671	-0.688	0.674
-0.747	0.602	-0.75	0.604
-0.801	0.528	-0.804	0.53
-0.848	0.449	-0.852	0.451

$\rho 21c_n$	$\rho 21s_n$	$\rho 22c_n$	$\rho 22s_n$
-0.888	0.367	-0.892	0.368
-0.92	0.282	-0.925	0.283
-0.945	0.194	-0.95	0.195
-0.961	0.106	-0.966	0.106
-0.969	0.017	-0.975	0.017
-0.969	-0.072	-0.975	-0.073
-0.96	-0.16	-0.967	-0.161
-0.944	-0.246	-0.951	-0.248
-0.919	-0.33	-0.926	-0.333
-0.887	-0.411	-0.894	-0.414
-0.848	-0.488	-0.855	-0.492
-0.801	-0.56	-0.808	-0.566
-0.748	-0.628	-0.755	-0.634
-0.689	-0.69	-0.695	-0.696
-0.624	-0.745	-0.63	-0.753
-0.554	-0.794	-0.56	-0.803
-0.48	-0.836	-0.485	-0.846
-0.402	-0.871	-0.406	-0.882
-0.321	-0.898	-0.325	-0.91
-0.238	-0.918	-0.241	-0.93
-0.153	-0.929	-0.155	-0.942

$\rho 11c_n$	$\rho 11s_n$	$\rho 12c_n$	$\rho 12s_n$
0.997	0.153	0.997	0.153
0.974	0.302	0.974	0.302
0.927	0.443	0.927	0.443
0.859	0.575	0.86	0.575
0.771	0.693	0.771	0.693
0.665	0.794	0.665	0.794
0.543	0.877	0.544	0.877
0.409	0.939	0.409	0.94
0.265	0.979	0.265	0.98
0.115	0.997	0.115	0.997
-0.037	0.99	-0.037	0.991
-0.189	0.961	-0.189	0.962
-0.336	0.909	-0.336	0.91
-0.474	0.836	-0.475	0.837
-0.602	0.743	-0.602	0.744
-0.715	0.633	-0.716	0.634
-0.811	0.509	-0.812	0.509
-0.888	0.372	-0.89	0.373
-0.944	0.227	-0.946	0.228
-0.978	0.078	-0.98	0.078
-0.989	-0.074	-0.991	-0.074
-0.977	-0.223	-0.979	-0.224
-0.941	-0.367	-0.944	-0.368
-0.884	0.501	-0.887	-0.503
-0.807	-0.624	-0.809	-0.626
-0.71	-0.732	-0.712	-0.734
-0.597	-0.822	-0.599	-0.825
-0.471	-0.893	-0.472	-0.897
-0.333	-0.943	-0.335	-0.947
-0.189	-0.97	-0.19	-0.975

$\rho 11c_n$	$\rho 11s_n$	$\rho 12c_n$	$\rho 12s_n$
-0.04	-0.975	-0.04	-0.979
0.109	-0.956	0.109	-0.961
0.255	-0.916	0.256	-0.921
0.394	-0.854	0.397	-0.859
0.524	-0.772	0.527	-0.777
0.641	-0.673	0.645	-0.677
0.743	-0.558	0.748	-0.562
0.827	-0.43	0.833	-0.434
0.891	-0.293	0.898	-0.296
0.934	-0.15	0.941	-0.151
0.955	-0.004	0.963	-0.004
0.953	0.142	0.962	0.143
0.929	0.284	0.938	0.286
0.884	0.418	0.893	0.422
0.818	0.542	0.827	0.548
0.733	0.653	0.741	0.66
0.631	0.748	0.639	0.757
0.516	0.824	0.522	0.835
0.388	0.882	0.393	0.893
0.253	0.918	0.256	0.93